2012

Applicability of MIKE SHE to simulate hydrology in heavily tile drained agricultural land and effects of drainage characteristics on hydrology

Andrew Steven Frana
Iowa State University

Applicability of MIKE SHE to simulate hydrology in heavily tile drained agricultural land and effects of drainage characteristics on hydrology

by

Andrew Steven Frana

A thesis submitted to the graduate faculty
in partial fulfillment of the requirements for the degree of
MASTER OF SCIENCE

Co-majors: Agricultural Engineering; Civil Engineering (Environmental Stewardship Engineering; Environmental Engineering)

Program of study committee:
Matthew Helmers, Co-major Professor
Chris Rehmann, Co-major Professor
Amy Kaleita

Iowa State University

Ames, Iowa

2012

TABLE OF CONTENTS

LIST OF FIGURES

LIST OF TABLES

LISTS OF SYMBOLS AND ABBREVIATIONS

α : curve shape factor in Rosetta model, used for soil water retention curve

l : empirical pore connectivity and tortuosity parameter, used for soil water retention curve

CRP : conservation reserve program

D.O.G : day of growth (crop cycle)

DTC : drainage time constant

EF% : Nash-Sutcliffe model efficiency

ET : evapotranspiration

ET_o : reference evapotranspiration

ET_p : potential evapotranspiration

E : error, accumulated in MIKE SHE over simulation period

FAO : food and agriculture organization

GLUE : generalized likelihood uncertainty estimation

K_c : crop coefficient

K_s : saturated hydraulic conductivity

LAI : leaf area index

M : Manning's M, reciprocal of Manning's surface roughness coefficient

M_Sf : modeled streamflow

n : curve shape factor in Rosetta, used for soil water retention curve

NCDC : National Climatic Data Center

O_Sf : observed streamflow

OVL : overland flow component

PBIAS : percent bias, form of statistical comparison of model to observed data

pF_{fc} : pressure head at field capacity

pF_w : pressure head at wilting point

PPT : precipitation

R^2 : coefficient of determination

RD : rooting depth

Re : recharge

SUBD : subsurface drainage exiting the watershed outlet

SZ : saturated zone

UZ : unsaturated zone

WM ; water movement, the main module for watershed simulation in MIKE SHE

θ_r : residual moisture content, volumetric basis

θ_{sat} : saturated moisture content, volumetric basis

ψ : pressure head

ACKNOWLEDGEMENTS

I would first like to thank Iowa State University and the departments of Agricultural and Biosystems Engineering and Civil Engineering for giving me the opportunity to pursue a Master's of Science degree. The journey to complete this degree has enabled me to grow more as a scholar, an engineer, and as a person than I would have had I not been accepted into the Master's of Science program at such a prestigious university. This degree will also open doors and create opportunities to

In addition, I would like to personally thank my committee that guided and advised me throughout the entire process. I could always rely on them to ask the tough questions that needed to be answered and point me in the right direction so I could find the solution and eventually learn what questions I should be asking myself. Dr. Helmers provided lead support as my major professor in the Agricultural and Biosystems Engineering department. I would like to thank him for accepting me into his staff and providing challenging yet rewarding research. Dr. Rehmann also deserves thanks, as a co-major professor he was a key liaison to the Civil Engineering department. I would also like to thank Dr. Kaleita, the final member of my committee; she was always able to make time to answer any questions I had.

My thanks to Kris Bell and Katherine Petersen, as secretaries of the graduate college departments of ABE and CCEE, respectively, they answered questions and helped keep deadlines from the beginning of this endeavor to the completion. Also, Dr. Freeman and Dr Hoff of the ABE department and Dr. Sritharan of the CCEE department acted as DOGE's and deserve my thanks as well.

My thanks also go to Dr. Gelder and his ArcGIS expertise, Greg Stenback for providing flow data, Carl Pederson for providing practical watershed knowledge, and special thanks go to Bob Zhou for his expertise with MIKE SHE and hydrological model simulation. I would also like to thank all other professors that I had the pleasure of taking classes from while at Iowa State.

I would like to thank my family and friends for providing continual support throughout the thesis process. I would especially like to thank my fiancé, Molly McHenry, for her understanding and patience dealing with long nights and weekends. She has always been there for me and I look forward to being there for her as well.

ABSTRACT

The watersheds of the Des Moines lobe in north central Iowa have fundamentally changed in the last 170 years. Where there was once prairie, row crop agriculture now dominates. This progress has enabled this small region of the Midwest to provide food, fuel, feed, and fiber for millions, but with recent flooding events of 2008 and 2010 questions have been raised about the hydrological impacts of these lands. These flood events are driven by peak flow and concerns about the effect of drainage on peak flow should be investigated. MIKE SHE, a watershed scale model, was used to simulate daily streamflow in a multisite comparison to determine if the model is suitable to simulate streamflow in heavily drained agricultural land. The model was tested for five years (2007-2011) in two similar watersheds (1127 ha and 1356 ha) in Palo Alto County, Iowa. In the testing watershed, the simulated streamflow correlated well with the observed streamflow, as shown by a daily Nash-Sutcliffe coefficient of 0.62 and a coefficient of determination of 0.66. Likewise, the model performed well in the validation watershed with a daily Nash-Sutcliffe coefficient of 0.73 and coefficient of determination of 0.79. This shows that the model can be used in the future to simulate flow in similar agricultural regions throughout the Midwest that employ tile drainage to maintain suitable water table levels needed for crop growth.

Changes in land use management and drainage design were simulated to better understand the hydrological impact that land use and tile drainage has on the landscape. It was shown that if row crops are converted to pasture or prairie, with drainage infrastructure intact, evapotranspiration would increase by 25% and the magnitude of peak events would decrease by over 50% in some cases. Likewise, if the drainage infrastructure was removed and only perennial grassland remained, similar to likely pre-settlement conditions for the region, then water table height becomes the main driver of surface flow and overall flow from both watersheds would decrease by 55%. Alternatively, if the depth of tile drains were decreased from 1.2m to 0.75m the effect would allow for 7 to 20 mm of extra surface runoff, while decreasing subsurface flow and maintaining the total flow. Lastly, if all drainage infrastructures were removed from the watersheds and row crop monoculture were to be maintained there would be an increased frequency of peak flow that may lead to damaging flood events. These results show that MIKE SHE could be used in land use management

decisions and assessment of drainage design for mitigation of hydrological impacts downstream of heavily drained agricultural watersheds. This may help target land areas for wetland placement by showing the effects of eliminating drainage structure will have on the watershed.

CHAPTER I – INTRODUCTION

1.1 Background

With the ever increasing need for food, feed, fuel, and fiber to drive the world's economies, agricultural producers are embracing diverse approaches targeted at increasing yield on currently productive land and transforming idle land into new productive land. These approaches include transforming plant phenotypes to thrive in previously inhospitable land (Reynolds and Borlaug, 2006), improving nutrition value of plant varietals (Borlaug, 1992), improving irrigation techniques in arid land (Fereres and Soriano, 2007), and applying subsurface drainage to increase yield (Skaggs et al.,, 1994). These improvements to land use management practices must also balance with the natural cycles of the planet, such as seasonal changes or drought-monsoon cycles, in order to provide a sustainable future; this must be done not only at the field level, but at the watershed level as well.

In Iowa, the vast majority of land is used for agricultural purposes and 3.6 million ha (25%) of this land is enhanced with subsurface drainage infrastructure (Baker et al., 2004). Not only does subsurface drainage allow for greater soil aeration, possible earlier planting dates, and overall better field conditions (Zhou et al., 2010), but some researchers have also concluded subsurface drainage has the potential to reduce surface runoff and pollutants associated with surface runoff (Bengston et al., 1995). There are many studies that have quantified benefits of draining agricultural land. In the Carolina coastal plains runoff was reduced 34 to 55% by installing subsurface drainage (Skaggs, 1994). Properly managed drainage can also increase infiltration rates (Shipitalo et al., 2004), change soil structure by increasing crop residue and decreasing water logging in wheat fields (Gardner et al., 1994), more importantly on a watershed scale drainage can reduce peak flow of flooding events in Carolina coastal plains (Skaggs and Broadhead, 1982). However, recent flooding events in Iowa during the summers of 2008 and 2010 has brought the impact of subsurface drainage on flooding back into discussion. The peak flow of a flood may be influenced by drainage, climate, decrease in storage capabilities of wetlands, row crop monoculture, or other land use factors. Therefore studies are needed to determine the extent that peak flow of floods are influenced at the watershed scale these various factors. Although factors contributing to peak flow of floods

are still being investigated, subsurface drainage has been linked to increased transport of soluble pollutants such as nitrate, a large contributor to the spread of the hypoxic zone in the Gulf of Mexico (Rabalais et al., 2001; Kanwar et al., 2005).

In order to quantify the effect that subsurface drainage has on peak floods or nitrate transport, data (streamflow and nutrient fate and transport) must be collected and analyzed so relevant conclusions can be made. Historically, the hydrogeological, meteorological, and agronomical data were collected by hand and conclusions were empirically based. This process was very intensive in both time and manual resources. Over the past few decades, great strides have been made in technology and modeling techniques that allow users to make informed and relatively accurate representations of ungaged watersheds that previously would have been impractical. Examples of models that have been extensively used to simulate hydrological conditions of watersheds include ANSWERS-2000, DRAINMOD, HEC-RAS, MIKE SHE, and SWAT. Physically based models like MIKE SHE have an advantage that at small enough grid scales basic physics can explicitly describe the watershed response, and when compared to empirically based models of equivalent grid scale, they can produce results with higher degrees of precision to observed values (Downer and Ogden, 2004). With proper calibration physically based models can be applied to widely varying landscapes with very useful results.

MIKE SHE, Système Hydrologique Européen, is a sub-model under the collection of models within the MIKE framework. This model was developed by a consortium of European institutes: the Danish Hydraulic Institute (DHI), the British Institute of Hydrology, and a French consulting agency SOGREAH. DHI has retained rights and revisions of all MIKE based hydrologic and hydraulic models. MIKE SHE has been applied in far reaching applications all over the world, ranging from Canada (Oogathoo, 2009) to Australia (Demetriou 1999), and Slovenia (Janža, 2009) to Hawaii (Sahoo, 2006), but limited work has been done with MIKE SHE on the effects of subsurface drainage. Studies calibrated MIKE SHE to drained and undrained marshes in England and found that theoretically eliminating drainage would increase peak flow but reduce overall annual streamflow (Al-Khudhairy 1997, and 1999). More recently, studies have been published about subsurface drainage in

Iowa (Zhou et al., 2011) that show MIKE SHE can model subsurface drainage in heavily drained agricultural land at the plot scale. However, no work to date has been done to validate the ability of MIKE SHE to simulate streamflow of heavily tile drained agricultural land on a watershed scale, which vastly increases the complexity and demands of the model. This task will be more encompassing than plot scale work, and it may help in land use management decisions throughout the Midwest as the effects of drainage become well understood.

1. 2 Objectives

The objectives for this study are

1. To evaluate the applicability of MIKE SHE, a physically-based, distributed, watershed-scale model, for simulating hydrology in heavily tile drained watersheds in North Central Iowa, United States. This will be accomplished by:

    1.a Evaluating the ability of the MIKE SHE model to predict observed flows using standard statistical measures (e.g. NSE (Nash-Sutcliffe efficiency), percent bias, and R^2 values), and

    1.b Performing a sensitivity analysis of various important parameters such as drainage time constant and detention storage.

2. To evaluate the impact various subsurface drainage and drain depth practices have on watershed hydrology.

3. To assess the impact different land use practices, such as land use change have on the hydrologic response of the watershed.

1.3 Scope of Study

The MIKE SHE model has the ability to simulate surface flow as runoff and subsurface flow as either drainage routed through tile drainage infrastructure or seepage out of the boundaries set forth within the model. There are other models with these capabilities, but may either be too simplistic with lumped parameters and non-continuous capabilities, or incomplete in nature, either only surface flow or surface flow and incomplete subsurface

flow. Since this study is aimed at simulating the hydrologic processes at a watershed-scale, it was necessary to choose the model that could most completely describe the hydrologic conditions without oversimplifications or missing features.

Although there are no rivers in the watersheds, there are drainage ditches that could be modeled using the MIKE 11 model. This was not done since the drainage ditches are very small relative to the rest of the flow area and flow data was collected at the headwaters of the drainage ditches making the modeling of the ditch unnecessary. Since the monitoring station was at the headwaters of the channel, the channel flow would not significantly effect the time of concentration within the MIKE SHE model.

The MIKE SHE model will be used to simulate overland and subsurface flow to reproduce the hydrologic conditions occurring at the outlet of two watersheds in the North central region of Iowa, specifically Palo Alto County. Climate data were obtained from two stations near the watershed. First, climate data for evapotranspiration including wind speed, temperature, solar radiation and relative humidity were obtained from a Mesonet station in Kanawha, Iowa. Precipitation data were obtained from the Emmetsburg NCDC station (S132689). Soil data were obtained from the Web Soil Survey and certain soil parameters used to calculate unsaturated hydraulic conductivity were calculated using the Rosetta soil model. Land cover information including leaf area index, rooting depth, and crop coefficient were obtained from literature. It should be noted that initial conditions of the water table and flow conditions were set at arbitrary startup values since the first year of the simulation was used as a “warm up” period. This study was limited to two watersheds overall, and future simulations of a similar nature on comparable watersheds should be done to solidify conclusions drawn to the model’s applicability in broader terms.

CHAPTER II – LITERATURE REVIEW

This section will provide a review of the literature concerning hydrologic modeling. This will include the hydrologic cycle, watershed hydrology, and past work done with the physically based watershed model MIKE SHE, as well as a description of the model.

2.1 Hydrologic Cycle

The hydrologic processes that affect the world are well known and have been studied in detail (Schwab et al., 1993.) As an air mass becomes saturated with moisture, precipitation falls through the atmosphere to the Earth's surface as rain, snow, sleet or hail. Before it reaches the soil surface, some of this precipitation can be intercepted on the canopy surface of vegetation, or is evaporated back into the atmosphere. The precipitation that does reach the soil surface may infiltrate into the soil, evaporate after a detention period on the surface, or flow over the surface as runoff. Evapotranspiration can occur from any saturated surface under the proper conditions, or within the stomata of leaves as plants transpire. The fraction of water that infiltrates through the surface can either be taken up by plants for growth processes or percolate deeper into the soil profile. The portion that enters the saturated zone will exit groundwater into streams and rivers or through baseflow eventually to the ocean (Dingman, 2002). Subsurface drainage can increase infiltration and export of water out of the soil profile by providing a path of least resistance for water in the soil above the drainage lines. This drainage of the upper soil profile can control the antecedent moisture content of the soil profile, which creates a more stable soil regime, which can in turn limit instances of peak flow that lead to flooding events.

2.2 Watershed Hydrology

The above mentioned processes occur at all scales, and it is possible to sum the water balance of any sized watershed as long as all inputs and outputs are accounted for the difference will be the change in storage of the watershed. A watershed is defined as the land area contributing surface runoff and subsurface drainage into a stream or to any point of interest (Chow et al., 1988). Thus depending on the scale, one watershed may consist of several sub-watersheds, or may be a smaller watershed within an overall larger watershed. A water balance of a watershed can be theoretically represented by the main laws in effect when

calculating the change in storage, which include the conservation of mass and Newton's laws concerning the conservation of momentum and energy (Newton, 1729). These forces become important when modeling the flow of water down the landscape, and in channel flow where backwater effects may take place (Fetter, 2001).

Input – Output = Net Change in Storage (1.2.1)

An object that is at rest will tend to stay at rest unless an unbalanced force acts upon it;
An object that is in motion will not change its velocity unless an unbalanced force acts upon it

$$\sum F = 0 \Rightarrow \frac{dv}{dt} = 0 \quad (1.2.2)$$

The net force on a particle is equal to the time rate of change of its linear momentum **ρ**

$$F = \frac{d\rho}{dt} = \frac{d(mv)}{dt} = m\frac{dv}{dt} = ma \quad (1.2.3)$$

2.3 Hydrology Models

A model is used in hydrology to understand why a flow system is behaving in a particular observed manner and to predict how a flow system will behave in the future (Fetter, 2001). These two uses, understanding observed flow and predicting future behavior, are integral in creating real world infrastructure that will be able to sustainably exist within the hydrologic and hydraulic systems. Models can be classified as physical, analog, or mathematical in nature.

Mathematical models can be represented in a number of ways depending on the input output relationships and what laws and principles they abide by. A mathematical model can use theoretical equations that follow the laws of nature and be classified as physically based, or the model can use experiment based relationships to draw equations and be classified as empirically based. A model that spatially or temporally varies the input parameters is a distributed model, in contrast to a lumped model, which has a spatially or temporally uniform input parameter set. Models can also either be event based which simulate a particular event of process for a short period; or a model can be continuous in nature and output several years' worth of data. The extent to which model parameters are determined can further

classify models. A deterministic model has every parameter fully determined by governing equations, a stochastic or probabilistic model has incomplete determination and some variable are totally or partially described by probability equations. (DHI, 2004)

2.3.1 MIKE SHE as a model

MIKE SHE is a fully integrated, physically based, distributed model, capable of both event based and continuous simulations. The model is capable of simulating hydrology in plot, field, and watershed scales, particle tracking of solutes, and can be linked with MIKE 11 to simulate watershed-river relationships. The MIKE SHE model was originally developed by three European organizations (Danish Hydraulic Institute, British Institute of Hydrology, and a French consulting company SOGREAH) in 1977. DHI has taken the lead in development and research of MIKE SHE for improvements and additions (DHI, 2004). The physically based nature of the model lends inclusion of natural topography and watershed characteristics such as vegetation, soil, and weather parameter sets. The distributed nature of the model allows the user to spatially and temporally vary parameter sets such as soil profiles, land use conditions, drainage practices, weather and evapotranspiration data sets, and overland flow values. The spatial distribution is accomplished through an orthogonal grid network that allows for horizontal or vertical discretization, as applicable within each parameter set (Abbot et al., 1986). Temporal distribution allows users to either vary parameters by timestep, or set constant values for parameters for the entirety of the simulation period. The user can also change the complexity of the model simulation by adjusting the modular setup of the model within the GUI (graphic user interface). One can choose to include the modules such as Overland Flow (OF), Rivers and Lakes (OC), Unsaturated Zone (UZ), Evapotranspiration (ET), and Saturated Flow (SF). If the saturated flow module is included than the unsaturated zone and evapotranspiration modules must be included as well.

2.3.2 MIKE SHE in literature

The following applications in literature elucidate the versatility of MIKE SHE as a hydrological model and, although not an exhaustive list, show that the potential for this model may be bounded by the imagination and creativity of the user.

2.3.2.a MIKE SHE in irrigation applications

Much of the early work involving MIKE SHE has been directed at irrigation (Carr et al., 1993; Punthakey et al., 1993; Singh et al., 1997 and 1999; Jayatilaka et al., 1998; Mishra et al., 2005). Carr (1993) and Punthakey (1993) both looked at the Berriquin irrigation district in New South Wales, Australia. The concerns in the region were rising groundwater levels that increased the salinity of the irrigated cropland. The MIKE SHE model was used to assess the impact of irrigation and water logging on water table levels with current farming practices (Punthakey, 1993) in order to propose more efficient structural practices with regard to water storage and best management practices for drainage applications. Carr (1993) sought to determine what temporal and spatial scales would work best with the model. It was determined that too fine of spatial resolution lengthened stream networks and increased the number of grid cells in the stream network. This in turn could lead to errors associated with groundwater loss to the steams. For this simulation it was deemed that a 500-750 m grid cell size could accurately predict rice crops grown in an area of 320,000 ha. Similar work has been done in the Wakool Irrigation District in New South Wales, Australia (Demetriou 1999). This investigation added to the work done by Punthakey and Carr dealing with rising water table levels and salinity issues stemming from increasingly wet winters and inadequate drainage. Demetriou used MIKE SHE to evaluate potential solutions in a land and water management plan. These solutions included revegetation alternatives like tree planting and introducing salt tolerant plants; engineering alternatives such as pumping to evaporation basins, land reforming, and utilizing recycling ponds. The model was used to simulate the extent to which near surface water table area would expand by 2020. It was concluded that using 48 pumps to pump water into evaporation basins and artificially lower the water table would stem the spread to only a 7% increase from 1995 levels. Confidence levels in this method are higher than other alternatives since pumping rates are known and salt recovery is predictable.

Singh (1999) used MIKE SHE in to optimize irrigation schedules of rice paddies in a small rain fed watershed in West Bengal, India. The rainfall was stored in tanks and released during dry periods as suggested by the irrigation schedule prepared with the assistance of a water balance modeled by MIKE SHE. The metrics that defined success in this instance were

water balance error, increased crop yield and enough stored water to maintain *rabi* crops, or winter season crops like wheat, mustard, and grain. Jayatilaka (1998) used MIKE SHE to model water flow and was calibrated to observe piezometric levels in wells throughout the 9 ha site in the Tragowel Plains, Australia. The model simulated many flow processes including infiltration, capillary rise, evapotranspiration, overland flow, and ground water flow. The Jayatilaka paper concluded that MIKE SHE adequately simulated the flow conditions of the region (correlation coefficients ranged from 0.803 – 0.924) but the model lacked the ability to accurately reflect the characteristics of the regional soil. The mostly clay soil would expand during wet time periods, then dry and crack, leaving large macropores that create preferential flow pathways for the subsequent rainfall event. MIKE SHE can allow users the option of including macropore flow, both as a simple bypass or as a full macropore flow. In full macropore flow the user can specify the maximum infiltration per timestep, and maximum exchange for each node and column. The model may not simulate the transient nature of the of the shrink-swell cycle of the clay soils in the study region, but it was found to adequately simulate salinity and quantity of drain flow despite this deficiency. Revised versions of MIKE SHE allow users to fine tune the macropore flow as a function of soil moisture (DHI, 2004). Another investigation coupled MIKE SHE with MIKE 11 (Mishra, 2005) in order to develop an optimal canal release schedule for the Right Bank Main Canal System in West Bengal, India. Three simulation scenarios were performed during the *kharif* season (Aug – Oct.) for three years (1995-1997). The scenarios compared were the (1) MIKE 11 and MIKE SHE simulation, (2) an integrated optimization simulation (IOS) which included canal hydrology for optimal release, (3) an IOS with an improved schedule. It was found that the MIKE 11 and MIKE SHE (MMS) simulation ran higher deficits towards the end of the growing season than the integrated optimization simulations. The discussion pointed out that the IOS, which is based off of limiting the route mean square error (RMSE) for several modules of the irrigation performs well enough that it was questionable whether sophisticated models such as MIKE 11 and MIKE SHE were needed.

2.3.2.b MIKE SHE in drainage applications

A series of papers (Al-Khudhairy, et al 1997, 1999, Thompson, et al 2004) investigated the effects of changes in hydrology of marshland in Southeast England. The former two papers

address a 10 km^2 area near the North Kent Marshes; the later paper by Thompson (2004) addresses the adjacent 8.7 km^2 of the Elmey Marshes on the Isle of Sheppey. This marshland was drained for grazing in the past century and the authors were investigating the effects that restoration of the ground to its former state would have (Al-Khudhairy, 1997; Thompson, 2004). A pseudo-differential split sample was used to assess the MIKE SHE predictions of the effects on hydrology of changes in land use. Coefficient of correlation values for observed monthly flow reached 0.87 for the baseline model flow and 0.92 with the baseline model with macropore flow. These results support Jayatilaka's conclusion that shrink-swell characteristics of soil profiles are important in describing preferential flow in the unsaturated zone (Al-Khudhairy, 1999). Thompson (2004) found that the coupling MIKE SHE with MIKE 11 to describe marshland piezometric head and surface water extent lead to a high degree of precision. Observed head values at piezometer locations throughout the research area had coefficient of correlation values ranging from 0.41 to 0.78 for testing and 0.56 to 0.92 for validation. Thompson (2004) concluded that the MIKE SHE model was sufficient to describe the water table elevation of marshland in the Southeastern region of England and postulated that it may be sufficient to model marshland area in other regions as well.

More recently, and closer to the study area of this investigation, work has been done using the MIKE SHE model at the field scale in heavily tile drained agricultural land in Iowa (Zhou et al., 2011). This investigation modeled 73 unique drained plots, each about 38 m in length and 15.2 m in width. Drains were installed along the border to minimize lateral subsurface flow, and drainage flow from the plots were monitored by a center drainage line under each plot using automatic pumping and volume monitoring system (Zhou, 2011). The MIKE SHE model showed a satisfactory performance with NSE values of 0.78 for the calibration period (2006 – 2007) and 0.73 for the validation period (2008 – 2009) for comparing modeled flow to observed flow at the site. The study concluded that macropore flow and the drainage time constant were the most sensitive to parameters to predicting drainage flow. This investigation also showed that MIKE SHE has the potential to be used as a land management use tool at the watershed scale if it can be proved that the model simulates flow adequately at the plot scale as well.

2.3.2.c MIKE SHE in additional applications

Several investigators have used MIKE SHE in dissimilar hydrological conditions to analyze and develop solutions to hydrological problems within the parent region. In the mountainous regions of Hawaii, irrigation is less of an issue than flash flooding resulting from short but intense rainfall events (Sahoo, 2004). The study area investigated included two watersheds in the Manoa-Palolo stream system adding up to 27.28 km^2 on the Hawaiian island of Oahu. Flow data was collected at 15 minute intervals in order to accurately describe the sudden onset of flash flood events within the watershed. Deviations from other investigations include unique topography (mountainous) and soil parameters (volcanic parent material); horizontal saturated hydraulic conductivity K_h was 190 times greater than the vertical saturated hydraulic conductivity K_v. It was concluded that MIKE SHE reached a correlation coefficient of 0.70 with watershed discharge and could be used to predict the severity of flood events with a given precipitation depth.

MIKE SHE and MIKE 11 were also successfully coupled to model water storage in a 95 ha canal-impoundment flood control structure that provides drainage for 720 ha of wetland grove in Florida (Jaber and Shukla, 2005). This investigation utilized two approaches; the first modeled canal flow as a one dimensional and overflow into the impoundment as two dimensional flows; the second modeled the canal and impoundment as a one dimensional link-node system. The second method, which used MIKE 11 to model the canal flow and MIKE SHE to model the seepage through sandy soil profiles, outperformed the first method with a coefficient of correlation value of 0.90 for simulated and observed impoundment water levels. The first method had a coefficient of correlation of 0.78. This paper showed that although MIKE SHE proved suitable for modeling two dimensional subsurface flow and seepage, MIKE 11 was not able to accurately represent the flooding process from the canal to the floodplain.

In the South Carolina coastal plain, a bi-criteria approach (streamflow and depth to water table) with MIKE SHE was used to determine if the model could satisfactorily simulate watersheds in the region (Dai et al, 2009). The 160 ha watershed has a nest of ten wells throughout the expanse to measure the water table depth. Statistical measures were more than satisfactory with R^2 values from 0.60 – 0.99 for daily and monthly streamflow, Nash

Sutcliffe's model efficiency (NSE) of 0.53 – 0.98 for daily and monthly calibrated streamflow; water table depth also had satisfactory statistical values with R^2 values of 0.52-0.91 and NSE values of 0.50 – 0.90 for calibration (Dai et al, 2009). The model showed that simulations of the Carolina coastal plains were highly sensitive to surface detention storage, drainage depth, surface roughness and horizontal hydraulic conductivity. However, the model showed that a multi criteria approach provides better optimization of parameter sets than a single criterion approach (streamflow or water table depth, but not both).

The MIKE SHE model was also put to use in simulating groundwater flow and aquifer recharge in a 200 km^2 catchment of the Rižana spring in Slovenia (Janža, 2009). This watershed is located above a karst aquifer region, characterized by limestone with large fissures and pathways for preferential flow. The model improved upon previous models utilizing a black box, or a linear guess and check approach (Labat et al., 2000), models using physically based data that requires resource intensive, site specific, geometric characteristics of the aquifer (Eisnelohr et al., 1997), and models using physically based approaches that are oversimplified (Quin et al., 2006). This work showed that with such a variable and unstructured saturated zone, coupled with marked preferential flow in the unsaturated zone, a small increase in precipitation can lead to a large downstream increase in spring discharge (Janža, 2009). Performance criteria achieved were calibration values for a 14 year period (1984 – 1997) as high as 0.80 for R^2, and validation values for a six year period (1998-2003) were comparable at 0.82 for the same statistical analysis.

2.3.2.d MIKE SHE advancement research

Several papers are devoted not to site investigations, but to internally optimizing the MIKE SHE model by increasing the precision in calculations involving soil, hydraulic, and internal parameters. (Christiaens and Feyen 2000, 2001, 2002; Vázquez and Feyen 2002; Vasquez et al.; Feyen et al. 2000). First, spatial uncertainty associated with soil hydraulic properties were measured in three distinct ways (Christiaens, 2000). These three ways include soil characteristics measured through laboratory means, calculated using a pedo-transfer function (PTF), and calculated with the PTF using soil texture values available through the USDA. It was determined that the simulated spatial uncertainty (100 m by 100 m grid cells) was smaller than the observed uncertainty in the field, possibly indicating that other parameters

are important when trying to define output, groundwater elevation in this case (Christiaens, 2000). Christiaens (2000) also recommended that more simulations with a greater array of parameter values should be tested to see if uncertainty is coming from parameters other than the ones considered in this paper. In 2001, Christiaens and Feyen further investigated the uncertainty propagation with soil hydraulic properties; this investigation also included a fourth way to calculate soil characteristics, a bootstrap neural network approach using field texture measurements (Christiaens and Feyen, 2001). Scaling issues were disregarded in this approach and the neural network had the smallest uncertainty, but median values were different from observed median values of output such as discharge, water level, and soil water content. A later investigation (Christiaens and Feyen, 2002) explored the output uncertainty of MIKE SHE using a generalized likelihood uncertainty estimation (GLUE) network. This GLUE network enabled the user to eliminate potential parameter ranges by 20-85% of the original size (Christiaens, 2002). For example, the logarithm of the hydraulic conductivity shape parameter *n* matched well with previous works value ranges after using the GLUE network. This investigation called for a continued study that further establishes parameter ranges for soil hydraulic characteristics. In addition to soil hydraulic parameters, there have been papers investigating the effect of various methods to calculate potential evapotranspiration ET_p as an input into the MIKE SHE model (Váquez, 2001). This study used three ways to calculate ET_p: Food and Agricultural Organization (FAO) FAO-24 approach, FAO-24 approach used with different coefficients for both the wind and Stefan-Boltzman equations, and the FAO-56 standard approach. Although the first method was linked to better model performance, it was indicated that coarse grid cell size and time step length may also be contributing to different outputs from the model scenarios. It was suggested that further research be done to investigate the link between output and spatiotemporal resolution. This led to the next paper in this series investigating the effect of grid size of effective parameters in MIKE SHE (Vázquez et al., 2002). This study used three spatial resolutions: 300 m square grid cell, 600 m grid cell, and 1200 m grid cell sizes. Of the three resolutions, the 600 m square grid cell run had the best statistical performance with a NSE of 0.769 for discharge at the gaging station, as opposed to the 300 m square grid cell, which had a NSE of 0.763. Although these values are close, since the larger grid cell size

outperformed the smaller size the paper concluded it could be from one of three causes: governing equations are not being solved effectively at much larger scales, the trial and error calibration failed to identify global optimums for all three scenarios, or the lumped time resolution for all three scenarios was not properly calibrated for all scales. It was concluded that further studies should be done on a sub daily time step in order to obtain more reliable and accurate results (Vázquez, 2002).

The preceding studies have shown that MIKE SHE is capable of modeling various extreme hydrological conditions such as irrigation (Mishra, 2005; Singh, 1997 and 1999; Carr 1993), mountainous stream networks (Sahoo, 2006), lowland periodic wetlands with drainage (Thompson 2004), coastal plains (Dai et al, 2009), complex karstic formations (Janža, 2009), cold climates (Oogathoo, 2009), tile drained agricultural land at the plot and field scale (Zhou, 2011). It is a justifiable investigation to see whether a plot and field scale model will be able to adequately reproduce observed flow at a watershed level. Satisfactory modeling of entire watersheds with highly drained agricultural land will provide a base to investigate land management decisions that can improve the hydrological quality of the watershed.

2.4 The MIKE SHE Model

This section will describe the model components used in this investigation and present the mathematical basis for each module. Special note will be taken to the saturated and unsaturated zones in regards to drainage within the model.

2.4.1 Hydrological Description

As stated earlier, MIKE SHE is a fully distributed, physically based, deterministic hydrological model capable of both continuous and single event analysis (DHI, 2004). The process starts with user input precipitation, a fraction of which is intercepted by vegetation before it reaches the surface. This intercepted precipitation is either stored on the plant material and later evaporated back into the atmosphere or detained on the soil surface where it can undergo surface runoff or infiltration, depending on soil conditions. As infiltration continues, the unsaturated zone will become saturated and after all surface storage areas are taken up overland flow will begin downward from one cell to the next based on topographic data. As this process is ongoing, moisture from the unsaturated zone is transferred to the

saturated zone at a rate dependent upon soil parameters within the vertical soil profile. This saturated zone flow can either continue down as deep percolation or continue laterally either as subsurface drainage, or interflow. This lateral flow will eventually contribute to inflow to surface lakes and streams and also contribute to groundwater in the form of recharge to the saturated zone. Subsurface flow will continue until released at an outlet structure, where is will in turn flow into surface bodies like those listed above.

2.4.2 Mathematical Description

The MIKE SHE model consists of two main modules, water quality (WQ) and water movement (WM). The water quality sub-modules are advection-dispersion (AD), particle tracking (PT), sorption and degradation (SD), geochemistry (GC), biodegradation (BD), and crop yield and nitrogen consumption (CN). The soil water movement module was utilized for this investigation and consists of many sub-modules: evapotranspiration (ET), soil water movement (SWM), overland flow (OF), channel flow (CF), ground water flow (GWF), and irrigation (IR) (DHI 2004). Other components used in the water movement module include unsaturated zone (UZ), saturated zone (SZ), snow melt and root zone models as shown in Figure 1.

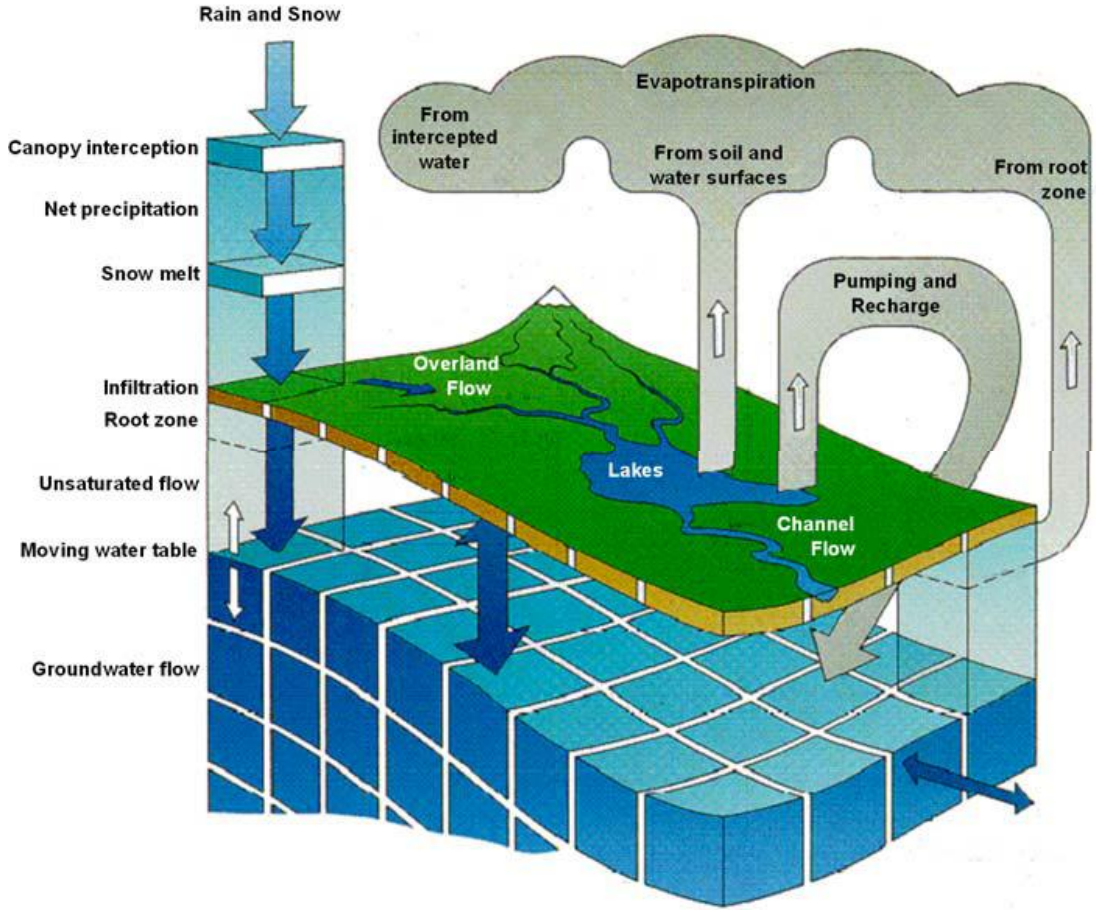

Figure 1 Three dimensional schematic representation of the MIKE SHE model (Refsgaard and Storm, 1995)

As MIKE SHE is a physically based model, the above mentioned modules are based on physical laws which are derived from forms of the laws of conservation of mass, momentum, and energy. The evapotranspiration model is calculated using the Kristensen and Jensen methods, although user input reference ET can be calculated in numerous ways. Channel flow is handled using one dimensional (1-D) diffusive wave Saint Venant equations and overland flow is calculated using two dimensional (2-D) diffusive wave Saint Venant equations. Water infiltrating into the unsaturated zone can be modeled using the 1-D Richards flow or gravity flow. The saturated zone is modeled using a three dimensional (3-D) Boussinesq equation which uses finite difference methods to solve the partial differential equations (PDE's). Some aspects of MIKE SHE are empirically based, however, these routines include snowmelt equations and coefficients dealing with interception (DHI, 2004).

2.4.2.a Interception and Evapotranspiration Component

The interception and evapotranspiration module of MIKE SHE is split up and modeled in four sections based on the time of contact with soil and canopy as shown in figure 1. Initially, a portion of the precipitation is intercepted by vegetative canopy, some of which evaporates back to the atmosphere. The remaining water that reaches the surface either produces runoff or infiltrates into the unsaturated zone. The water reaching the unsaturated one can either evaporate from the upper part of the root zone, be transported by plant roots, or recharge groundwater into the saturated zone (DHI 2004).

i. Kristensen Jensen method

The Kristensen Jensen method was developed through empirical work done at the Royal Veterinary and Agricultural University (KVL) in Copenhagen, Denmark. Empirical equations are based on field measurements and require inputs of reference evapotranspiration (ET_{ref}), leaf area index (LAI), root depth (AROOT), and several user controlled empirical parameters (Refsgaard and Storm 1995). The first step in this method is to determine the maximum interception storage capacity of the vegetative canopy, I_{max} which can be defined by:

$$I_{max} = C_{int} * LAI \quad (2.1)$$

where

C_{int} is an interception coefficient [L]

LAI is a leaf area index [-]

The default value of C_{int} in the MIKE SHE model is 0.05 mm. LAI values are empirically calibrated to vegetation and region and can be found in literature as well. If sufficient water is intercepted, evaporation from canopy storage can occur, this is given by:

$$E_{can} = \min (I_{max}, E_p \Delta t) \quad (2.2)$$

where

E_{can} is evaporation from canopy vegetation [LT^{-1}]

E_p is potential evapotranspiration rate [LT^{-1}]

Δt is the time step length for the simulation [T]

In addition to evaporation from canopy storage, transpiration from vegetation is important for determining a water balance. This depends on the density of the crop material above and below ground. Thus, the actual transpiration is given as:

$$E_{at} = f_1(LAI) * f_2(\theta) * RDF * E_p \quad (2.3)$$

where

E_{at} is actual transpiration [LT-1]

f_1 is a function based on leaf area index [-]

f_2 is a function based on soil moisture content of root zone [-]

RDF is a root distribution function [-]

The f_1(LAI) function is given by:

$$f_1(LAI) = C_2 + C_1 * LAI \quad (2.4)$$

where C_1 and C_2 are empirical parameters [-].

The $f_2(\theta)$ function is given by:

$$f_a(\theta) = 1 - \left(\frac{\theta_{FC} - \theta}{\theta_{FC} - \theta_W}\right)^{\frac{C_3}{Ep}} \quad (2.5)$$

where

θ_{FC} is the volumetric moisture content at field capacity [$L^3 L^{-3}$]

θ_W is the volumetric water content at the wilting point [$L^3 L^{-3}$]

θ is the actual volumetric water content at the time step [$L^3 L^{-3}$] and

C_3 is an empirical parameter [LT^{-1}]; higher values of C_3 will lead to higher values of transpiration, which means the soil will dry out faster. The default value for MIKE SHE is 20 mm day^{-1}.

The root distribution function, RDF, is a time varying distribution of root depth for a given vegetation type. Root extraction of water from the soil is assumed to vary exponentially by:

$$RDF_i = \frac{\int_{z1}^{z2} R(z)dz}{\int_0^{L_R} R(z)dz} \quad (2.6)$$

where

i is the specific layer of soil profile being calculated

Z_1 and Z_2 are boundary conditions [L] with L_R being the maximum root depth

R(z) is a function of depth and assumed to vary logarithmically by depth as:

$$\log R(z) = \log R_0 - AROOT * z \quad (2.7)$$

where

R_0 is root extraction at the soil surface

AROOT is a parameter that describes root mass distribution [L^{-1}]; the MIKE SHE default, and typical value is 0.25 m^{-1}

Z is depth below ground surface [L]

The last component needed for calculating canopy interception and evapotranspiration is the evaporation occurring in the top layer of the soil profile. Soil evaporation, E_s, is given by:

$$E_s = E_p * f_3(\theta) + \left(E_p - E_{at} - E_p * f_3(\theta) * f_4(\theta) * (1 - f_1(LAI)\right) \quad (2.8)$$

where

E_s is the calculated soil evaporation

E_p is the calculated potential evapotranspiration

E_{at} is the actual transpiration from eq. 1.3

f_1(LAI) is the leaf area index function from eq. 1.3.a

$f_3(\theta)$ and $f_4(\theta)$ are empirical functions based on soil moisture and are given by:

$$f_3(\theta) = \begin{cases} C_2 & for\ \theta \geq \theta_w \\ C_2 \frac{\theta}{\theta_w} & for\ \theta_r \leq \theta \leq \theta_w \\ 0 & for\ \theta \leq \theta_r \end{cases} \quad (2.9)$$

$$f_4(\theta) = \begin{cases} \frac{\theta - \frac{\theta_W + \theta_{FC}}{2}}{\theta_{FC} - \frac{\theta_W + \theta_{FC}}{2}} & for\ \theta \geq \frac{\theta_W + \theta_{FC}}{2} \\ 0 & for\ \theta \geq \frac{\theta_W + \theta_{FC}}{2} \end{cases} \quad (2.10)$$

where

C_2 is an empirical parameter with a default MIKE SHE value on 0.2 [-],

This parameter (C_2) influences the distribution between soil evaporation and transpiration. Higher values of C_2 allocate a larger percentage of the actual ET to soil evaporation. In the absence of vegetation (bare ground) the f_1(LAI) function would equal zero and the evaporation from the soil occurs only in the upper node of the soil profile, which should be the top 10 centimeters or less.

2.4.2.b Overland and Channel Flow Components

There are two methods to determine overland flow in MIKE SHE; the first follows the physically-based diffusive wave approximation of the Saint Venant equations and the second is a simplified version of overland flow routing which is a semi-distributed approach based on the Manning's equation. The former of these two was used in this investigation to model overland flow. Overland flow depends on a variety of factors including topography (slope), soil properties, detention storage, evaporation, and infiltration.

i. Diffusive Wave Approximation of the Saint Venant Equations

The approximations of the fully dynamic Saint Venant equations neglect the momentum losses due to local and convective acceleration and lateral inflows perpendicular to the flow of the direction. Therefore momentum equations in two dimensions are:

$$S_{fx} = S_{O_x} - \left(\frac{\partial h}{\partial x}\right) - \left(\frac{u}{g}\frac{\partial u}{\partial x}\right) - \left(\frac{1}{g}\frac{\partial u}{\partial t}\right) - \left(\frac{qu}{gh}\right) \quad (2.11)$$

$$S_{fy} = S_{O_y} - \left(\frac{\partial h}{\partial y}\right) - \left(\frac{v}{g}\frac{\partial v}{\partial y}\right) - \left(\frac{1}{g}\frac{\partial v}{\partial t}\right) - \left(\frac{qv}{gh}\right) \quad (2.12)$$

In the x direction this reduces to:

$$S_{fx} = S_{O_x} - \left(\frac{\partial h}{\partial x}\right)$$

where

S_{fx} is the friction slope and [L L^{-1}]

S_{O_x} is the ground slope [L L^{-1}]

h is the flow depth above the ground surface [L]

x is the direction of flow [L]

simplifying slope, the original equation in the x direction reduces to:

$$S_{fx} = \frac{\partial z_g}{\partial x} - \left(\frac{\partial h}{\partial x}\right) \quad (2.13)$$

where

z_g is the ground surface level [L] the relationship $z = z_g + h$ further reduces to

$$S_{fx} = -\frac{\partial z}{\partial x} \quad (2.14)$$

and in the y direction:

$$S_{fy} = -\frac{\partial z}{\partial y}$$

The uses of these approximations allow the depth of flow to vary significantly between cells and can create backwater effects under the right conditions. In addition, if the Manning's equation is used to determine the friction slope further assumptions can be made that a constant surface roughness and velocity occur over the channel surface:

$$S_{fx} = \frac{u^2}{K_x^2 h^{4/3}} \tag{2.15}$$

$$S_{fy} = \frac{v^2}{K_y^2 h^{4/3}} \tag{2.16}$$

where

u and v are velocity components in the x and y direction, respectively [L T^{-1}]

K_x and K_y are Manning M or Strickler coefficients, respectively [-] it should be noted that the Strickler number and Manning M are inverses of the Manning's *n* roughness coefficient

Combining Manning's equation and the diffusive wave approximations of the Saint Venant equations yields:

$$uh = K_x \left(-\frac{\partial z}{\partial x}\right)^{1/2} h^{5/3} \tag{2.17}$$

$$vh = K_y \left(-\frac{\partial z}{\partial y}\right)^{1/2} h^{5/3} \tag{2.18}$$

where

uh and *vh* represent discharge per unit length [L^2T^{-1}] along the cell boundary in the x and y directions, respectively

Finally, flow between grid cells can be given by

$$Q = \frac{K\Delta x}{\Delta x^{1/2}} (Z_U - Z_D)^{1/2} h_u^{5/3}$$

where

Q is flow from one cell to another [L^3T^{-1}]

K is now the appropriate Strickler number

Z_U and Z_D are the maximum and minimum water levels, respectively [L]

h_u is the depth of water that can freely flow into the next cell [L]

If h_u is zero, no flow will occur. Water is added or removed from the cell, due to infiltration, evaporation, recharge, or precipitation at the beginning of every overland flow step. With the modified Gauss Seidel method, overland flows are reduced in some situations to avoid internal errors to the water balance and possible divergence from a solution. With these precautions in mind, flow split into inflow and outflow becomes:

$$\sum|Q_{out}| \leq \sum Q_{in} + I + \frac{\Delta x^2 h(t)}{\Delta t}$$

The above shows how the flow in one grid cell in one time step is calculated. In order to satisfy the equal sign, calculated outflows may be reduced for the aforementioned reasons. Also, in order to ensure inflows are summed first, grid cells are treated in order of descending ground level (topography) during the iterations in each time step.

2.4.2.c Unsaturated Zone Components

Unsaturated zone flow in MIKE SHE is one dimensional and assumed to be vertical throughout the soil profile. The model allows users to pick one of three methods:

- Richards equation
- simplified gravity flow
- two layer water balance

This investigation uses the Richards equation since it is precise and robust than the simplified gravity flow and more appropriate for the soil profile than the simple two layer water balance. The Richards equation is based on Darcy's law and the continuity equation. It assumes the soil matrix to be incompressible, of constant density, and the gradient of hydraulic head as the driving force. First the gradient is given by:

$$h = z + \psi \tag{2.19}$$

where

h is the hydraulic head [L]

z is the gravitational component [L] (positive assumed upwards)

ψ is the pressure component [L] (negative in unsaturated conditions)

For vertical flow, transporting water in the vertical gradient is the driving force thus:

$$\Delta h = \frac{\partial h}{\partial z} \tag{2.19}$$

The volumetric flux $\frac{\partial h}{\partial z}$, can also be obtained from Darcy's law:

$$q = -K(\theta)\frac{\partial h}{\partial z} \tag{2.20}$$

where

q is discharge per unit area [LT^{-1}]

K(θ) is the unsaturated hydraulic conductivity [LT^{-1}]

If the above assumptions hold for the soil profile (incompressible, constant density), the continuity equation will be:

$$\frac{\partial \theta}{\partial t} = -\frac{\partial q}{\partial z} - S(z) \tag{2.21}$$

where

θ is the volumetric soil moisture [-] or [L^3 L^{-3}]

S is a root extraction (sink) term [LT^{-1}]

It is now possible to combine the above three equations into the Richards equation:

$$\frac{\partial \theta}{\partial t} = \frac{\partial}{\partial z}\left(K(\theta)\frac{\partial K(\theta)}{\partial z}\right) + \frac{\partial K(\theta)}{\partial z} - S(z) \tag{2.22}$$

where the soil moisture content (θ) and pressure head (ψ) are dependent and related through the soil moisture retention curve. The Richards equation works well with homogeneous soil profiles, but when heterogeneity is introduced it is necessary to solve numerically using the finite difference implicit approximation method, similar to the Gauss-Seidel formula. Boundaries for this method are the ground surface (upper bound) and the water table (lower bound). The lower boundary is generally a pressure boundary. The model is set up for hydrostatic initial conditions (equilibrium, no flow).

In order to enable water table fluctuation between the saturated zone (SZ) and unsaturated zone (UZ) several steps must be taken. First, the saturated zone time step must be equal to the unsaturated zone time step or a whole number multiple of the unsaturated zone time step. Second, the uppermost level of the saturated zone must be slightly higher than the lower bound level of the unsaturated zone; coupling does not apply to lower levels of the saturated zone. Therefore during the simulation, if the water table is below the first layer of the saturated zone, the unsaturated zone treats the first layer as a free drainage boundary. In addition, the specific yield, S_y, must be properly set in order to decrease water balance errors between the unsaturated and saturated zones.

2.4.2.d Saturated Zone Components

MIKE SHE allows the user to pick one of two methods to calculate flow in the saturated zone module of the model. The first is a three dimensional finite difference method and the second is a linear method. In this investigation, the former was selected and will be discussed in this section.

(i) 3-D Finite Difference Method

Like the Richards equation for unsaturated flow, this method takes advantage of Darcy's law and continuity with a similar approach using finite difference techniques. Unlike the unsaturated zone, it is now calculated in three dimensions and can either use a preconditioned conjugate gradient (PCG) or the successive over-relaxation solution (SOR) technique. The preconditioned conjugate gradient was chosen for this investigation because of the difference in formulation of potential flow and the way source and sink terms are treated. In the PCG

method, sources and sinks interact with the saturated zone either implicitly or explicitly in the 3-D partial differential equation given as:

$$\frac{\partial}{\partial x}\left(K_{xx}\frac{\partial h}{\partial x}\right)+\frac{\partial}{\partial y}\left(K_{yy}\frac{\partial h}{\partial y}\right)+\frac{\partial}{\partial z}\left(K_{zz}\frac{\partial h}{\partial z}\right)-L=S\frac{\partial h}{\partial t} \quad (2.23)$$

where

x, y, z are unique axes in the Cartesian coordinate system [L]

K_{xx}, K_{yy}, K_{zz} are hydraulic conductivities along the x, y, and z axes [LT^{-1}]

h is the hydraulic head [L]

L is the sink/source term [T^{-1}] and

S is the specific storage coefficient [L^{-1}]

Two special features should be noted about the above equation. First the equation is non-linear when the flow is confined. Second, the storage coefficient switches between the specific storage coefficient when confined and the specific yield for unconfined conditions.

(ii) The Preconditioned Conjugate Solver (PCG)

The PCG is an alternative to the successive over relaxation (SOR) solver. The PCG keeps both an inner iteration loop (where dependent boundaries are constant), and an outer iteration loop (where head dependent terms are updated). The default user settings are set up for convergence, but if individual simulations encounter slow convergence or divergence then adjusting the solver settings is recommended. The PCG is also identical to the solver used in MODFLOW (McDonald and Harbaugh, 1988). The potential flow calculated is obtained using Darcy's law:

$$Q = \Delta hC \quad (2.24)$$

where

Δh is the piezometric head difference [-]

C is the conductance of the cell [L^2T^{-1}]

The horizontal conductance is calculated using the horizontal conductivity and the geometric mean of the layer thickness; this creates a harmonic mean. On the other hand, the vertical conductance is the weighted serial connection vertical hydraulic conductivity which is calculated from the middle of one layer to the middle of another. In dewatering situations, the saturated zone cells are calculated with a correction term added to the right side of the differential equation using the head of the last iteration:

$$q_c = C_{v_{k+½}}\left(h_{k+1} - Z_{\text{top,k+1}}\right) \tag{2.25}$$

where

C_v is the vertical conductance [L^2T^{-1}]

Z is the layer thickness [L]

k + 1 is the number of the node

The storage capacity for the cell is calculated by:

$$\frac{\Delta w}{\Delta t} = \frac{S2\left(h^n - z_{top}\right) + S1\left(z_{top} - h^{n-1}\right)}{\Delta t} \tag{2.26}$$

where

n is the time step

S1 is the storage capacity at the start of the iteration

S2 is the storage capacity at the last iteration

So for confined cell the storage capacity is given as:

$$S = \Delta x^2 \Delta z S_{art} \tag{2.27}$$

where

S_{art} is storage capacity of the confined cell

and in unconfined aquifers the storage capacity is given as:

$$S = \Delta x^2 s_{free} \quad (2.28)$$

where

S_{free} is the storage capacity of an unconfined cell

The limits and boundary conditions for the saturated zone are similar to the unsaturated zone. The hydraulic head is subject to Dirichlet's conditions, which specifies the value of the solution since the value of the hydraulic head is specified in the unsaturated layer. Nuemann's boundary conditions are based off of the gradient (derivative) of hydraulic head, and Fourier's boundary conditions are used when there is a head dependent flux.

2.5 Description of Study Areas

The watersheds modeled in this investigation are in northcentral Iowa, in Palo Alto County, approximately 13 miles northeast from Emmetsburg, IA and slightly closer to smaller towns as shown in figure 2. Stars in each watershed indicate the monitoring stations where flow was recorded location near the outlet. They are part of the Upper Des Moines River watershed by HUC-8 boundaries (MLRA 103).

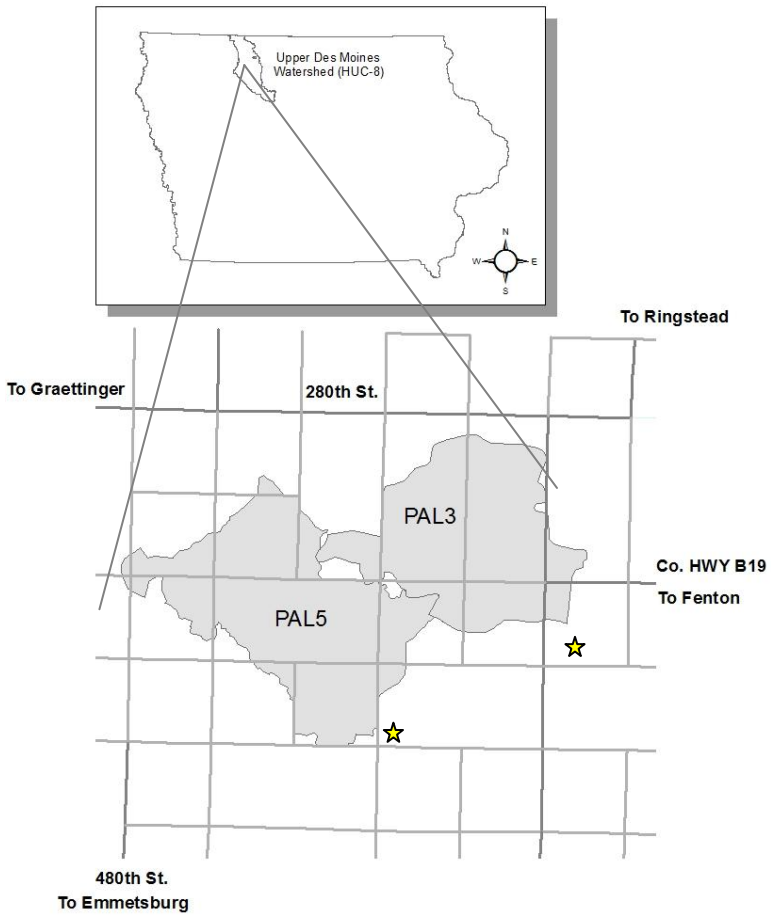

Figure 2 PAL 3 watershed in relation to surrounding towns and state.

The elevation of the watershed study areas vary from highs of 403.2 m and 400.8 in the PAL5 and PAL3, respectively, to lows of 390.2 m and 382.0 m at the outlets of PAL 5 and PAL 3, respectively. The average elevations for PAL5 and PAL3 are 398.2 m and 390.8 m, respectively. The average slope for both watersheds is very low at 0.5%. Predominant soils in the watersheds are Canisteo (fine-loamy, mixed, superactive, calcareous, mesic Typic Endoaquolls), Clarion (fine-loamy, mixed, superactive, mesic Typic Hapludolls), Webster (fine-loamy, mixed, superactive, mesic Typic Endoaquolls), and Nicollet (fine-loamy, mixed, superactive, mesic Aquic Hapludolls), as shown in Figure 3. Table 1 shows the percent area in relation to the total area for each soil, Canisteo has a plurality in both watersheds with 34.1% of the total area (384.4 ha) in PAL3 and 45.5% of the total area (616.9 ha) in PAL5. These soils tend to naturally be poorly to somewhat poorly drained with characteristic pothole formations and periods of standing water.

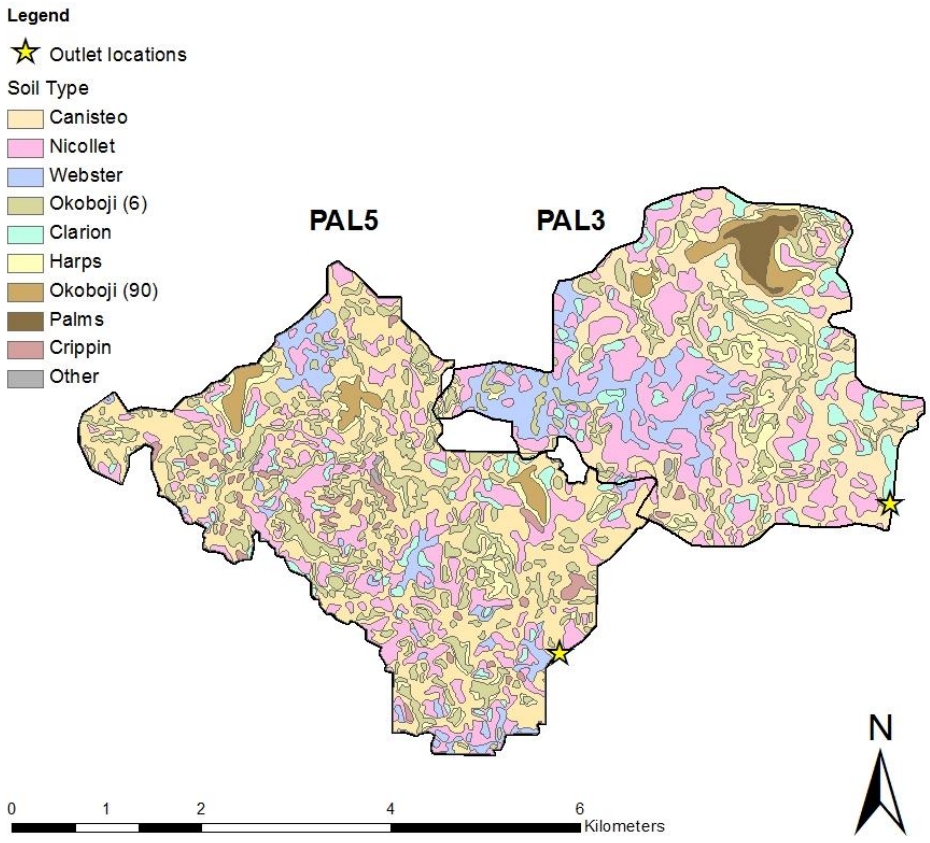

Figure 3 Soil types of the PAL3 and PAL5 watersheds

Table 1 Soil types, area, and percent total for PAL3 and PAL5 watersheds

Soil MUSYM	Soil Type	PAL 3 Area (ha)	PAL 3 Percent Total (%)	PAL5 Area (ha)	PAL 5 Percent Total (%)
507	Canisteo	384	34.1	617	45.5
55	Nicollet	297	26.4	290	21.4
107	Webster	123	10.9	70	5.2
6	Okoboji	95	8.4	203	15.0
138B and 138C2	Clarion	87	7.7	44	3.3
95	Harps	79	7.0	64	4.7
90	Okoboji	34	3.0	33	2.5
221	Palms	25	2.2	---	---
655	Crippin	3	0.25	32	2.4
---	Other	1	0.11	2	0.2
	Total	1128	100	1354	100

Information gathered through personal site inspections on several spring and fall dates, orthographic photography for all years spanning the study area, LANDSAT images, and Web Soil Survey maps have shown that the main land use of the watersheds is row crop agriculture, compiled in Table 2 and shown in Figure 4. The table shows the majority of this area, 73.7% and 62.7% for PAL3 and PAL5, respectively, are under a corn-soybean rotation. Land under continuous corn management in both watersheds tends to center around confined animal feeding operations, since an applicable fertilizer source is readily available. The bulk of land not utilized for row crop production is classified as types of perennial grassland with 5.3% and 5.1% of the total land use in PAL3 and PAL5, respectively. The rest of the land in the watersheds are residential area, road surfaces, and hog confinements.

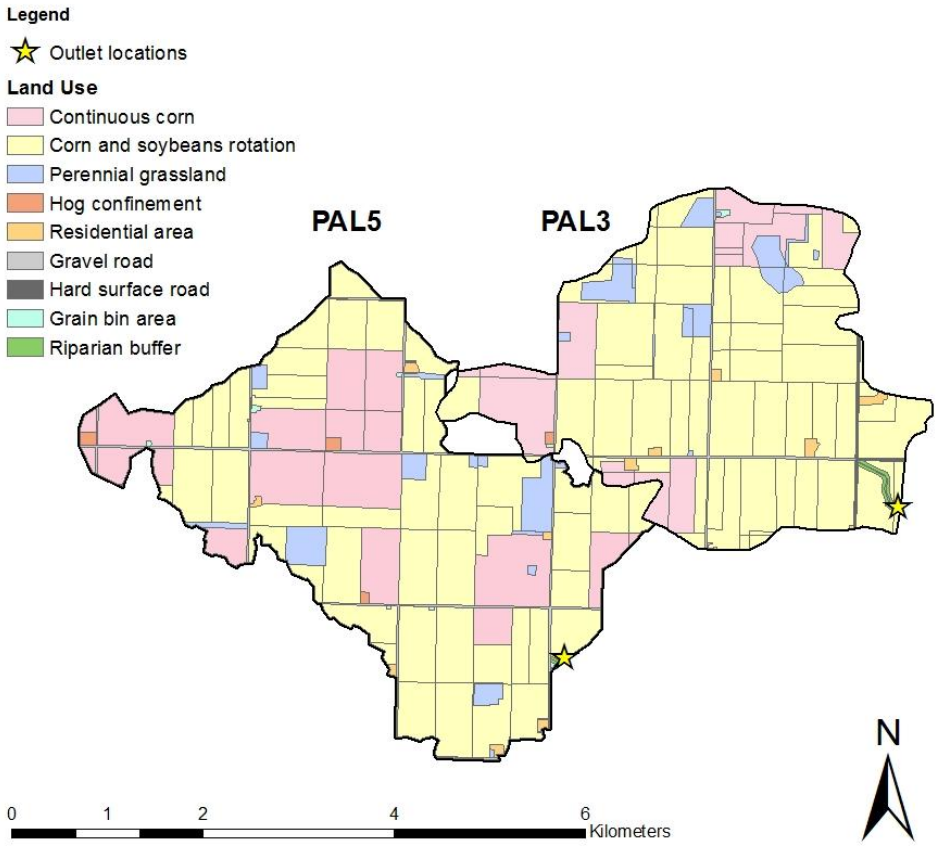

Figure 4 Land use in the PAL3 and PAL5 watersheds

Table 2 Land use in PAL3 watershed, corn and soybean rotation assumed to be a single land use system

Description of land cover	PAL3 Area (ha)	PAL3 Percent Total (%)	PAL5 Area (ha)	PAL5 Percent Total (%)
Agriculture:	1090	96.7	1305	97.1
-Continuous row crop (corn)	198	17.6	390	29.1
-Row crop rotation (corn/bean)	830	73.7	838	62.4
-Perennial grassland	59	5.3	69	5.1
-Hog confinement area (CAFO)	~2	0.1	6	0.4
-Grain bin areas	~1	0.1	2	0.1
Other:	38	3.3	38	2.9
-Residential area	10	0.9	7	0.5
-Hard surface road	7	0.6	---	---
-Gravel road	15	1.3	30	2.3
-Watershed outlet	6	0.5	~1	0.1
Total	1128	100	1343	100

2.6 Input Data

As a physically based model, MIKE SHE relies upon physical laws of nature and representative data from the site undergoing hydrological modeling. This section will outline the data types and sources used for all inputs involved in testing and validation of MIKE SHE in this application.

2.6.1 Meteorological Data

Climatic conditions in the watershed are similar to the Upper Midwest region and are characterized by wet springs, hot and dry summers, and cold winters comparable to other continental locations around similar latitudes, according to the Köppen climate classification system (Traintafyllou and Tsonis, 1994). The climate portion of the MIKE SHE investigation consisted of three main inputs: air temperature, reference evapotranspiration, and precipitation rate (as total rainfall and snow equivalent rainfall). Reference evapotranspiration (ET_{ref}) and precipitation rate were input as daily values and temperature as bi-daily to facilitate freeze-thaw cycles in winter months that may occur with daytime temperatures above freezing and nighttime temperatures below freezing. Since the time step for the model was sub-daily, the precipitation rate was amortized over the 24 hours according to the time step. Thus, if there was a two hour time step and 24 mm of rain that day, each timestep would simulate 2 mm. Rainfall data were collected from two National Climatic Data Center locations southwest and northeast of the study area. The SW station (Station No. 132724) was located in Emmetsburg, IA and the NE station (Station No. 138026) was located in Swea City, IA. Air temperature and ET_{ref} data were gathered from the Iowa Environmental Mesonet, IEM site in Kanawha, Iowa. ET_o was calculated using the FAO modified Penman-Montieth method. Daily minimum and maximum temperature, wind speed, relative humidity, and solar radiation were gathered for the computation of ET_o. The FAO Penman-Montieth equation is given as:

$$ET_o = \frac{0.408\Delta(R_n - G) + \gamma\frac{900}{T+273}u_2(e_s - e_a)}{\Delta + \gamma(1 + 0.34u_2)} \quad (2.29)$$

where all values are in SI units

ET_o is the reference evapotranspiration [LT^{-1}]

R_n is the net radiation at the crop surface [MT^{-3}]

G is the soil heat flux density [MT^{-3}]

T is the air temperature at a 2 m height [°C]

U_2 is the wind speed at a 2m height [LT^{-1}]

E_s is the saturation vapor pressure [$ML^{-1}T^{-2}$]

E_a is the actual vapor pressure [$ML^{-1}T^{-2}$] and (e_s-e_a) is the vapor pressure deficit

Δ is the slope vapor pressure curve [$ML^{-1}T^{-2}$ °C^{-1}] or force per degree Celsius

γ is a psychometric constant dependent on elevation [$ML^{-1}T^{-2}$ °C^{-1}]

At the beginning of the simulation, initial conditions from the first iteration of the first timestep were for January 1st, 2006.

2.6.2 Hydro-geological data: surface and subsurface geology

Input into the MIKE SHE model concerning the hydro-geological composition of the study are a crucial for determining overland flow, subsurface drainage, and deep seepage out of the watershed. The critical inputs to determine overland flow are topography and soil hydraulic parameters. One way to increase precision within the MIKE SHE model is to increase the resolution in the upper unsaturated zone by decreasing the cell height in the vertical discretization of the soil profile. The difference between equal cell height and increased resolution in the upper unsaturated zone is shown in Figure 5, and it can lead to Hortonian ponding at the ground surface, characterized by high rainfall intensity on dry, low permeable soil, with the increased resolution profile (DHI, 2004). The ponding occurs in the model at higher resolutions when the relationship between moisture content and soil profile depth can more accurately reproduce the nonlinear aspect of observed infiltration and ponding by allowing more points in the soil profile to be explicitly described, as opposed to a lower resolution approach, which may be more linear in nature as shown below. The rest of the soil profile parameters, drain location, and depth help determine the influence of subsurface drainage on each simulation as well. Deep seepage can be affected by confined aquifers,

karst topography (Janža, 2009), lenses (DHI, 2004) and multiple layers of permeable glacial till like in this study.

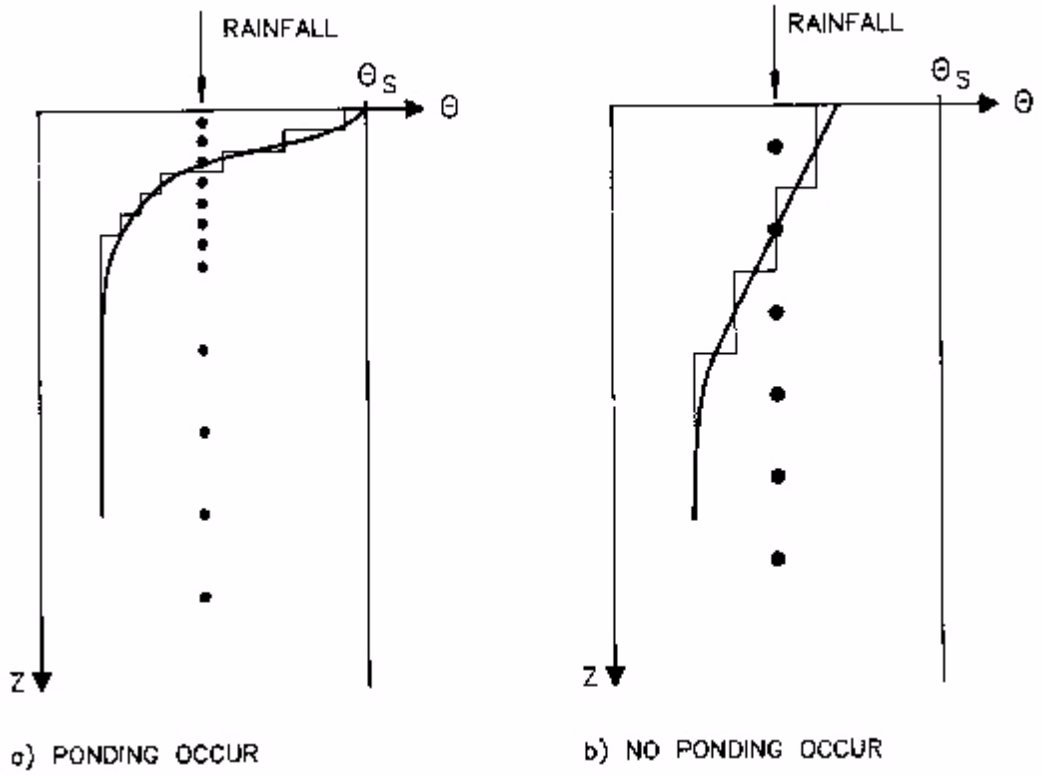

Figure 5 Example of two soil profile vertical discretization paradigms, one with increased upper profile resolution, and one with equal cell height.

2.6.2.1 Topography

The topography input data was obtained with the help of Dr. Gelder of Iowa State University. The digital elevation model (DEM) that was acquired used 3 m x 3 m resolution LiDAR data, which was converted into a point file suitable for MIKE SHE using ArcGIS 10.1. The elevations in the point file were bi-linearly interpolated into a 10 by 10 meter resolution inside MIKE SHE. Figures 6 and 7 show the topography as it appears in MIKE SHE for PAL3 and PAL5; the 10 x 10 m resolution still allows the pothole topography typical of region to be seen, as well as finer features like roads and ditches. Dr. Gelder, of Iowa State University, utilized a subroutine he created in ArcGIS 10.1 using the Python programming language that identified major underground drainage infrastructure such as aluminum cylindrical culverts bisecting residential driveways and concrete box culverts allowing

surface flow to flow between road ditches underneath the surface roads and driveways. This was done by locating the lowest point on either side of the driveway or road top and eliminating the surface in between, and creating a uniform slope allowing flow to continue unimpeded despite the original surface topography.

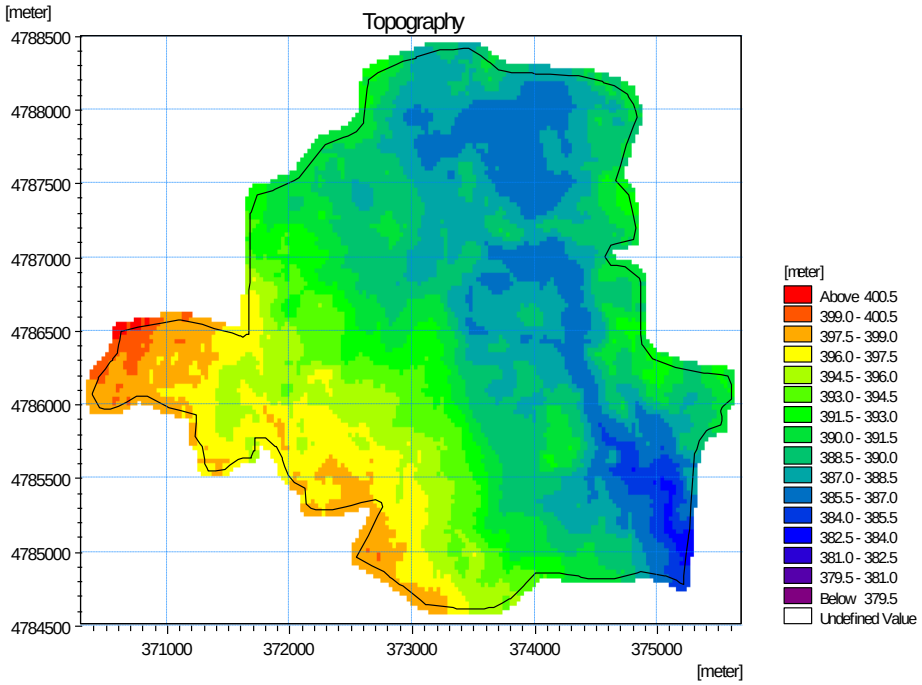

Figure 6 Topography map of PAL3 watershed as an input file in MIKE SHE

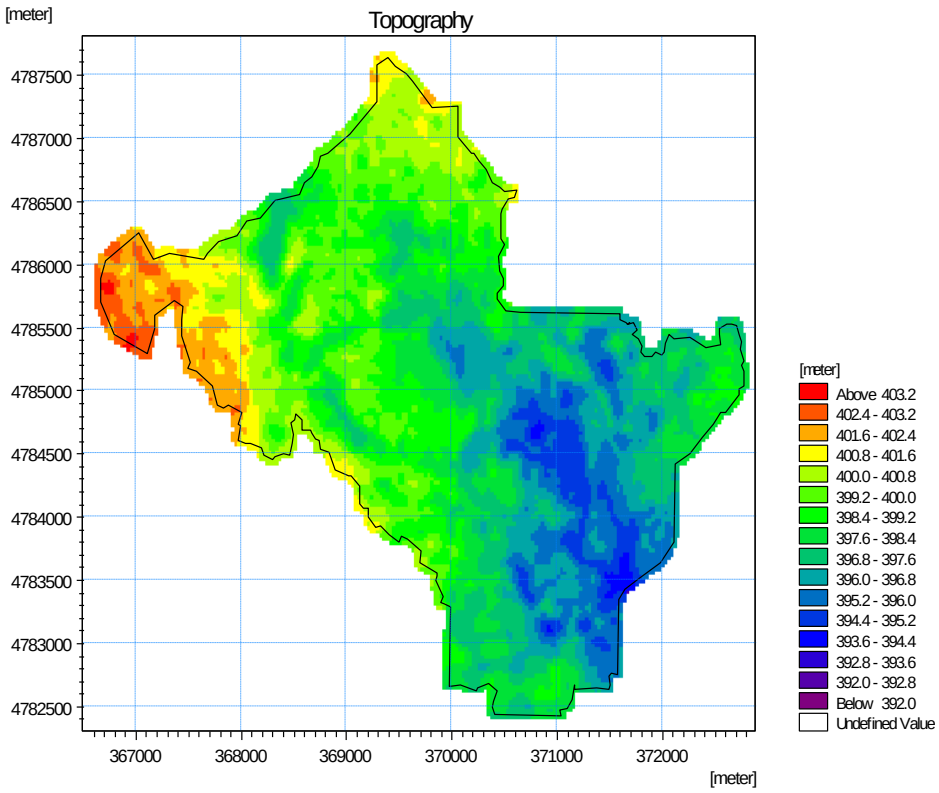

Figure 7 Topography map of PAL5 watershed as an input file in MIKE SHE

2.6.2.2 Soil composition and properties

The soil makeup of PAL3 and PAL5 are very similar and are typical soils of the region. Soil maps of the watershed were obtained using the Web Soil Survey tool available through the National Resources Conservation Service (NRCS). These maps were converted to polygon shapefiles in ArcGIS 10.1 and input into the MIKE SHE model. Each soil has a unique value set for hydro-geological properties which also differ throughout the vertical profile of the soil. Soil texture classes using percent sand, silt, and clay, in addition to bulk densities from the survey area were input in the neural network approach of the Rosetta model (Schaap et al., 2001) to obtain van Genuchten parameters which were then input into MIKE SHE soil property files. The Rosetta output parameters used are: saturated moisture content θ_{sat}, residual moisture content θ_r, pressure head at field capacity pF_{fc}, pressure head at wilting point pF_w, α, n, and l. The last three parameters are empirical constants, α [L^{-1}] and n [-] are curve shape factors while l [-] is a pore tortuosity/connectivity parameter. The van Genuchten formula for determining the unsaturated hydraulic conductivity is given by:

$$K(\psi) = K_s \frac{\left((1+|\alpha\psi|^n)-|\alpha\psi|^{n-l}\right)^2}{(1+|\alpha\psi|^n)^{m(l+2)}} \quad (2.30)$$

and the van Genuchten formula for the retention curve is:

$$\theta(\psi) = \theta_r + \frac{(\theta_s-\theta_r)}{[1+(\alpha\psi)^n]^m} \quad (2.31)$$

where

ψ is the pressure head of the soil matrix [L]

K(ψ) is the hydraulic conductivity function with respect to pressure head

θ(ψ) is the soil moisture function with respect to pressure head

Tables 3-6 show the empirical values for n, α, θ_r, θ_{sat}, have for 0 - 0.4 m, 0.4 - 0.6 m, 0.6 - 1.0 m, and 1.0 – 4 m, respectively. Some clear relationships are how bulk density and soil water holding capacity relate to soil profile depth. The bulk density increases with depth, which decreases effective pore space available for water thus decreasing the soil moisture at which saturation occurs. A less intuitive relationship can be made with the empirical constant α as soil profile depth increases. The constant, α, is related to the inverse of air entry suction of the soil. A coarse, consolidated material like large particles of sand will have the highest value for α (0.15 cm^{-1}), while an unconsolidated mixture of fine and medium sized particles like a silty clay will provide the most resistance to air entry into the soil (0.005 cm^{-1}). As soil depth increases, especially towards the glacial till that comprises the parent material of the Des Moines lobe, there is less silt and clay which increases the average pore size having an effect of lowering the air entry suction and increasing α. However, Palms muck has a profile in which α decreases with depth, most likely due to the layers of silt and clay that make up the bulk of the soil profile.

Table 3 Soil water retention curve characteristics (0 - 0.4m)

Soil name	Soil Symbol	Bulk density (kg m^{-3})	θ_{sat} (%)	θ_r (%)	α (cm^{-1})	n (---)	K_s (m s^{-1})	Model grid cell depth (m)
Canisteo	207	1300	46.0	8.3	0.010	1.48	1.9×10^{-6}	0.05
Nicollet	55	1200	47.0	7.7	0.010	1.52	3.5×10^{-6}	0.05
Webster	107	1380	44.4	8.3	0.008	1.52	1.3×10^{-6}	0.05
Okoboji	6	1350	48.1	9.4	0.010	1.45	1.3×10^{-6}	0.05
Clarion	138	1430	40.1	6.3	0.011	1.50	1.4×10^{-6}	0.05
Harps	95	1380	42.6	7.3	0.011	1.49	1.4×10^{-6}	0.05
Okoboji	90	1230	46.1	7.8	0.007	1.60	3.4×10^{-6}	0.05
Palms	221	500	73.5	11.8	0.013	1.46	6.2×10^{-5}	0.05

Table 4 Soil water retention curve characteristics (0.4 - 0.6m)

Soil name	Soil Symbol	Bulk density (kg m^{-3})	θ_{sat} (%)	θ_r (%)	α (cm^{-1})	n (---)	K_s (m s^{-1})	Model grid cell depth (m)
Canisteo	507	1390	42.8	7.6	0.010	1.49	1.3×10^{-6}	0.05
Nicollet	55	1260	46.1	7.9	0.010	1.50	2.5×10^{-6}	0.05
Webster	107	1440	42.2	7.8	0.011	1.46	9.3×10^{-7}	0.05
Okoboji	6	1350	48.1	9.4	0.010	1.45	1.3×10^{-6}	0.05
Clarion	138	1550	38.2	6.5	0.012	1.43	6.7×10^{-7}	0.05
Harps	95	1450	40.7	6.9	0.010	1.48	1.0×10^{-6}	0.05
Okoboji	90	1340	48.1	7.8	0.010	1.46	1.4×10^{-6}	0.05
Palms	221	500	73.5	11.8	0.013	1.46	6.2×10^{-5}	0.05

Table 5 Soil water retention curve characteristics (0.6 - 1.0m)

Soil name	Soil Symbol	Bulk density (kg m^{-3})	θ_{sat} (%)	θ_r (%)	α (cm^{-1})	n (---)	K_s (m s^{-1})	Model grid cell depth (m)
Canisteo	507	1430	41.3	7.2	0.010	1.50	1.1×10^{-6}	0.2
Nicollet	55	1300	45.6	8.1	0.010	1.49	2.0×10^{-6}	0.2
Webster	107	1440	42.2	7.8	0.011	1.46	9.3×10^{-7}	0.2
Okoboji	6	1360	47.9	9.4	0.010	1.44	1.2×10^{-6}	0.2
Clarion	138	1600	36.9	6.2	0.013	1.40	5.6×10^{-7}	0.2
Harps	95	1450	41.9	7.7	0.011	1.45	9.0×10^{-7}	0.2
Okoboji	90	1360	47.8	9.4	0.010	1.44	1.2×10^{-6}	0.2
Palms	221	1060	51.0	8.2	0.006	1.62	9.0×10^{-6}	0.2

Table 6 Soil water retention curve characteristics (1.0 - 4.0m)

Soil name	Soil Symbol	Bulk density ($kg\ m^{-3}$)	θ_{sat} (%)	Θ_r (%)	α (cm^{-1})	n (---)	K_s ($m\ s^{-1}$)	Model grid cell depth (m)
Canisteo	507	1600	35.2	5.0	0.014	1.42	9.7×10^{-8}	0.2
Nicollet	55	1450	41.2	7.2	0.011	1.46	9.5×10^{-8}	0.2
Webster	107	1540	38.8	6.8	0.012	1.43	6.4×10^{-8}	0.2
Okoboji	6	1390	46.9	9.3	0.010	1.45	1.0×10^{-7}	0.2
Clarion	138	1600	35.2	5.0	0.014	1.42	2.0×10^{-7}	0.2
Harps	95	1580	37.6	6.4	0.013	1.41	5.7×10^{-8}	0.2
Okoboji	90	1390	47.7	9.4	0.010	1.45	1.0×10^{-6}	0.2
Palms	221	1600	36.9	6.3	0.007	1.55	6.7×10^{-9}	0.2

Geologic properties of the soil profile will have a great impact on the interaction of water between the unsaturated and saturated zone. Soils that are considered "tighter," or more restrictive to flow contribute less water to subsurface activities than a less tight soil, such as Clarion, which tends to be moderately permeable and well drained. Properties affecting subsurface activities include saturated hydraulic conductivity of the saturated zone layers, specific yield, and specific storage. Values for these properties are shown in Table 7; note the factor of 1.5 between vertical and horizontal saturated hydraulic conductivities is due to natural anisotropy of soils (Zhou, 2011). Specific yield and specific storage were kept at default values in the MIKE SHE model since the aquifer was considered to be unconfined and established values for similar soil types fit the default values. This investigation used three layers to simulate deep seepage out of the watershed system. The first layer simulated the surface level to the depth of the natural water table, when the unsaturated zone became saturated; properties in this layer were used. The middle layer was composed of the layer simulating the depth below the surface that would comprise the seasonal fluctuations of the water table -3.8 to -8 m with respect to the surface. The last layer simulated groundwater activity down to a depth of -20 m, any water leaving this layer was considered outside the system and contributed to the subsurface flow out of the system in the water balance. (DHI, 2004).

Table 7 Hydraulic properties of saturated zone layers

Layer	Upper Level (m below surface)	Lower Level (m below surface)	Vertical K_s ($m\ s^{-1}$)	Horizontal K_s ($m\ s^{-1}$)
Upper	0	3.8	1.5×10^{-6}	1.0×10^{-6}
Middle	3.8	8	7.5×10^{-7}	5.0×10^{-7}
Lower	8	20	7.5×10^{-8}	5.0×10^{-8}

2.6.3 Vegetative Properties

Many processes in MIKE SHE depend on inputs directly related to the vegetative land cover of the watershed. ET depends on the crop growth cycle of the vegetation and the LAI, rooting depth, and crop coefficient at various stages of this cycle. Overland flow depends on canopy interception values, and more importantly the Manning's roughness coefficient of various vegetative cover. Infiltration can be influenced by soil moisture, which can be influenced by evapotranspiration in the root zone and rooting depth.

a. Crop Cycle

Each cropping cycle in the watershed has values typical for that plant species and geographical region. Corn, (*Zea mays*), soybeans (*Glycine max*), and perennial grasses (chiefly Big bluestem – *Andropogon gerardii*, Little bluestem - *Schizachyrium scoparium*, and Indian grass - *Sorghastrum nutans*) are the chief plant varieties and were simulated in MIKE SHE. The three prairie grasses were aggregated into a single vegetative state within the model as perennial grasses. The assumption that all three are typical to a stand of conservation reserve program (CRP) is based on the standard seed mix for the region, IA CP25 Mesic Prairie Mix, which bears all three species previously mentioned in addition to other forbs and grasses in smaller percentages. Values for crop and prairie grass parameters were taken from literature (Nippert et al., 2011a; Nippert et al., 2011b; Oogathoo, 2009; Al-Kaisi, 2000; Zhou, 2011). These parameters are summarized by day of growth (D.O.G.) in Table 8. Within MIKE SHE land use areas consisting of residential areas, confinements, and road surfaces were modeled as perennial grass for spatial resolution reasons.

Table 8 Crop cycle input parameters for corn, soybeans, and perennial grass mix: LAI, RD, K_c as they relate to D.O.G.

Crop stage of development	Corn (grain/silage)				Soybean			
	D.O.G[a]	LAI[b]	RD[c]	K_c[d]	D.O.G.[a]	LAI[b]	RD[c]	K_c[d]
Planting	121	0	0	0.3	135	0	0	0.3
Crop development	146	0.6	300	0.5	152	0.4	300	0.45
Mid-season	188	6	900	1.2	179	2.5	300	1.075
Late-season	238	5	900	1.2	237	5.5	900	1.075
Harvest	271	0	900	0.5	261	4.22	900	0.3

Crop stage of development	Prairie grass mix			
	D.O.G[a]	LAI[b]	RD[c]	K_c[d]
Beginning of year	0	1	300	0.1
New growth	120	2.4	600	0.8
Early season	150	4	700	1.0
Mid season	180	4.5	700	1.0
Late season	270	5.5	700	1.0
End of year	365	1	300	0.1

Terms and references
a. D.O.G. - day of growth (Julian)
b. LAI - leaf area index (m^2 m^{-2})
c. RD - rooting depth (mm)
d. K_c - crop coefficient (---)
a. (Zhou, 2011)
b. (Oogathoo, 2009; Zhou, 2009; Nippert 2011b)
c. (Jong and MacDonald, 2001)
d. (Zhou, 2009; Doorenbos and Pruit, 1977, Nippert 2011a)

b. Manning's coefficient of roughness

The MIKE SHE input parameter associated with surface roughness is the inverse of the Manning's roughness coefficient, Manning's M, both are shown in Table 9. The MIKE SHE model interpolates the input values when distributed points are used, therefore cells in Figures 8 and 9 near the boundary of perennial grass and crop ground may have values in between perennial grass and crops that are not specifically specified in Table 9.

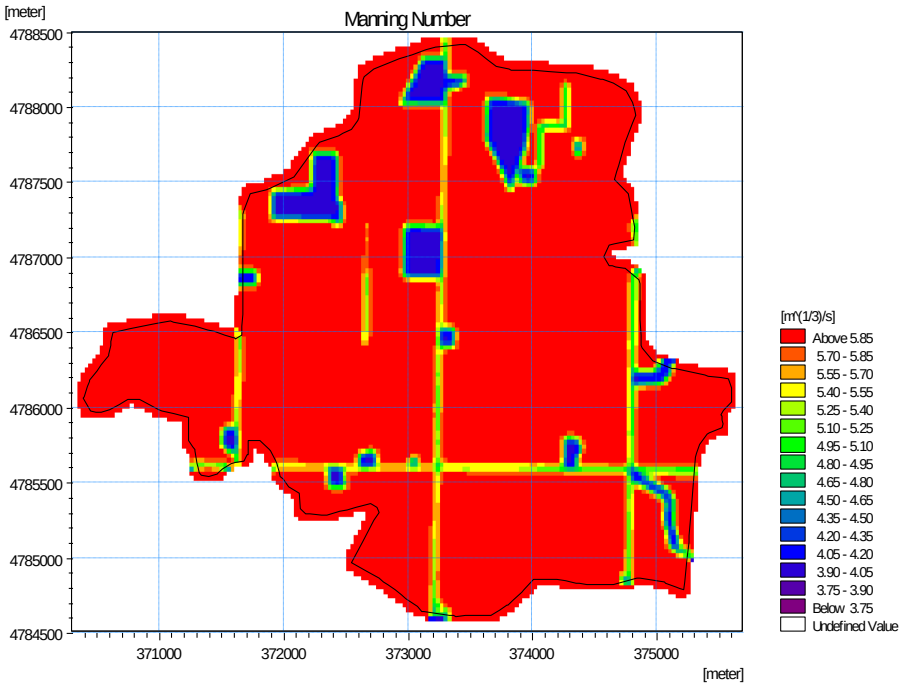

Figure 8 Manning M for PAL3 watershed

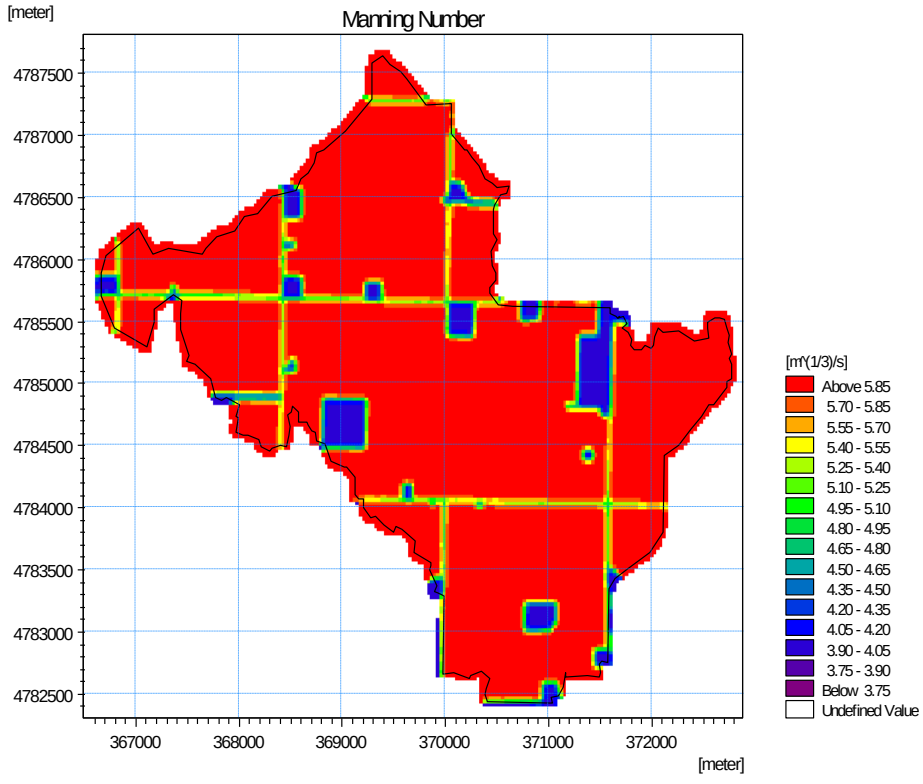

Figure 9 Manning M for PAL5 watershed

Table 9 Manning's roughness coefficient and Manning's M for land use in the PAL 3 and PAL5 watersheds

Vegetation in PAL3 and PAL5	Manning's n	Manning's M
Continuous corn[a]	0.17	6
Corn-soybean rotation[a]	0.17	6
Perennial grassland[b]	0.25	4

Source: a - Ward and Trimble (2004), b - Zhou (2011)

The surface roughness also can affect detention storage within common land units in the model. A detention storage value of 25.4 mm (1 in) was input in the overland flow parameter set based off of common land management practices in the region, as well as literature (Dai et al, 2009). Detention storage will be investigated further as a sensitive parameter during initial model testing.

2.7 Initial model set up

Many of the above listed parameter sets have initial values that be assumed on the first iteration of the first time step of the simulation. A static equilibrium is assumed for the first timestep and adjusts to hydrologic conditions as they change. This assumption does not affect model performance since the first year of simulation (2006) is used as a warm up period and the subsequent years are used for model testing and validation in both the PAL3 and PAL5 watersheds.

2.8 Model simulation time step

The time steps used in the model for efficient simulation are: initial unsaturated zone time step (hr); maximum unsaturated zone time step (1 hrs); maximum saturated zone time step (4 hrs); minimum overland flow time step (1 hr); maximum overland flow time step (1 hr). Precipitation and evapotranspiration were input as daily values, but then redistributed over the time steps above during the iterative calculation process. If the time step is too large, this will oversimplify the model and can lead to an imprecise description of the hydrology of the watersheds. If the timestep is too short, the computational and temporal resources required will surpass an allowable limit. This limit was fine tuned to the above time steps during preliminary model testing. The proper time step settings are crucial for minimizing water

balance errors that appear in simulations which should account for less than 1% of the total error in order to ensure a precise relationship between observed and modeled flow.

2.9 Statistical Methods to Determine Model Performance

Hydrologic performance evaluation has been guided by the efforts of Moriasi et al. (2007) to establish certain statistical tests and performance ratings to determine the fit of a model to the observed watershed. These tests are the Nash-Sutcliffe efficiency (NSE), percent bias (PBIAS), a visual regression analysis plot showing R^2 values and slope and intercept values for observed and modeled flow data points. A model can be judged as satisfactory if the value for NSE > 0.50, the PBIAS is ± 25% and R^2 > 0.50 for daily values of streamflow (Moriasi et al., 2009).

The Nash-Sutcliffe efficiency measures the goodness-of-fit between observed and modeled streamflow. Possible values range from -∞ to 1, with 1 representing a perfect model and values of 0 indicates a modeled prediction is less accurate to using the mean of the observed data. Negative values indicate the model prediction is worse than applying the mean of observed values to predict future values. The NSE equation is given by:

$$NSE = 1 - \left[\frac{\sum_{i=1}^{n}\left(Y_i^{obs} - Y_i^{sim}\right)^2}{\sum_{i=1}^{n}\left(Y_i^{obs} - Y^{mean}\right)^2}\right] \quad (2.32)$$

where

Y_i^{obs} is the observed streamflow value of the i^{th} time step

Y_i^{sim} is the simulated streamflow values of the i^{th} time step

Y^{mean} is the mean of all observed streamflow values

The NSE was chosen as an indicator of model fit as it objectively reflected the overall fit of the hydrograph the best (Sevat and Dezetter, 1991; Moriasi et al., 2007).

The PBIAS, or percent bias, measures the average tendency of simulated data to be larger or smaller than their observed counterparts (Gupta et al., 1999). The optimal value of PBIAS is

0.0 indicating perfect fit. Positive values indicate model underestimation bias and negative values indicate model overestimation bias. The equation for PBIAS is given by:

$$PBIAS = \left[\frac{\sum_{i=1}^{n}\left(Y_i^{obs} - Y_i^{sim}\right)*100}{\sum_{i=1}^{n}\left(Y_i^{obs}\right)}\right] \quad (2.33)$$

where variables are similar in nature to the NSE equation.

The coefficient of determination (R^2) value is also useful in describing the degree of fit of modeled to observed data. This measure is widely used because a visual representation of a plot of modeled and observed data points is easy to interpret, and R^2 values can point to the magnitude of error variance within the data set. The correlation coefficient ranges from -1 to 1 and is an index of degree of linear relationship between observed and simulated data (Moriasi et al, 2007). If r = 0, no linear relationship exists. Likewise, if r = 1 a perfect positive relationship exists, and r = 1 indicates a perfect negative relationship, or an inverse relationship between modeled and observed data. R^2 values range from 0 to 1, with higher values indicating less error (Van Liew et al., 2003). Values exceeding 0.50 are indicators of acceptable fit of modeled flow to observed streamflow (Moriasi et al., 2007). Although the coefficient of determination and Nash-Sutcliffe efficiency are congruent equations, graphs depicting points with coordinates of modeled values (Y axis) and observed values (X axis) and the respective position from an ideal line with a slope of 1. The statistical analyses used in subsequent chapters use daily flow values for NSE and PBIAS calculations, and weekly flow values for R^2 calculations and graphs depicting R^2 values.

CHAPTER III – MODEL TESTING AND VALIDATION

The MIKE SHE model was run under various land management scenarios to investigate the effect that land use has on the hydrological integrity of the watershed. Total surface and subsurface flow were compared to observed flow data to provide evidence for significant deviations from observed flow

3.1 Pre-Calibration Model Simulation

The model was initially run on a six year time period. For both watersheds, the first year of the simulation (2006) was used as a warm up period to assimilate natural values into the parameters concerning saturated zone and lower level hydrology where default values were utilized. This ensures that the initial values at the start of the testing period are more representative of the conditions in the watershed at that time.

3.2 Model Testing Validation and Performance

The MIKE SHE model investigated five years of hydrological measurements in the PAL3 watershed (2007 to 2011). PAL3 was chosen as the testing watershed according to multi site watershed model comparisons set out by Vázquez et al., (2002). PAL5 served as the validation watershed with the same time period (2007 to 2011). With sufficient data, physical models do not need to be calibrated, but the calibration and validation process in a multi site comparison helps to validate internal parameters such as local soil properties and vegetation parameters (Vázquez et al., 2002). As stated above, an additional year was simulated in order for a natural equilibrium to be struck between default parameters difficult to measure values in the watershed.

3.2.1 Model Testing

The initial investigation into the PAL3 watershed illuminated several watershed parameters that were sensitive in relation to the hydrological outputs of the model. Usually it is necessary for each sensitive parameter to undergo a trial and error procedure while all other parameters and inputs were kept constant in order to determine the appropriate range of values to adequately represent the system (Ma et al., 2000). However, formal sensitivity analysis was not performed during this study, due to the high computational demand needed

by the distributed, rather than lumped nature of the simulation. The number of parameters being adjusted during testing should also be as small as possible in order to avoid over defining relationships (Refsgaard and Storm, 1995), yet the calibration parameters should still fully characterize all the important hydrological processes in MIKE SHE. The parameters subject to adjustment in this investigation are drainage time constant (DTC) and overland detention. Testing took place in the PAL3 watershed from 2007 through 2011; these years were representative of normal, wet, and dry conditions in the region. The first year of simulation used as initialization for parameters was excluded from the testing process.

3.2.1.a Drainage Time Constant

In the MIKE SHE model, the drainage time constant parameter characterizes the density of the drainage system and the permeability around the drains, which can be used to determine the velocity of subsurface drainage flow (DHI, 2004). Default values in MIKE SHE range between 10^{-6} and 10^{-7} s^{-1}; however site specific adjustments and calibration should be done with every new model site. Values from literature supporting the need for adjustment and calibration include 4.9×10^{-4} s^{-1} (5.6 hours to drain) for a plot scale watershed, (Zhou et al., 2011) and 2×10^{-8} s^{-1} for a watershed of similar size, 1000 ha, (Al-Khudhairy, 2009)Upon model initialization, it was deemed that the DTC for PAL3 and PAL5 would need to be tested to ensure a proper value was reached since the values depend highly on the size of the watershed and the default value in MIKE SHE is not representative of the size of PAL3 and PAL5. The following Figures 10-14 show the effects that changing the drainage time constant have on overall flow, and how the total simulated flow compares to observed flow. The differences are the least noticeable in years of average or below average rainfall; however, the distinct DTC values show a visible contrast in years of concentrated high flow, like in 2010 and 2011.

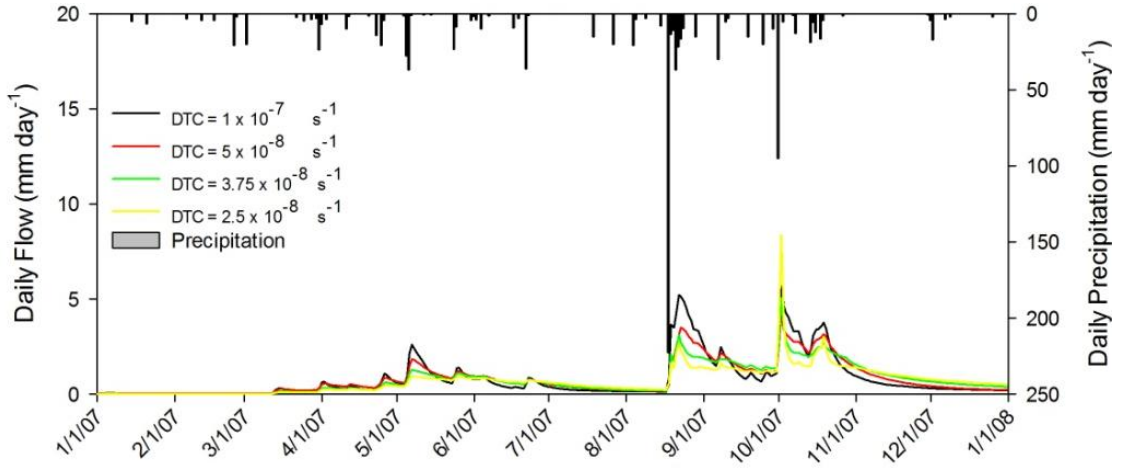

Figure 10 Drainage time constant comparison for PAL3 in 2007

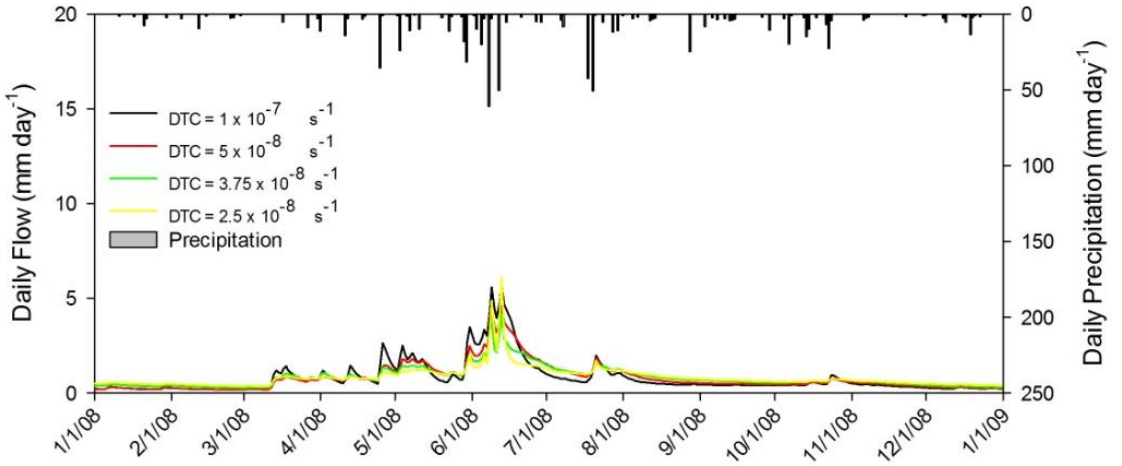

Figure 11 Drainage time constant comparison for PAL3 in 2008

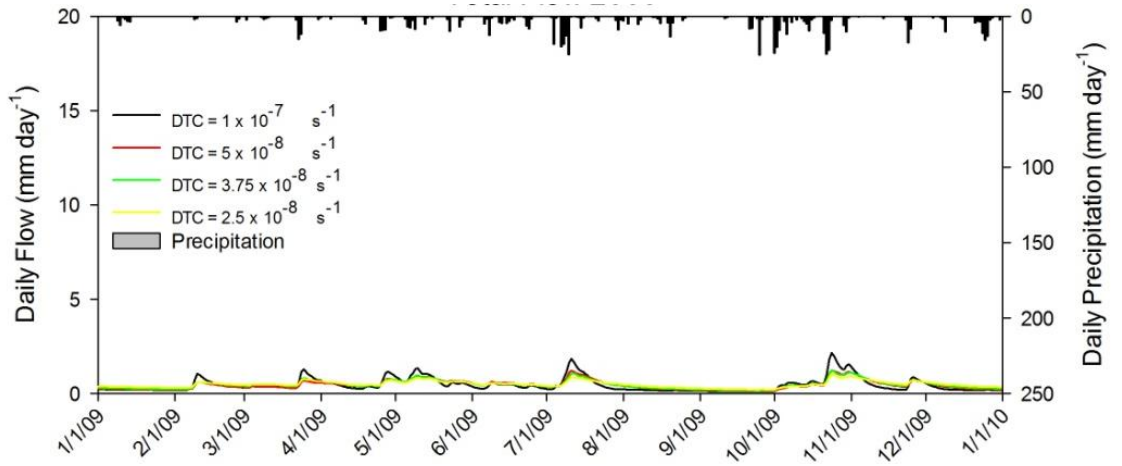

Figure 12 Drainage time constant comparison for PAL3 in 2009

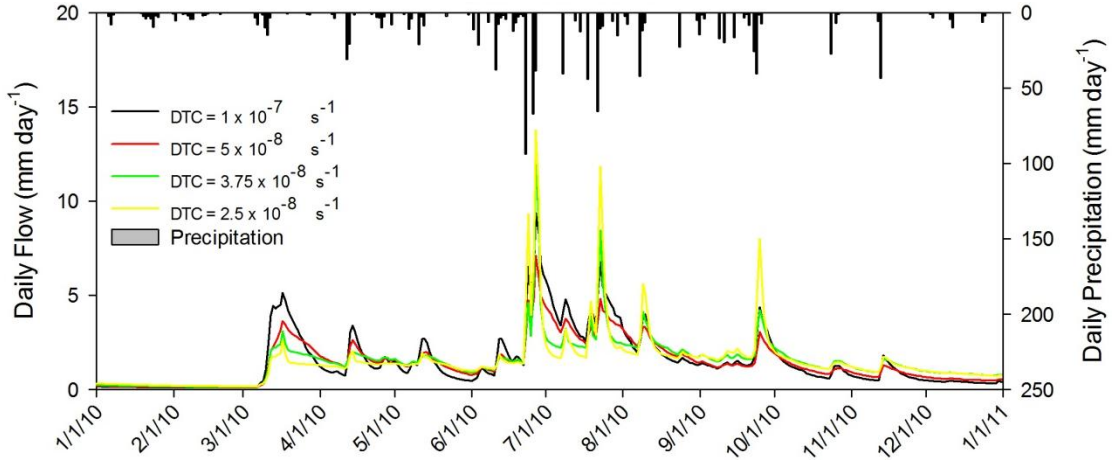

Figure 13 Drainage time constant comparison for PAL3 in 2010

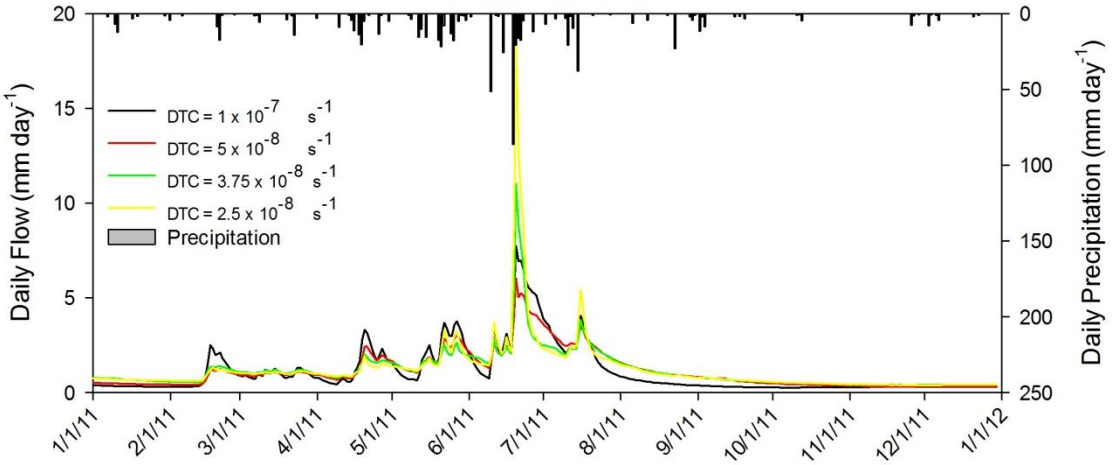

Figure 14 Drainage time constant comparison for PAL3 in 2011

In order to pick the most representative value it is also useful to compare water balances of each parameter value to show whether or not the ratio of surface to subsurface flow matches ratios seen elsewhere in literature across Iowa (Malone et al., 2008). Values for PAL3 are reported as the average over the simulation period from 2007-2011. Table 10 indicates that when surface to subsurface flow ratios are compared, the site investigated has the lowest value (0.022), but is also in the upper Des Moines lobe, an area very conducive to subsurface flow due to the extremely flat terrain and water holding capacity of pothole depressions typical of the area.

Table 10 Average surface and subsurface flow ratios for PAL3 drainage time constant values and similar areas in Iowa

Drainage time constant (s^{-1})	Surface flow (mm)	Subsurface flow (mm)	Total flow (mm)	Ratio $\left(\frac{surface}{subsurface}\right)$	Ratio in Des Moines	Ratio in Mason City	Ratio in Sioux City
1×10^{-7}	7.7	330	338	0.023	0.084	0.081	0.065
5×10^{-8}	7.3	280	287	0.026			
3.75×10^{-8}	28.6	315	343	0.083			
2.5×10^{-8}	64.9	281	346	0.231			

In order to determine which value for drainage time constant will be the most suitable to model the remainder of simulations for PAL3 and PAL5. A simple statistical analysis comparing modeled daily streamflow for each parameter value to observed daily streamflow using the Nash-Sutcliffe efficiency and PBIAS was done to determine the appropriate value. Table 11 shows each simulation, the daily and weekly NSE and PBIAS for each parameter value with respect to the observed flow for PAL3 over the duration of the simulation period. Although the PBIAS values are slightly better in other simulations, the most suitable value based on these studies for daily and weekly NSE values were calculated with the drainage time constant of 5×10^{-8} s^{-1}. NSE values for the DTC peaked at 0.59 and 0.61 for daily and weekly values, respectively. For this reason, the drainage time constant of 5×10^{-8} s^{-1} will be used for the remainder of the investigation.

Table 11 Daily and weekly statistical values for drainage time constant comparison in the PAL3 watershed

Drainage time constant (s^{-1})	Daily NSE	Daily PBIAS	Weekly NSE	Weekly PBIAS
1×10^{-7}	0.56	-1.21	0.60	-0.88
5×10^{-8}	0.62	0.39	0.66	2.13
3.75×10^{-8}	0.54	-1.31	0.62	-0.83
2.5×10^{-8}	0.29	-1.30	0.47	-0.84

3.2.1.b Detention Storage

The detention storage parameter was tested in a similar fashion in order to determine the magnitude of sensitivity for the parameter and to isolate the value that best represents the PAL3 and PAL5 watersheds. Figures 15-19 show the effect of total flow of surface and

subsurface water out of the PAL3 watershed over the duration of the simulation period (2007-2011).

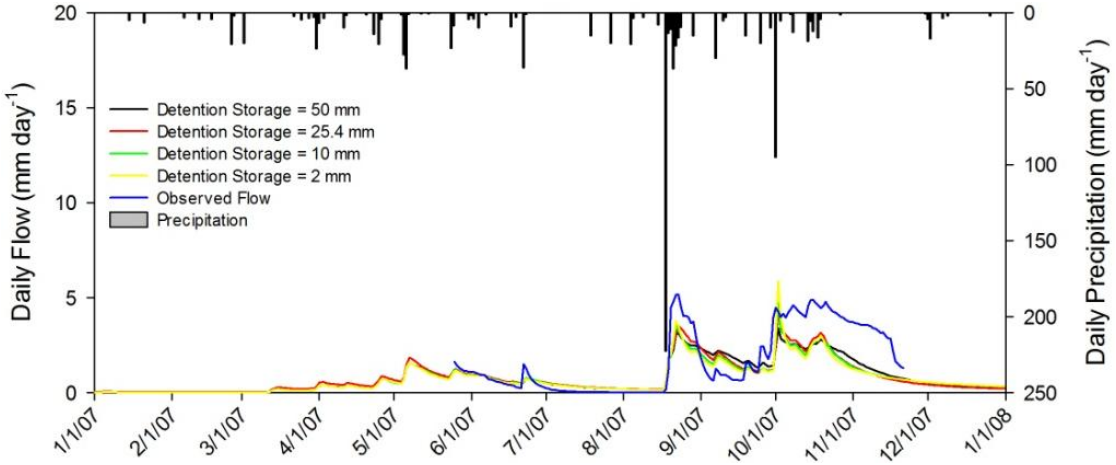

Figure 15 Detention storage comparison for PAL3 in 2007

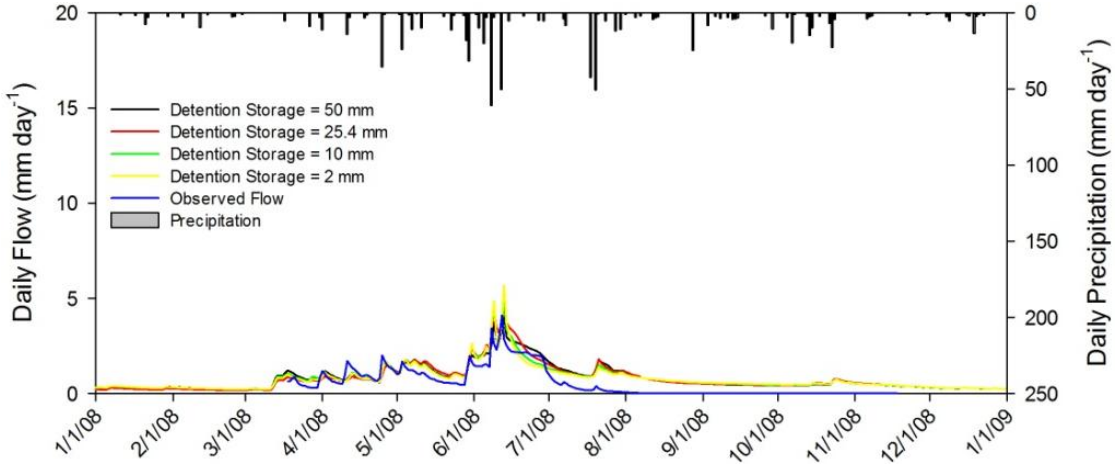

Figure 16 Detention storage comparison for PAL3 in 2008

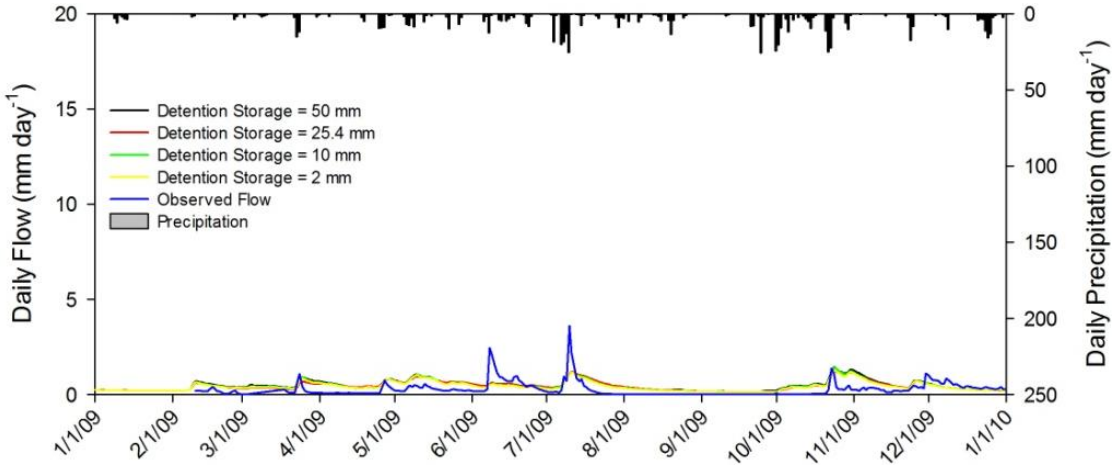

Figure 17 Detention storage comparison for PAL3 in 2009

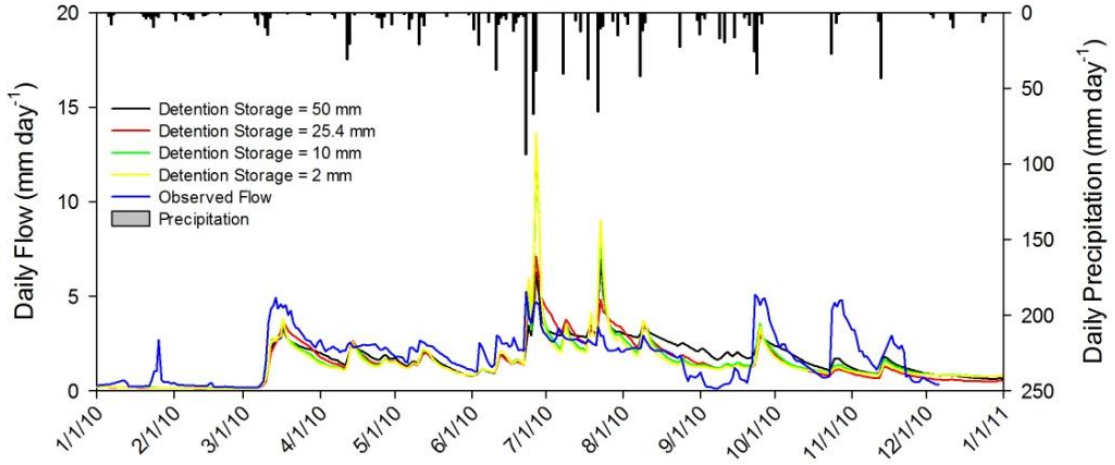

Figure 18 Detention storage comparison for PAL3 in 2010

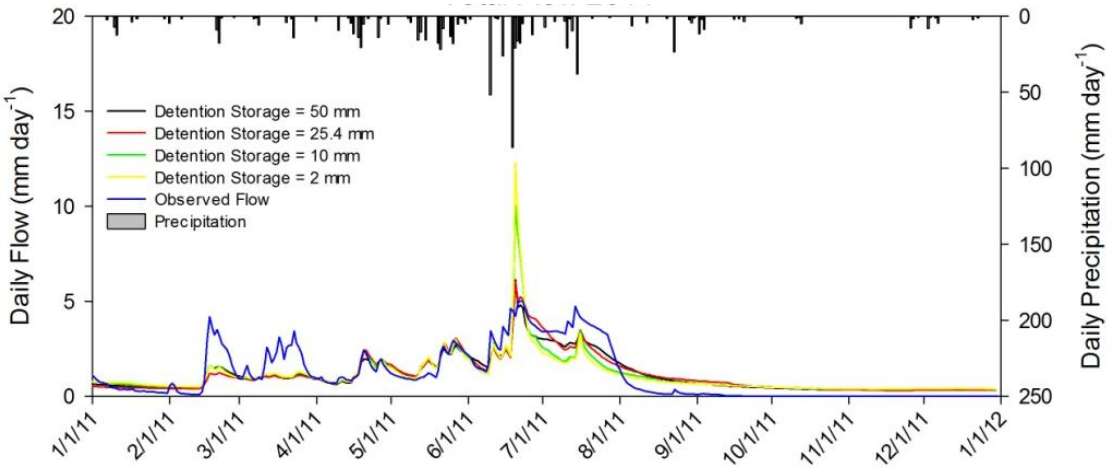

Figure 19 Detention storage comparison for PAL3 in 2011

The ratios of surface runoff to subsurface drainage were compared to regional values in a similar manner with the values of detention storage that were investigated. Table 12 shows this relationship for each parameter value. Although regional values for the ratio of surface to subsurface flow are more closely related to lower values of detention storage, such as 10mm or 2mm, the majority of land use in PAL3 and PAL5 consists of roughly tilled agricultural ground and pothole formations more conducive of detention storage with higher values.

Table 12 Surface and subsurface flow ratios for PAL3 detention storage values and similar areas in Iowa

Detention storage depth (mm)	Surface flow (mm)	Subsurface flow (mm)	Total flow (mm)	Ratio $\left(\frac{surface}{subsurface}\right)$	Ratio in Des Moines, IA	Ratio in Mason City, IA	Ratio in Sioux City, IA
50	6.0	336	342	0.014	0.084	0.081	0.065
25.4	7.3	327	334	0.022			
10	21.8	311	332	0.046			
2	25.9	199	325	0.086			

A statistical analysis was done with the detention storage parameter values to determine the most suitable value for the remainder of the investigation. Like drainage time constant, the analysis compared daily and weekly flow values for the detention storage values and calculated NSE and PBIAS values for daily and weekly flow. Table 13 shows that the 50 mm detention storage value performed slightly better than the 25.4 mm value, with a daily NSE value of 0.60 compared to 0.59. Although 50 mm is slightly more suitable, 25.4 mm will be used in all subsequent simulations for two reasons. First, 50 mm or about 2 in is less intuitive than 25.4 mm or about 1 in, a site inspection shows that although pockets of 50 mm storage are possible, the majority are greater than 10 mm and less than 50 mm. Also, an inspection of the above figures, particularly figure (2008) show that the flow from 25.4 mm tends to recover back to baseline flow more quickly than flow from 50 mm storage.

Table 13 Daily and weekly statistical values for detention storage comparison in the PAL3 watershed

Detention storage depth (mm)	Daily NSE	Daily PBIAS	Weekly NSE	Weekly PBIAS
50	0.63	-2.87	0.67	-0.36
25.4	0.62	0.39	0.66	2.13
10	0.56	1.51	0.63	0.62
2	0.51	3.96	0.60	0.25

3.2.2 Model Validation

The model was validated using the PAL5 watershed following multi site comparison guidelines. Using this method, testing values can be changed slightly to reflect the differences between testing and validation watershed, although PAL3 and PAL5 are very similar and the only appreciable difference was the absence of Palms soil from the PAL5 watershed. Like the testing period, the first year of the simulation was excluded from the validation and model performance evaluation.

3.3 Management Scenario Analysis

Several management scenarios were analyzed in order to quantify the effect that various practices have on streamflow at the watershed scale. Modeled streamflow from these scenarios were compared to testing and validation streamflow for current conditions in both watersheds.

3.3.1 Drainage Analysis

In order to quantify the effect that drainage has on the land, it is important to model the alternate drainage management practices, in addition to current drainage management practices. Much of the Des Moines lobe of Iowa is drained at a depth of about 1.2 m (4 ft). Throughout the entire state approximately 3.6 million ha of cropland are artificially drained; this amount accounts for more than 25% of the total agricultural land for the state (Baker et al., 2004). In the PAL3 and PAL5 watersheds, areas to be drained were determined by site inspection and soil type and thus were spatially varied within the MIKE SHE model. Site inspections showed a large kettle formation in the north central part of the PAL3 watershed that had consistent standing water and no visible surface intake drains. This shows that the area may not be drained, and therefore subsurface drainage was excluded from this area. Clarion soils were also assumed to not be drained in both watersheds. Although there is increasing prevalence of pattern draining entire fields, the Clarion soil type dominates upland areas and is moderately well drained soil (National Cooperative Soil Survey, 2011). For these reasons, Clarion was not drained.

The main drainage scenarios analyzed in this investigation were conventional drainage with a depth of 1.2 m (4 ft), shallow drainage depth with a drain level at 0.75 m (2.5 ft), and no

subsurface drainage. The general trend is for conventional drainage over a wide area that may include entire fields. This can lead to a buffer effect by increased storage for rainfall events which can reduce peak flow volumes (Skaggs and Broadhead, 1982). On the other hand, this may increase infiltration which in turn is a major transport pathway for soluble chemicals such as nitrate (Shipitalo et al., 2004).

3.3.2 Land Management Analysis

In addition to drainage analysis, land use and management was also analyzed in order to describe how changing land use may affect the hydrology of the watershed. The current land use consists of spatially distributed row crops and perennial grasses. The areas of perennial grassland are either perennial vegetation, unplanted portions of field, or homestead and ditch space. Other scenarios to be analyzed include all perennial grassland that has no drainage, which may simulate pre-settlement conditions, all perennial grassland with drainage, which could simulate a change from the current land use; and land management which is completely corn and soybean without drainage.

The simulation regarding pre-settlement conditions will help establish a baseline that will help show how the hydrology of the watershed has changed in the last 150 years. This may help make land management decisions similar to urban low impact developments (LID's) where the goal is to reduce flood peak flow to pre-urbanization periods (Bedan and Clausen, 2009).

The management scenario that excludes perennial grass and solely focuses on a corn and bean rotation may show what future land management would look like if the general trend to bring more area under agriculture to increase food production is to continue (Oogathoo, 2009). This scenario would, in practice, include hog confinements as a food source as well, but the scenario will consider confinement land to be cropped in order to model a hypothetical scenario. Although the percent land use of perennial grassland is minor compared to corn and soybeans, the effect of no grassland may be significant.

CHAPTER IV – TESTING AND VALIDATION RESULTS AND DISCUSSION

4.1 Model Testing

With the multi site approach, one watershed was used for testing, PAL3, the other watershed is to be used for validation, PAL5. The first year of simulation (2006) was used to initialize the output data for both time periods and was not included in statistical evaluations of model accuracy or otherwise. The one year model initialization period was important because initial conditions put forth may not reflect actual conditions at the time; conditions will stabilize over a one year period. These conditions stabilized by the initialization period include initial water table depth, water content in the unsaturated zone, and outputs that rely on past rainfall events like drainage and overland flow. In addition, parameter values for drainage time constant and detention storage were tested to determine the most acceptable values for the watersheds. The simulation used for final testing included the most appropriate values for drainage time constant (5×10^{-8} s^{-1}) and detention storage (25.4 mm).

4.1.1 Testing and Analysis of Hydrographs

The first year of the six year simulation period was considered model initialization or "warming up," and was excluded from statistical analysis. Annual precipitation over the simulation period was analyzed and determined to have an average of 858 mm of rainfall per year. Years outside of the range of mean ± one standard deviation (STDEV = 186 mm) were considered 'wet' if above this range, and 'dry' if below this range. This is slightly below the annual average for Iowa of 880 mm (NCDC) but higher than the annual average of North Central Iowa 750 mm (NCDC Station MIF14, Milford, IA). This is most likely due to the two 'wet' years of 2007 and 2011. The observed stream flow data that were not directly collected from the outlet of the PAL3 watershed were either estimated from the downstream USGS gaging station 05479000 East Fork Des Moines River at Dakota City, IA; or interpolated between observed flow data. The six year period of observed stream flow data had some gaps estimates include: (m/d/y), (8-23-06 to 5-25-07), (11-22-07 to 3-17-08), (11-19-08 to 2-09-09), (3-3-09 to 3-17-09); interpolated dates include: (9-15-08 to 10-5-08), (12-25-09), (1-7-10 to 1-11-10), (2-15-10), (10-12-10 to 10-18-10); missing points include (12-6-09 to 12-31-09).

Temperature and weather input related discrepancies

There seem to be a few anomalies in figures 20-24, both temperature and weather input related with the observed data. Most noticeably in late fall of 2007, instead of a gradual recession there is sustained flow on the trailing leg of the hydrograph starting around Nov. 1st and continuing until Dec. 1st. This could be from one of several scenarios: first, the flow is accurately reflecting conditions in the watershed and the model performs poorly in this period. Second, the drainage ditch is at capacity downstream and due to the flat nature of the channel bed, subcritical flow could be causing backwater effects at the monitoring station which would cause overprediction of streamflow. Finally, a period of sub zero temperatures starting around the beginning of November could freeze water near the monitoring station, which would cause overprediction and the observed sustained "flow" while the ice is present. Another event that stands out is the spike in observed flow in January, 2010. This could easily be attributed to a thawing event, which would release large quantities of stored water in the form of snow and ice. Thawing events were successfully modeled in 2007 and 2011. The magnitude of the thawing events, however, was under-predicted by the model. This may stem from refreezing of melt water which can in turn place an inordinate amount of pressure on the streamflow measuring pressure transducers as the ice expands, causing an over-estimate of observed flow during this time. This hypothesis is supported by temperature input data that indicates possible conditions for refreezing of melt water. Likewise, peak streamflow events in the modeled data that are not reflected in the observed data may be due to precipitation inputs that do not completely reflect with actual rainfall events. Some of these modeled peaks that are not matched with observed peaks are in late October 2008, and early October 2009.

Soil profile input discrepancies

The MIKE SHE soil profiles are assumed to be uniform throughout the simulation period, only varying with depth. However, real world operations such as tillage and cultivation can increase parameters such as hydraulic conductivity which would increase infiltration. Non-tillage field operations such as fertilization and harvest can increase compaction, which would have the reverse effects. Likewise, annual root development and burrowing activities

of earthworms and other organisms can create macropores which will result in preferential flow and decreased overland flow during peak events. Macropore flow can be simulated in MIKE SHE; however, it is applied to the entire simulation period, which makes it difficult to simulate seasonal variations in hydraulic conductivity (Zhou, 2011). Fall tillage operations could be responsible for the lack of flow in the late fall of 2008 and decreased flow in the late fall of 2009 by increasing the amount of macropore pathways and available detention storage of cropland areas.

The MIKE SHE model performed well, with respect to graphically matching modeled flow to observed flow, under varying times throughout the simulation period, as shown in Figures 20-24; most notably, May 1st through mid-August 2007, March 1st through mid-June 2010, and mid-August through late October 2010. The model also performed satisfactorily through 2011, despite the over predicted peak flow after the rainfall event on June 20th when 90 mm of rain fell. Differences in spatial and temporal values for vegetation and soil properties could explain why these periods were simulated better than other portions of the annual hydrograph. For example, corn and soybean plant dates were considered to be constant from year to year, when in practice these dates can vary by as much as several weeks from year to year, depending on weather and soil bed conditions. Modeled years with a more accurate representation of actual crop growth may also have a better representation of streamflow, since important factors like ET and LAI will better reflect actual conditions. Year to year differences in vegetation cover and soil properties could also explain why some seasonal periods were simulated better than corresponding seasonal periods in different years of the simulation. For example, a spring with delayed planting would lead to later germination of crops. Less dense crop cover would lead to a higher Manning's M (lower Manning's roughness coefficient *n*) which would increase overland flow, possibly allowing the model to under-predict surface flow for this period.

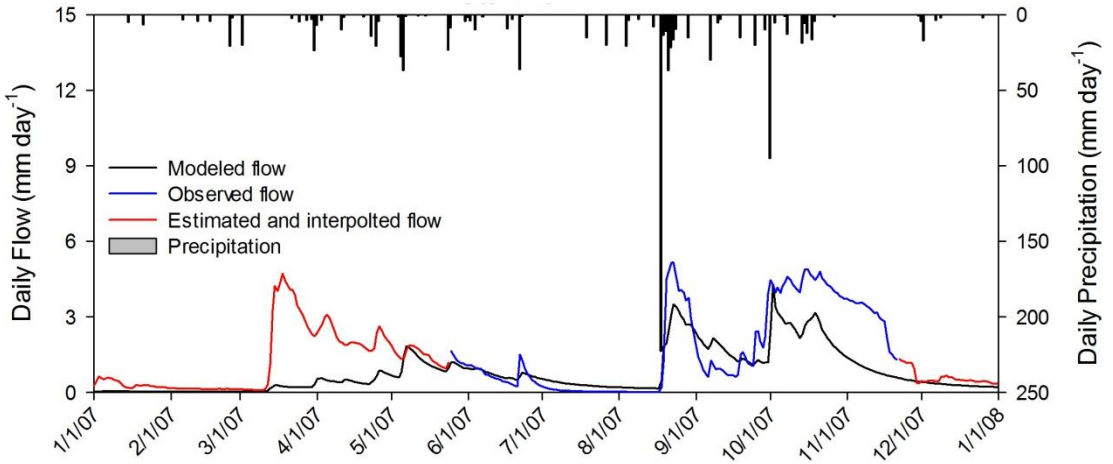

Figure 20 Testing hydrograph and hyetograph for PAL3, 2007

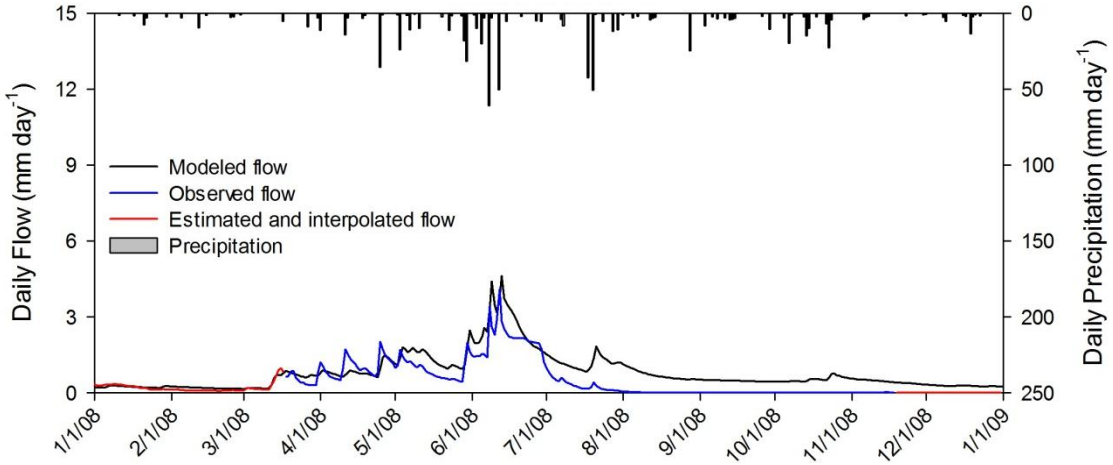

Figure 21 Testing hydrograph and hyetograph for PAL3, 2008

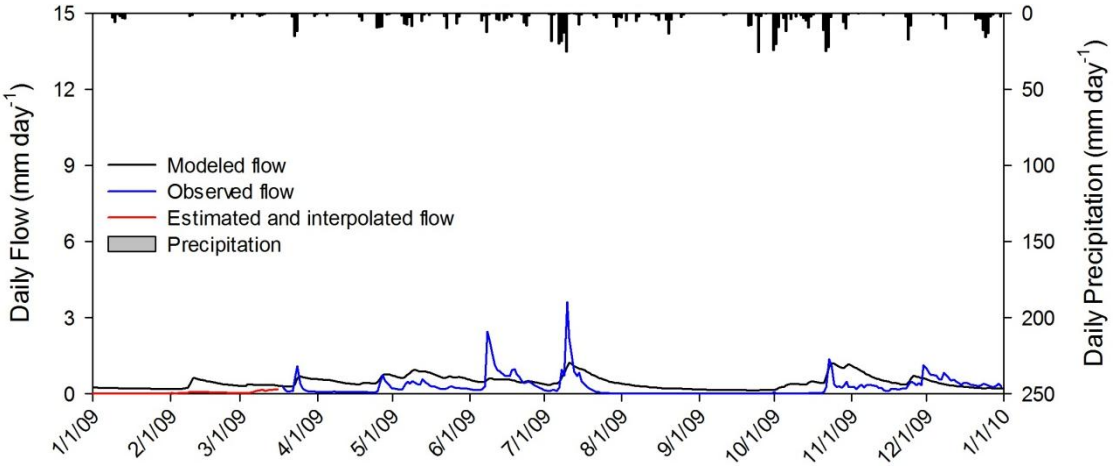

Figure 22 Testing hydrograph and hyetograph for PAL3, 2009

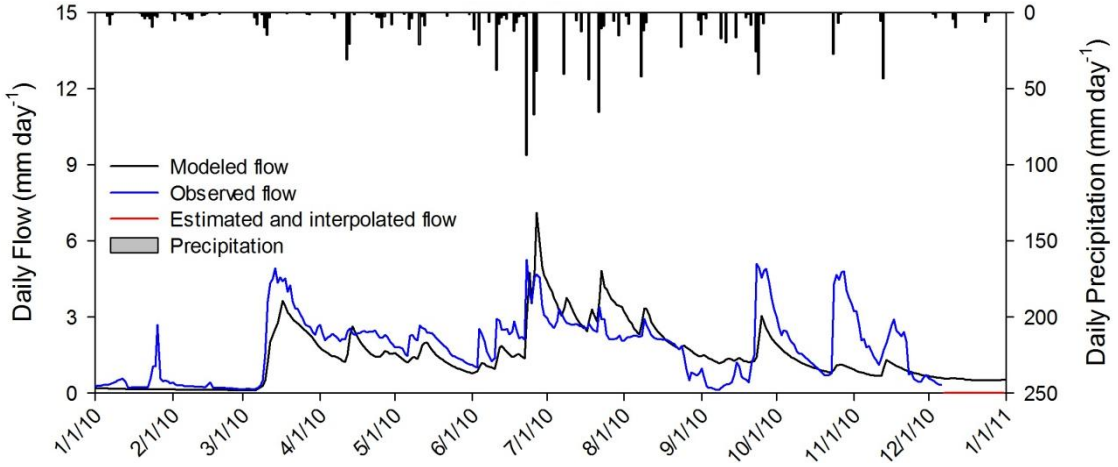

Figure 23 Testing hydrograph and hyetograph for PAL3, 2010

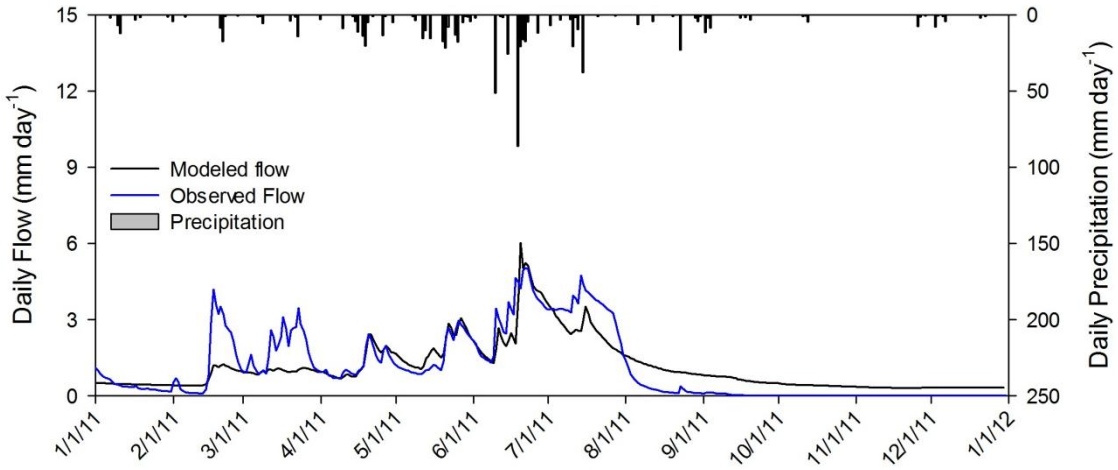

Figure 24 Testing hydrograph and hyetograph for PAL3, 2011

4.1.2 Statistical Analysis of Hydrographs

The average coefficient of determination was above 0.66 for the entirety of the simulation when weekly streamflow was used in the regression analysis. Table 14 shows regression parameters and R^2 values for each year of the simulation, while Figure 25 shows the regression analysis for weekly flow throughout the simulation period (2007-2011). The coefficient of determination only dropped below the acceptable 0.50 value in 2009, which may be attributed to an over-prediction of modeled streamflow. This is supported by a highly negative PBIAS value for 2009, another indicator of over-prediction. The average daily NSE value for the simulation period was 0.62; an indicator that the model matched observed streamflow quite well, overall. PBIAS values indicate a trend of under-prediction by the model, which is supported by the 148 mm difference between modeled and observed

streamflow over the simulation period. However, if the possibility that freezing events may have corrupted flow data for short periods of time in late fall of 2007 and 2010 and spring of 2010 and 2011 (and 2007, although not included in statistical analysis) would bring the PBIAS values closer to the ideal value of 0, and also increase the degree of fit in other statistical parameters over the course of the simulation.

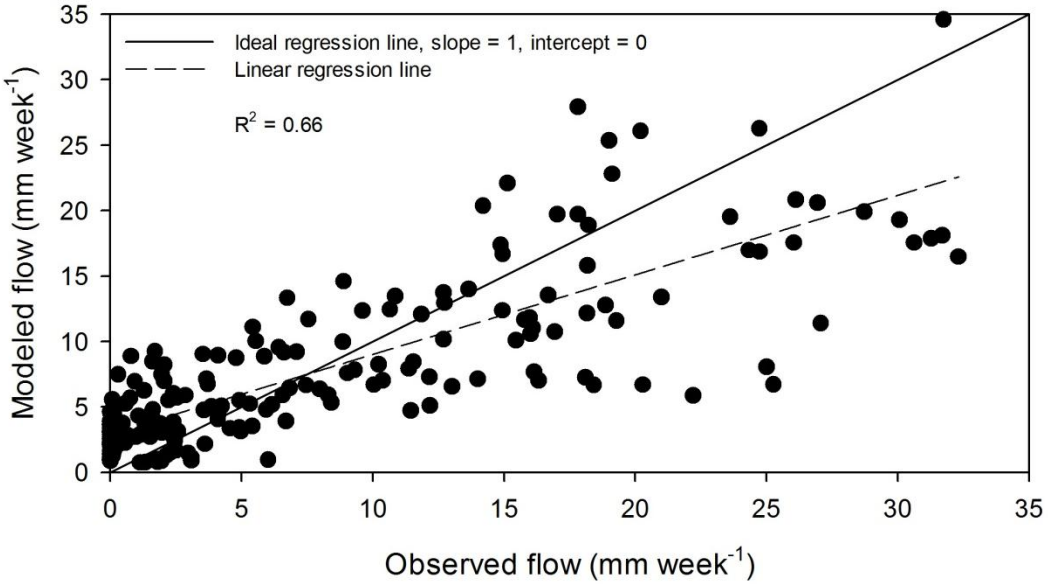

Figure 25 Scatter plot of observed vs. modeled weekly flow for testing period of PAL3

Table 14 Model performance during testing of PAL3 watershed with daily streamflow

Year	Observed streamflow (mm)	Simulated streamflow (mm)	PBIAS	EF (%)	R^2	Regression parameters	
						Intercept (mm)	Slope
2007	546	283	29.2	0.51	0.70	3.2*	0.45*
2008	167	286	-79.5	0.34	0.71	3.75*	0.82*
2009	91	160	-79.3	-0.11	0.13	2.74*	0.29*
2010	667	525	16.8	0.36	0.53	1.55*	0.71*
2011	406	414	-2.0	0.73	0.79	2.78*	0.66*
Total	1818	1670	0.39	0.62	0.66	2.94*	0.61*

PBIAS – percent bias based on daily flow; EF – Nash-Sutcliffe coefficient based on daily flow; R^2 – coefficient of determination based on weekly flow; * – slope and intercept are significantly different ($P \leq 0.05$) from their ideal values of 1 and 0, respectively.

4.2 Model Validation

Observed data for the validation watershed had similar time periods where streamflow was estimated from downstream gages or interpolated from previous values. The six year period of observed stream flow data had some gaps, estimates include: (m/d/y), (8-23-06 to 5-15-07), (11-22-07 to 3-17-08), (7-1-08 to 8-3-08), (11-19-08 to 2-22-09), and (3-3-09 to 3-17-09); interpolated dates include: (12-8-09 to 12-9-09), (12-25-09), (1-7-10 to 1-10-10), and (2-15-10 to 2-16-2010); there were no missing data points from the time period. PAL5 was subject to the same discrepancies in weather input and soil profile input values. Constant plant and harvest dates for corn and soybean crops may lead to less than exact prediction of ET which may affect the annual water balance, which may in turn, attribute more or less water to streamflow than would have otherwise occurred. Also, PAL5 experienced the same peaks in streamflow in the fall of 2010, and springs of 2007, 2010, and 2011. These peaks may have resulted from streamflow freezing above the pressure transducers that measure flow. The increased pressure caused by expanding ice may have indicated a large volume of streamflow to be recorded by the flow-meter, when in fact; the stream may have been frozen. Bi-daily temperature values for the above time periods indicate that freezing temperatures were attained during the intervals, supporting this hypothesis.

4.2.1 Testing and Analysis of Hydrographs

The MIKE SHE model performed very well over the simulation period for PAL5, and exceedingly well over specific periods during the simulation. Figures 26-30 show daily streamflow modeled by MIKE SHE, observed flow of the watershed, estimated and interpolated flow, and precipitation for each year of the simulation period. Periods of exceedingly good fit are the summer and early fall of 2007, including the August 17th storm which produced 220 mm of precipitation; the majority of 2008, with the exclusion of periods of estimated and interpolated flow; 2009, with the exclusion of peaks most likely produced by surface runoff; the majority of 2010 until possible freezing events in early fall; and the majority of 2011 starting on April 1st and including the abnormally dry fall and winter.

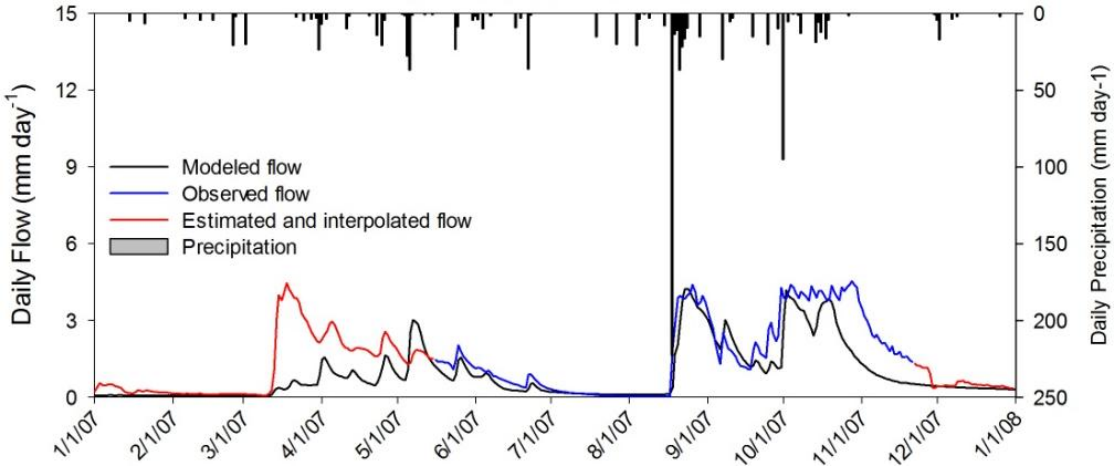

Figure 26 Validation hydrograph and hyetograph for PAL5, 2007

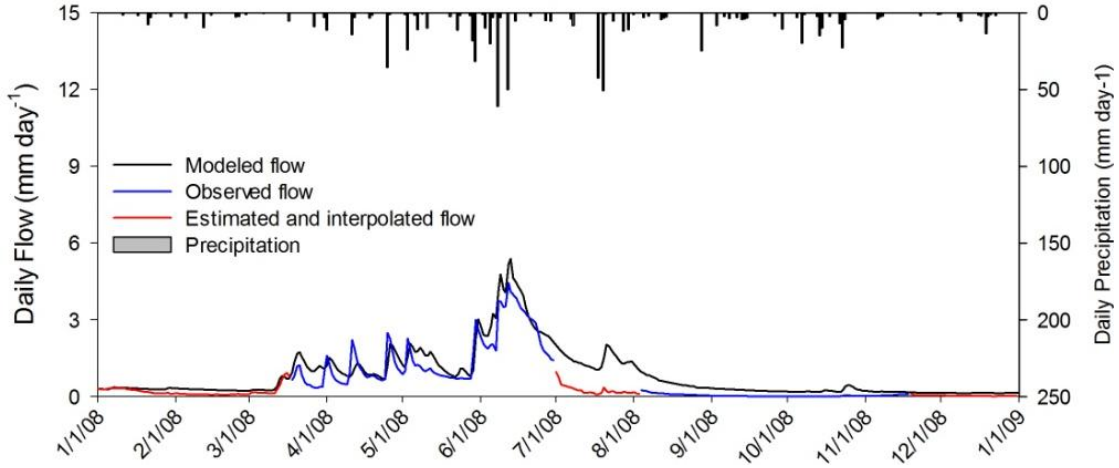

Figure 27 Validation hydrograph and hyetograph for PAL5, 2008

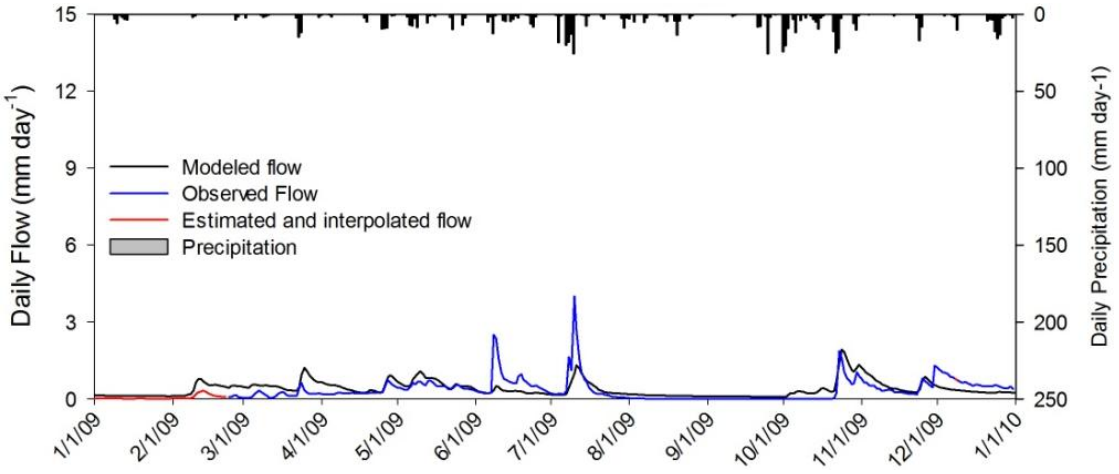

Figure 28 Validation hydrograph and hyetograph for PAL5, 2009

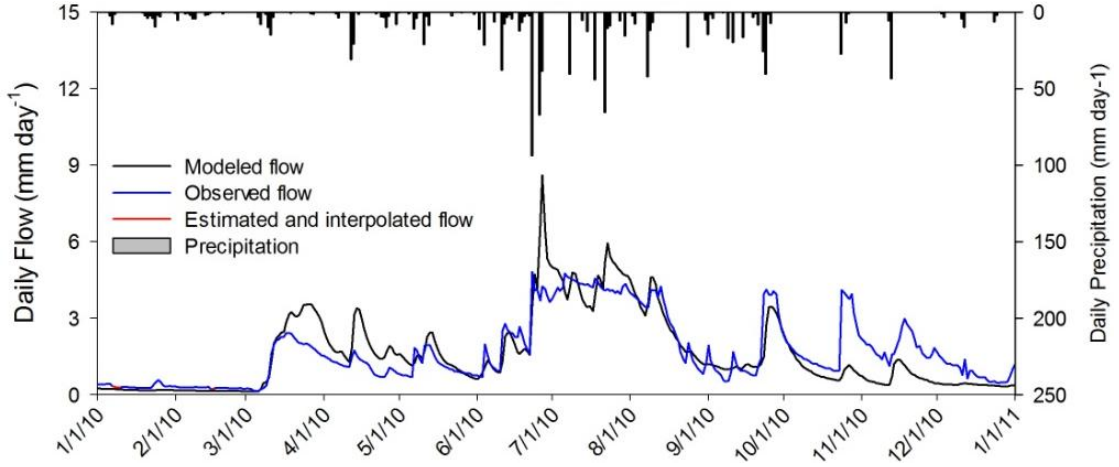

Figure 29 Validation hydrograph and hyetograph for PAL5, 2010

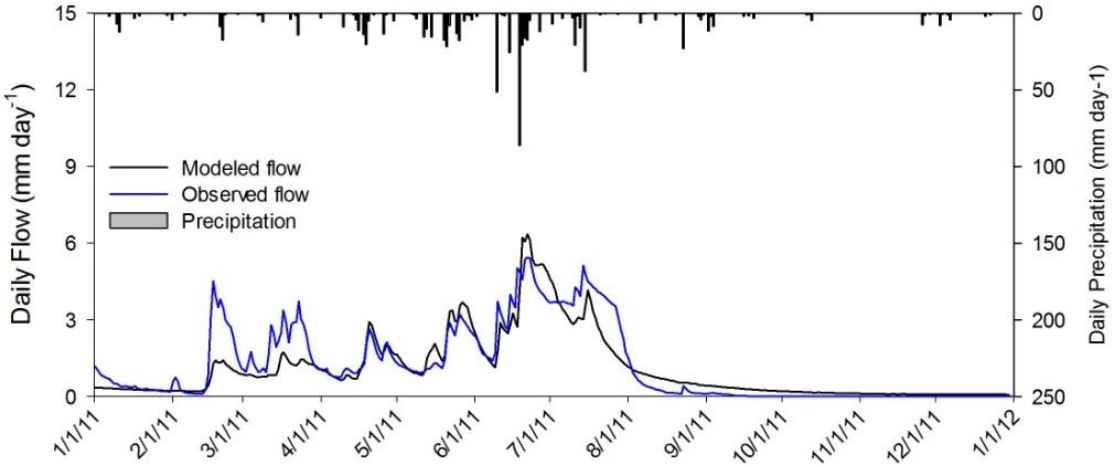

Figure 30 Validation hydrograph and hyetograph for PAL5, 2011

4.2.2 Statistical Analysis of Validation Hydrographs

Overall, PAL5 performed better than PAL3 in most aspects of statistical comparison. The average coefficient of determination over the simulation period was over 0.78 with values as high as 0.96 in 2008 and 0.82 in 2011. Likewise, daily NSE values for streamflow were a very good fit, with average simulation period NSE of 0.73 and a maximum value of 0.91 in 2008. Similar to PAL3, 2009 was the year of minimal fit with observed data. These values are summarized in Table 15, while Figure 31 shows the regression analysis for weekly flow in PAL5 over the simulation period (2007-2011). Also similar to PAL3, freezing events in the fall of 2010 and springs of 2010 and 2011 may have attributed to a portion the under-prediction of total streamflow throughout the simulation period.

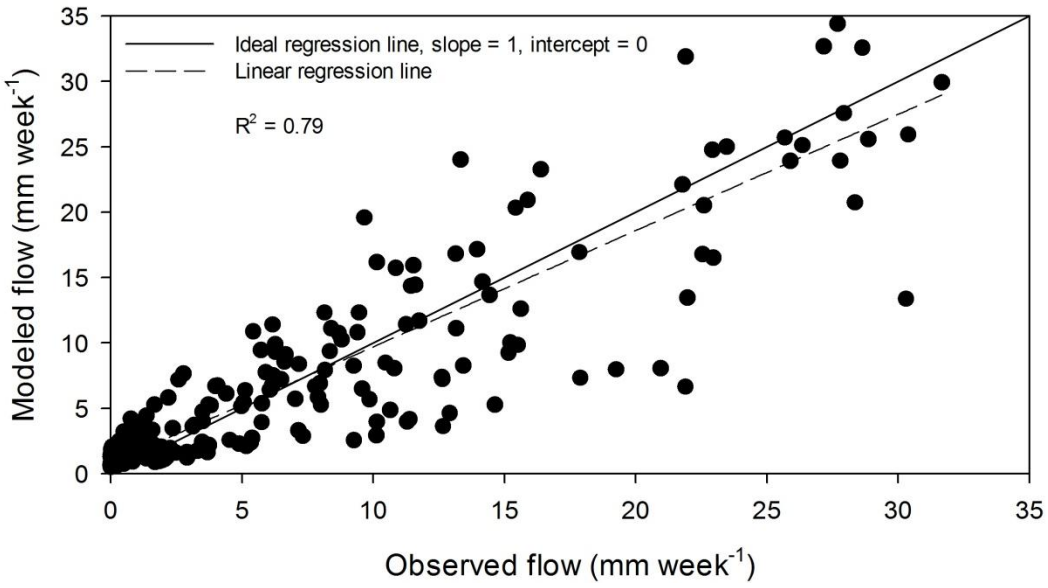

Figure 31 Scatter plot of observed vs. modeled weekly flow for validation period of PAL5

Table 15 Model performance during validation of PAL5 watershed

Year	Observed streamflow (mm)	Simulated streamflow (mm)	PBIAS	EF (%)	R^2	Regression parameters	
						Intercept (mm)	Slope
2007	518	324	27.3	0.66	0.80	-0.05	0.73*
2008	188	305	-38.6	0.82	0.96	1.73*	1.06
2009	115	141	-15.8	0.26	0.31	0.91*	0.52*
2010	614	588	4.1	0.59	0.72	-0.24*	0.98
2011	394	397	-7.7	0.75	0.81	0.68*	0.97
Total	1830	1757	0.43	0.73	0.77	0.89*	0.88*

PBIAS – percent bias based on daily flow; EF – Nash-Sutcliffe coefficient based on daily flow; R^2 – coefficient of determination based on weekly flow; * – slope and intercept are significantly different ($P \leq 0.05$) from their ideal values of 1 and 0, respectively.

4.3 Water Balance Analysis

After model simulation, a water balance module is undertaken to catalog each mechanism for water transport throughout the simulation. The complete water balance for the PAL3 and PAL5 watersheds appear in Tables 16 and 17, respectively. The water balance module tracks cumulative evapotranspiration, overland flow, subsurface drainage, recharge, and time step error throughout the model time period. The results show that the model simulated water processes much like the processes would occur in nature. For example, in wet years (2007 and 2010) evapotranspiration accounted for 57% and 51% of total water lost throughout the watershed, in normal years (2008, 2009, and 2011) ET was 62%, 68%, and 63%, respectively. The ratio of overland flow as surface runoff to drainage also corresponds well to expected real world results in similar landscapes on smaller scales (Zhou, 2011). Recharge for the watershed also tends to be close to regional values in literature of between 18.7 to 33.2 mm y^{-1} (Ella et al., 2002). The error accumulated for each year is a byproduct of time step; one would expect a model with a rather large time step to accumulate more error than an equal model with a smaller time step. The error divided by the annual precipitation can then be shown as a percent instead of a depth. The model performed exceptionally well in both testing and validation phases with a relative error of 5% and close to 0% for PAL3 and

PAL5, respectively. Water balance errors of less than 5% of total precipitation were desired, and reached in testing and validation.

Table 16 Water balance for PAL3 over the simulation period (2007-2011)

Year	PPT (mm)	ET (mm)	Re (mm)	ΔS (mm)	OVL (mm)	SUBD (mm)	Error (mm)	Total Flow (mm)
2007	1065	606	23	99	4.1	280	-18	284
2008	767	473	28	-22	5.8	281	-10	287
2009	752	512	24	13	0.0	161	5	161
2010	1162	597	30	33	16.3	509	-29	525
2011	796	505	32	-137	10.2	404	30	414
Average	908	539	27	-3	7.3	327	-4	334

PPT – precipitation; ET – evapotranspiration; Re – subsurface recharge; ΔS – change in subsurface storage; OVL – surface runoff; SUBD – subsurface drainage

Table 17 Water balance for PAL5 over the simulation period (2007-2011)

Year	PPT (mm)	ET (mm)	Re (mm)	ΔS (mm)	OVL (mm)	SUBD (mm)	Error (mm)	Total Flow (mm)
2007	1060	585	26	108	1.3	323	0	324
2008	768	478	30	-41	3.3	302	0	302
2009	752	510	25	28	0.0	141	0	141
2010	1162	575	32	23	11.7	576	0	588
2011	758	503	32	-153	6.8	390	1	397
Mean	900	530	30	-7	4.6	346	0	351

PPT – precipitation; ET – evapotranspiration; Re – subsurface recharge; ΔS – change in subsurface storage; OVL – surface runoff; SUBD – subsurface drainage

The annual water balances can be further broken down into the four seasons, as shown in Tables 18 and 19. The individual parcels will show when each aspect of the water balance is most prevalent, and analyzing the seasons together can show intra-annual changes and how the modules interact with each other as well. Upon inspection, recharge occurs at a nearly uniform rate throughout the year, while the other components fluctuate depending on the time of the year and hydrological impact of the other water balance components. Storage in the unsaturated zone depends on precipitation and ET within the season; seasons with low precipitation and high ET will have negative storage values, and vice versa. Evapotranspiration occurs predominantly in the hot, dry periods of summer and fall, compounded by plant growth during this same time period. Overland flow is driven by excess rainfall and will not have a large long time from heavy event to surface runoff, while drainage can occur from March to November fairly regularly and can show a slight lag from a precipitation event to drainage flow downstream.

Table 18 Water balance for PAL3 showing seasonal variations (2007-2011)

Year	**Winter (Jan., Feb., March)**								**Spring (April, May, June)**							
	PPT (mm)	ET (mm)	Re (mm)	ΔS (mm)	OVL (mm)	SUBD (mm)	M_Sf (mm)	O_Sf (mm)	PPT (mm)	ET (mm)	Re (mm)	ΔS (mm)	OVL (mm)	SUBD (mm)	M_Sf (mm)	O_Sf (mm)
2007	115	9	4.8	88	0.0	6.2	16.1	80	233	192	5.0	-31	0.0	70.9	70.9	132
2008	69	8	6.2	41	0.1	27.7	27.8	23	343	124	6.9	12	5.0	143.2	148.2	134
2009	73	14	6.0	42	0.0	29.0	29.0	9	162	157	6.0	-48	0.0	52.4	52.4	35
2010	113	14	5.6	65	1,6	62.2	63.8	108	464	169	7.0	42	10.2	147.9	158.1	222
2011	95	7	7.1	39	0.0	64.7	64.7	107	467	154	8.4	2	9.4	175.2	184.6	180
Mean	91	10	5.9	55	0.3	38	38.3	66	314	159	6.7	-4	4.9	117.9	122.8	141
Year	**Summer (July, Aug., Sept.)**								**Fall (Oct., Nov., Dec.)**							
	PPT (mm)	ET (mm)	Re (mm)	ΔS (mm)	OVL (mm)	SUBD (mm)	M_Sf (mm)	O_Sf (mm)	PPT (mm)	ET (mm)	Re (mm)	ΔS (mm)	OVL (mm)	SUBD (mm)	M_Sf (mm)	O_Sf (mm)
2007	600	318	5.7	62	1.6	94.3	95.9	99	113	86	7.1	-20	2.5	108.5	111.0	235
2008	220	282	7.6	-105	0.7	72.1	72.8	11	135	58	6.8	28	0.0	37.7	37.7	0
2009	256	279	5.9	-79	0.0	32.6	32.6	15	263	62	5.8	98	0.0	46.5	46.5	31
2010	473	329	9.4	-52	4.4	220.3	224.7	203	112	86	8.3	-22	0.0	78.9	78.9	134
2011	161	302	9.2	-173	0.8	132.6	13.4	119	36	42	7.0	-4	0.0	31.5	31.5	0
Mean	328	302	7.6	-69	1.5	110.4	111.9	89	125	67	7.0	16	0.5	60.6	61.1	80

PPT – precipitation (mm); ET – evapotranspiration (mm); Re – recharge (mm); ΔS – change in storage (subsurface and mm); OVL – surface runoff; SUBD – subsurface drainage; M_Sf – modeled streamflow (mm); O_Sf – observed streamflow (mm)

Table 19 Water balance for PAL5 showing seasonal variations (2007-2011)

Year	**Winter (Jan., Feb., March)**								**Spring (April, May, June)**							
	PPT (mm)	ET (mm)	Re (mm)	ΔS (mm)	OVL (mm)	SUBD (mm)	M_Sf (mm)	O_Sf (mm)	PPT (mm)	ET (mm)	Re (mm)	ΔS (mm)	OVL (mm)	SUBD (mm)	M_Sf (mm)	O_Sf (mm)
2007	115	5	5.6	101	0.0	13.0	13.0	72	233	189	6.1	-37	0.0	84.6	84.6	132
2008	69	4	7.0	36	0.0	41.1	41.1	24	343	117	8.3	37	3.3	173.4	176.7	150
2009	73	10	6.3	47	0.0	33.3	33.3	10	162	159	6.4	-45	0.0	42.1	42.1	45
2010	113	8	6.0	91	0.5	73.0	73.5	63	464	167	7.9	48	8.6	168.7	177.3	140
2011	95	3	7.3	39	0.0	60.8	60.8	70	467	147	9.1	46	6.8	200.7	207.5	195
Mean	91	6	6.5	62	0.1	44.2	44.3	48	314	156	7.6	10	3.7	133.9	137.6	132
Year	**Summer (July, Aug., Sept.)**								**Fall (Oct., Nov., Dec.)**							
	PPT (mm)	ET (mm)	Re (mm)	ΔS (mm)	OVL (mm)	SUBD (mm)	M_Sf (mm)	O_Sf (mm)	PPT (mm)	ET (mm)	Re (mm)	ΔS (mm)	OVL (mm)	SUBD (mm)	M_Sf (mm)	O_Sf (mm)
2007	600	312	6.6	76	0.4	102.5	102.9	117	113	79	8.2	-31	0.9	123.0	123.9	195
2008	220	300	8.4	-144	0.0	71.1	71.1	12	135	57	7.0	30	0.0	16.3	16.3	2
2009	256	282	6.2	-77	0.0	20.2	20.2	18	263	60	6.2	104	0.0	46.0	46.0	43
2010	473	317	10.7	-68	2.6	269.6	272.2	267	112	83	8.3	-48	0.0	65.4	65.4	143
2011	161	311	9.2	-216	0.0	119.2	119.2	128	36	43	6.8	-22	0.0	9.7	9.7	0
Mean	328	304	8.2	-86	0.6	116.5	117.1	108	125	64	7.3	7	0.2	52.1	52.3	77

PPT – precipitation (mm); ET – evapotranspiration (mm); Re – recharge (mm); ΔS – change in storage (subsurface and mm); OVL – surface runoff; SUBD – subsurface drainage; M_Sf – modeled streamflow (mm); O_Sf – observed streamflow (mm)

CHAPTER V – SCENARIO SIMULATIONS

Based on past land use and possible future land management change, four scenarios were tested in order to quantify the hydrological impact of each: converting row crop entirely to pasture or perennial grassland while retaining drainage infrastructure, land use conversion to grassland without drainage infrastructure, reducing subsurface drain depth from 1.2m to 0.75m, and entirely eliminating drainage from row crop agriculture. The first scenario, land use conversion to grassland while maintaining tile drains, would simulate a land use management change of present day from agriculture to government subsidized programs like CRP, upland prairies, and lowland riparian buffers. The second land use conversion scenario excluding tile drains would simulate pre-settlement conditions of the region. By comparing pre-settlement conditions to current practices, and possible future practices, one can quantify the effect agriculture and tile drainage have had on the landscape, in terms of streamflow and peak events. The hydrographs for all scenarios were compared with the reference hydrograph and the observed hydrograph for the watershed using tested and validated inputs from earlier simulations (Figures 20-30). The simulation timeline was the same as previous simulations (2007-2011).

5.1 Land Use Conversion to Perennial Grassland with Drainage Infrastructure

In this scenario, the dominant land use of row crop agricultural was converted to perennial grassland while maintaining the drainage infrastructure in both watersheds. Land use in the MIKE SHE model was altered from distributed and diverse to uniform and constant; this allows the hydrological impact of row crop versus perennial grassland to be quantified while keeping the variable of watershed drainage constant. Further scenarios will explore the effects that changes in drainage have on hydrology.

5.1.1 Hydrograph Analysis

Figures 32-41 show hydrographs of total flow, while appendix A breaks down surface and subsurface flow into annual figures as well. Nearly all peaks are decreased when the current conditions are replaced with perennial grassland while keeping the drainage infrastructure intact. Most notably, the low flow year of 2009 (figure 34) shows almost no flow with perennial grassland, most likely due to increased ET from perennial grassland during an

intense period of water stress on vegetation. In addition, peaks in 2007 (fig. 32 and 37, mid August and Sept. 1st) and 2010 (fig. 35 and 40, late June) show reductions of over 50% of the total flow when the current conditions are replaced with perennial grassland.

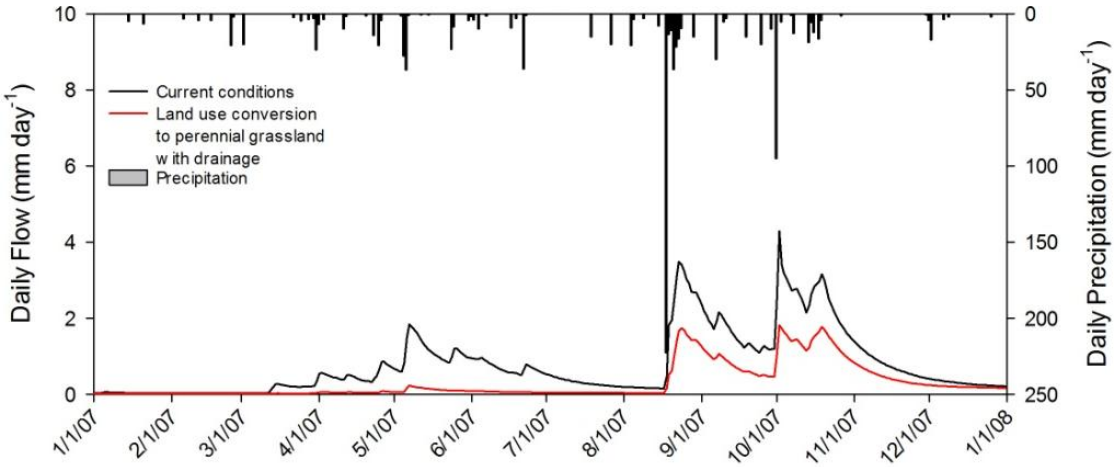

Figure 32 PAL3 current conditions to land use conversion with drainage infrastructure, 2007

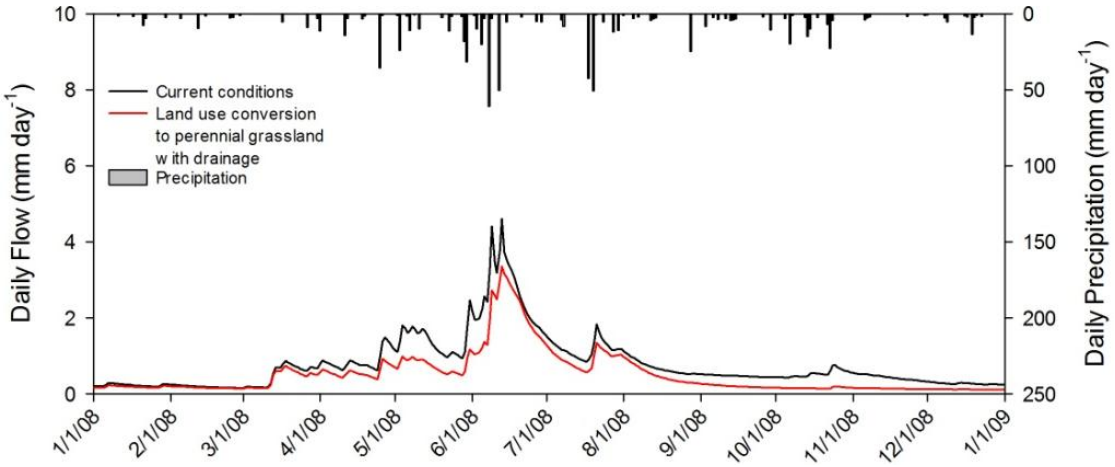

Figure 33 PAL3 current conditions to land use conversion with drainage infrastructure, 2008

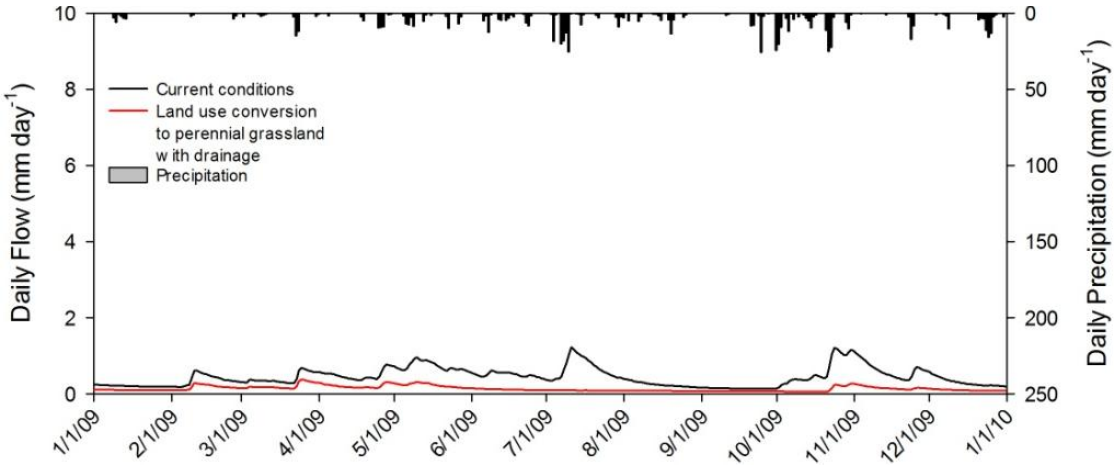

Figure 34 PAL3 current conditions to land use conversion with drainage infrastructure, 2009

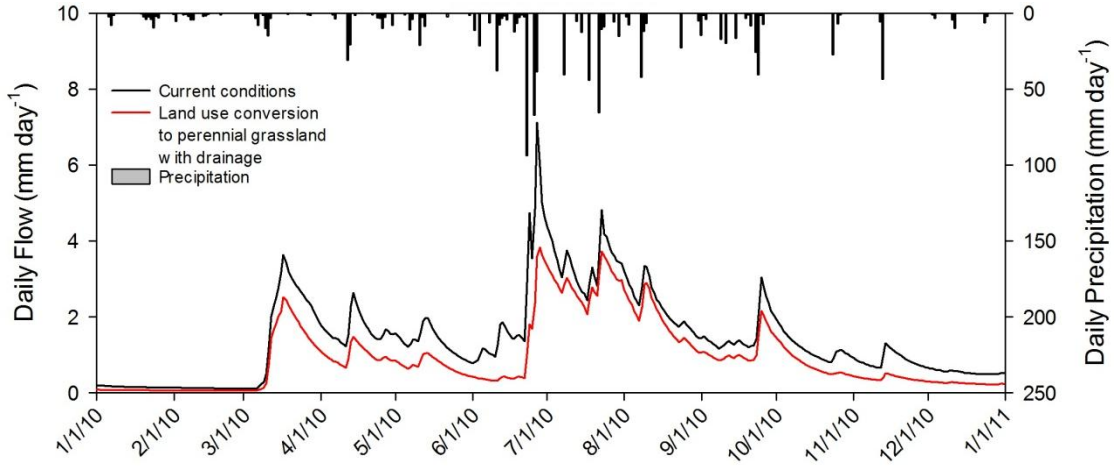

Figure 35 PAL3 current conditions to land use conversion with drainage infrastructure, 2010

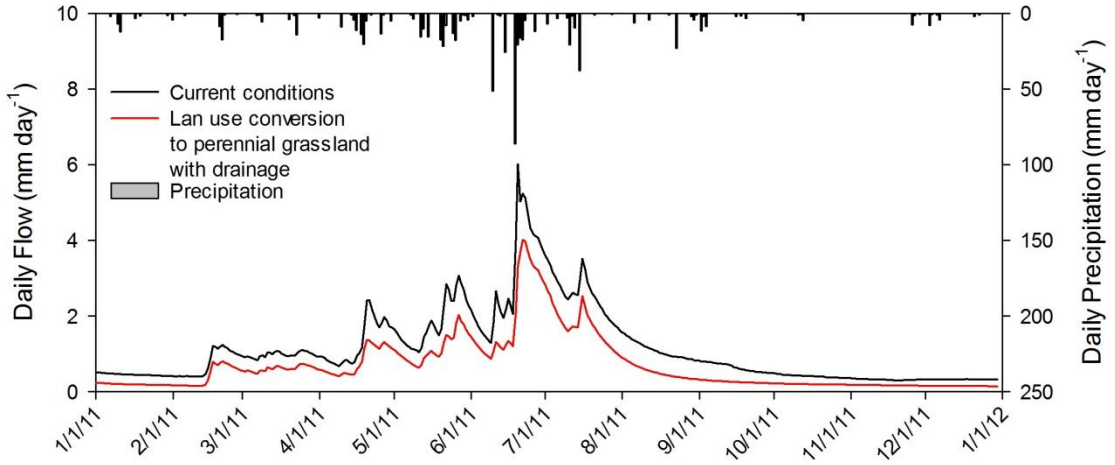

Figure 36 PAL3 current conditions to land use conversion with

drainage infrastructure, 2011

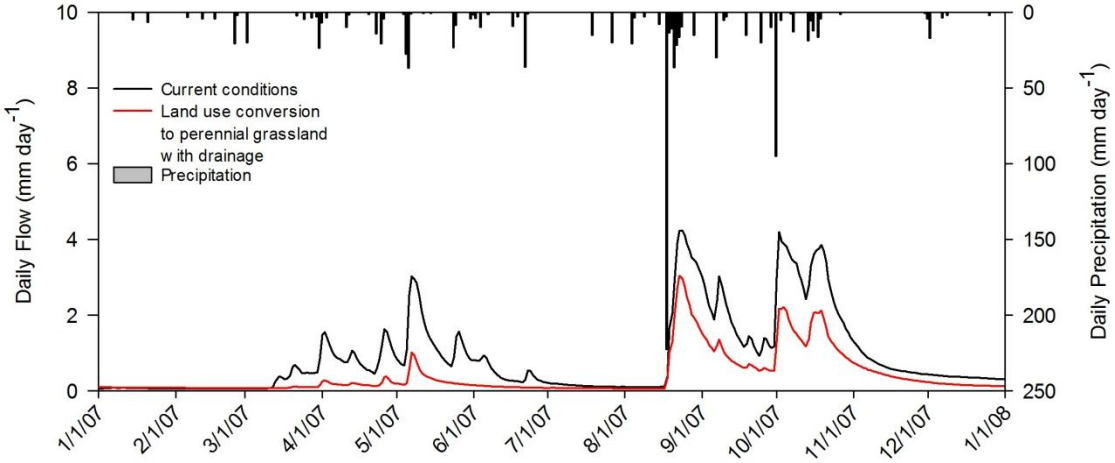

Figure 37 PAL5 current conditions to land use conversion with drainage infrastructure, 2007

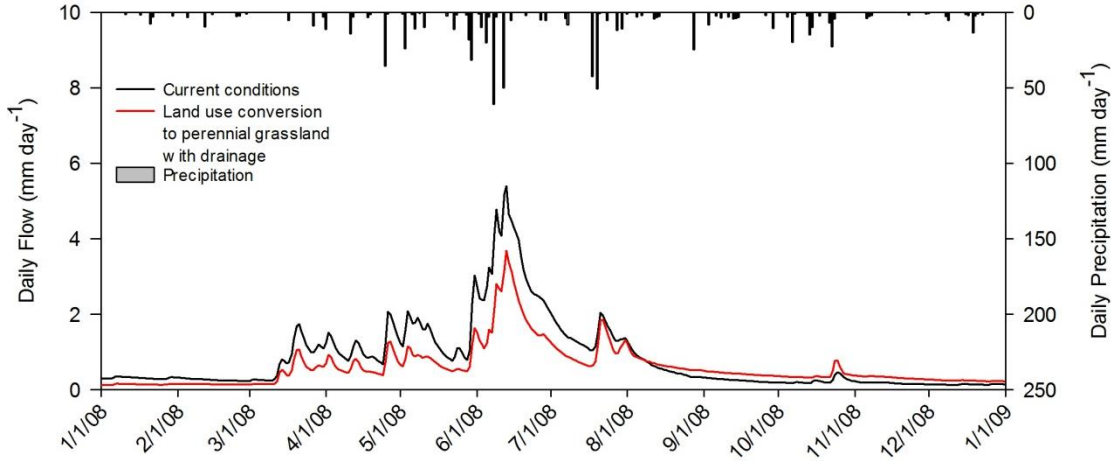

Figure 38 PAL5 current conditions to land use conversion with drainage infrastructure, 2008

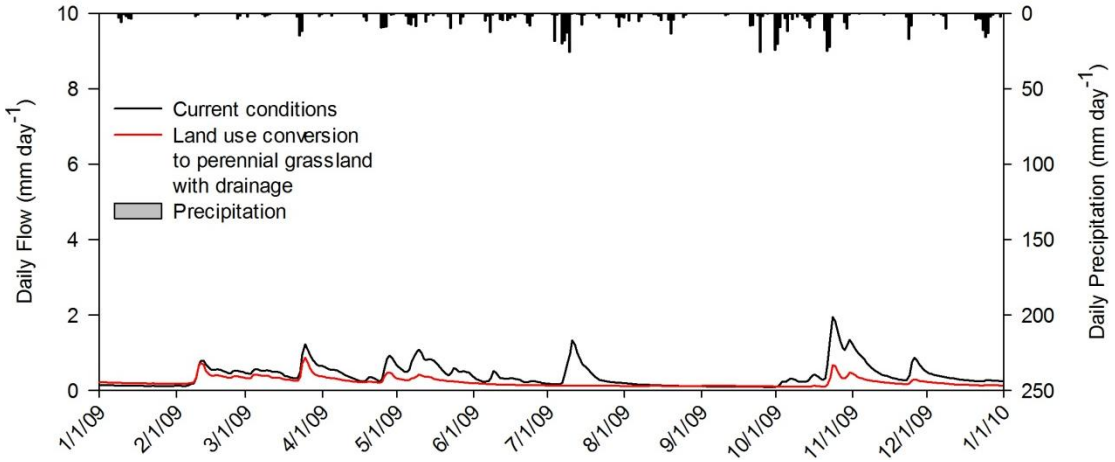

Figure 39 PAL5 current conditions to land use conversion with drainage infrastructure, 2009

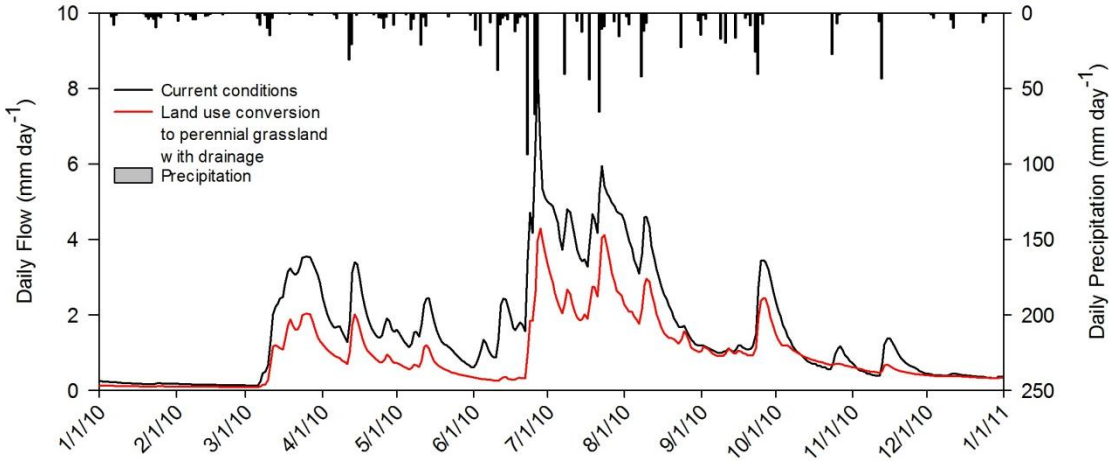

Figure 40 PAL5 current conditions to land use conversion with drainage infrastructure, 2010

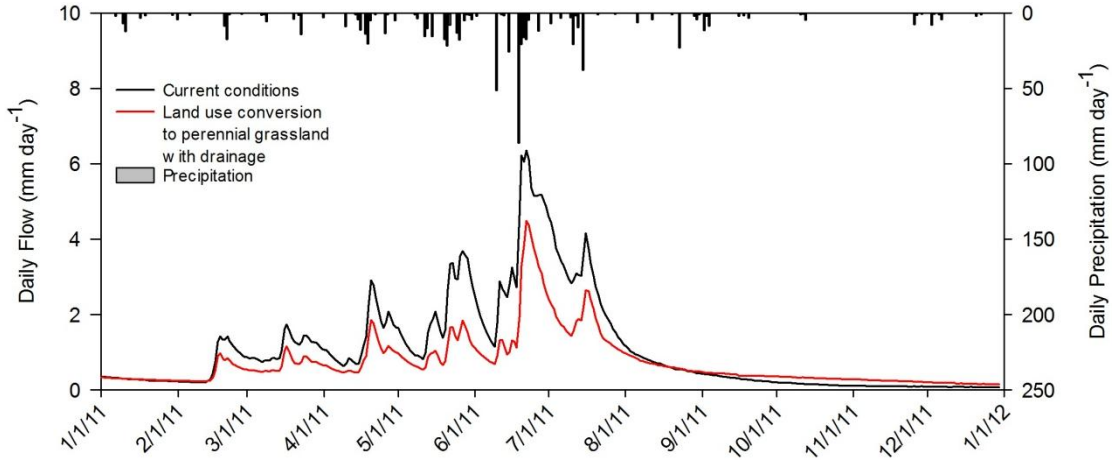

Figure 41 PAL5 current conditions to land use conversion with

drainage infrastructure, 2011

5.1.2 Water Balance Analysis

The annual water balances in Table 20 and 21 show an overall decrease in surface runoff by 95% in PAL3 and 84% in PAL5, and a 42% decrease in drainage flow in PAL3 and 40% in PAL5.This was offset by a 27% increase in average annual evapotranspiration in PAL3 and 25% PAL5. The main mechanisms driving the change in streamflow in this scenario are the vegetative properties of perennial grassland compared to the vegetative properties of corn or soybeans. The persistent nature of perennial grass root structure allows water uptake in early spring prior to row crop planting, and late fall after harvest and fall tillage operations. This decreases streamflow for both time periods. Likewise, perennial grasses have consistent above ground growth throughout the year which has a two-fold effect: first, the LAI of perennial grasses is non-zero in the early spring and late fall, which also decreases streamflow in these periods; second, the stem-surface relationship of perennial grassland creates a rougher surface (Manning's roughness coefficient) which in turn retards surface runoff that does occur.

Table 20 PAL3 water balance comparison of current conditions to grassland with drainage infrastructure

Year	PAL3	Current Conditions					Land use conversion to perennial grassland with drainage infrastructure				
	PPT	ET	Δ_S	OVL	SUBD	TOT	ET	Δ_S	OVL	SUBD	TOT
2007	1060	606	99	4.1	279.9	280.0	731	152	0.1	111.7	111.
2008	767	473	-22	5.8	280.7	286.5	597	-27	0.1	187.	187.3
2009	752	512	13	0.0	160.5	160.5	641	-7	0.0	48.6	48.6
2010	1162	597	33	16.3	509.1	525.4	776	63	0.5	347.1	347.6
2011	759	505	-137	10.2	403.9	414.1	671	-169	1.0	249.4	250.5
Mean	900	537	-3	7.3	326.8	334.1	683	11	0.3	188.8	189.1

PPT – precipitation; ET – evapotranspiration; ΔS – change in subsurface storage; OVL – surface runoff; SUBD – subsurface drainage

Table 21 PAL5 water balance comparison of current conditions to land use conversion with drainage infrastructure

Year	PAL5	Current Conditions					Land use conversion to perennial grassland with drainage infrastructure				
	PPT	ET	Δ_S	OVL	SUBD	TOT	ET	Δ_S	OVL	SUBD	TOT
2007	1060	585	108	1.3	323.1	324.4	716	159	0.2	146.9	147.1
2008	767	478	-41	3.3	301.9	305.2	527	-2	0.5	219.4	219.9
2009	752	510	29	0.0	141.6	141.6	635	-30	0.0	78.4	78.4

2010	1162	574	23	11.7	576.4	588.1	778	62	1.7	347.1	348.8
2011	759	503	-153	6.8	390.4	397.2	666	-184	1.1	265.2	266.3
Mean	900	530	-42	4.6	346.7	351.4	664	7	0.7	211.4	212.1

PPT – precipitation; ET – evapotranspiration; ΔS – change in subsurface storage; OVL – surface runoff; SUBD – subsurface drainage

Table 22 Percent (%) change from baseline values for PAL3 and PAL5 with land use change to all perennial grassland with drainage

Year	PAL3 percent (%) change from baseline values					PAL5 percent (%) change from baseline values				
	ΔET	Δ_S	ΔOVL	ΔSUB	ΔTOT	ΔET	Δ_S	ΔOVL	ΔSUB	ΔTOT
2007	21	53	-98	-60	-61	23	48	-82	-55	-55
2008	26	22	-99	-33	-35	10	-95	-83	-27	-28
2009	25	-157	---	-70	-70	25	-201	---	-45	-45
2010	30	90	-97	-32	-34	36	179	-86	-40	-41
2011	33	24	-90	-38	-40	32	20	-84	-32	-33
Mean	27	-183	-95	-42	-43	26	-116	-85	-39	-40

PPT – precipitation; ET – evapotranspiration; ΔS – change in subsurface storage; OVL – surface runoff; SUBD – subsurface drainage

5.2 Land use conversion Scenario- Drainage Infrastructure Excluded

This scenario, like the previous one, transforms all row crop land to perennial grassland for the entirety of the simulation period; however, unlike the previous scenario the model does not consider either watershed to possess subsurface drainage infrastructure thereby mimicking the pre-settlement conditions of the region. This scenario will give a baseline as to how hydrologic conditions have changed over the years as a result of alteration in landuse and drainage.

5.2.2 Hydrograph Analysis

Figures 42-51 illustrate the total flow comparison of current conditions to pre-settlement conditions in PAL3 and PAL5, while a breakdown of surface and subsurface annual flow by watershed appears in the appendices. The main mechanism driving streamflow in this scenario is subsurface storage, and more directly, antecedent moisture content. Precipitation throughout 2006 and early 2007 was below average, driving the water table lower than usual and drying out the soil. This had the effect of increasing subsurface storage (allowing the soil to act in a sponge-like manner) and allowing for a greater portion of macropore flow to take place caused by fractures associated with the shrink-swell relationship of wet and dry soils. The effects were so great that the rainfall event on August 17th, 2007 that produced 223 mm

(8.8 in) over a 24 hour period produced no flow. Conversely, a rainfall event on June 22nd, 2010 of 94 mm (3.7 in) produced a surface runoff peak flow of 13.7 mm. Other than the severity of the rainfall event, the major appreciable differences in these two situations were the antecedent moisture content of the soil and the water table level just prior to the rainfall event. Although the water table levels were not explicitly recorded for this scenario, an analog would be subsurface storage, the greater the subsurface storage at a point in time, the deeper the water table in general. Streamflow in the days preceding the 2010 event shows that soil moisture content was higher than 2007, and water table levels were at or near the surface. Likewise, lower subsurface storage values indicate a higher water table, which would explain periods of higher flow in the pre-settlement scenario than in the current conditions.

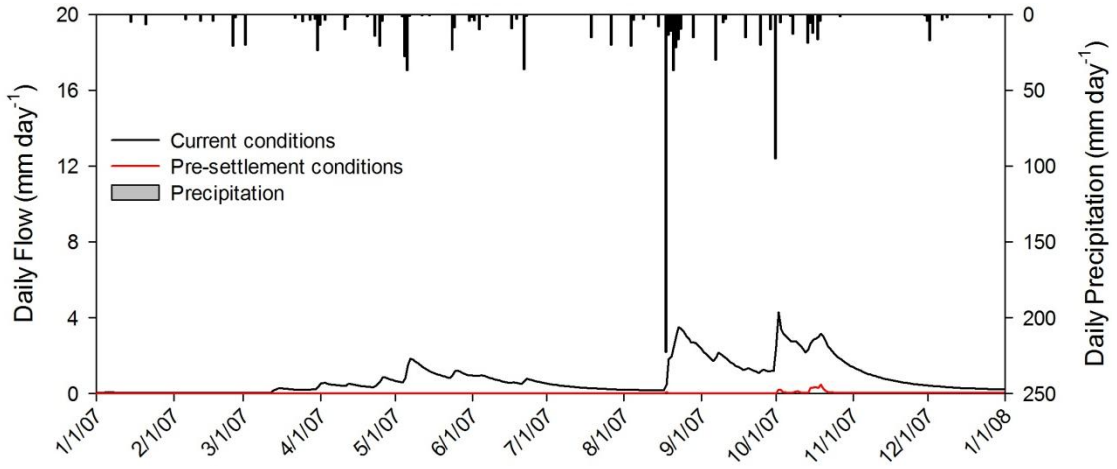

Figure 42 PAL3 current conditions to likely pre-settlement conditions, 2007

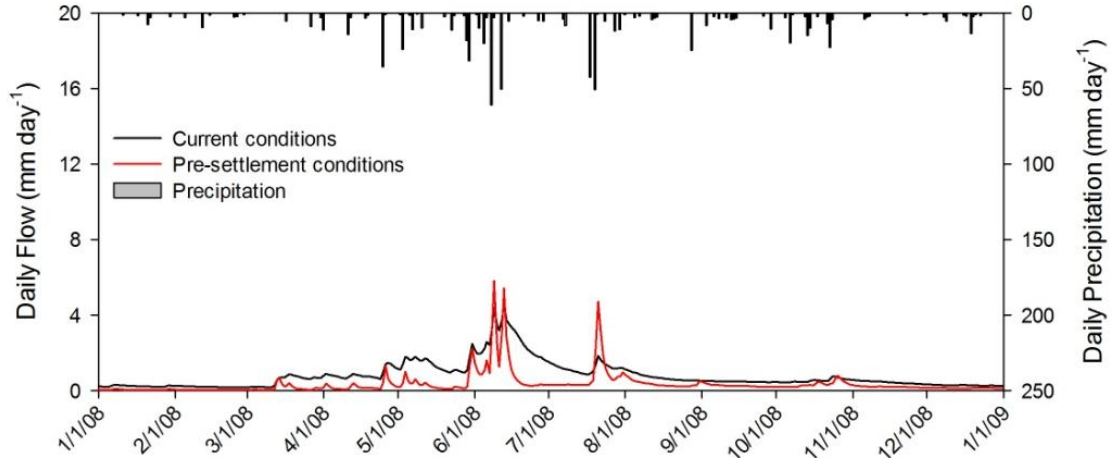

Figure 43 PAL3 current conditions to likely pre-settlement conditions, 2008

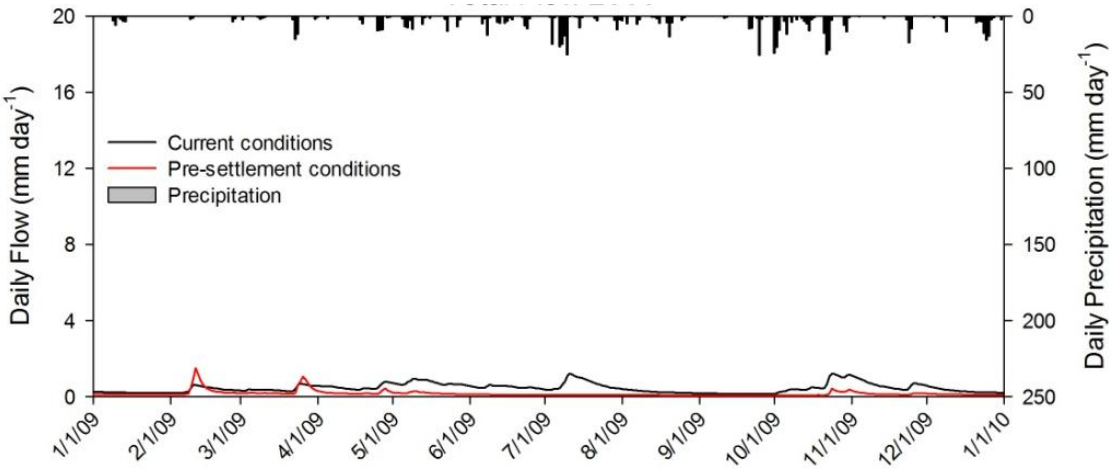

Figure 44 PAL3 current conditions to likely pre-settlement conditions, 2009

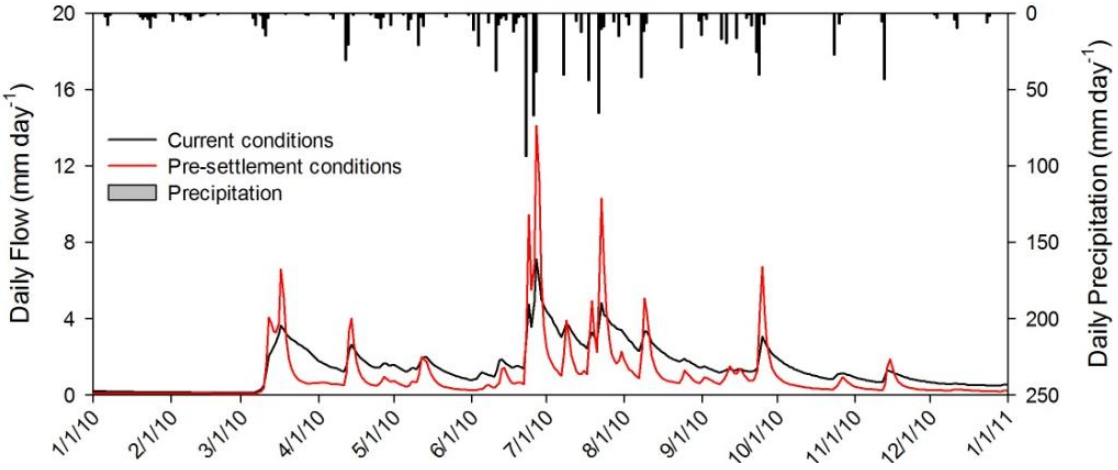

Figure 45 PAL3 current conditions to likely pre-settlement conditions, 2010

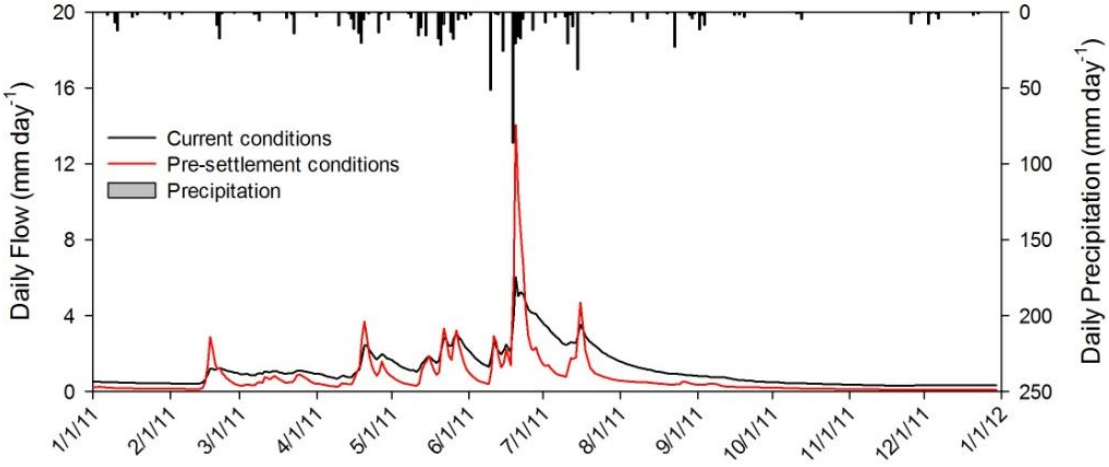

Figure 46 PAL3 current conditions to likely pre-settlement conditions, 2011

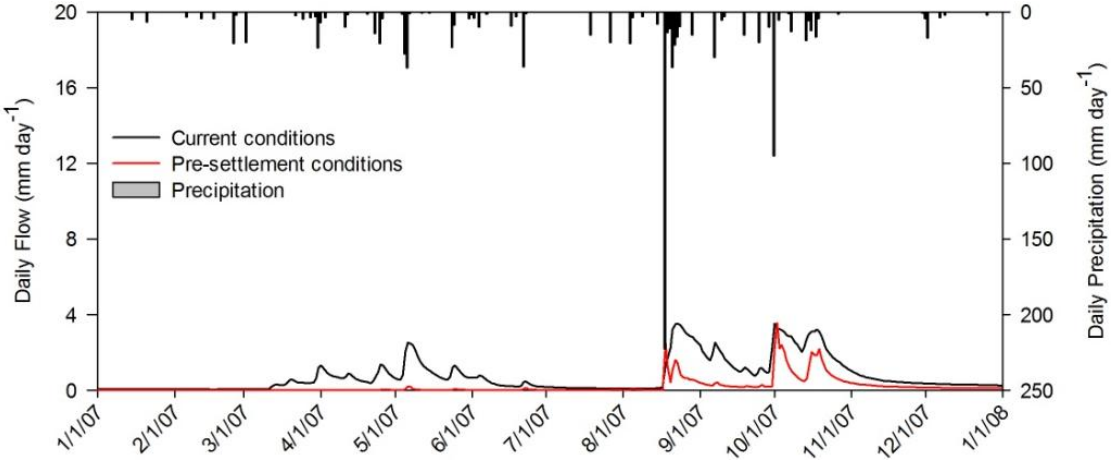

Figure 47 PAL5 current conditions to likely pre-settlement conditions, 2007

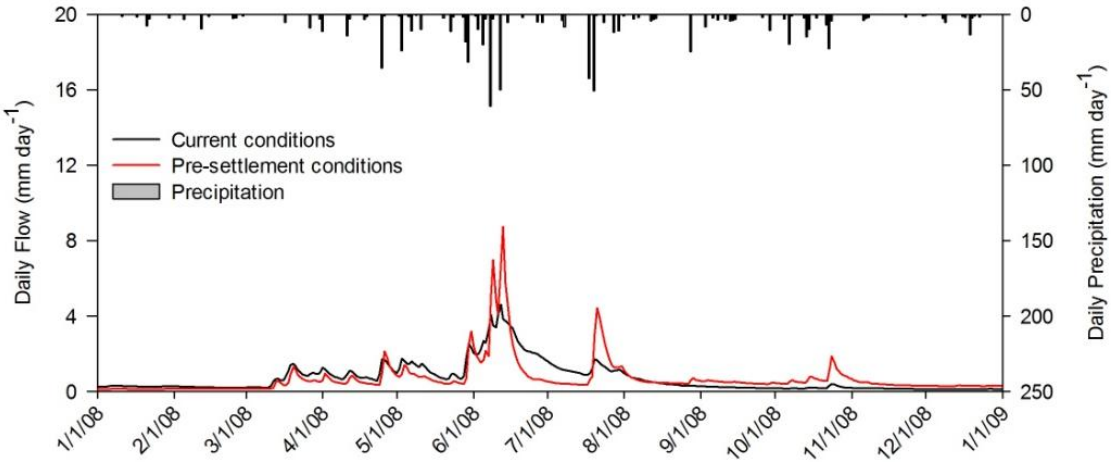

Figure 48 PAL5 current conditions to likely pre-settlement conditions, 2008

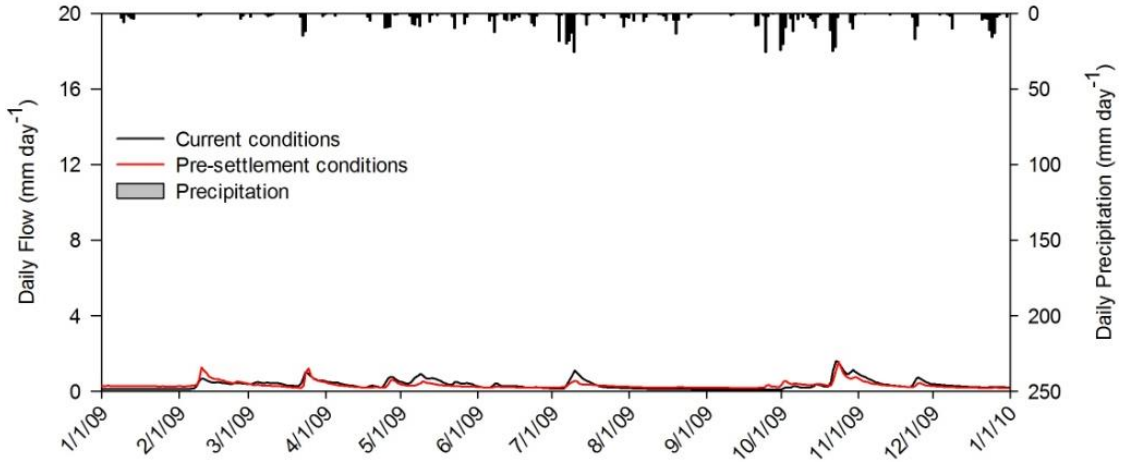

Figure 49 PAL5 current conditions to likely pre-settlement conditions, 2009

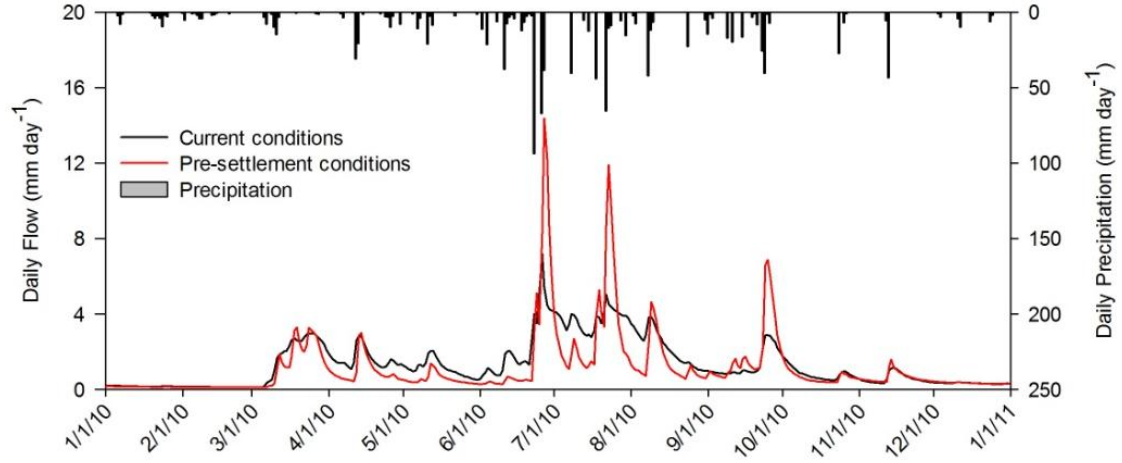

Figure 50 PAL5 current conditions to likely pre-settlement conditions, 2010

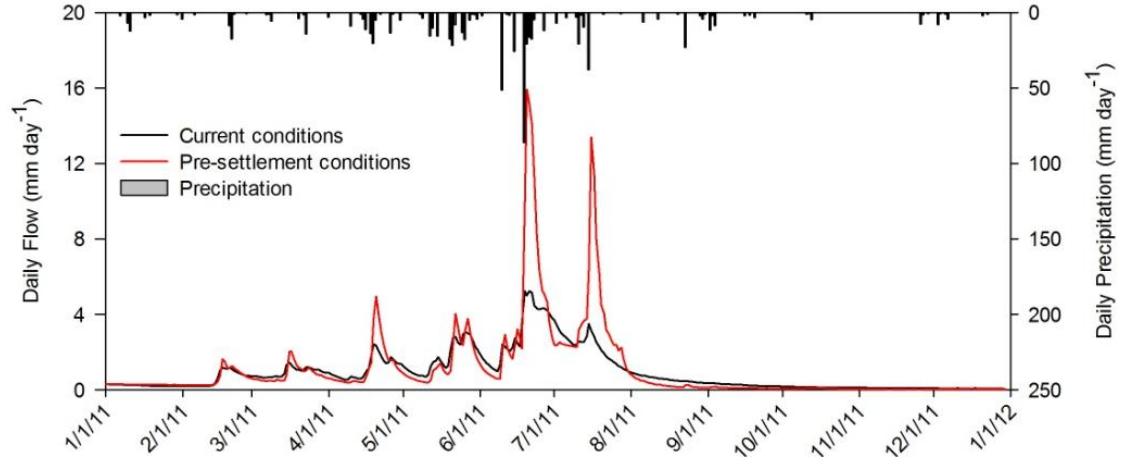

Figure 51 PAL5 current conditions to likely pre-settlement conditions, 2011

5.2.2 Water Balance Analysis

The water balances in Tables 22 and 23 show total streamflow decreased by 50% in PAL3 and 28% in PAL5. The most pronounced losses occurred in 2007-2009 with a decrease of 74% in total streamflow in PAL3. Evapotranspiration in the pre-settlement conditions was 23% higher with the average annual ET rising from 537 mm to 662 mm. Storage was more volatile in the pre-settlement scenario as well. The largest deficit in storage was -137 mm for the pre-settlement conditions as opposed to -149 for current conditions, while the largest deposit of water into storage was 222 mm opposed to 99 mm for PAL3.

Table 23 PAL3 water balance comparison of current conditions to likely pre-settlement conditions

Year	PAL3	Current Conditions					Pre-settlement conditions, perennial grassland with no drainage infrastructure				
	PPT	ET	Δ_S	OVL	SUBD	TOT	ET	Δ_S	OVL	SUBD	TOT
2007	1060	606	99	4.1	279.9	280.0	733	222	5.1	0.0	5.1
2008	767	473	-22	5.8	280.7	286.5	570	-12	127.2	0.0	127.2
2009	752	512	13	0.0	160.5	160.5	644	-10	53.8	0.0	53.8
2010	1162	597	33	16.3	509.1	525.4	731	61	378.1	0.0	378.1
2011	759	505	-137	10.2	403.9	414.1	634	-149	265.3	0.0	265.3
Mean	900	537	-3	7.3	326.8	334.1	662	23	165.9	0.0	165.9

PPT – precipitation; ET – evapotranspiration; ΔS – change in subsurface storage; OVL – surface runoff; SUBD – subsurface drainage

Table 24 PAL5 water balance comparison of current conditions to likely pre-settlement conditions

Year	PAL5	Current Conditions					Pre-settlement conditions, perennial grassland with no drainage infrastructure				
	PPT	ET	Δ_S	OVL	SUBD	TOT	ET	Δ_S	OVL	SUBD	TOT
2007	1060	585	108	1.3	323.1	324.4	673	191	71.3	0.0	71.3
2008	767	478	-41	3.3	301.9	305.2	468	6	254.2	0.0	254.2
2009	752	510	29	0.0	141.6	141.6	603	-29	113.8	0.0	113.8
2010	1162	574	23	11.7	576.4	588.1	682	57	424.6	0.0	424.6
2011	759	503	-153	6.8	390.4	397.2	527	-142	394.1	0.0	394.1
Mean	900	530	-42	4.6	346.7	351.4	591	17	251.6	0.0	251.6

PPT – precipitation; ET – evapotranspiration; ΔS – change in subsurface storage; OVL – surface runoff; SUBD – subsurface drainage

Table 25 Percent (%) change from baseline values for PAL3 and PAL5 with land use change to all perennial grassland without drainage (pre-settlement)

Year	PAL3 percent (%) change from baseline values					PAL5 percent (%) change from baseline values				
	ΔET	Δ_S	ΔOVL	ΔSUB	ΔTOT	ΔET	Δ_S	ΔOVL	ΔSUB	ΔTOT
2007	21	124	25	---	-98	15	78	5260	---	-78
2008	20	-47	2090	---	-56	-2	-113	7550	---	-17
2009	26	-173	---	---	-66	18	-199	---	---	-20
2010	22	83	2220	---	-28	19	156	3500	---	-28
2011	25	9	2400	---	-36	5	-8	5540	---	-1
Mean	23	-930	2180	---	-50	12	-323	5260	---	-29

PPT – precipitation; ET – evapotranspiration; ΔS – change in subsurface storage; OVL – surface runoff; SUBD – subsurface drainage

5.3 Conventional vs. Shallow Drainage

A possible alternate to current drainage practices is to decrease the depth at which tile drains are placed upon installation. Shallow drainage may have the effect of decreasing subsurface drainage, which could in turn decrease nitrate export from agricultural based watersheds that rely on fertilizer inputs throughout the growing season (Sands et al., 2003). This scenario simulated a nearly identical subsurface drainage infrastructure to that used in testing and validation except with a modification to drain depth, 0.75 m as opposed to 1.2 m below ground.

5.3.1 Hydrograph Analysis

Figures 52-61 show a remarkable agreement with current conditions in both watersheds despite the change in drainage depth from 1.2 m to 0.75 m. Although hydrograph comparisons show an increase in peak flow between 59 – 297% for PAL3 and between 75 – 187 % for PAL5, total streamflow as shown by the hydrographs remained nearly unchanged for both watersheds. Peak flows increased slightly since with a shallow drainage infrastructure there is more soil available to store water, and when this soil becomes saturated overland flow occurs instead of increased drainage. This also has the effect of slightly decreasing subsurface drainage (1% for PAL3 and 2% for PAL5) for the entire simulation period in both watersheds, as shown visually in appendix A and numerically in tables 24 and 25.

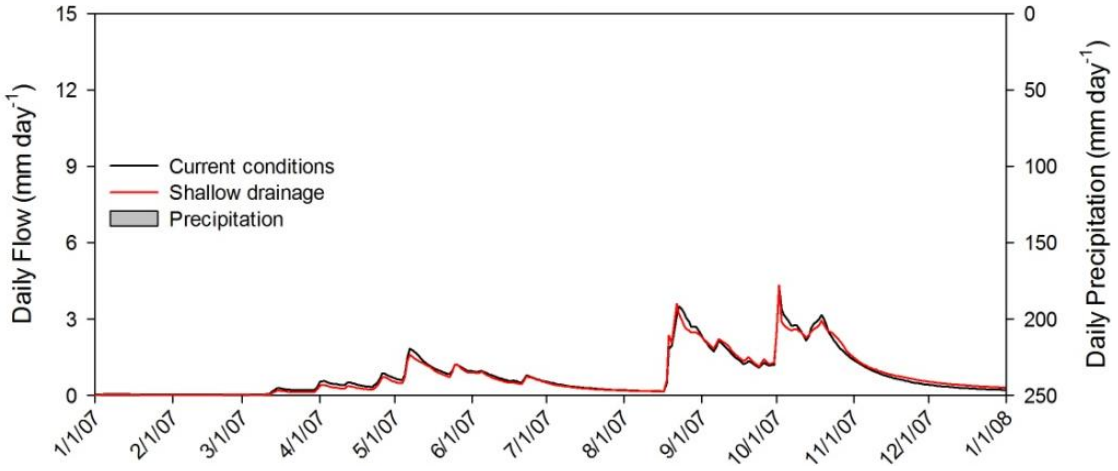

Figure 52 PAL3 current conditions to shallow drainage depth, 2007

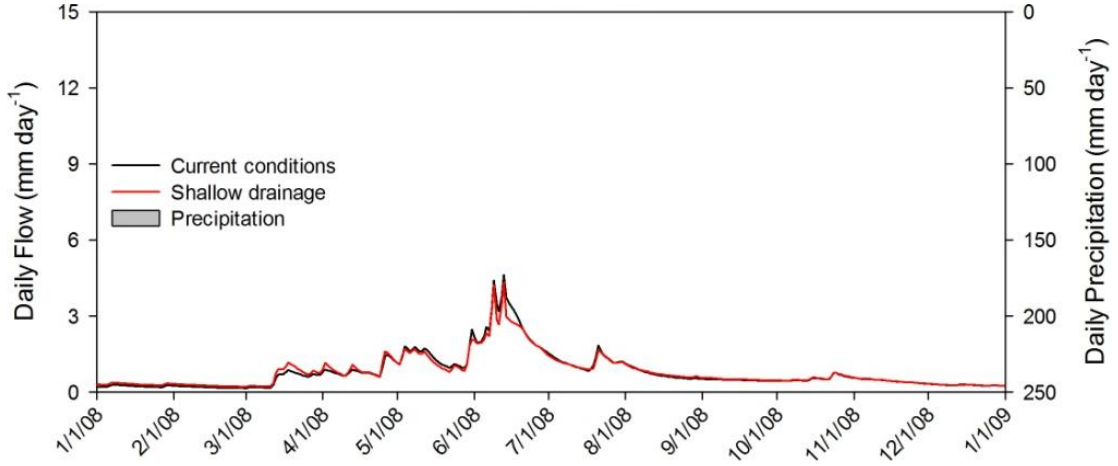

Figure 53 PAL3 current conditions to shallow drainage depth, 2008

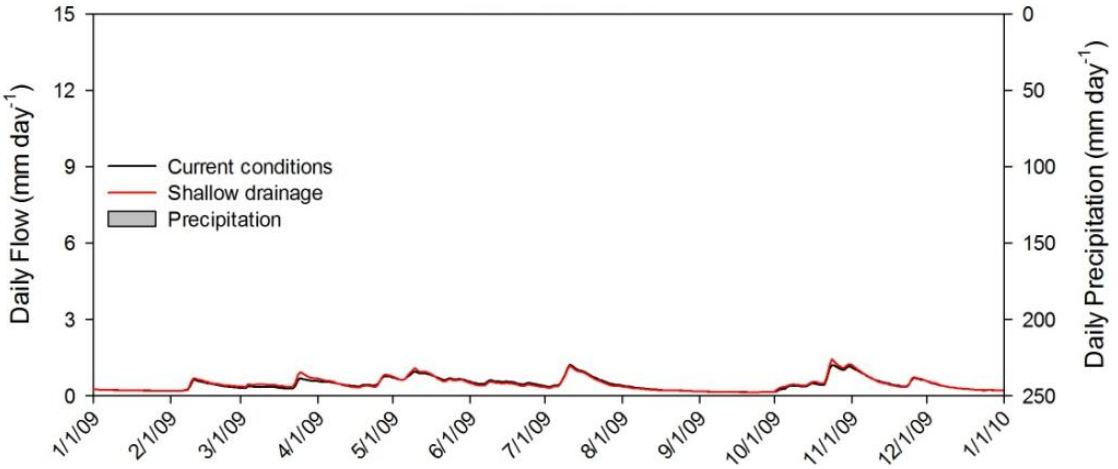

Figure 54 PAL3 current conditions to shallow drainage depth, 2009

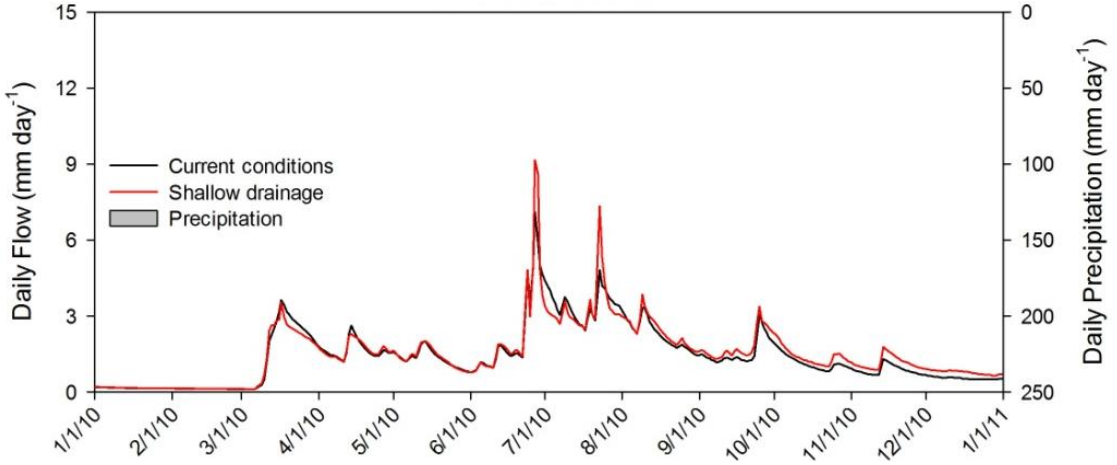

Figure 55 PAL3 current conditions to shallow drainage depth, 2010

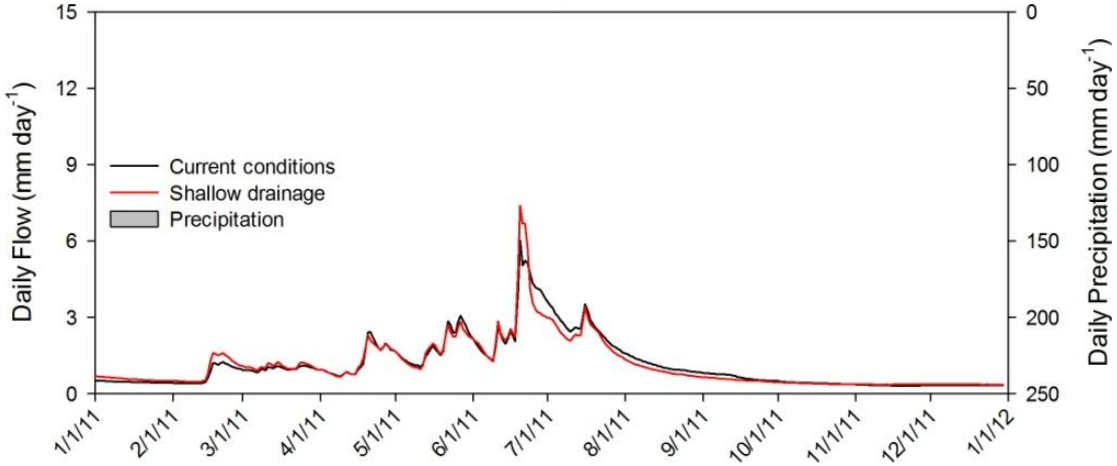

Figure 56 PAL3 current conditions to shallow drainage depth, 2011

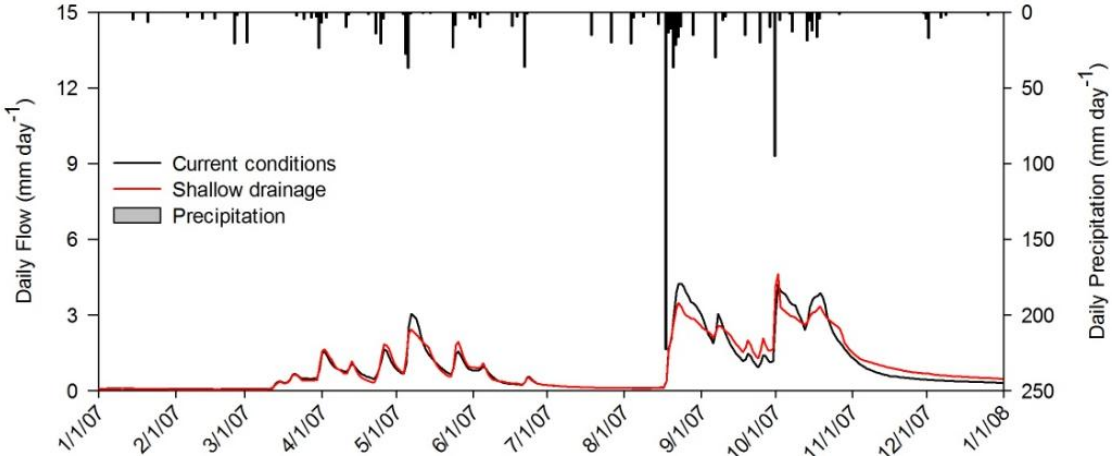

Figure 57 PAL5 current conditions to shallow drainage depth, 2007

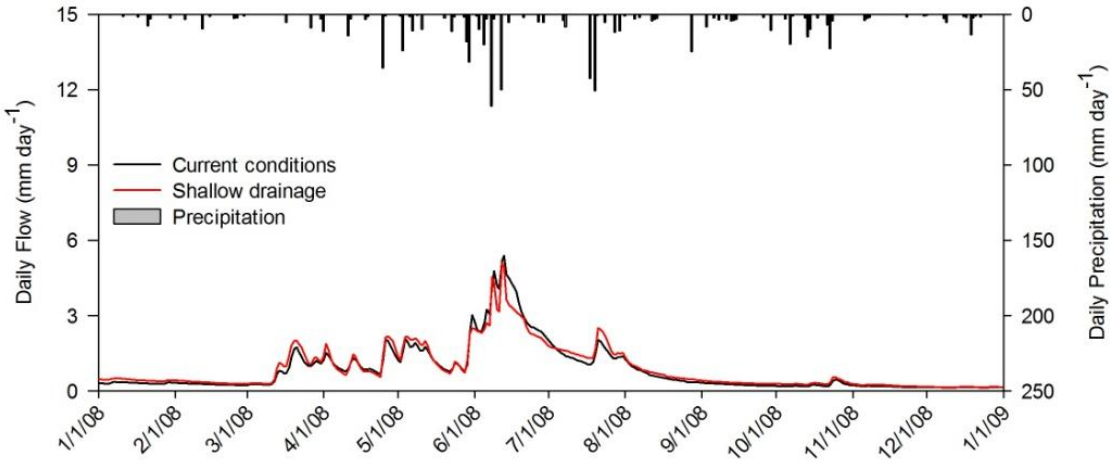

Figure 58 PAL5 current conditions to shallow drainage depth, 2008

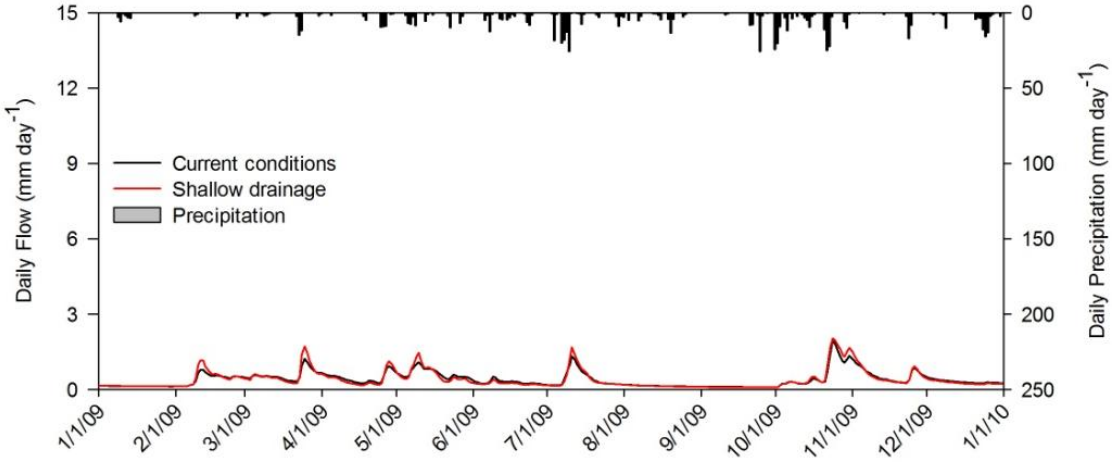

Figure 59 PAL5 current conditions to shallow drainage depth, 2009

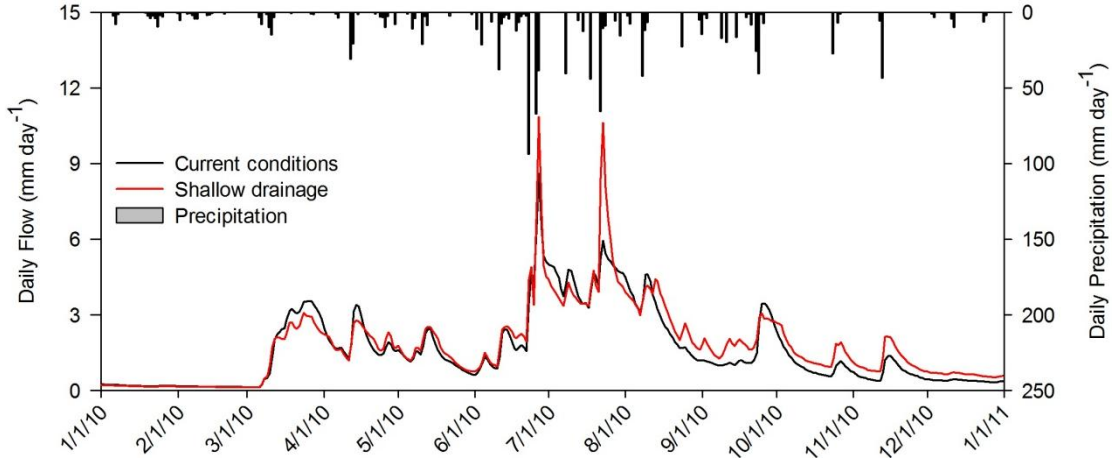

Figure 60 PAL5 current conditions to shallow drainage depth, 2010

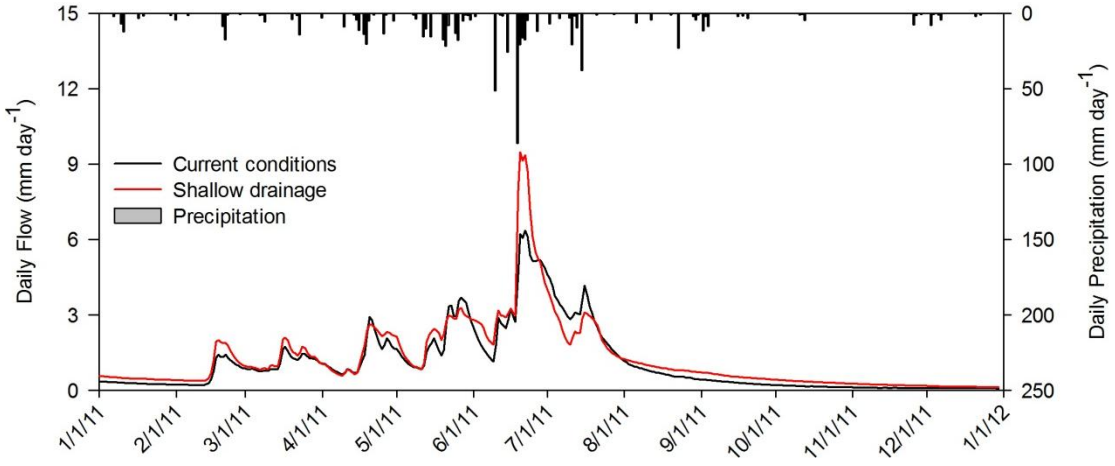

Figure 61 PAL5 current conditions to shallow drainage depth, 2011

5.3.2 Water Balance Analysis

An annual water balance comparison shows remarkable similarities between conventional and shallow drainage, evapotranspiration, surface runoff, and total flow were all within 10% difference with current conditions in PAL3 and PAL5, as shown in Tables 24 and 25. Total flow was increased, mainly through increased surface runoff up from an annual average of 6.0 mm to 13.4 mm in PAL3 and 3.7 mm to 23.1 mm in PAL5.

Table 26 PAL3 water balance comparison of current conditions to shallow drainage

Year	PAL3	Current Conditions					Shallow drainage depth, 0.75 m as opposed to 1.2 m				
	PPT	ET	Δ_S	OVL	SUBD	TOT	ET	Δ_S	OVL	SUBD	TOT
2007	1060	606	99	4.1	279.9	280.0	598	110	7.2	270.3	277.5
2008	767	473	-22	5.8	280.7	286.5	474	-19	5.7	283.5	289.2
2009	752	512	13	0.0	160.5	160.5	508	12	0.8	162.9	163.6
2010	1162	597	33	16.3	509.1	525.4	554	20	42.3	517.2	559.5
2011	759	505	-137	10.2	403.9	414.1	496	-123	24.9	383.5	408.4
Mean	900	537	-3	7.3	326.8	334.1	530	0	16.2	323.5	339.7

PPT – precipitation; ET – evapotranspiration; ΔS – change in subsurface storage; OVL – surface runoff; SUBD – subsurface drainage

Table 27 PAL5 water balance comparison of current conditions to shallow drainage

Year	PAL5	Current Conditions					Shallow drainage depth, 0.75 m as opposed to 1.2 m				
	PPT	ET	Δ_S	OVL	SUBD	TOT	ET	Δ_S	OVL	SUBD	TOT
2007	1060	585	108	1.3	323.1	324.4	564	118	6.7	327.0	333.7
2008	767	478	-41	3.3	301.9	305.2	467	-42	8.0	315.3	323.3
2009	752	510	29	0.0	141.6	141.6	508	27	0.1	142.7	142.8
2010	1162	574	23	11.7	576.4	588.1	478	30	77.9	575.0	652.9

2011	759	503	-153	6.8	390.4	397.2	455	-153	48.2	410.6	458.7
Mean	900	530	-42	4.6	346.7	351.4	494	-21	28.2	354.1	383.3

PPT – precipitation; ET – evapotranspiration; ΔS – change in subsurface storage; OVL – surface runoff; SUBD – subsurface drainage

Table 28 Percent (%) change from baseline values for PAL3 and PAL5 with shallow drainage replacing conventional drainage

Year	PAL3 percent (%) change from baseline values					PAL5 percent (%) change from baseline values				
	ΔET	Δ_S	ΔOVL	ΔSUB	ΔTOT	ΔET	Δ_S	ΔOVL	ΔSUB	ΔTOT
2007	-1	11	75	-3	-2	-3	9	393	0	2
2008	0	-15	-2	1	1	-2	1	141	4	6
2009	-1	-6	---	1	2	0	-6	---	1	1
2010	-7	-39	159	2	7	-16	36	561	-1	10
2011	-2	-10	144	-5	-1	-10	0	589	5	15
Mean	-2	-104	122	-1	2	-7	-42	500	2	8

Δ ET – change in evapotranspiration; ΔS – change in subsurface storage; ΔOVL – change in overland flow; ΔSUB – change in subsurface flow; ΔTOT – change in total flow

5.4 No Drainage Infrastructure

In order to investigate the impact that subsurface drainage has on agricultural watersheds, it is useful to simulate watersheds with row crop agriculture in the absence of subsurface drainage. In contrast to other simulations, this scenario will illuminate only the effects of drainage, as opposed to drain depth or land use. Even though a shift to non-drained agriculture in the Des Moines lobe is not expected, it is a useful exercise to provide evidence for benefits of drainage that may not be as intuitive as controlling moisture content of the soil to ensure ease of planting, growth, and harvest.

5.4.1 Hydrograph Analysis

Figures 62-71 show a clear relationship between increased peak flow events and the absence of subsurface drainage infrastructure. Peak flows increased in intensity by 500-2000 % in PAL3 and similar rates in PAL5. Like the scenario with shallow drainage, no drainage has an increased soil volume able to store water. This leads to more surface flow in wet periods than would occur with current drainage practices. In addition to increased peak flow values, the frequency of peak flows, defined by total flow above 5 mm, also increased in both watersheds with 25 occurrences of simulated peak flows over 5 mm as opposed to two occurrences with current conditions in PAL3 throughout the simulation period. This significant increase in frequency and intensity of high flow events could allow flash flooding

to be a common event in a landscape dominated by non drained agriculture in the Des Moines lobe and areas of similar topography and soil composition.

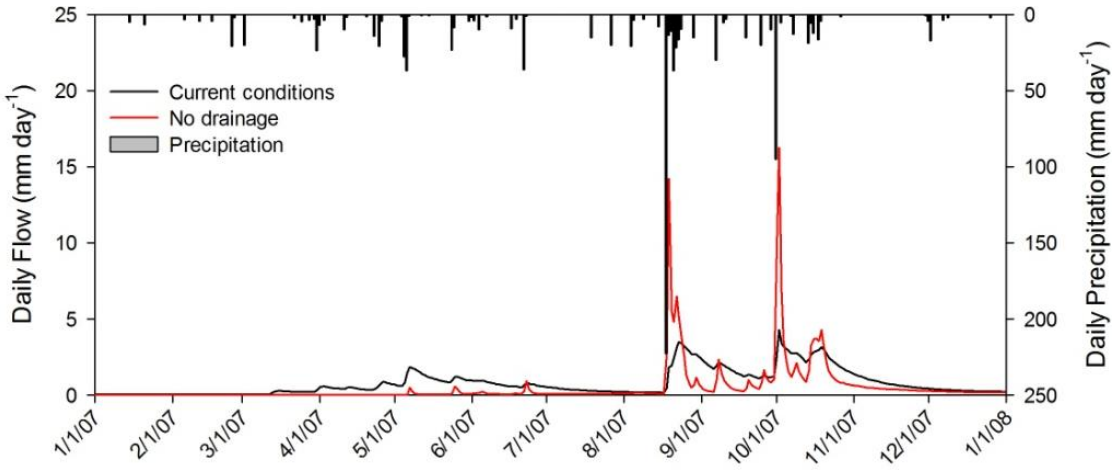

Figure 62 PAL3 current conditions to row crop agriculture without drainage, 2007

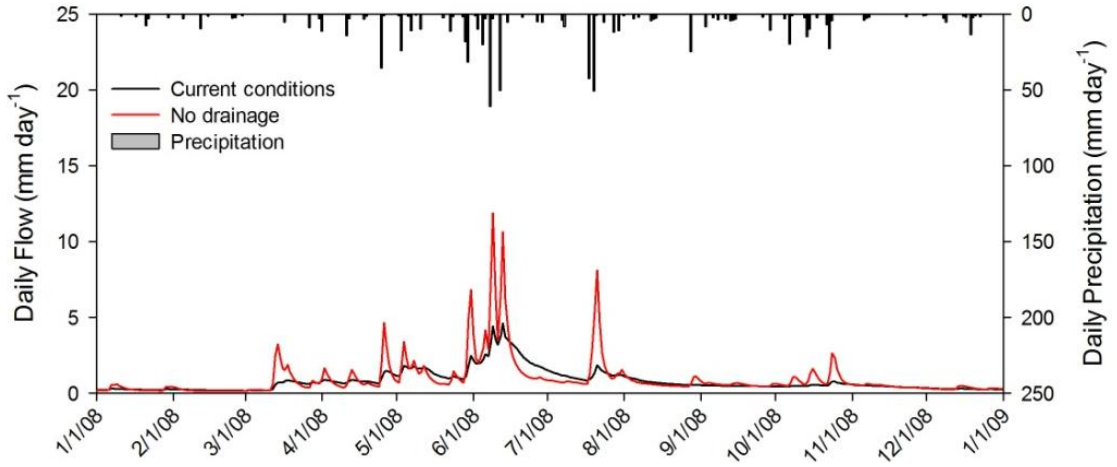

Figure 63 PAL3 current conditions to row crop agriculture without drainage, 2008

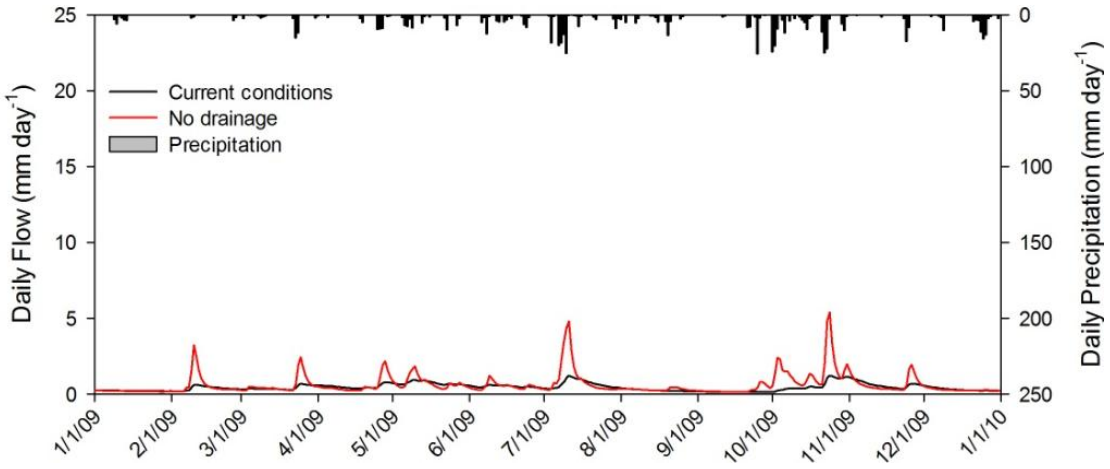

Figure 64 PAL3 current conditions to row crop agriculture without drainage, 2009

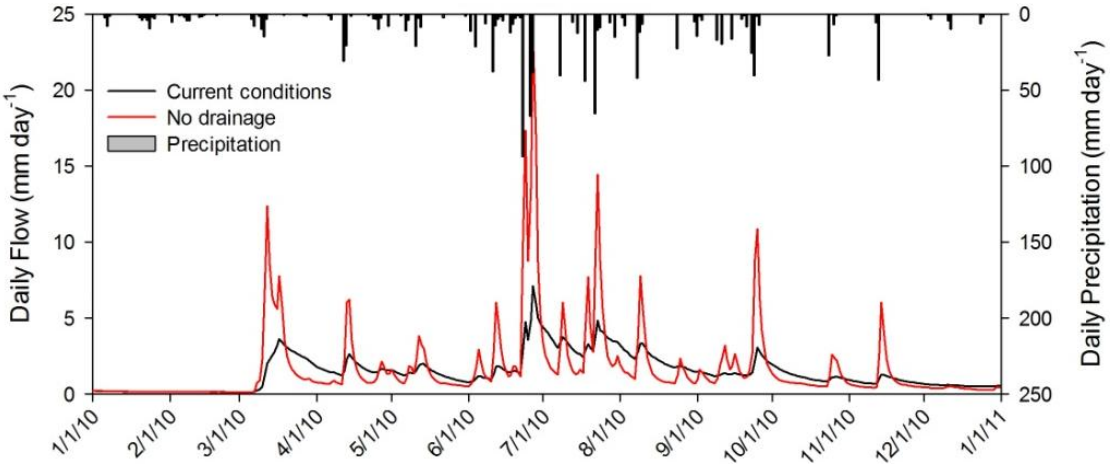

Figure 65 PAL3 current conditions to row crop agriculture without drainage, 2010

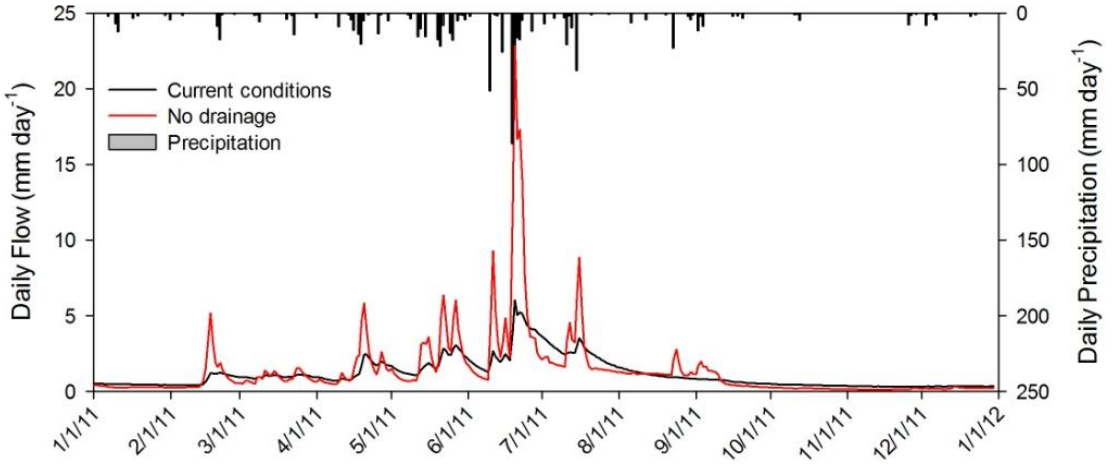

Figure 66 PAL3 current conditions to row crop agriculture without drainage, 2011

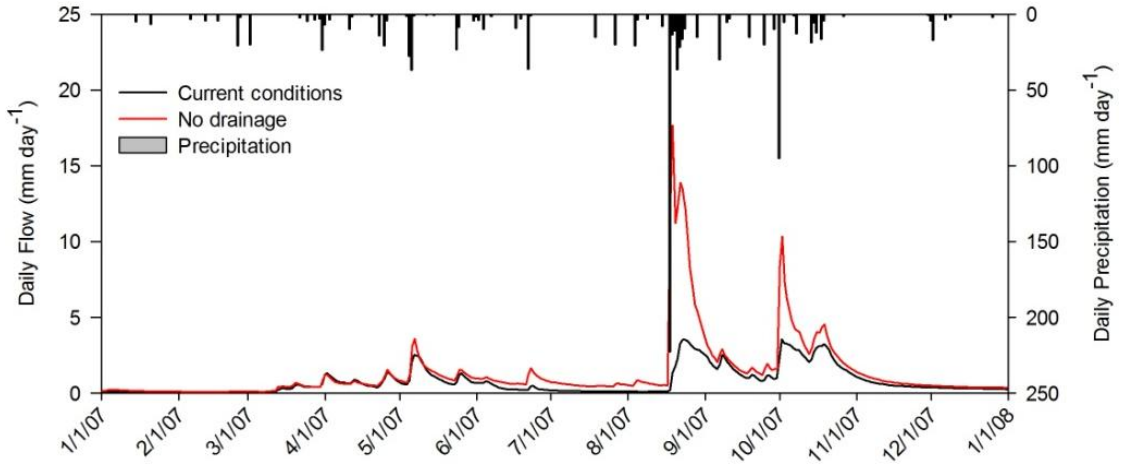

Figure 67 PAL5 current conditions to row crop agriculture without drainage, 2007

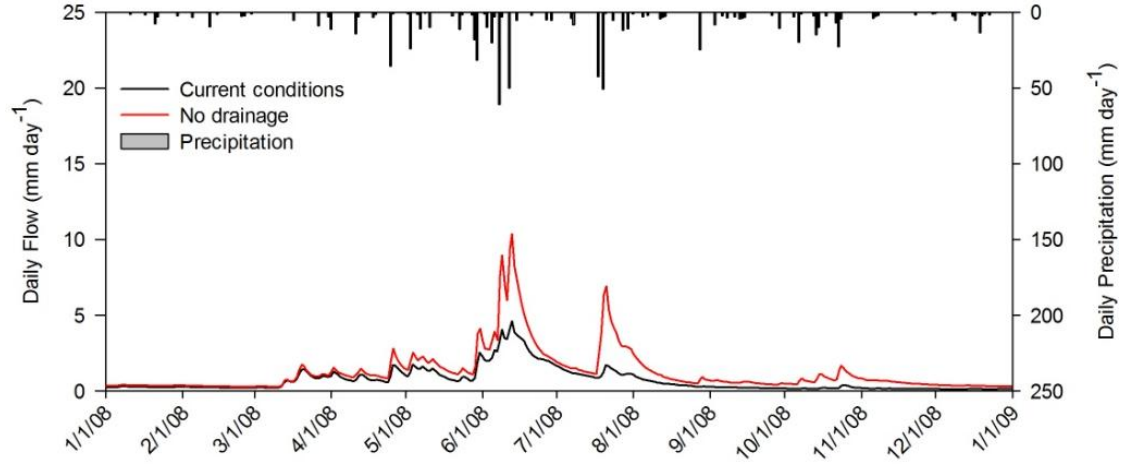

Figure 68 PAL5 current conditions to row crop agriculture without drainage, 2008

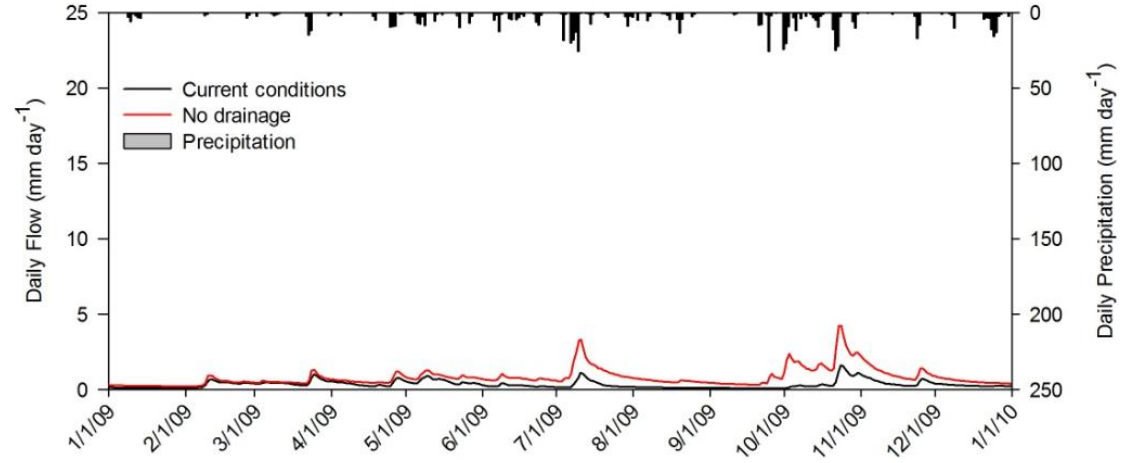

Figure 69 PAL5 current conditions to row crop agriculture without drainage, 2009

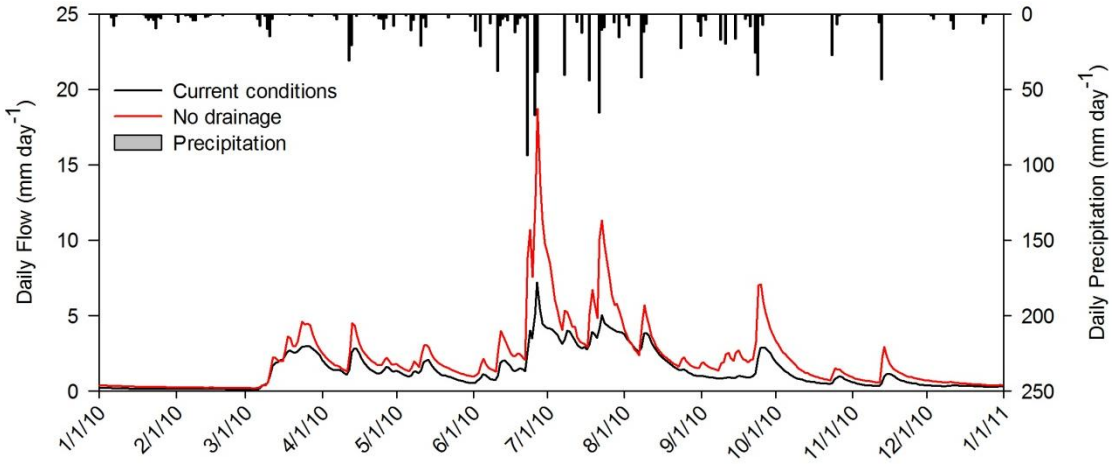

Figure 70 PAL5 current conditions to row crop agriculture without drainage, 2010

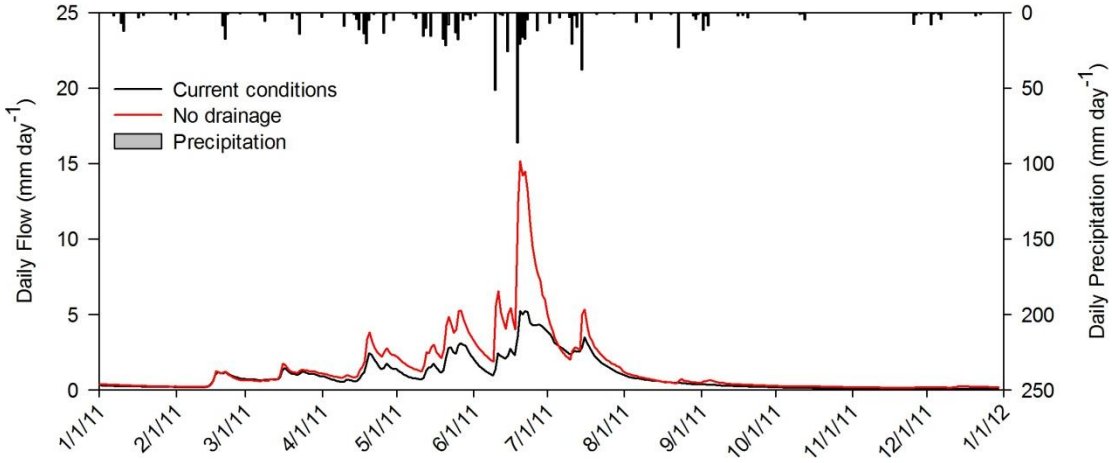

Figure 71 PAL5 current conditions to row crop agriculture without drainage, 2011

5.4.2 Water Balance Analysis

The annual water balance in Tables 26 and 27 provide evidence as to the hydrological impact on the watershed in a scenario absent of drainage. Evapotranspiration decreased by 15% and 34% (68 mm and 153 mm) in PAL3 and PAL5, respectively. This was offset by an increase in total flow of 13% and 45% (25 mm and 132 mm) in PAL3 and PAL5, respectively, with the remaining decrease in ET balanced by increases in subsurface storage and recharge. PAL5 results seem to show a larger magnitude of change from current conditions. This may in part, be due to increased overland storage in PAL3 compared to PAL5, while the less irregular surface topography of PAL5 also allows for a more even release of surface runoff. The flashy nature of surface runoff in PAL3 and periods of PAL5 decrease the residence time of water before export out of the watershed, which in turn, decreases the water available for

ET processes. In addition, without subsurface drainage water is allowed to saturate the upper profile of the unsaturated zone, which also increases the amount of water available for deep recharge into the groundwater supply.

Table 29 PAL3 water balance comparison of current conditions to row crop agriculture without drainage infrastructure

Year	PAL3	Current Conditions					Row crop agriculture without drainage infrastructure				
	PPT	ET	Δ_S	OVL	SUBD	TOT	ET	Δ_S	OVL	SUBD	TOT
2007	1060	606	99	4.1	279.9	280.0	557	139	183.0	0.0	183.0
2008	767	473	-22	5.8	280.7	286.5	402	-16	352.5	0.0	352.5
2009	752	512	13	0.0	160.5	160.5	443	9	224.0	0.0	224.0
2010	1162	597	33	16.3	509.1	525.4	491	-2	626.2	0.0	626.2
2011	759	505	-137	10.2	403.9	414.1	368	-57	499.7	0.0	499.7
Mean	900	537	-3	7.3	326.8	334.1	452	73	377.1	0.0	377.1

PPT – precipitation; ET – evapotranspiration; ΔS – change in subsurface storage; OVL – surface runoff; SUBD – subsurface drainage

Table 30 PAL5 water balance comparison of current conditions to row crop agriculture without drainage infrastructure

Year	PAL5	Current Conditions					Row crop agriculture without drainage infrastructure				
	PPT	ET	Δ_S	OVL	SUBD	TOT	ET	Δ_S	OVL	SUBD	TOT
2007	1060	585	108	1.3	323.1	324.4	393	85	478.8	0.0	478.8
2008	767	478	-41	3.3	301.9	305.2	306	-24	456.8	0.0	456.8
2009	752	510	29	0.0	141.6	141.6	354	17	292.1	0.0	292.1
2010	1162	574	23	11.7	576.4	588.1	373	12	787.1	0.0	787.1
2011	759	503	-153	6.8	390.4	397.2	308	-81	523.4	0.0	523.4
Mean	900	530	-42	4.6	346.7	351.4	347	2	509.5	0.0	509.5

PPT – precipitation; ET – evapotranspiration; ΔS – change in subsurface storage; OVL – surface runoff; SUBD – subsurface drainage

Table 31 Percent (%) change from baseline values for PAL3 and PAL5 with no drainage infrastructure

Year	PAL3 percent (%) change from baseline values					PAL5 percent (%) change from baseline values				
	ΔET	Δ_S	ΔOVL	ΔSUB	ΔTOT	ΔET	Δ_S	ΔOVL	ΔSUB	ΔTOT
2007	-8	40	4347	---	-36	-33	-21	36000	---	49
2008	-15	-29	5966	---	23	-36	-42	13640	---	49
2009	-13	-33	---	---	40	-31	-41	---	---	106
2010	-18	-106	3737	---	19	-35	-48	6677	---	33
2011	-27	-58	4795	---	21	-38	-47	7390	---	32
Mean	-16	-640	5072	---	13	-35	-121	11350	---	44

Δ ET – change in evapotranspiration; ΔS – change in subsurface storage; ΔOVL – change in overland flow; ΔSUB – change in subsurface flow; ΔTOT – change in total flow

CHAPTER VI – SUMMARY AND CONCLUSIONS

The focus of this investigation was to evaluate the ability of the physically based, hydrological model, MIKE SHE to simulate surface runoff, and subsurface flow from drainage infrastructure in the heavily tile drained, agriculturally based, land of North Central Iowa. MIKE SHE was chosen over other models since it has a proven track record in a wide range of applications ranging from mountainous streamflow in Hawaii, to draining marshes in England. The impacts of land use management change on the watershed response were also evaluated in order to determine what effect tile drainage has on peak streamflow during flooding events.

A multisite testing and validation approach was used to determine the applicability of MIKE SHE in the region. PAL3 and PAL5 were two watersheds of similar size (1126 and 1356 ha, respectively), land use (row crop), and soils (drained, Canisteo), and geographical area (Palo Alto County, IA). Meteorological data for the two watersheds including rainfall, air temperature, and evapotranspiration were collected from the same weather stations over the entire simulation period (2006-2011). The PAL3 watershed was used for initial model set up and testing, while the PAL5 watershed was used for validation. The first year in both simulations (2006) was used for initialization of internal parameters. During initial testing, it was found that the model is sensitive to drainage time constant, macropore flow, and detention storage for the simulation period.

The MIKE SHE annual water balance during testing and validation simulations had error of less than 3% over the entire simulation period. The seasonal water balance showed the relationship that weather patterns and crop growth cycles have on the hydrological equilibrium of the watersheds. Heavy rainfall in spring before crops were established led to more overland flow, while established crops in summer produced the bulk of evapotranspiration for the year. Crop growth also led to a deficit in subsurface storage during summer months, while precipitation over winter months led to an increase of water being stored in the soil profile since sinks, such as plant uptake and evapotranspiration, are generally not present to a high degree in winter months. There is also an interesting lag effect that drainage has on the seasonal water balance, falls that follow wetter than average

summers (2007 and 2010) will show a higher amount of subsurface drainage flow than total precipitation for the current fall.

The statistical analyses showed that correlation between observed and modeled daily streamflow was good, as represented by coefficients of determination ranging from 0.13 to 0.79 for the testing simulation and 0.29 to 0.96 for the validated model. The mean Nash-Sutcliffe efficiency value for the testing period was 0.62 and 0.73 during validation, with a high value of 0.82 during the year 2008. This shows that MIKE SHE is more than suitable for modeling streamflow in heavily tile drained agricultural land, like that found in the Des Moines lobe in Iowa.

The investigation also covered hypothetical land use management change scenarios including land use conversion to perennial grassland, both with and without subsurface drainage infrastructure, and shallow depth (0.75 m) subsurface drainage infrastructure as opposed to conventional depth (1.2 m) subsurface drainage infrastructure, and elimination of subsurface drainage from the watersheds. In both watersheds, converting to perennial grassland increases annual ET amounts and decreases overall streamflow. While eliminating drainage infrastructure entirely, as in pre-settlement conditions, causes streamflow to chiefly stem from surface runoff. Although the pre-settlement conditions scenario had slightly less annual streamflow, a greater percent of the flow came with surface runoff events, as opposed to a relatively steady drainage output. Also, when high intensity rainfall events completely saturate the soil peak flow from non-drained scenarios exceeded peak flow from current conditions in both PAL3 and PAL5. This shows the importance of subsurface drainage with respect to intense precipitation events. When comparing shallow drainage to scenarios that excluded subsurface drainage, both with and without land use conversion, there is a considerable decrease in surface flow and peak flow events. The difference can be attributed to an increased ability for the soil to retain water in periods of high precipitation; the drains keep the soil above from becoming completely saturated. The following tables 32 and 33 show the comparison of overall change from baseline values for PAL3 and PAL5, as well as percent change from baseline flow values for surface and subsurface flow.

Table 32 Scenario comparison of overall change from baseline surface and subsurface flow values for PAL3 and PAL5

Scenario conditions	PAL3			PAL5		
	Average surface flow, mm	Average drainage flow, mm	Total flow, mm	Average surface flow, mm	Average drainage flow, mm	Total flow, mm
Current conditions	7.1	327.0	334.1	4.6	346.0	350.6
Perennial grass, with drainage	0.3	188.8	189.1	0.7	211.4	212.1
Perennial grass, pre-settlement	165.9	---	165.9	251.6	---	251.6
Shallow drainage	16.2	323.5	339.7	28.2	354.1	383.3
Row crop, no drainage	377.1	---	377.1	509.5	---	509.5

Table 33 Scenario comparison of percent overall change from baseline surface and subsurface values for PAL3 and PAL5

Scenario conditions	PAL3			PAL5		
	Surface flow change (%)	Drainage flow change (%)	Total Flow change (%)	Surface flow change (%)	Drainage flow change (%)	Total Flow change (%)
Current conditions	---	---	---	---	---	---
Perennial grass, with drainage	-95	-42	-43	-85	-36	-40
Perennial grass, pre-settlement	2180	---	-50	5260	---	-29
Shallow drainage	122	-1	2	500	2	8
Row crop, no drainage	5070	---	13	11350	---	44

Since damaging flood events are mainly caused by levee, and stream bank overtopping, as opposed to sustained heavy flow below design limits of water storage structures, peak flow of flood events were considered to be the driving force in devastating floods, as opposed to overall annual, or seasonal streamflow. Several factors may affect annual floods associated with peak flow events: climate change, decrease in storage capabilities of wetlands, row crop monoculture, but this investigation has shown drainage infrastructure does not increase the severity of peak flow events associated with flood damage and in fact, has the potential to reduce peak flow during potential flood situations at the scale studied within this investigation.

This study shows that the model performed well in simulating surface runoff and subsurface drainage in two watersheds of heavily tile drained agricultural land. Furthermore, it can be used to aid in decision making strategies in regards to land use management change. Future studies could be done in similar watersheds to strengthen the conclusions done in this

investigation. Alternatively, future studies in watersheds with dissimilar soil and weather conditions but still subject to subsurface drainage would help strengthen the relationship that drainage has on watershed hydrology characteristics.

REFERENCES

Abbott, M.B., J.C. Bathurst, J.A Cunge, P.E. O'Connell, and J. Rasmussen. 1986a. An introduction to the European Hydrological System - Système Hydrologique Européen, "SHE", 1: History and philosophy of a physically-based, distributed modelling system. *Journal of Hydrology*. 87(1): 45-59.

Abbott, M.B., J.C. Bathurst, J.A Cunge, P.E. O'Connell, and J. Rasmussen. 1986b. An Introduction to the European Hydrological System - Système Hydrologique Européen, "SHE", 2: Structure of a physically based, distributed modeling system. *Journal of Hydrology*. 87(1): 61-77.

Al-Khudhairy, D. H. A., Thompson, J. R., Gavin, H., 1999. Hydrological modeling of a drained grazing marsh under agricultural land use and the simulation of restoration management scenarios. *Hydrological Sciences Journal*. 44(6): 943-971

Baker, J.L., Melvin, S.W., Lemke, D.W., Lawlor, P.A., Crumpton, W.G., Helmers, M.J., 2004. Subsurface drainage in Iowa and the water quality benefits and problem. Drainage VIII Proceedings of the Eighth International Symposium. ASAE Meeting Paper No. 701P0304. St. Joseph, MI

Bedan, E.S., Clausen, J. C., 2009. Stormwater runoff quality and quantity from traditional and low impact development watersheds. Journal of the American Water Resources Association. 44(4): 998-1008

Bengtson, R.L., Carter, C. E., Fouss, J.L., Southwick, L.M., Willis, G.H., 1995. Agricultural drainage and water quality in Mississippi Delta. *Journal of Irrigation and Drainage Engineering*. 121, 292-295.

Brooks, K.N., P.F. Folliott, H.M. Gregersen, and J.L. Thames. 1991. *Hydrology and the Management of Watersheds*. A**m**es, IA: Iowa State University Press.

Carr, R. S., Punthakey J. F., Cooke, R. 1993. *Large scale catchment simulation using the* MIKE SHE model: 1. Process simulation of an irrigation district. *Environmental Management Geo-water and Engineering Aspects: Proceedings of the International Conference on Environmental Geo-water and Engineering Aspects*, 401-405. Robin N. Chowdhury, S.M. Sivakumar, eds. Leiden, The Netherlands: A.A. Balkema

Chow, V.T, D.R. Maidment, and L.W. Mays. 1988. *Applied Hydrology*. New York: McGraw-Hill.

Christiaens K, Feyen J. 2001. Analysis of uncertainties associated with different methods to determine soil hydraulic properties and their propagation in the distributed hydrological MIKE SHE model. *Journal of Hydrology* 246: 63–81.

Christiaens K, Feyen J. 2002. Constraining soil hydraulic parameter and output uncertainty of the distributed hydrological MIKE SHE model using the GLUE framework. *Hydrological Processes*. 16. 373-391.

Dai, Z., Li, C., Trettin, G., et al. 2010. Bi-criteria evaluation of the MIKE SHE model for a forested watershed on the South Carolina coastal plain. *Hydrology and Earth Sciences,*14, 1033-1046.

DHI. 2004. *MIKE SHE User Manual*. Hørsholm, Denmark: Danish Hydraulic Institute.

Dingman, S.L. 2002. *Physical Hydrology*. 2nd ed. Upper Saddle River, New Jersey: Prentice Hall.

Downer, C. W., Ogden, F. L., 2004. GSSHA: Model to simulate diverse stream flow producing processes. Journal of Hydrologic Engineering. 9(3): 161-174.

Eisenlohr L., Bouzelboudjen, M., Király, L., Rossier, Y. 1997. Numerical versus statistical modelling of natural response of a karst hydrogeological system. *Journal of Hydrology* 202(1–4):244–262.

Ella, V. B., Melvin, S. W., Kanwar, R. S., 2002. Inverse three-dimensional groundwater modeling using the finite-difference method for recharge estimation in a glacial till aquitard. *Trans. ASAE*, 45(3): 703-715.

Fereres, E., Soriano, M. A. 2007. Deficit irrigation for reducing agricultural water use. *Journal of Experimental Botony*. 58(2): 147-159.

Fetter, C. W., 2001. Applied Hydrology. 4th ed. New Jersey: Prentice Hall.

Feyen L, Vázquez R, Christiaens K, Sels O, Feyen J. 2000. Application of a distributed physically-based hydrological model to a medium size catchment. *Hydrology and Earth System Sciences* **4**(1): 47–63.

Gardner, W.K., Drendel, M.F., McDonald, G.K., 1994. Effects of subsurface drainage, cultivation and stubble retention on soil porosity and crop growth in a high rainfall area. *Australian Journal of Experimental Agriculture*. 34, 411-418.

Gupta, H. V., S. Sorooshian, and P. O. Yapo. 1999. Status of automatic calibration for hydrologic models: Comparison with multilevel expert calibration. *J. Hydrologic Eng.* 4(2): 135-143.

ISPAID 7.0, 2004. Iowa Soil Properties and Interpretations Database (ISPAID) Version 7.0. Iowa Agriculture and Home Economics Experiment Station, University Extension Service, Iowa State University, Ames, IA.

Jaber, F.H., and S. Shukla. 2005. Hydrodynamic modeling approaches for agricultural storm water impoundments. *Journal of Irrigation and Drainage Engineering.* 131 (4): 307-315.

Janža, Mitja. 2009. Hydrological modeling in the karst area, Rižana spring catchment, Slovenia. Environmental Earth Science. 61:909-920.

Jong, R.D, and K.B. MacDonald. 2001. Water balance components in the Canadian mixed wood ecozone. In: *Sustaining the Global Farm*. (*10th International Soil Conservation Organization Conference*), 1144-1151. D.E. Stott, R.H. Mohtar, and G.C. Steinhardt, eds. West Lafayette, IN: International Soil Conservation Organization, USDA-ARS National Soil Erosion Research Laboratory, and Purdue University. Available at: 99

http://www.tucson.ars.ag.gov/isco/isco10/SustainingTheGlobalFarm/P255-DeJong.pdf#search=%22Water%20Balance%20Components%20In%20The%20Canadian%20Mixed%20Wood%20Ecozone%22 Accessed 28 August 2006.

Kanwar, R.S., Cruse, R.M., Ghaffarzadeh, M., Bakhsh, A., Karlen, D.L., Bailey, T.B., 2005. Corn soybean and alternative cropping systems effected on NO3-N leaching losses in subsurface drainage water. *Applied Engineering in Agriculture*. 21,181-188.

Labat D, Ababou R, Mangin A (2000) Rainfall-runoff relations for karstic springs. Part I: convolution and spectral analyses. Journal of Hydrology 238(3–4):123–148.

Ma, L., J. C. Ascough II, L. R. Ahuja, M. J. Shaffer, J. D. Hanson, and K. W. Rojas. 2000. Root zone water quality model sensitivity analysis using Monte Carlo simulation. *Trans. ASAE* 43(4): 883-895.

McDonald, M.G., and Harbaugh, A.W., 1988, A modular three-dimensional finite-difference ground-water flow model: Techniques of Water-Resources Investigations of the United States Geological Survey, Book 6, Chapter A1, 586 p

Mishra, A., R. Singh, and N.S. Raghuwanshi. 2005. Development and application of an integrated optimization-simulation model for major irrigation projects. *Journal of Irrigation and Drainage Engineering*. 131(6): 504-513.

Newton, Isaac. 1726. Mathematical principles of natural philosophy. English translation based on 3rd Latin edition (1729).

Nippert, J. B., Ocheltree T. W., Skibbe, A. M., et al. 2011a. Linking plant growth responses across topographic gradients in tallgrass prairie. *Oecologia* 166(4):1131-42.

Nippert, J. B., Wieme, R. A., Oceltree, T. W., et al. 2011b. Root characteristics of C4 grasses limit reliance on deep soil water in tallgrass prairie. *Plant Soil* 355(1-2):385-394.

Oogathoo, S., 2009. Runoff simulation in the Canagagigue creek watershed watershed using the MIKE SHE Model. M.S. thesis. Sainte Anne-de-Bellevue, QC: McGill University, Department of Agricultural and Biosystems Engineering.

Punthakey J.F., R. Cooke, N.M. Somaratne, R.S. Carr, and K.K. Watson. 1993. Large-scale catchment simulation using the MIKE-SHE model: 2. Modelling the Berrigin irrigation district. *Environmental Management Geo-water and Engineering Aspects: Proceedings of the International Conference on Environmental Geo-water and Engineering Aspects*, 467-472. Robin N. Chowdhury, S.M. Sivakumar, eds. Leiden, The Netherlands: A.A. Balkema

Quinn JJ, Tomasko D, Kuiper JA (2006) Modeling complex flow in a karst aquifer. *Sed Geology*. 184(3–4):343–351.

Rabalais, N.N., Turner, R.E., Wiseman, Jr., W.J., 2001. Hypoxia in the Gulf of Mexico. *Journal of Environmental Quality*. 30, 320-329.

Refsgaard, J.C, and B. Storm. 1995. MIKE SHE. *In Computer Models of Watershed Hydrology*, 809-846. V.P. Singh, ed. Highlands Ranch, CO: Water Resources Publications.

Reynolds, M. P., Borlaug, N. E., 2006. Impact of breeding on international collaborative wheat improvement. Journal of Agricultural Science. 144: 3-17

Sahoo, G.B, C. Ray, and E.H. De Carlo. 2006. Calibration and validation of a physically distributed hydrological model, MIKE SHE, to predict streamflow at high frequency in a flashy mountainous Hawaii stream. *Journal of Contaminant Hydrology*. In Press.

Sands, G.R., Busman, L.M., Ruger, W.E., Hansen, B., 2003. The impact of drain depth on water quality in a cold climate. In: ASAE Annual International Meeting, Paper no. 032365, Las Vegas, NV, July 20–27, 2003.

Schaap, M. G., Leij, F. J., van Genuchten, M. T., 2001. ROSETTA: a computer program for estimating soil hydraulic parameters with hierarchical pedotransfer functions. *Journal of Hydrology*. 251 (2001) 163-176.

Schwab, G.O, D.D. Fangmeier, W.J. Elliot, and R.K. Frevert. 1993. *Soil and Water Conservation Engineering*. 4th ed. New York: Wiley.

Sevat, E., and A. Dezetter. 1991. Selection of calibration objective functions in the context of rainfall-runoff modeling in a Sudanese savannah area. *Hydrological Sci. J.* 36(4): 307-330.

Shipitalo, M.J., Nuutinen, V., Butt, K.R., 2004. Interaction of earthworm burrows and cracks in a clayey, subsurface drained, soil. Applied Soil Ecology 26, 209-217.

Singh, R., J.C. Refsgaard, L. Yde, G.H. Jorgensen, and M. Thorsen. 1997. Hydraulic-hydrological simulations of canal-command for irrigation water management. *Irrigation and Drainage Systems*. 11(3): 185-213.

Singh, R., K. Subramanian, and J.C. Refsgaard. 1999. Hydrological modeling of a small watershed using MIKE SHE for irrigation planning. *Agricultural Water Management*. 41(3): 149-166.

Singh, R., Helmers, M.J., Qi, Z., 2006. Calibration and validation of DRAINMOD to design subsurface drainage systems for Iowa's tile landscape. Agricultural Water Management 85, 221-232.

Skaggs, R.W., Broadhead, R.G., 1982. Drainage strategies and peak flood flows. ASAE Paper, St. Joseph, MI.

Skaggs, R.W., Breve, M.A., Gilliam, J.W., 1994. Hydrologic and water quality impact of agricultural drainage. Critical Reviews in Environmental Science and Technology 24, 1-32.

Thompson, J.R., H.R. Sorenson, H. Gavin, and A. Refsgaard. 2004. Application of the coupled MIKE SHE/MIKE 11 modeling system to a lowland wet grassland in southeast England. *Journal of Hydrology*. 293(2): 151-179.

Thorp, K. R., Jaynes, D. B., Malone, R. W., 2008. Simulating the long-term performance of drainage water management across the Midwestern United States. *Trans. ASAE* 51(3): 961-976.

Traiantafyllou, G. N., Tsonis, A. A., 1994. Assessing the ability of the Köppen system to delineate the general world pattern of climates. *Geophysical Research Letters*. 21(25): 2809-2812.

Vázquez, R. F., Feyen, L., Feyen, J., Refsgaard, J. C. 2002. Effect of grid size on effective parameters and model performance of the MIKE-SHE code. *Hydrological Processes*. 16: 355-372.

Van Liew, M. W., J. G. Arnold, and J. D. Garbrecht. 2003. Hydrologic simulation on agricultural watersheds: Choosing between two models. *Trans. ASAE* 46(6): 1539-1551.

Ward, A.D., and S.W. Trimble. 2004. *Environmental Hydrology*. Boca Raton, Fl.: Lewis Publishers.

Zhou, X., Helmers, M. Qi, Z. 2011. Field scale modeling of subsurface tile drainage using MIKE SHE. Submitted to *Applied Engineering in Agriculture.*

APPENDIX

SURFACE RUNOFF AND SUBSURFACE DRAINAGE HYDROGRAPHS

A. 1. Initial Parameter Sensitivity

The following images will show the relationship that drainage time constant and detention storage have on surface and subsurface runoff.

A. 1. 1. Drainage Time Constant

Surface Runoff

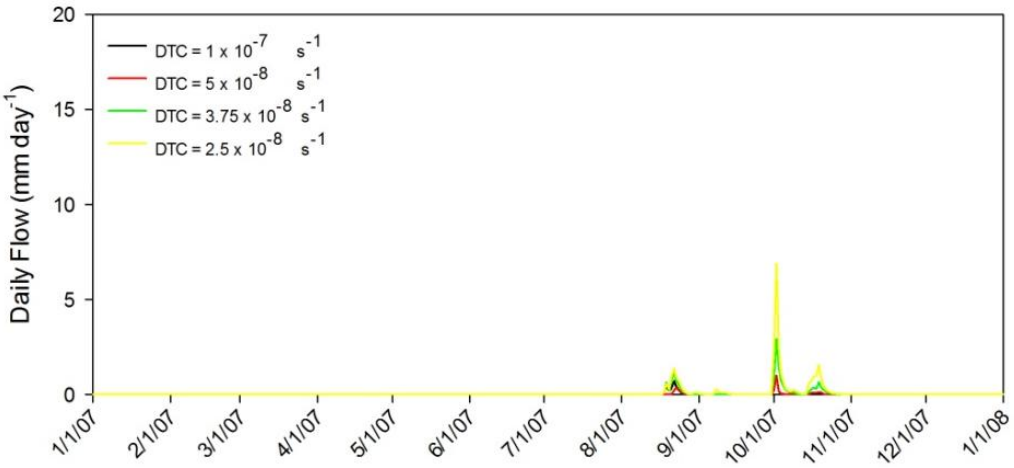

Figure 72 Surface flow for drainage time constant comparison in PAL3, 2007

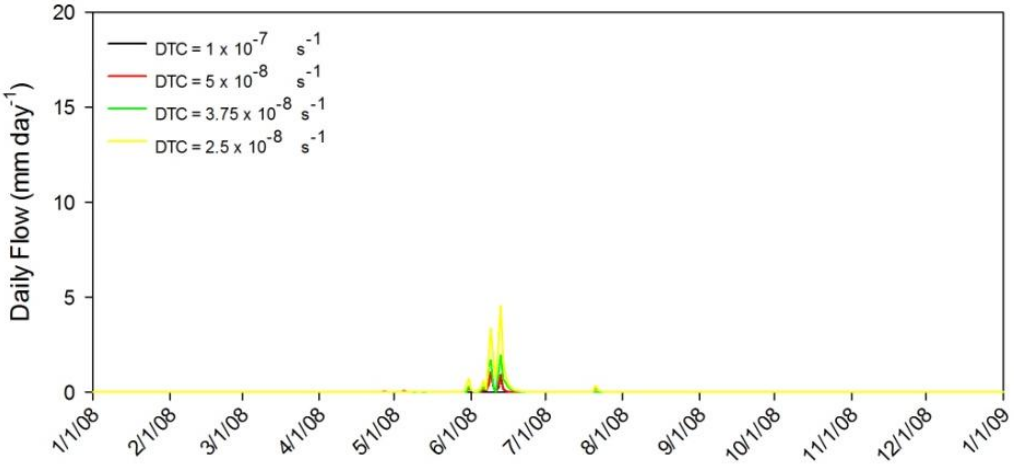

Figure 73 Surface flow for drainage time constant comparison in PAL3, 2008

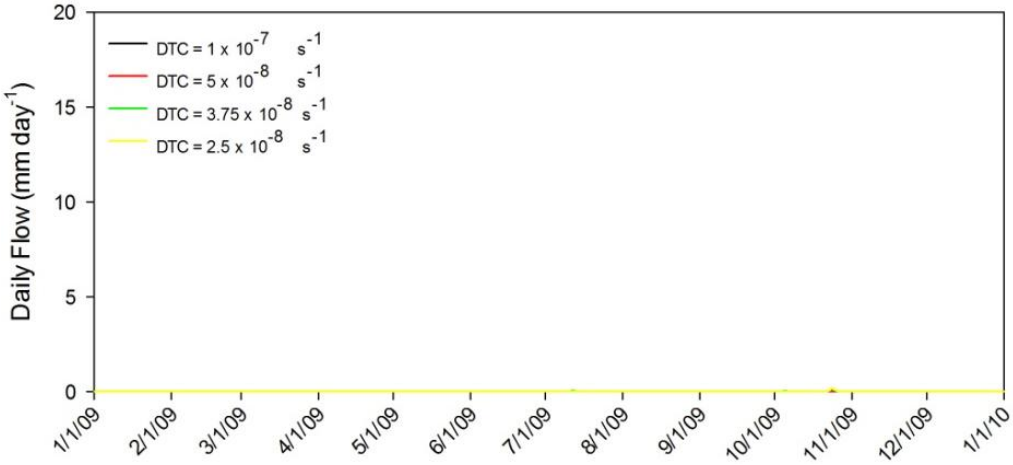

Figure 74 Surface flow for drainage time constant comparison in PAL3, 2009

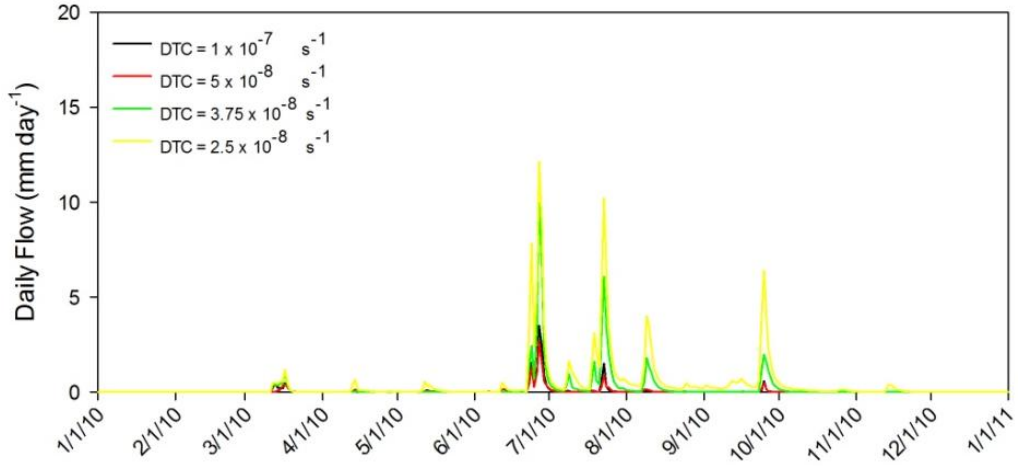

Figure 75 Surface flow for drainage time constant comparison in PAL3, 2010

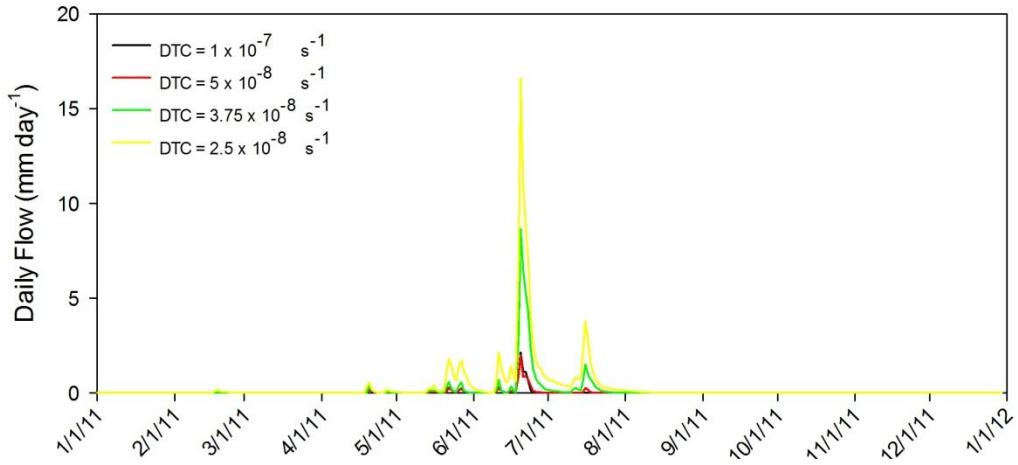

Figure 76 Surface flow for drainage time constant comparison in PAL3, 2011

Subsurface flow

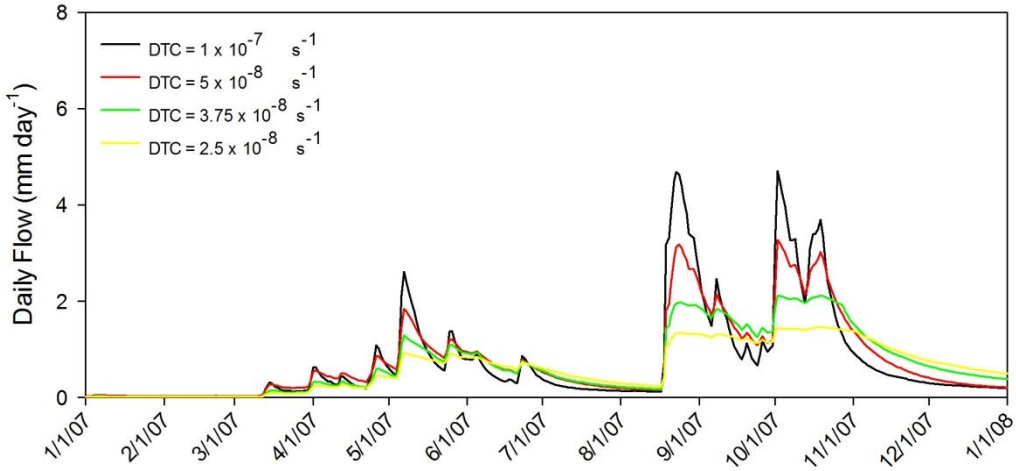

Figure 77 Subsurface flow for drainage time constant comparison in PAL3, 2007

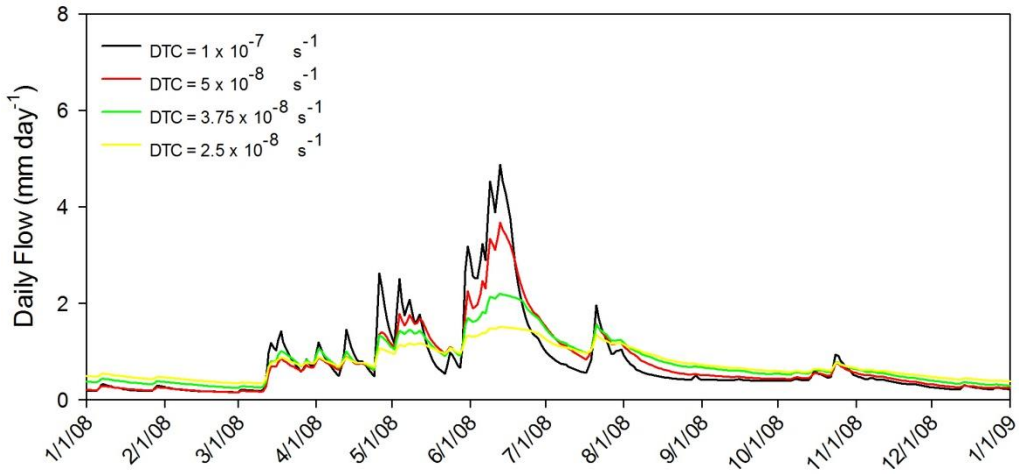

Figure 78 Subsurface flow for drainage time constant comparison in PAL3, 2008

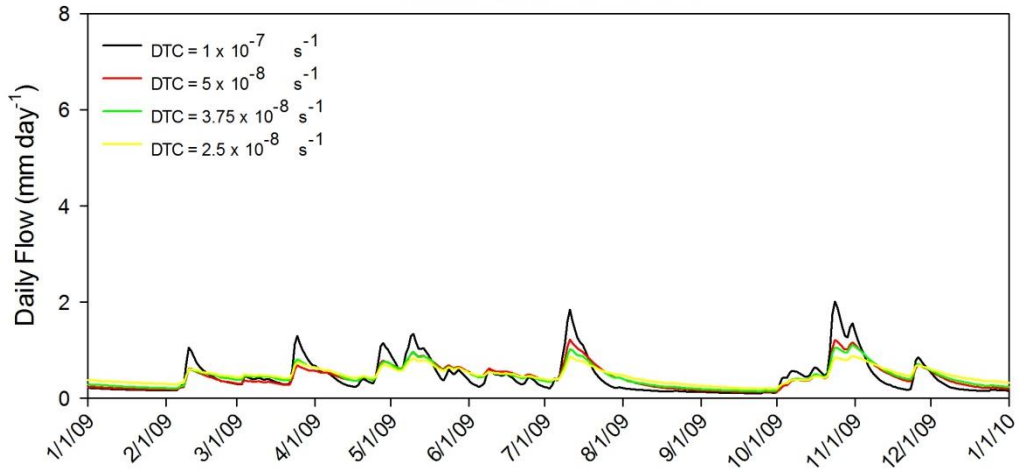

Figure 79 Subsurface flow for drainage time constant comparison in PAL3, 2009

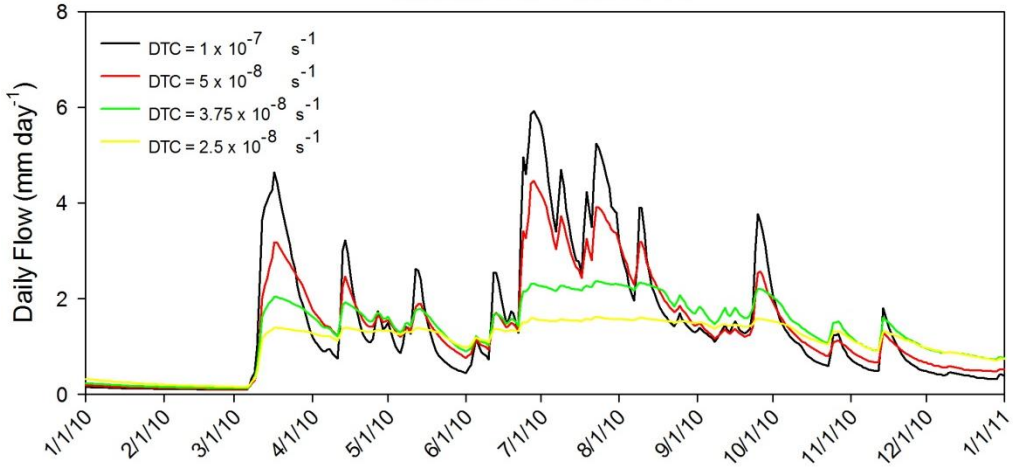

Figure 80 Subsurface flow for drainage time constant comparison in PAL3, 2010

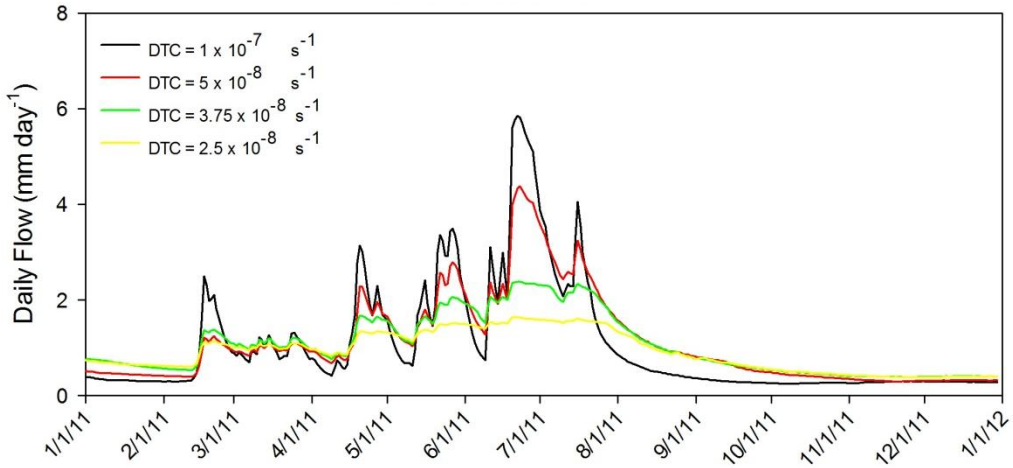

Figure 81 Subsurface flow for drainage time constant comparison in PAL3, 2011

A. 1. 2. Detention Storage

Surface Flow

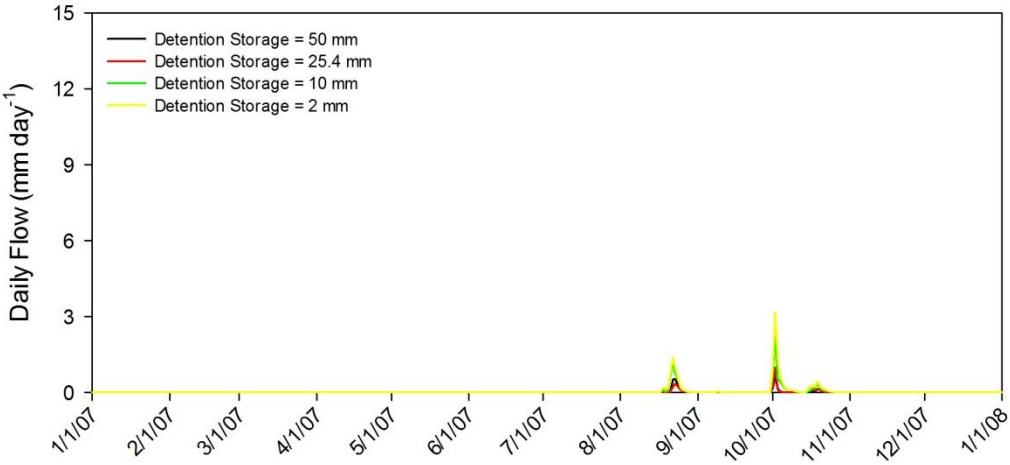

Figure 82 Surface flow for detention storage comparison in PAL3, 2011

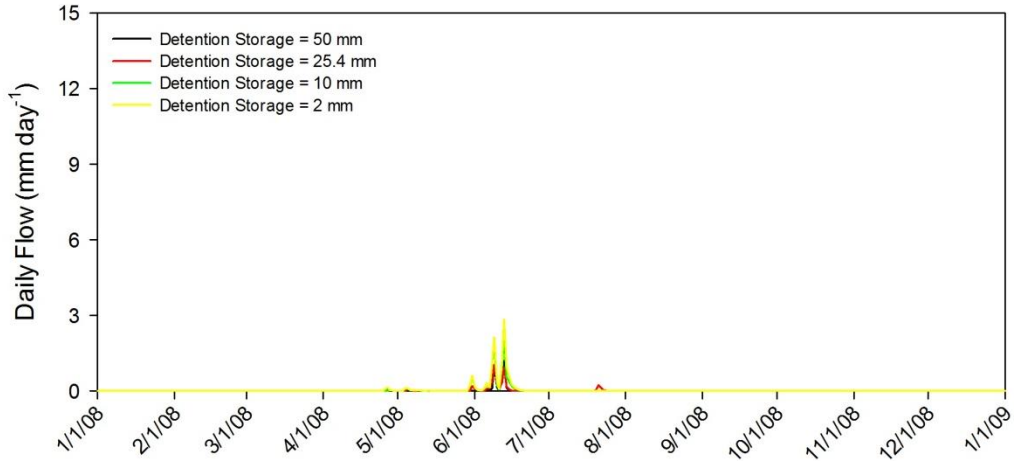

Figure 83 Surface flow for detention storage comparison in PAL3, 2008

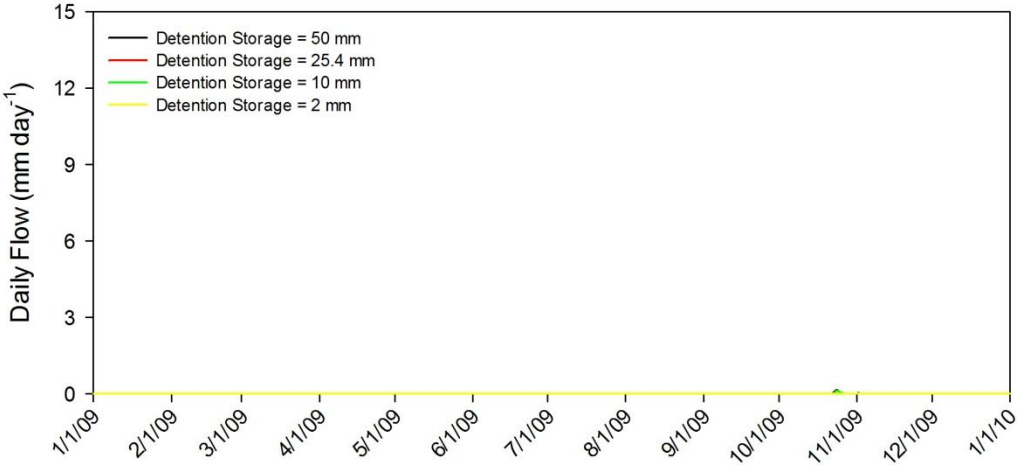

Figure 84 Surface flow for detention storage comparison in PAL3, 2009

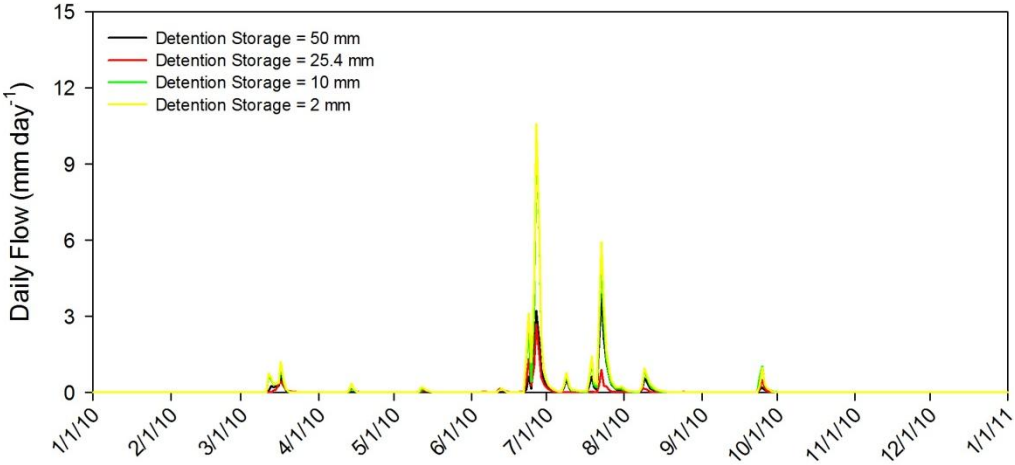

Figure 85 Surface flow for detention storage comparison in PAL3, 2010

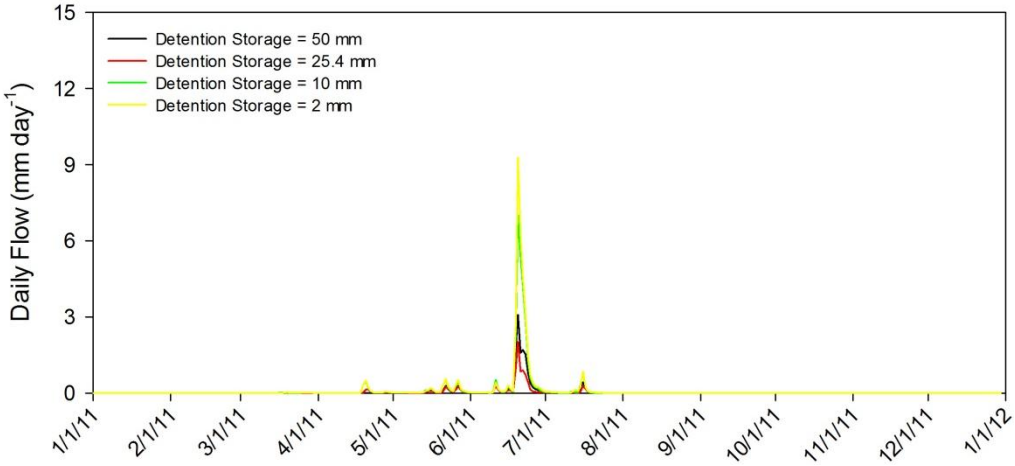

Figure 86 Surface flow for detention storage comparison in PAL3, 2011

Subsurface Flow

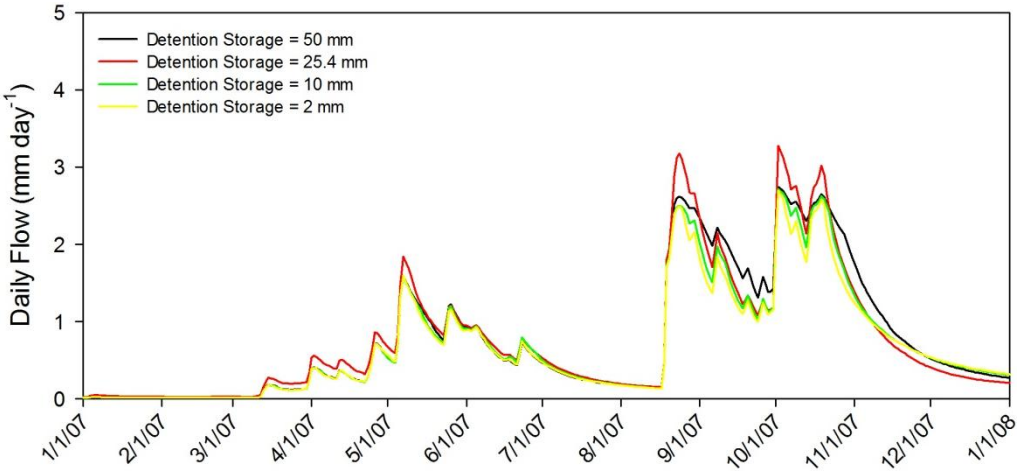

Figure 87 flow for detention storage comparison in PAL3, 2007

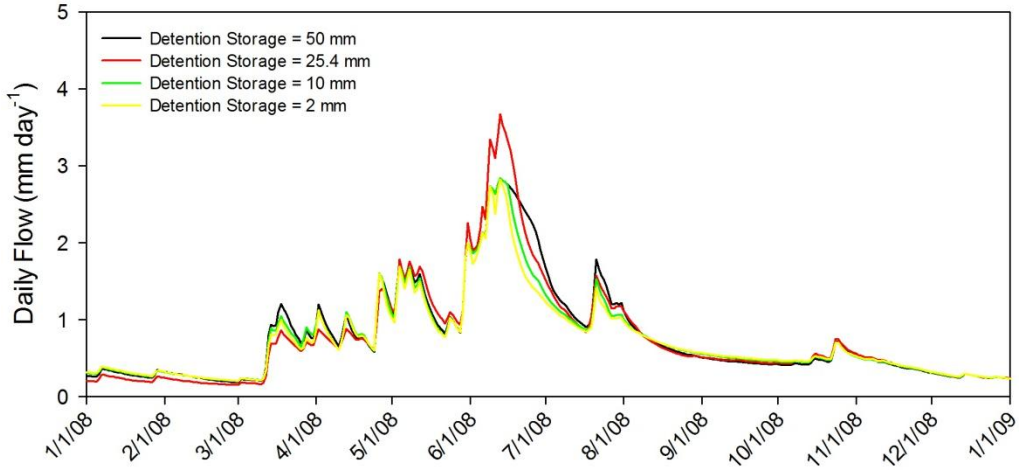

Figure 88 flow for detention storage comparison in PAL3, 2008

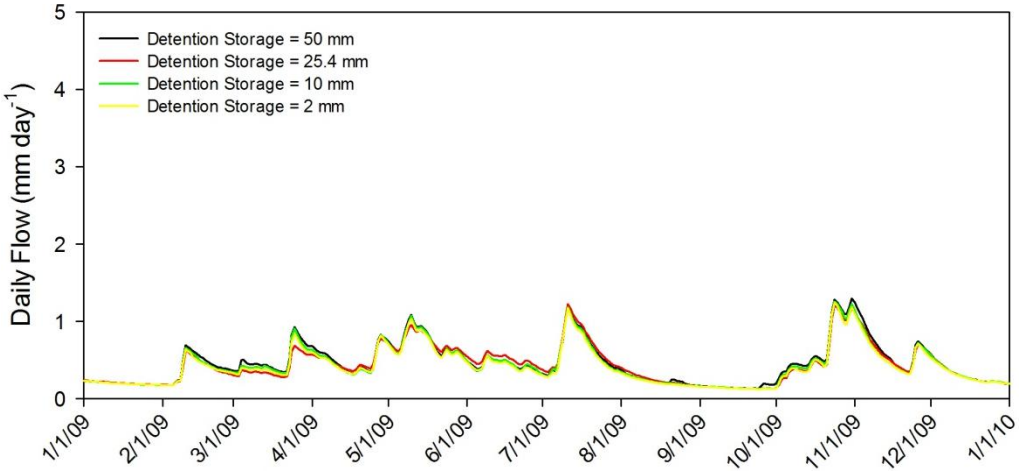

Figure 89 flow for detention storage comparison in PAL3, 2009

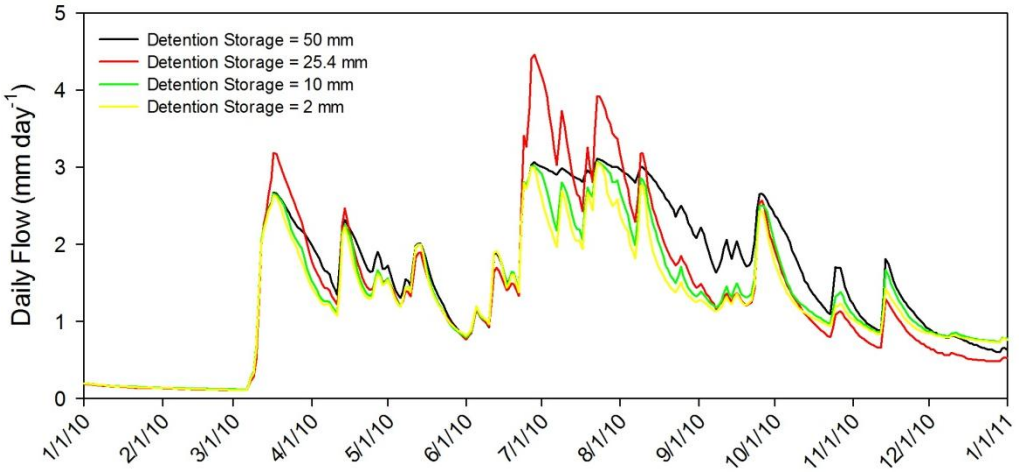

Figure 90 flow for detention storage comparison in PAL3, 2010

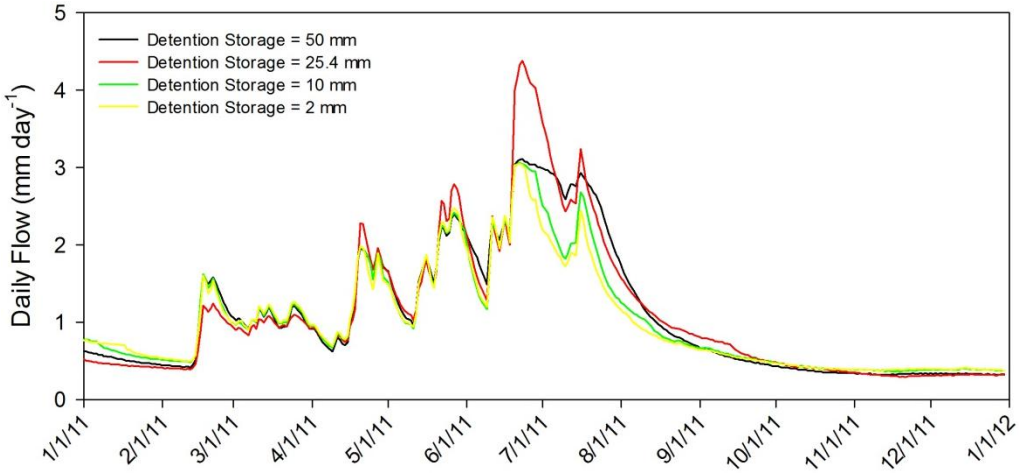

Figure 91 Subsurface flow for detention storage comparison in PAL3, 2011

A. 2. Testing and Validation Hydrographs

The following graphs will show surface and subsurface flow for the testing and validation stages of the MIKE SHE model investigation.

A. 2. 1. PAL3 Testing Hydrographs

Surface Runoff PAL3

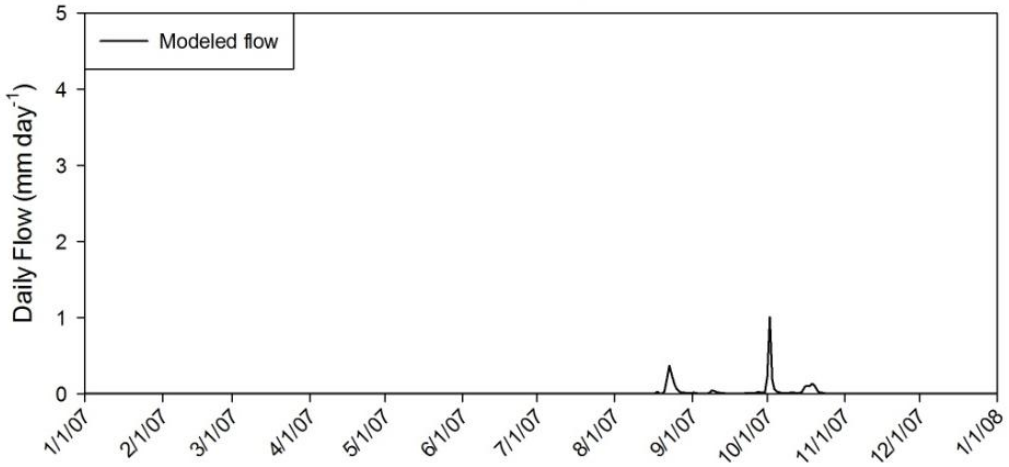

Figure 92 Surface flow for PAL3 in testing stage, 2007

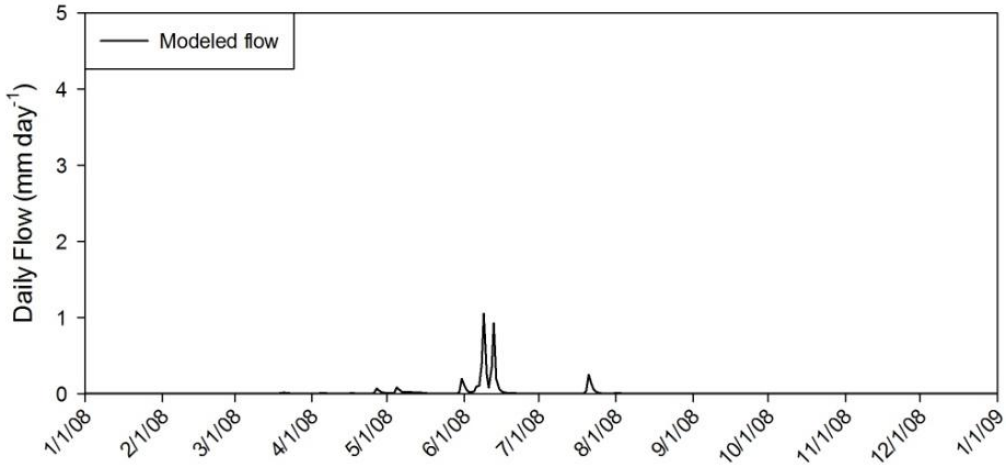

Figure 93 Surface flow for PAL3 in testing stage, 2008

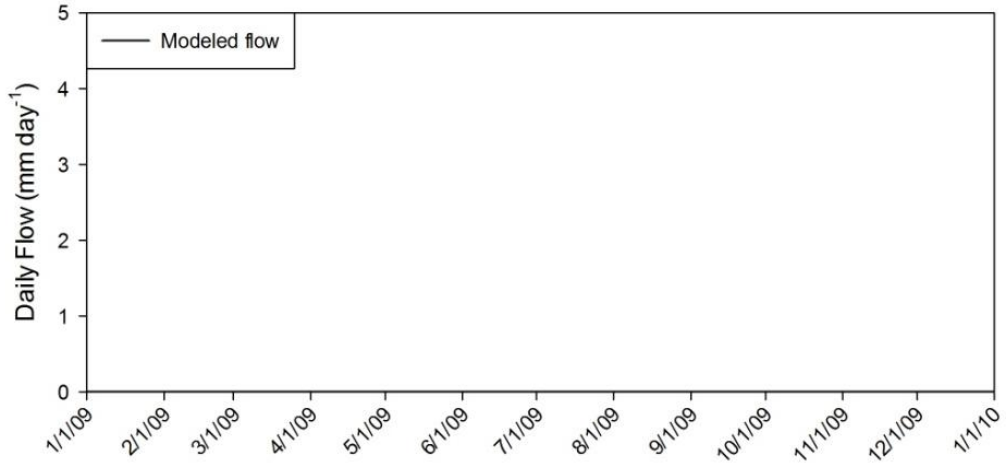

Figure 94 Surface flow for PAL3 in testing stage, 2009

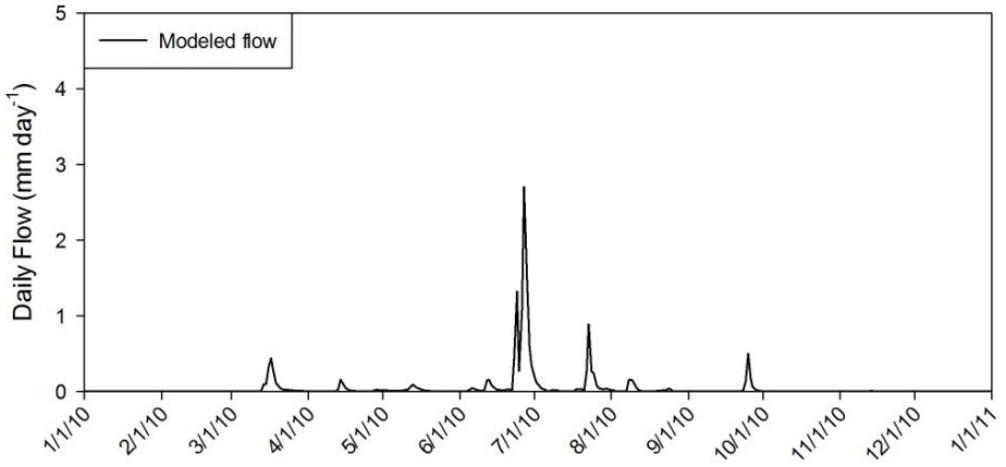

Figure 95 Surface flow for PAL3 in testing stage, 2010

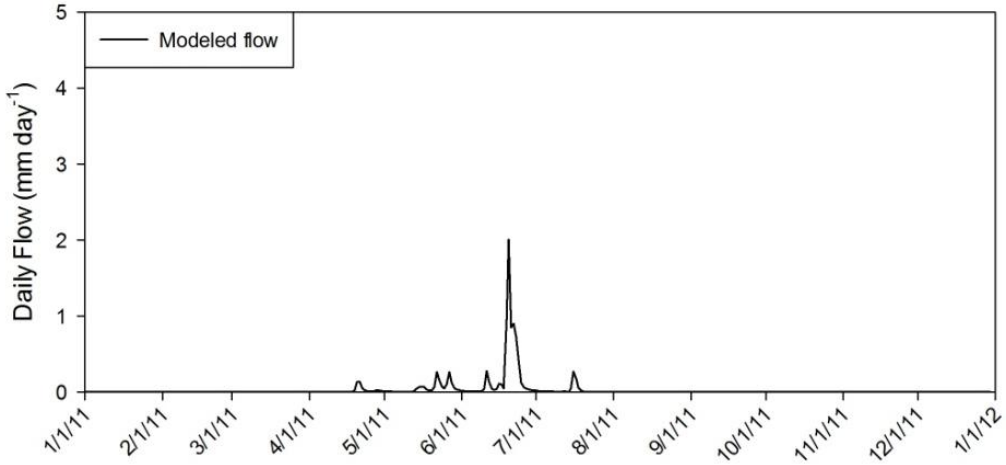

Figure 96 Surface flow for PAL3 in testing stage, 2011

Subsurface PAL3

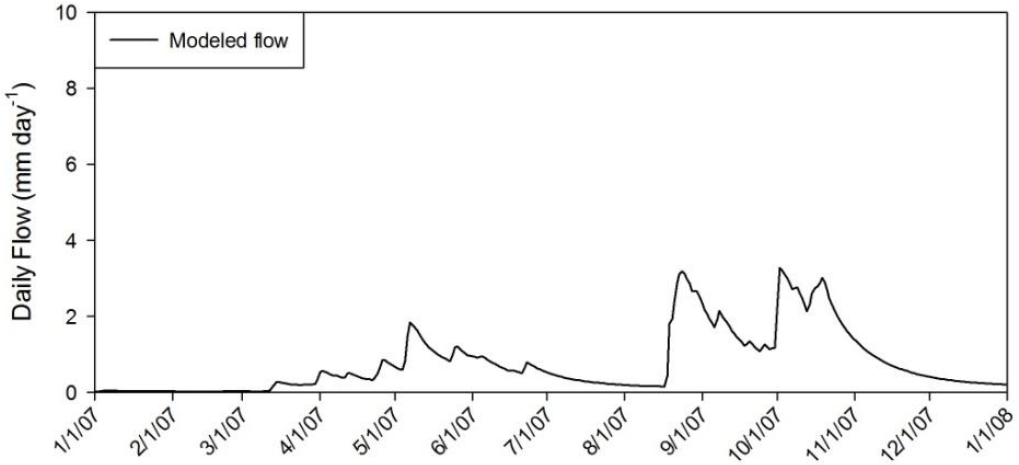

Figure 97 Subsurface flow for PAL3 in testing stage, 2007

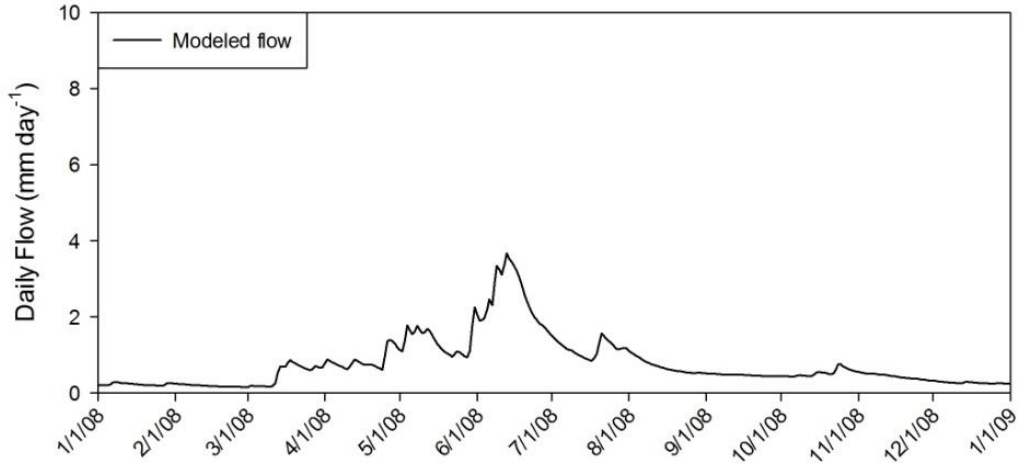

Figure 98 Subsurface flow for PAL3 in testing stage, 2008

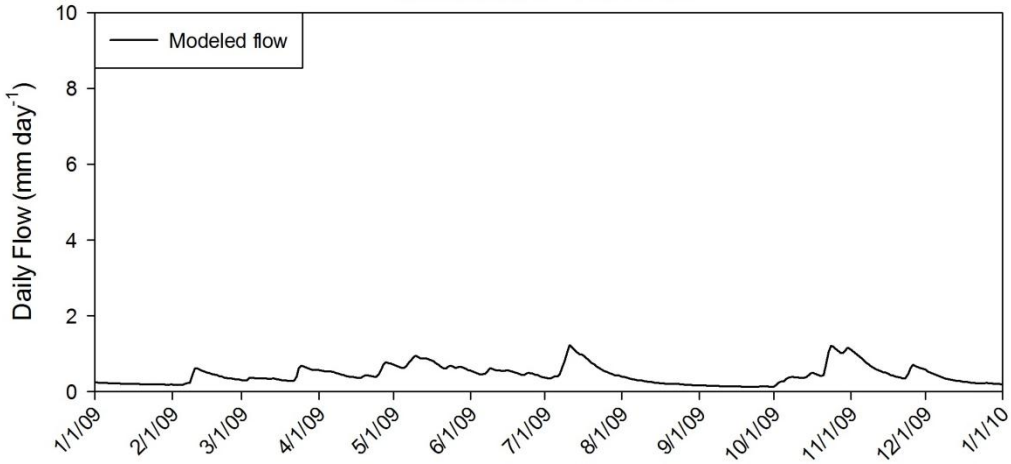

Figure 99 Subsurface flow for PAL3 in testing stage, 2009

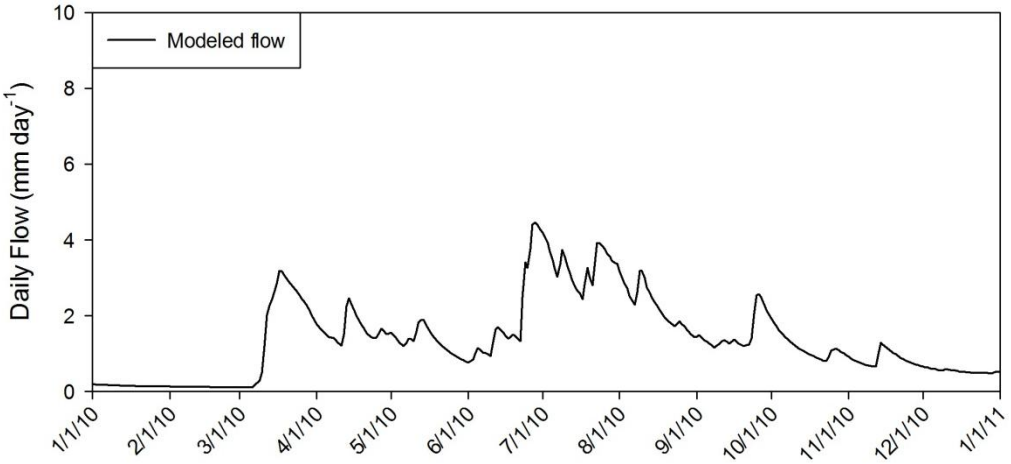

Figure 100 Subsurface flow for PAL3 in testing stage, 2010

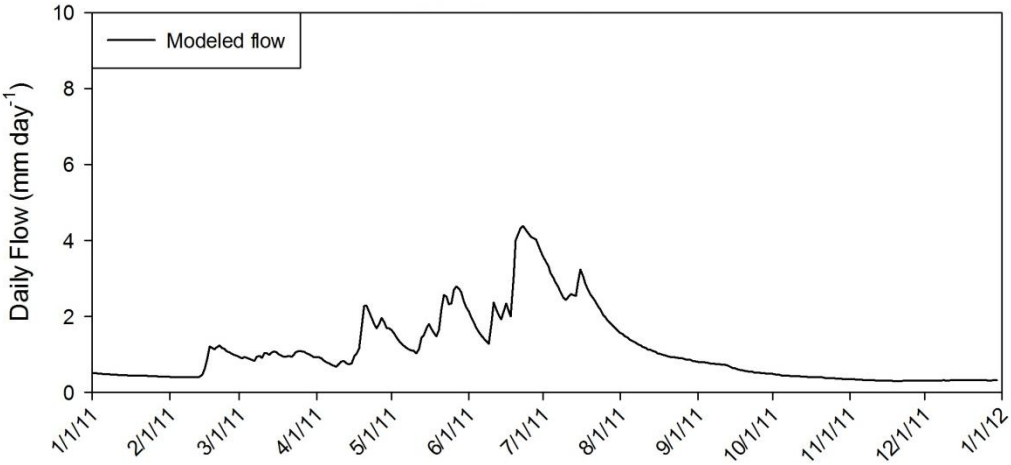

Figure 101 Subsurface flow for PAL3 in testing stage, 2011

A. 2. 1. PAL5 Validation Hydrographs

Surface Runoff PAL5

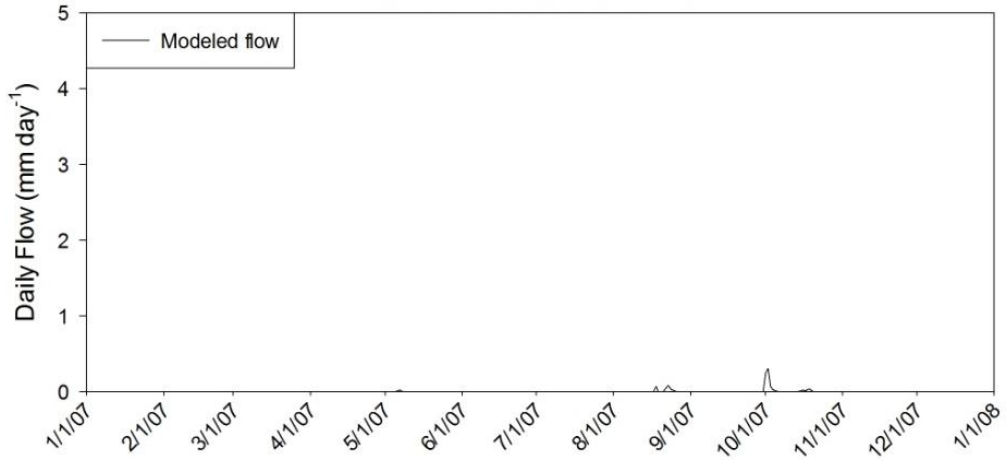

Figure 102 Surface flow for PAL5 in validation stage, 2007

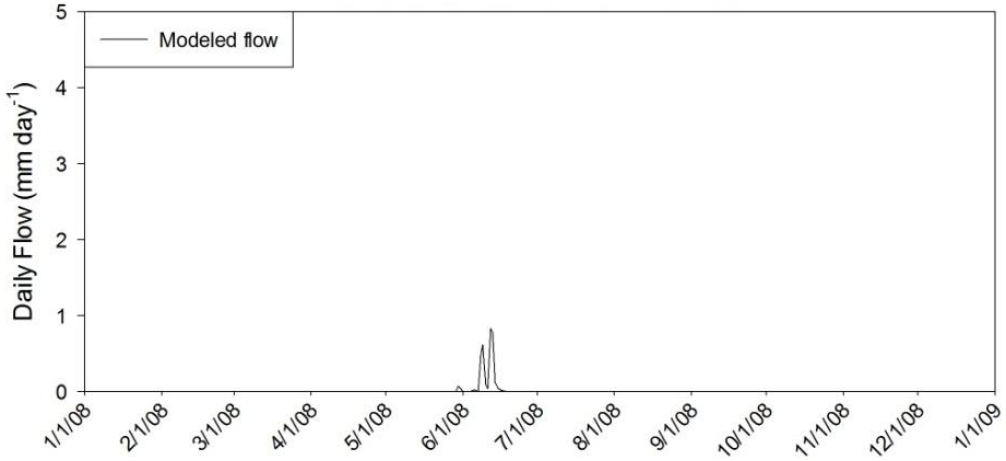

Figure 103 Surface flow for PAL5 in validation stage, 2008

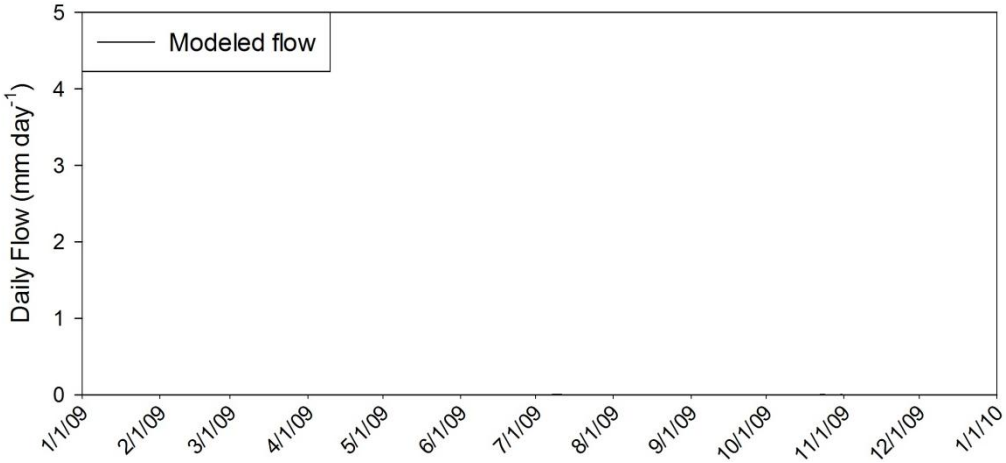

Figure 104 Surface flow for PAL5 in validation stage, 2009

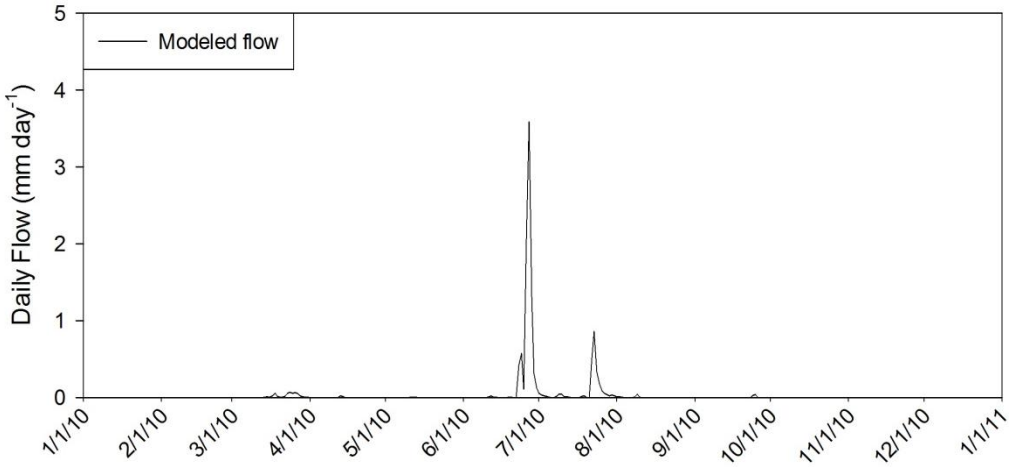

Figure 105 Surface flow for PAL5 in validation stage, 2010

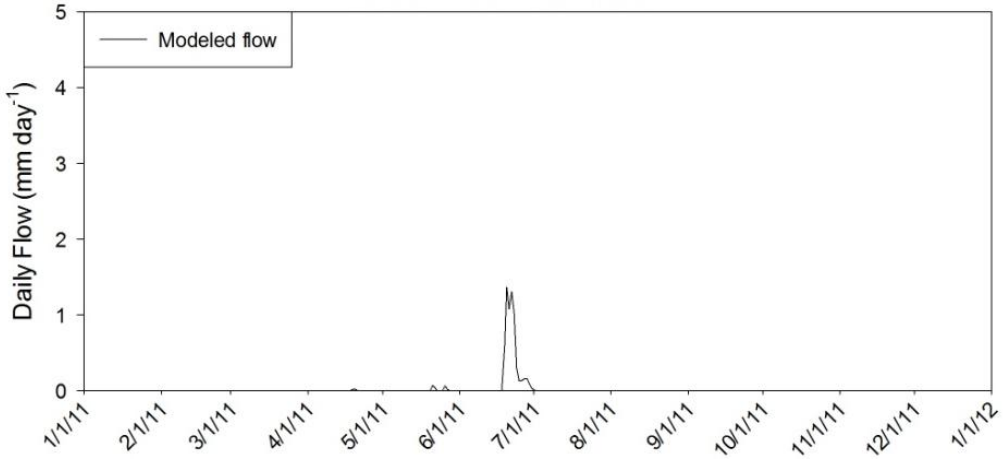

Figure 106 Surface flow for PAL5 in validation stage, 2011

Subsurface PAL5

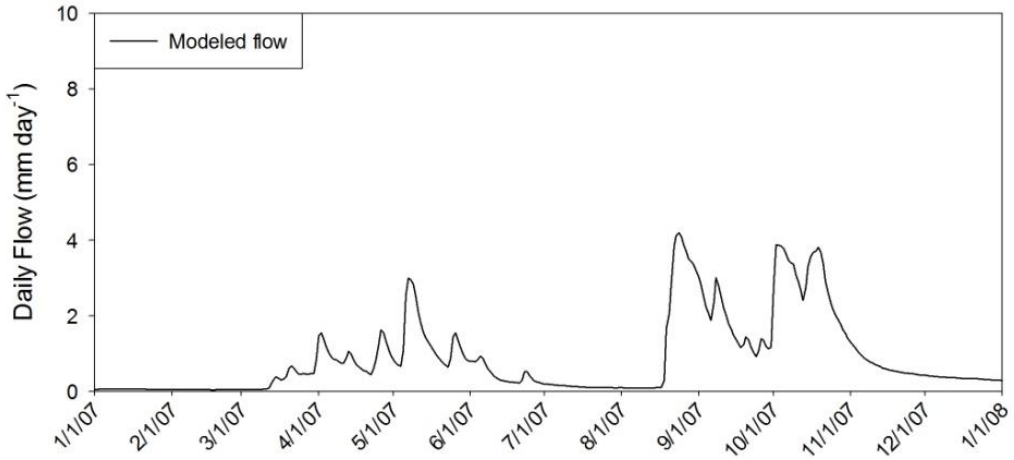

Figure 107 flow for PAL5 in validation stage, 2007

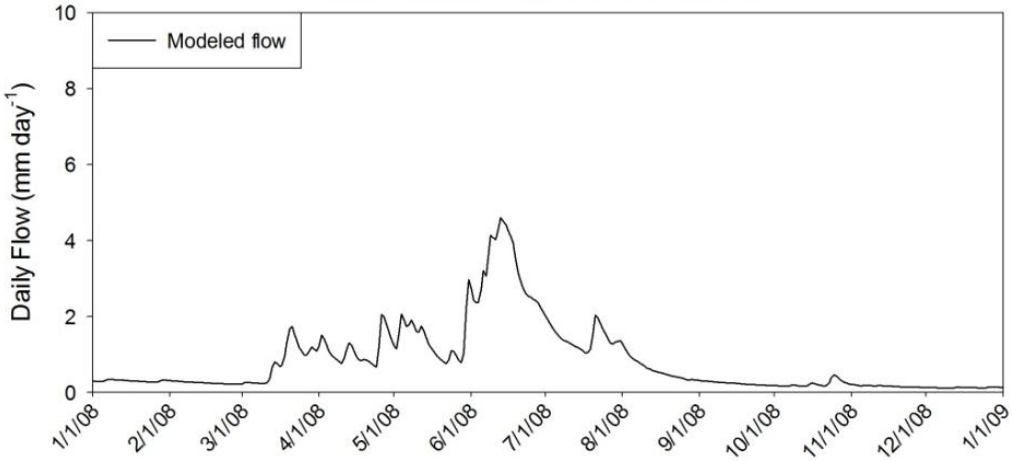

Figure 108 flow for PAL5 in validation stage, 2008

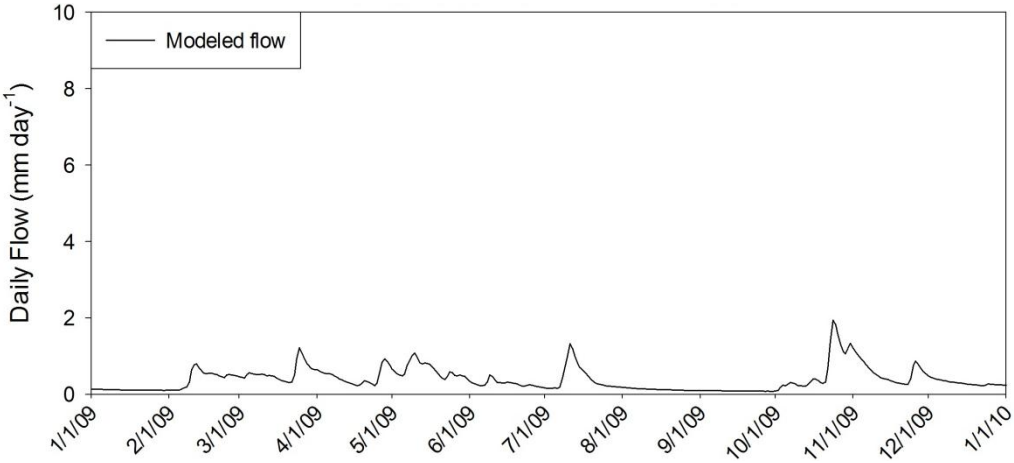

Figure 109 flow for PAL5 in validation stage, 2009

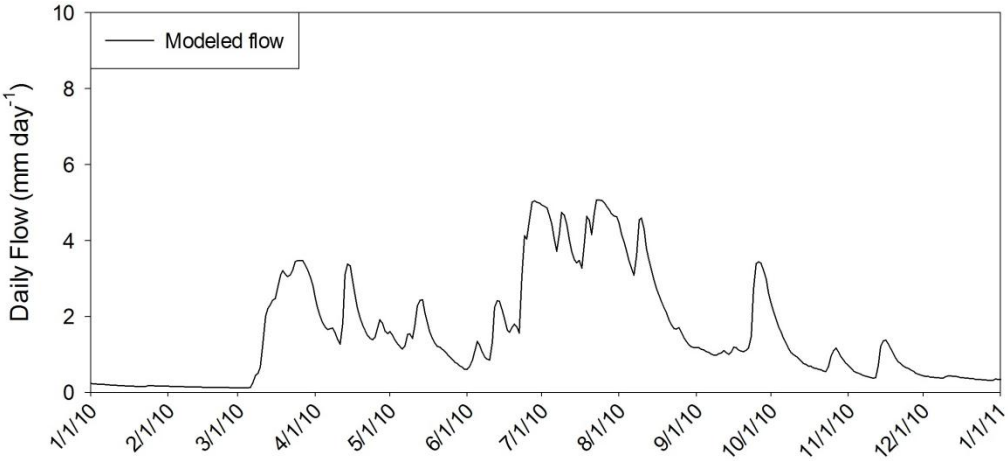

Figure 110 flow for PAL5 in validation stage, 2010

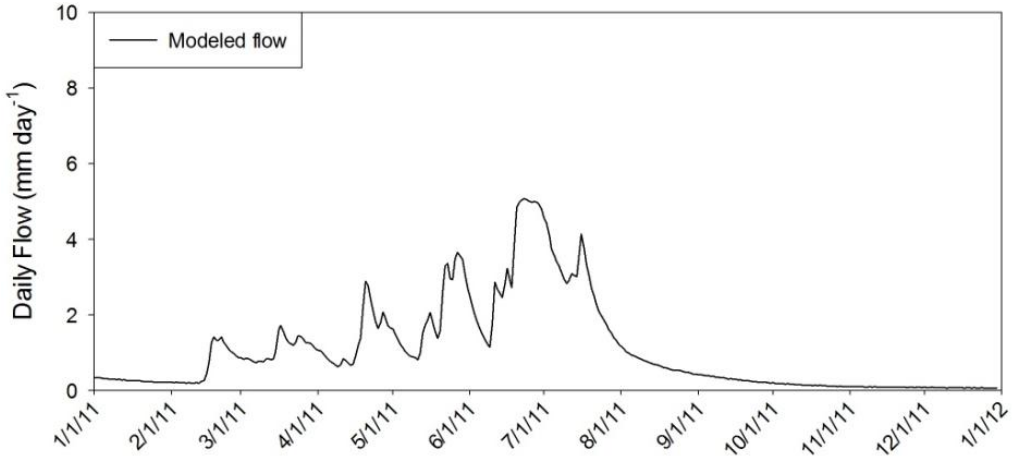

Figure 111 Subsurface flow for PAL5 in validation stage, 2011

A. 3. Land Use Management Scenarios

The following graphs will compare the relationships between the PAL3 testing scenario, PAl5 validation scenario, and the various scenarios investigated for surface and subsurface. Scenarios without subsurface drainage will have the subsurface comparison excluded from the sub appendices.

A. 3. 1. Land use conversion to perennial grassland with drainage infrastructure included

Surface Runoff

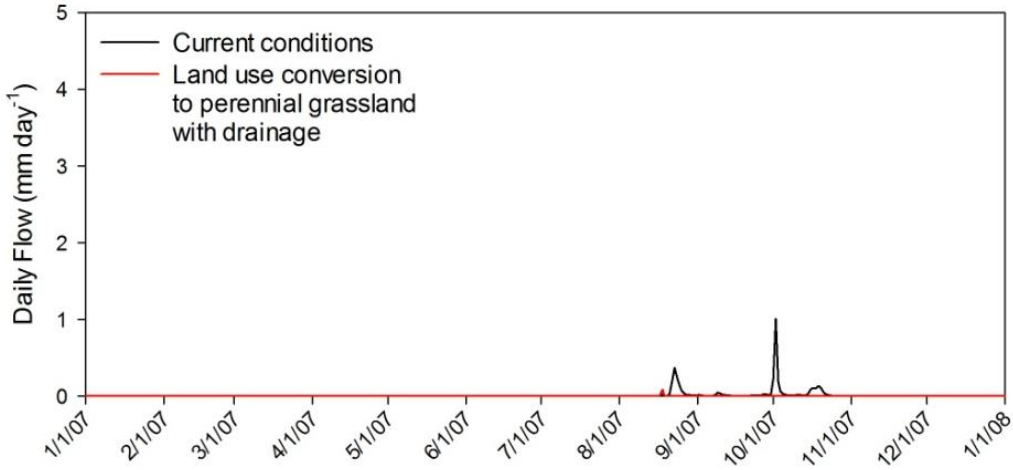

Figure 112 Surface flow for land use conversion with drainage infrastructure in PAL3, 2007

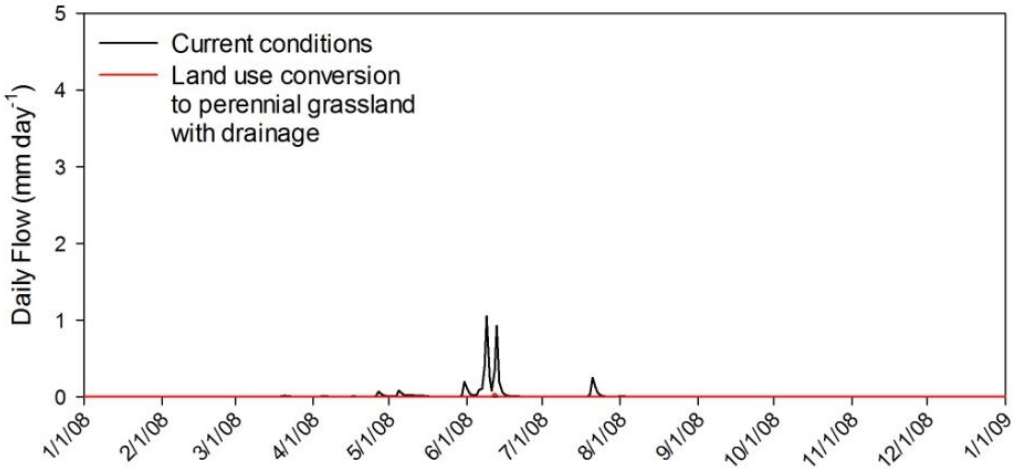

Figure 113 Surface flow for land use conversion with drainage infrastructure in PAL3, 2008

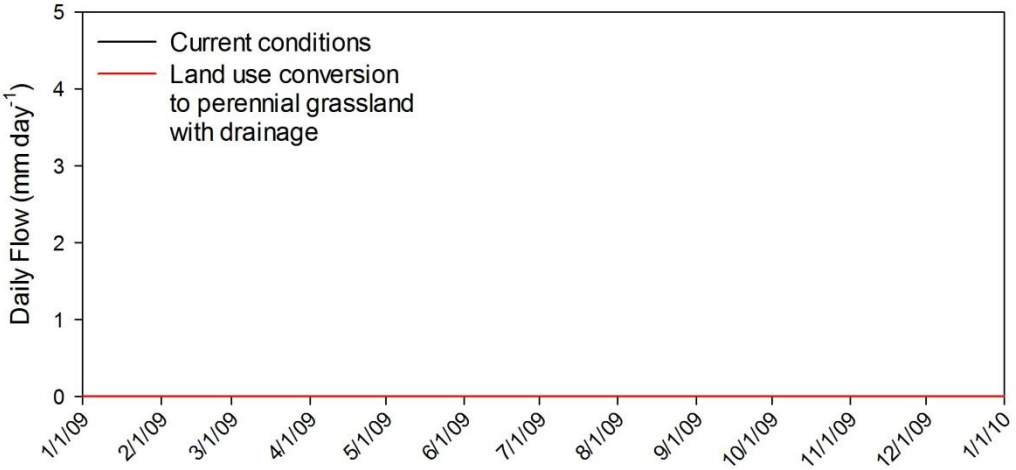

Figure 114 Surface flow for land use conversion with drainage infrastructure in PAL3, 2009

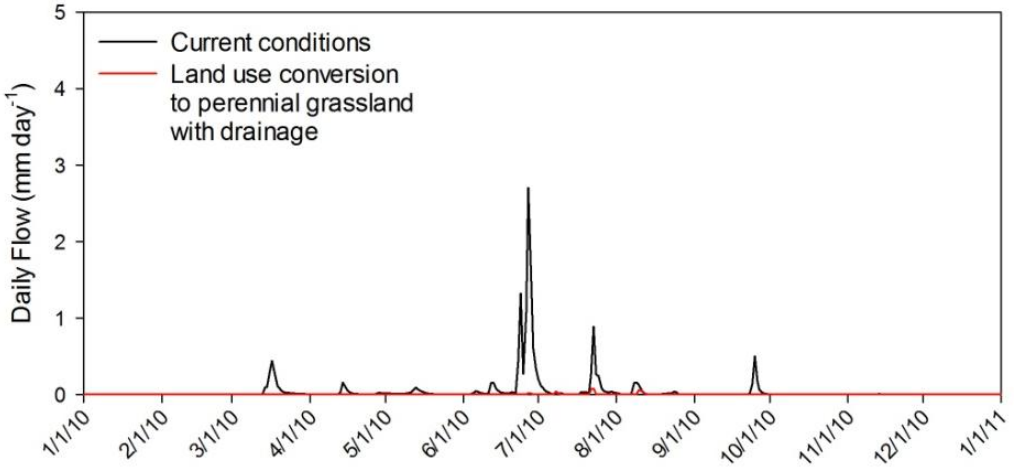

Figure 115 Surface flow for land use conversion with drainage infrastructure in PAL3, 2010

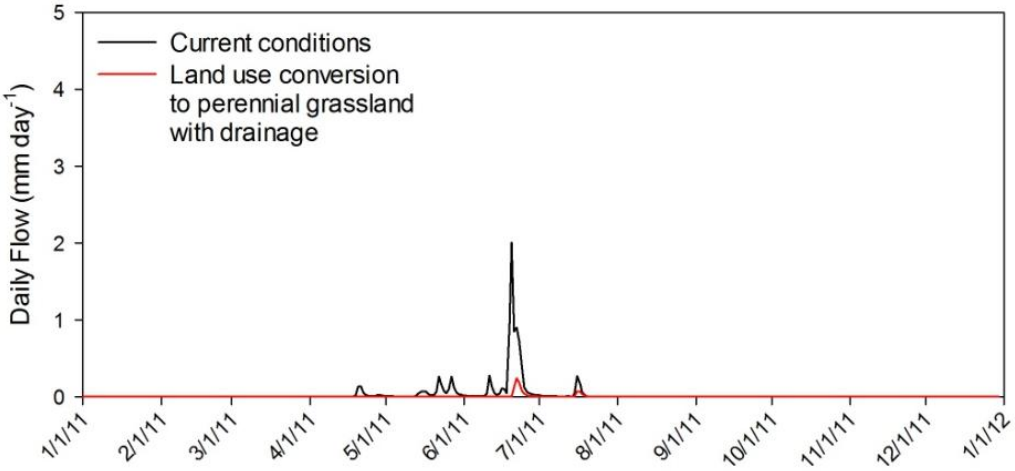

Figure 116 Surface flow for land use conversion with drainage infrastructure in PAL3, 2011

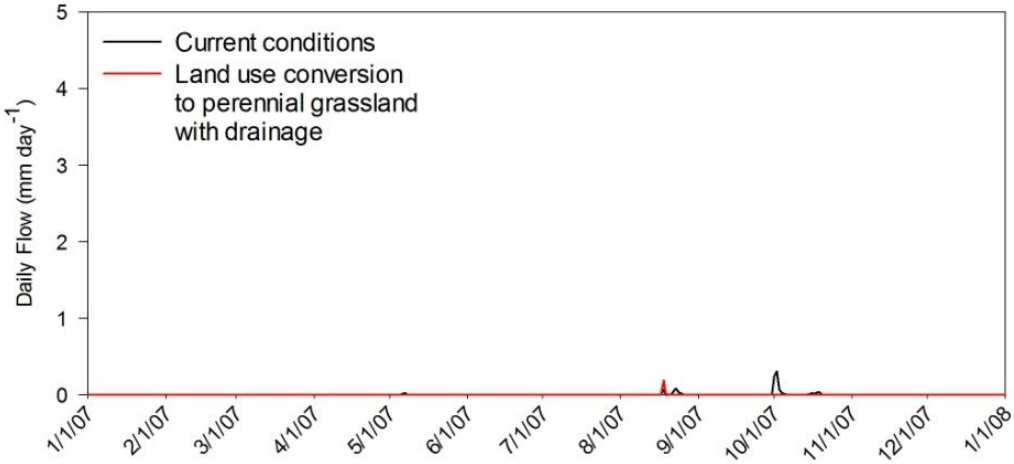

Figure 117 Surface flow for land use conversion with drainage infrastructure in PAL5, 2007

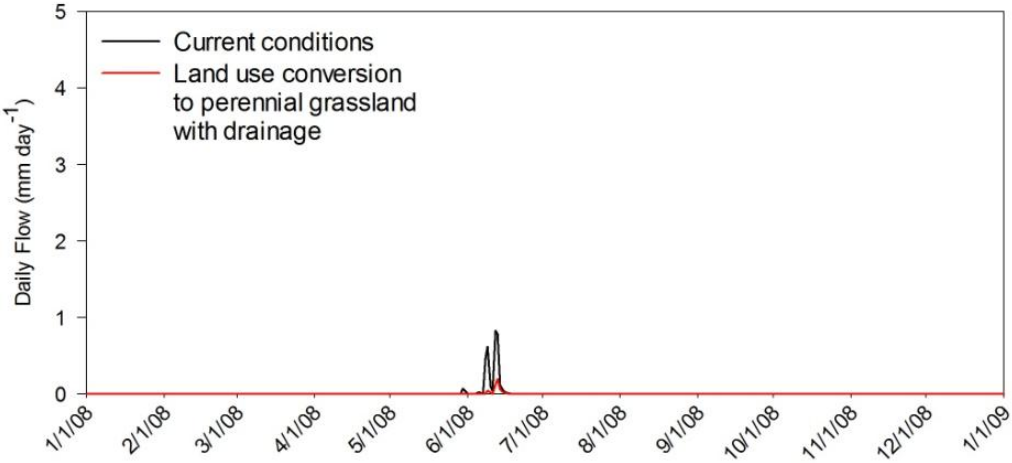

Figure 118 flow for land use conversion with drainage infrastructure in PAL5, 2008

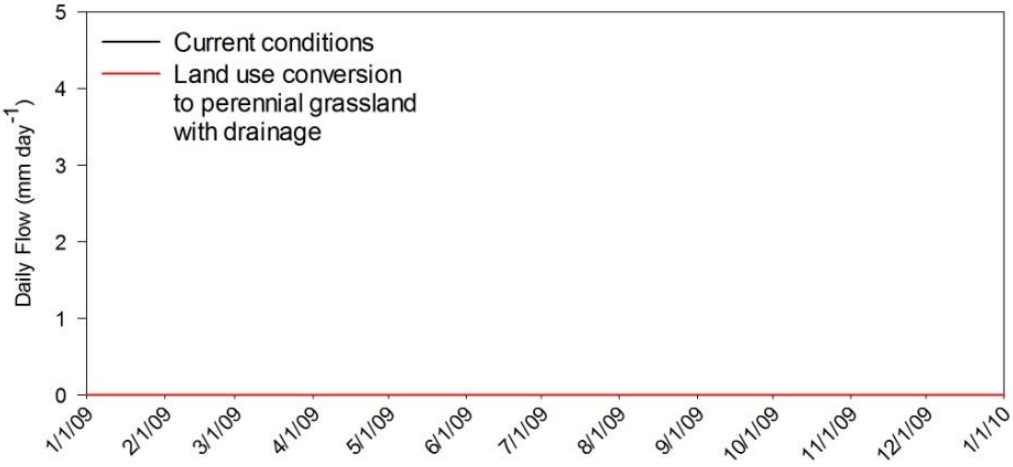

Figure 119 flow for land use conversion with drainage infrastructure in PAL5, 2009

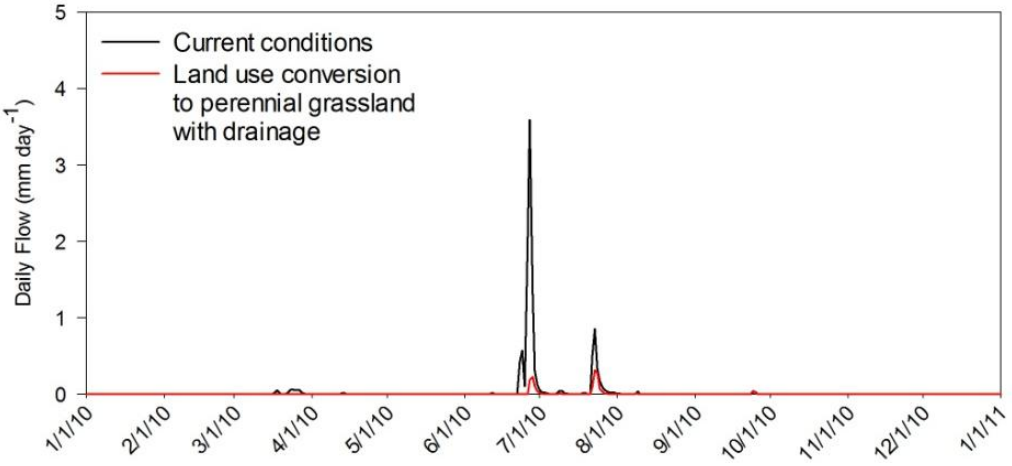

Figure 120 flow for land use conversion with drainage infrastructure in PAL5, 2010

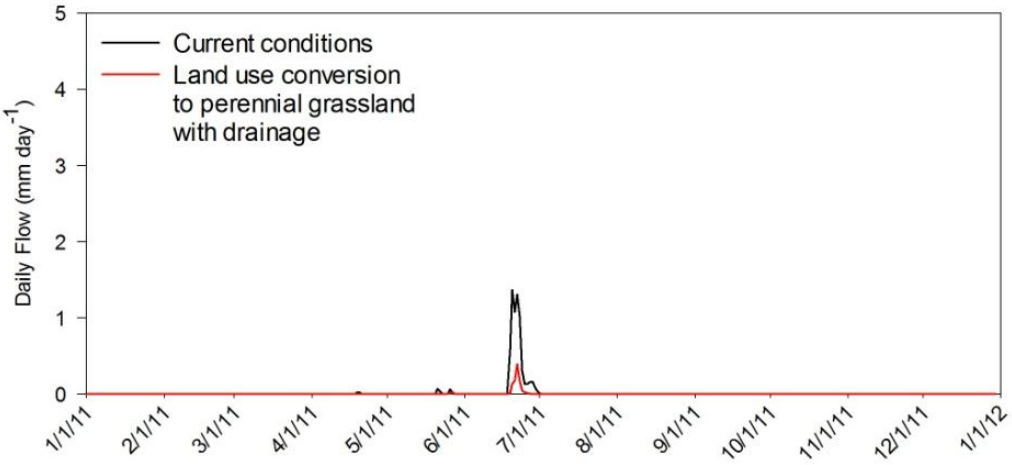

Figure 121 flow for land use conversion with drainage infrastructure in PAL5, 2011

Subsurface flow

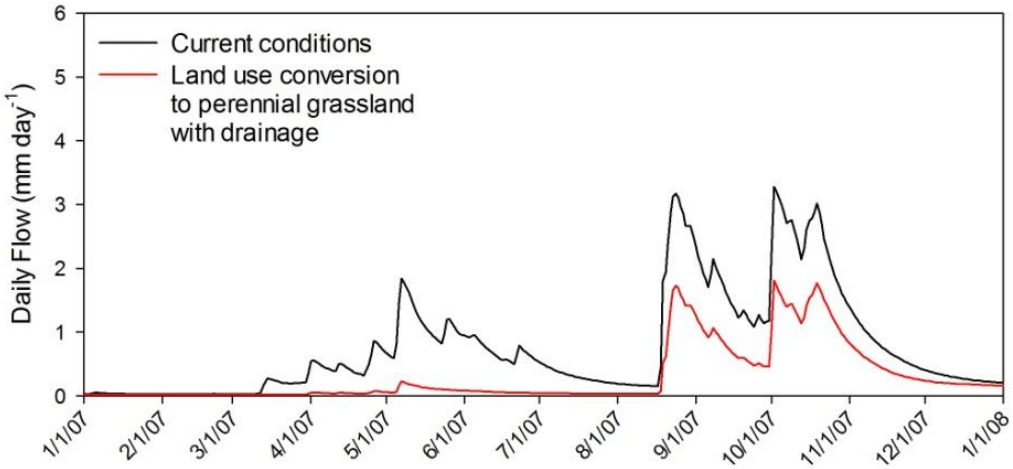

Figure 122 Subsurface flow for land use conversion with drainage infrastructure in PAL3, 2007

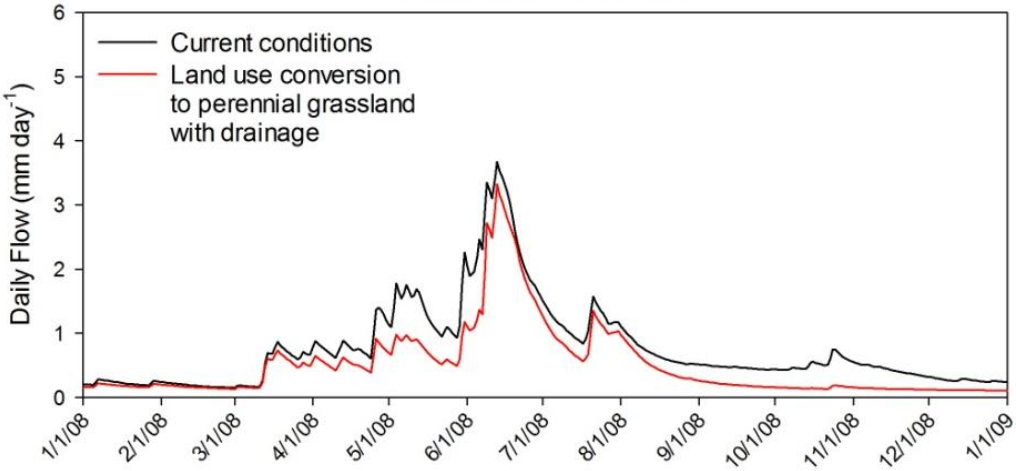

Figure 123 Subsurface flow for land use conversion with drainage infrastructure in PAL3, 2008

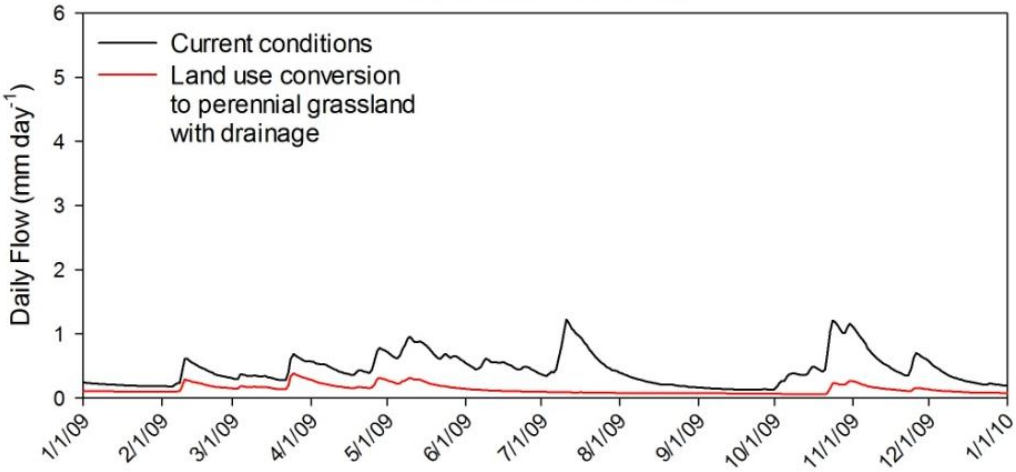

Figure 124 Subsurface flow for land use conversion with drainage infrastructure in PAL3, 2009

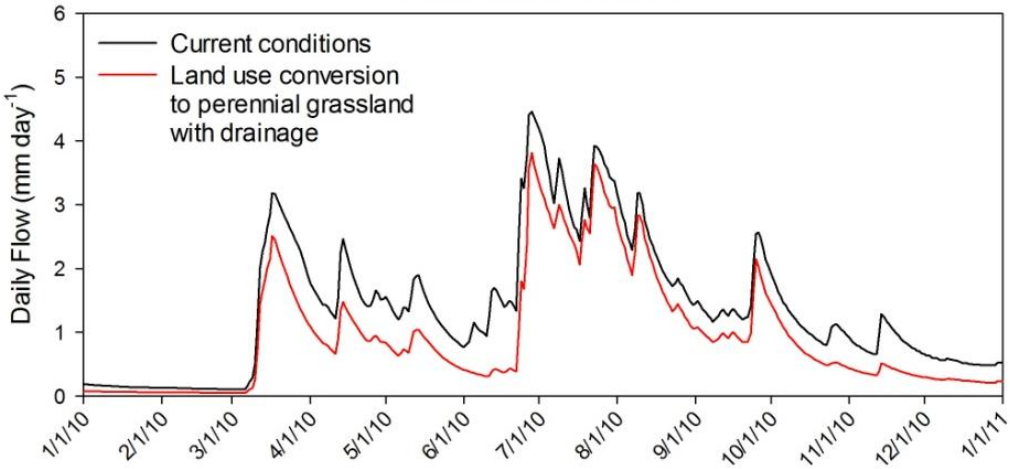

Figure 125 Subsurface flow for land use conversion with drainage infrastructure in PAL3, 2010

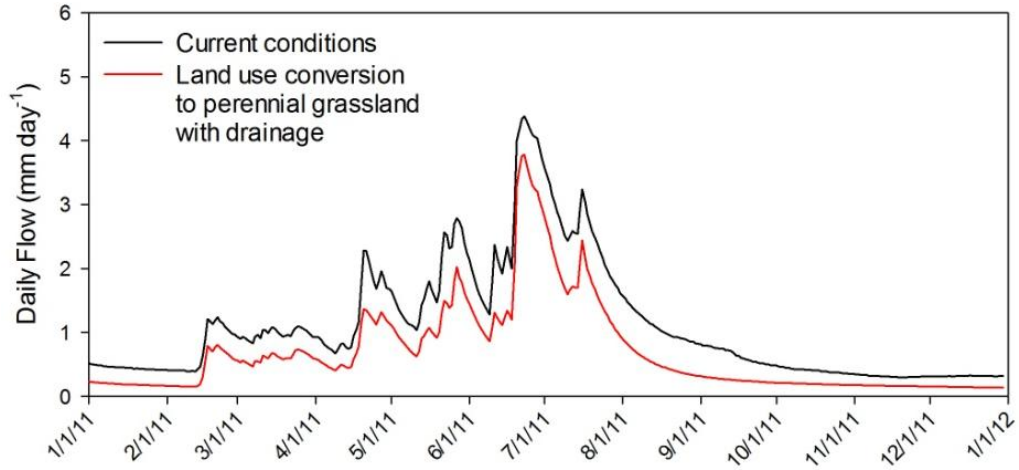

Figure 126 Subsurface flow for land use conversion with drainage infrastructure in PAL3, 2011

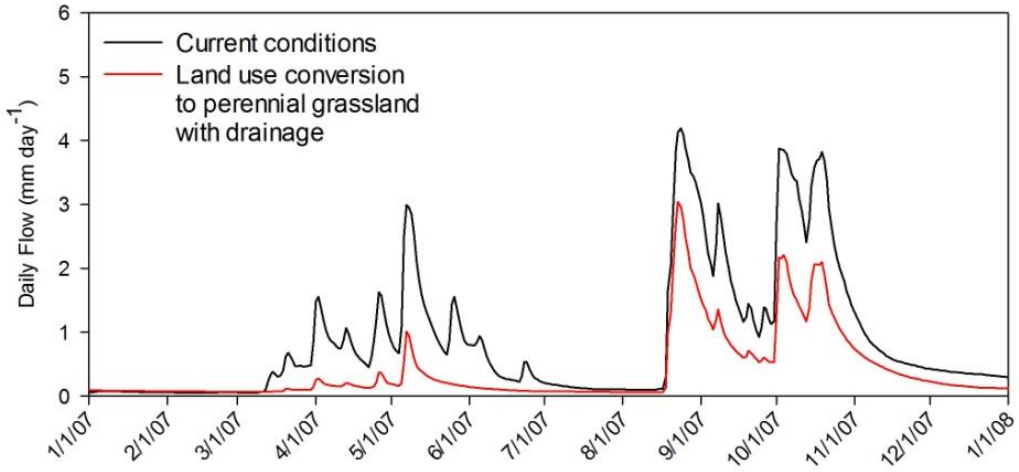

Figure 127 Subsurface flow for land use conversion with drainage infrastructure in PAL5, 2007

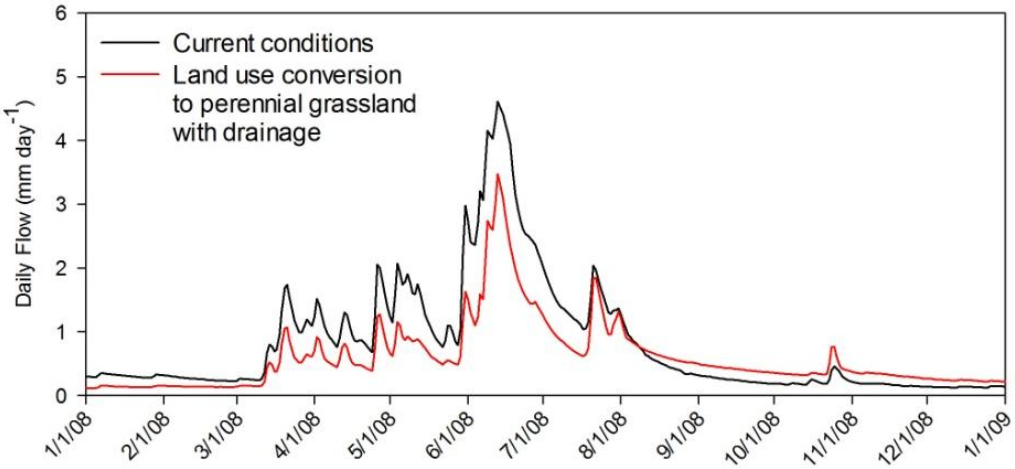

Figure 128 Subsurface flow for land use conversion with drainage infrastructure in PAL5, 2008

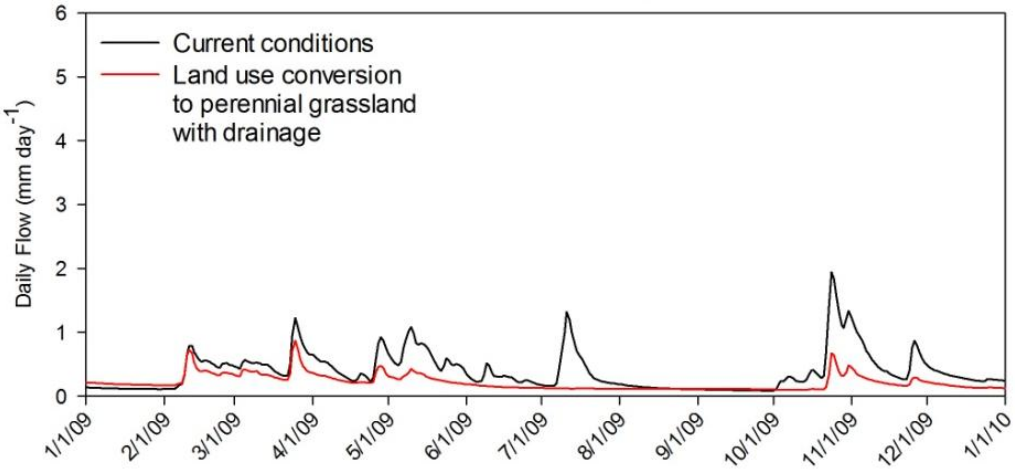

Figure 129 Subsurface flow for land use conversion with drainage infrastructure in PAL5, 2009

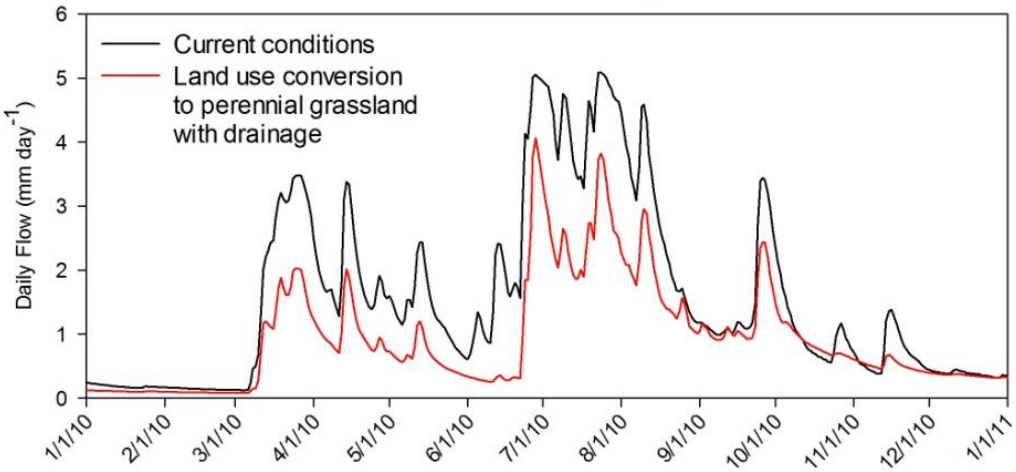

Figure 130 Subsurface flow for land use conversion with drainage infrastructure in PAL5, 2010

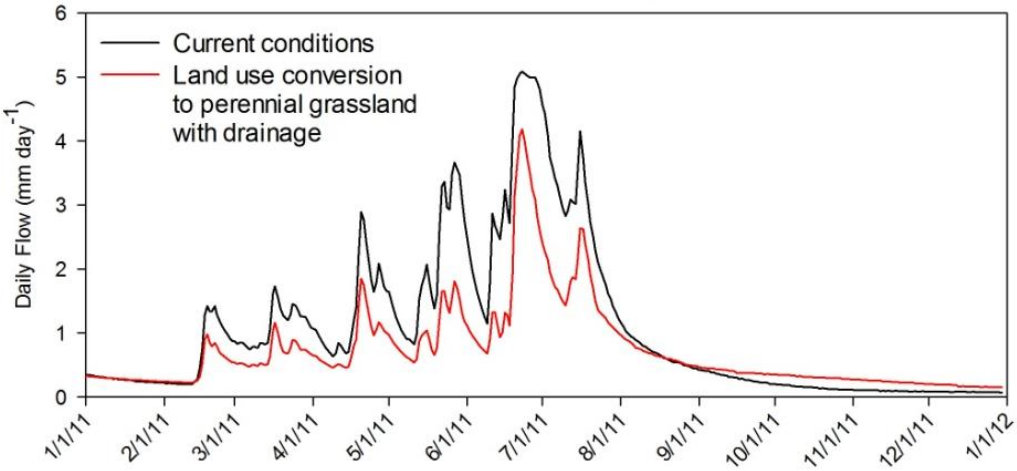

Figure 131 Subsurface flow for land use conversion with drainage infrastructure in PAL5, 2011

A. 3. 2. Likely pre-settlement conditions

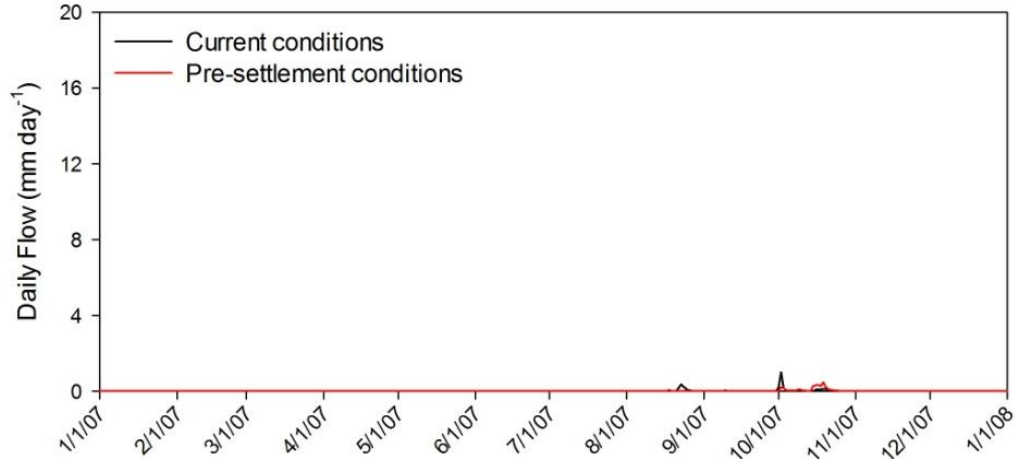

Figure 132 Surface flow for likely pre-settlement conditions in PAL3, 2007

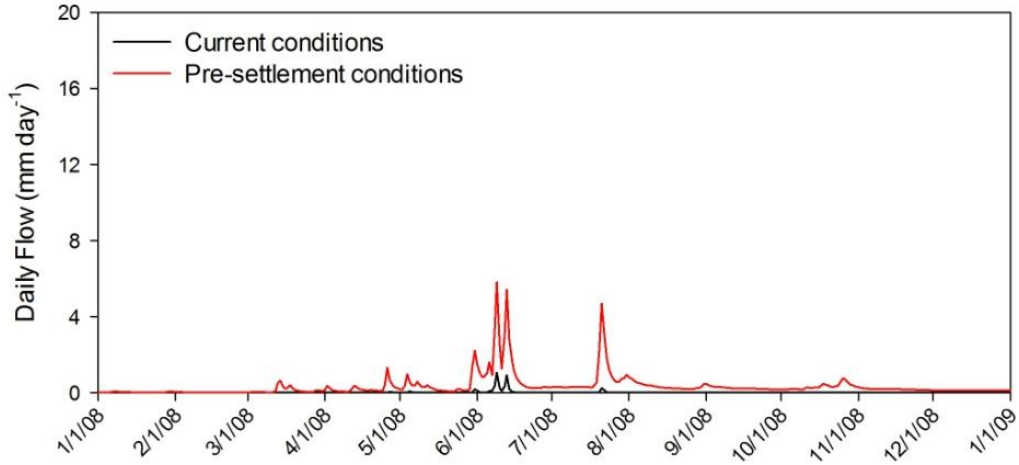

Figure 133 Surface flow for likely pre-settlement conditions in PAL3, 2008

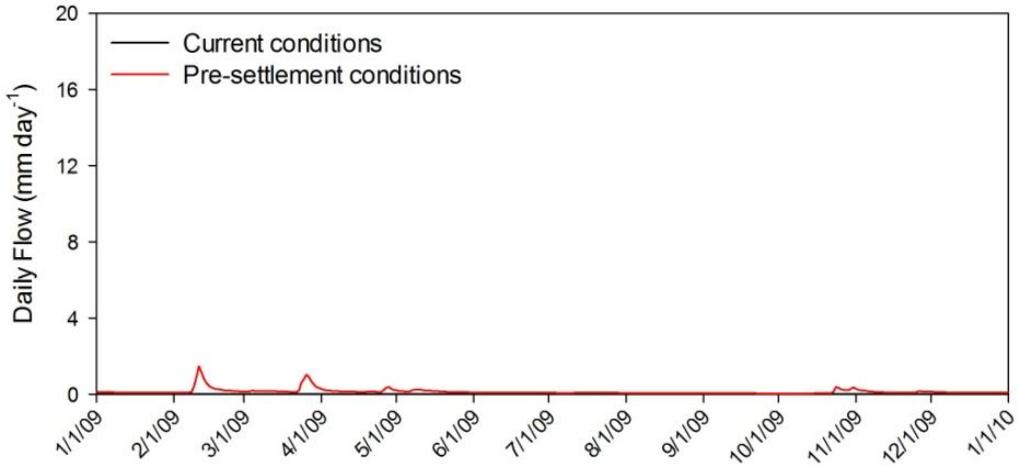

Figure 134 Surface flow for likely pre-settlement conditions in PAL3, 2009

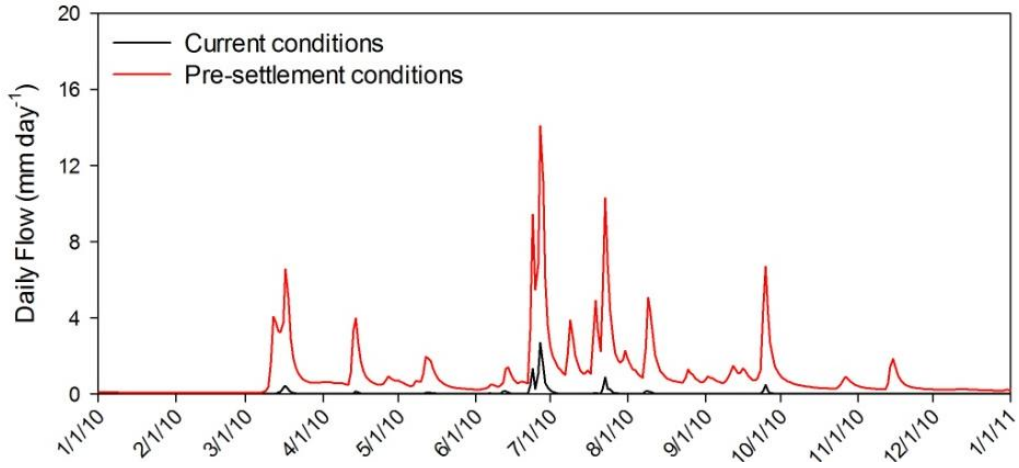

Figure 135 Surface flow for likely pre-settlement conditions in PAL3, 2010

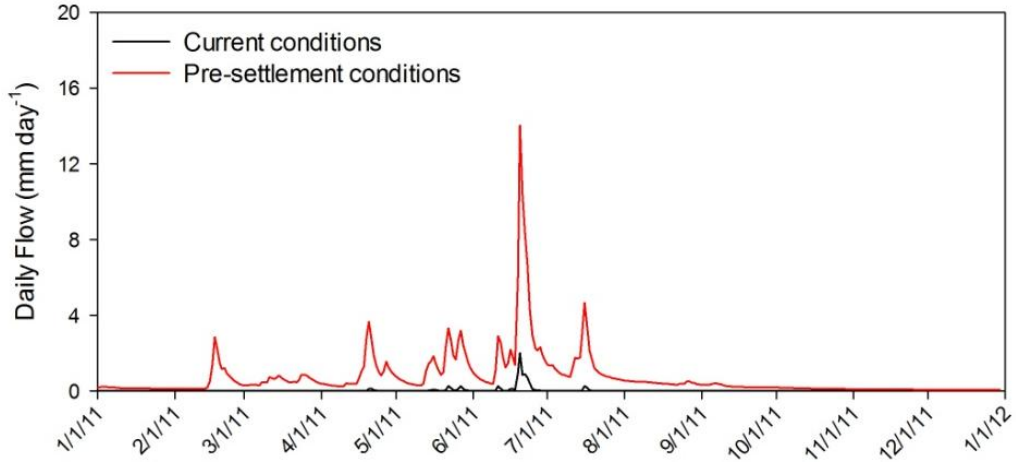

Figure 136 Surface flow for likely pre-settlement conditions in PAL3, 2011

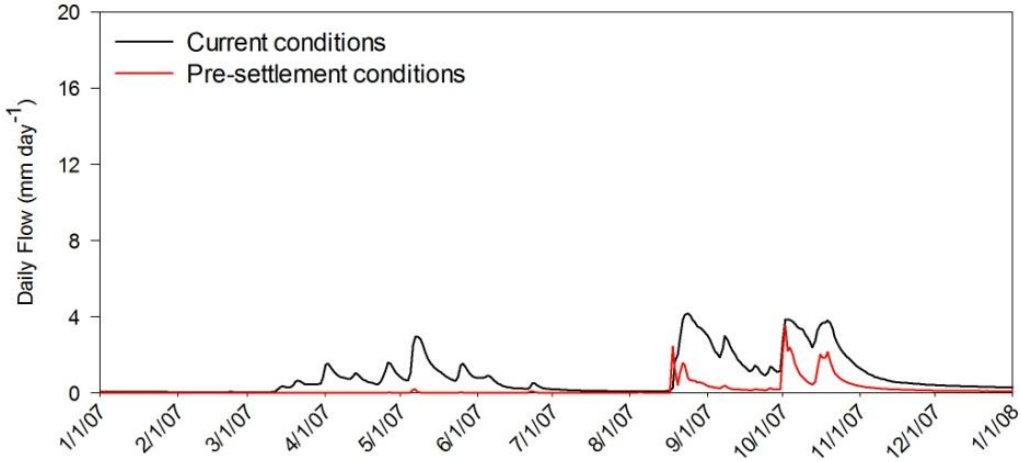

Figure 137 Surface flow for likely pre-settlement conditions in PAL3, 2007

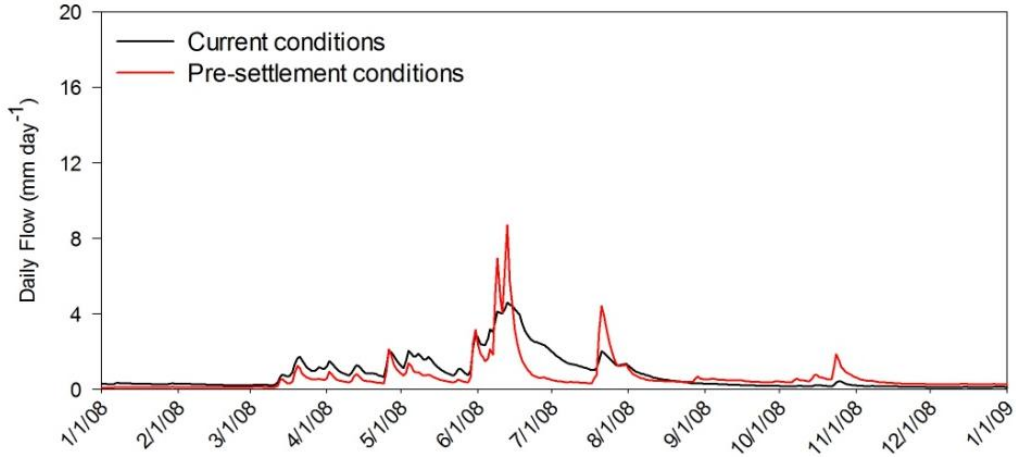

Figure 138 Surface flow for likely pre-settlement conditions in PAL3, 2008

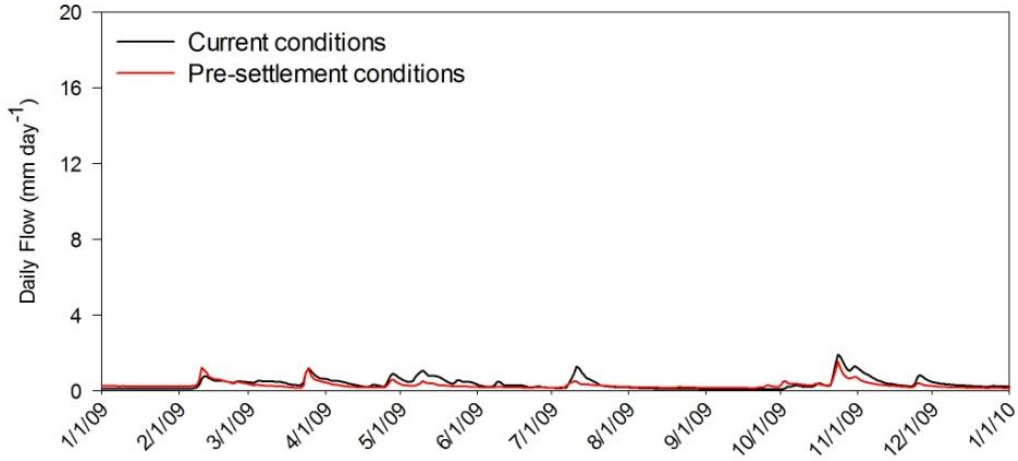

Figure 139 Surface flow for likely pre-settlement conditions in PAL3, 2009

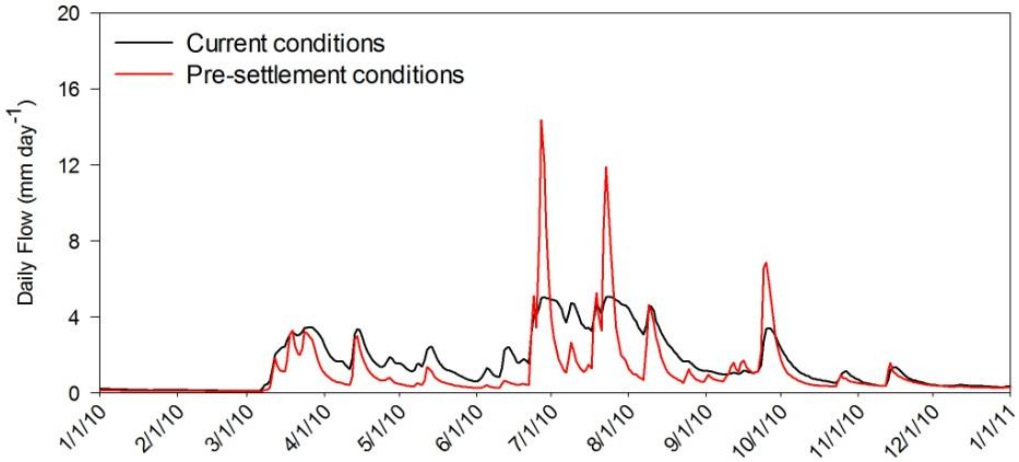

Figure 140 Surface flow for likely pre-settlement conditions in PAL3, 2010

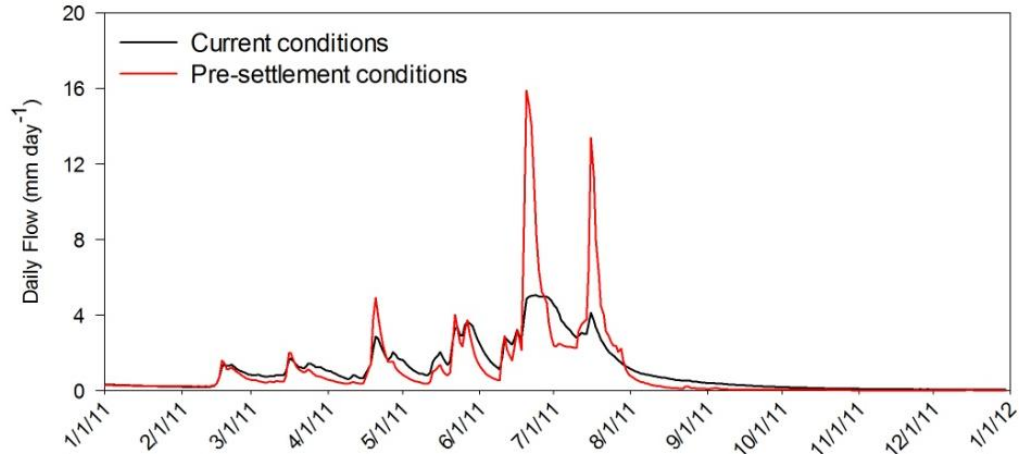

Figure 141 Surface flow for likely pre-settlement conditions in PAL3, 2011

A. 3. 3. Shallow drainage conditions

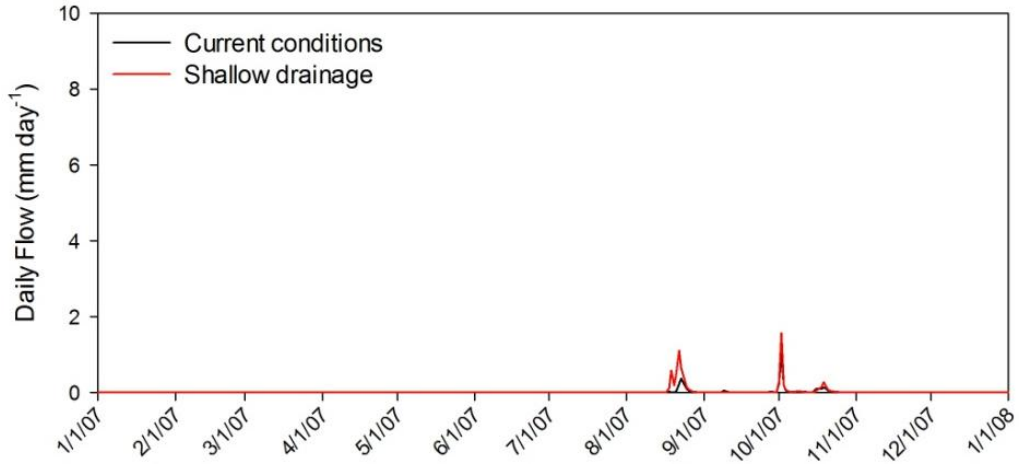

Figure 142 Surface flow for shallow drainage conditions in PAL3, 2007

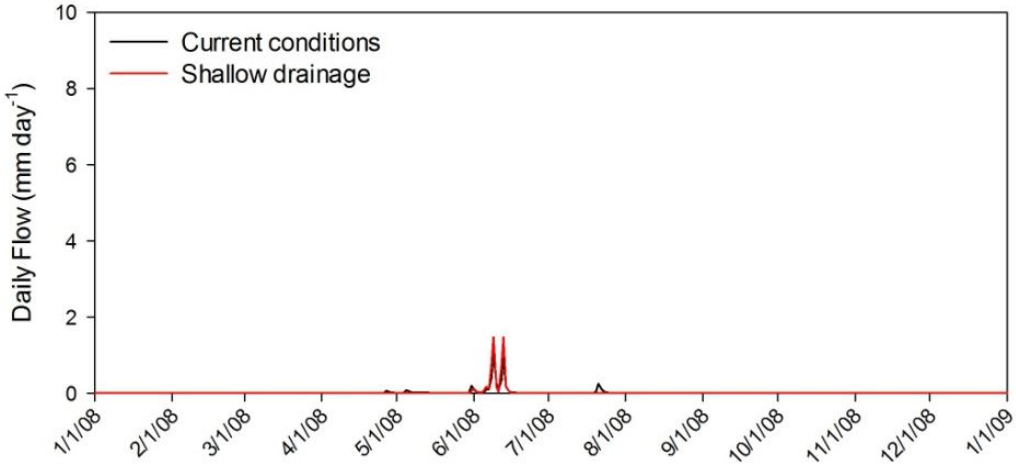

Figure 143 Surface flow for shallow drainage conditions in PAL3, 2008

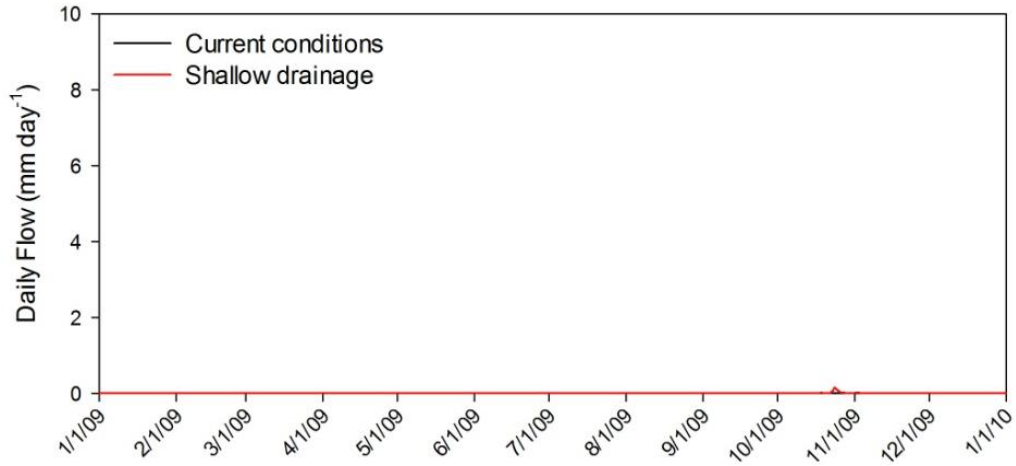

Figure 144 Surface flow for shallow drainage conditions in PAL3, 2009

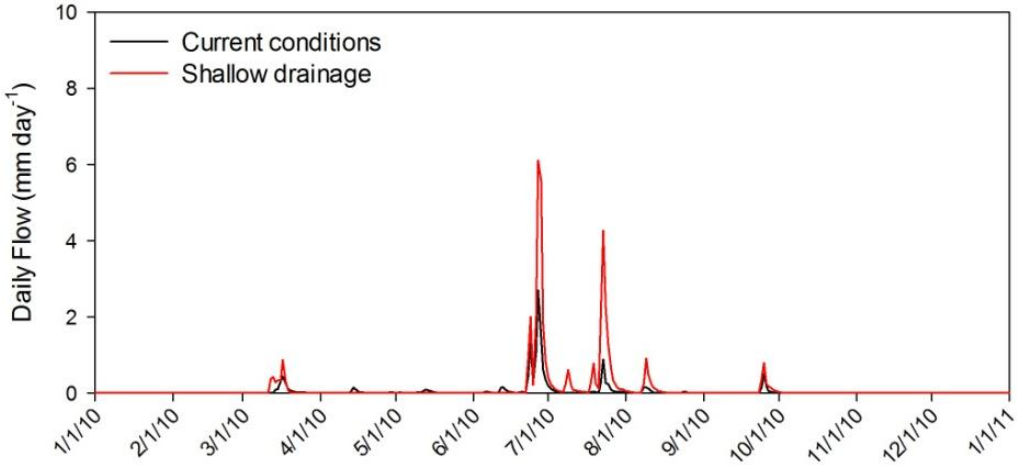

Figure 145 Surface flow for shallow drainage conditions in PAL3, 2010

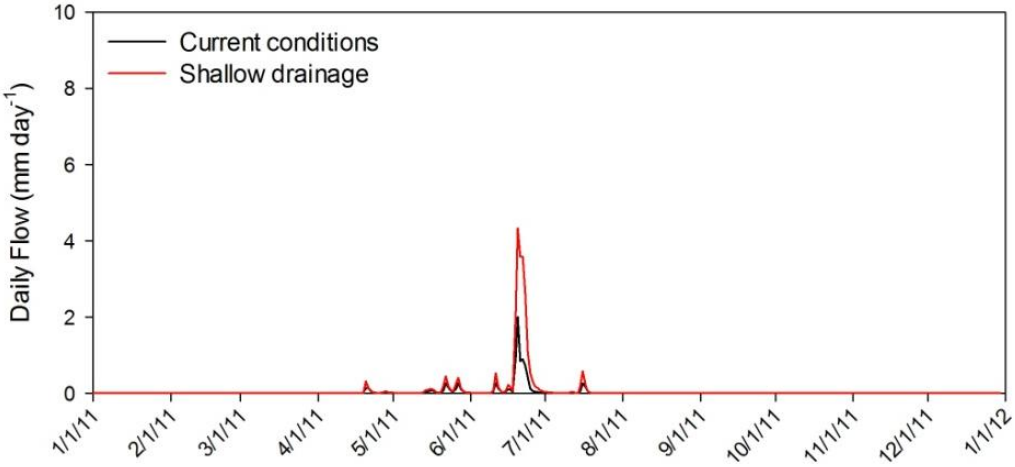

Figure 146 Surface flow for shallow drainage conditions in PAL3, 2011

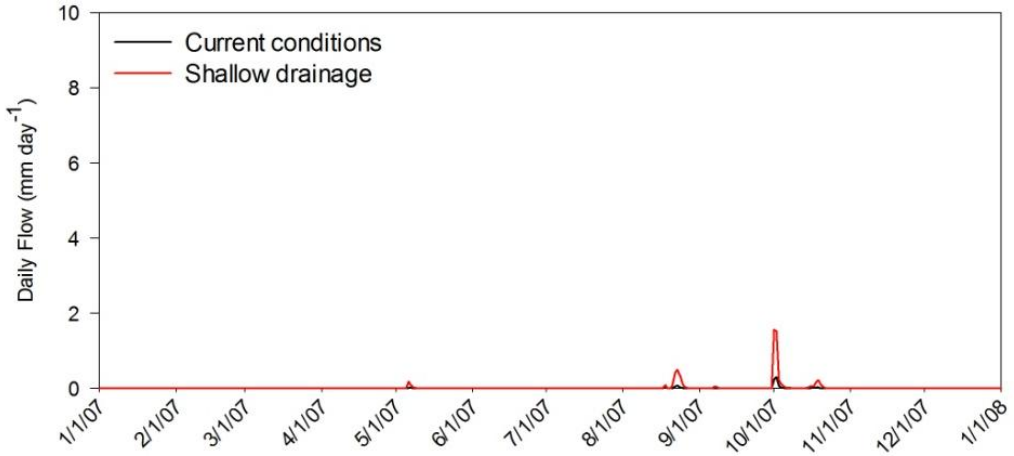

Figure 147 Surface flow for shallow drainage conditions in PAL5, 2007

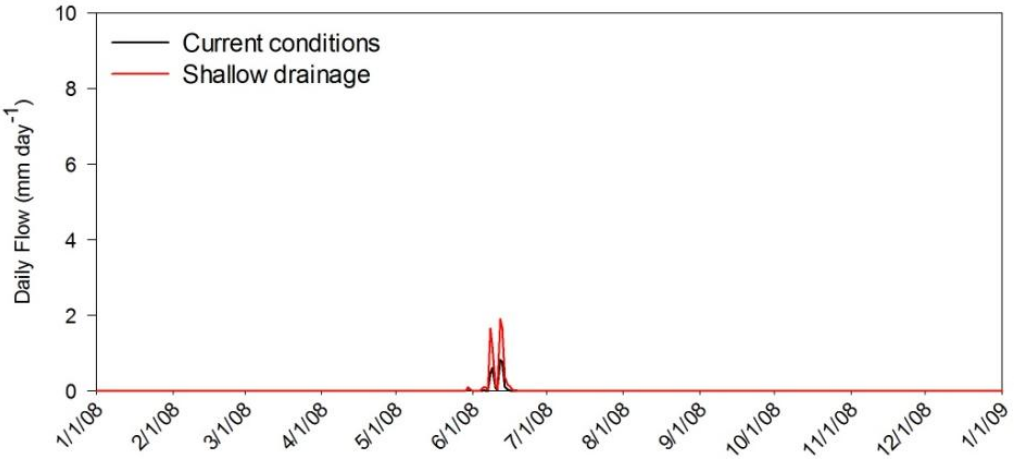

Figure 148 Surface flow for shallow drainage conditions in PAL5, 2008

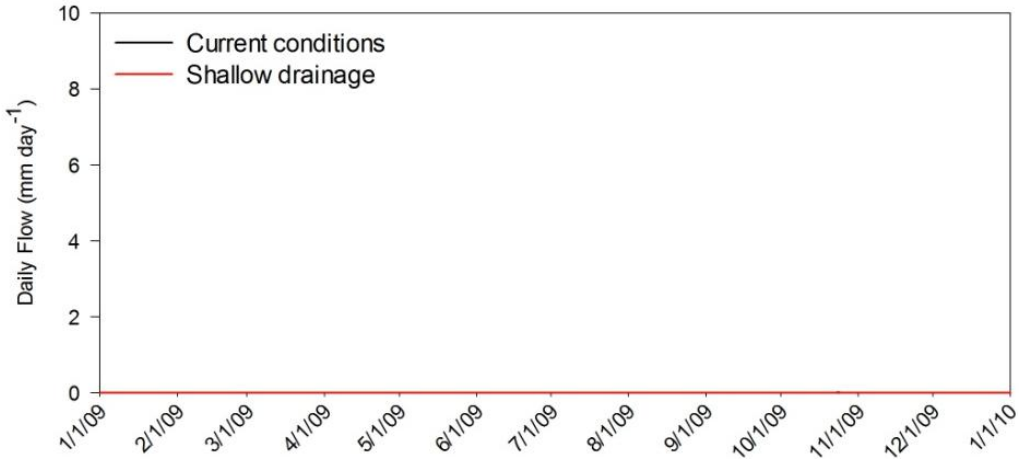

Figure 149 Surface flow for shallow drainage conditions in PAL5, 2009

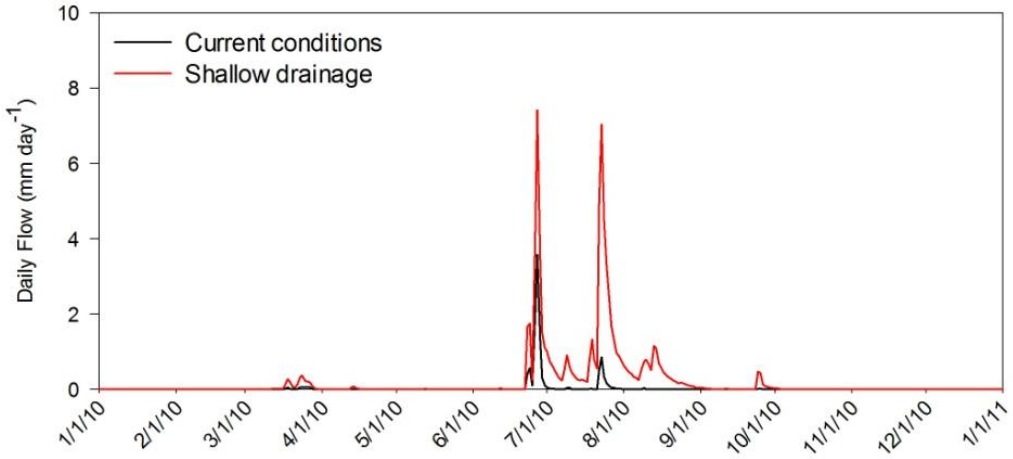

Figure 150 Surface flow for shallow drainage conditions in PAL5, 2010

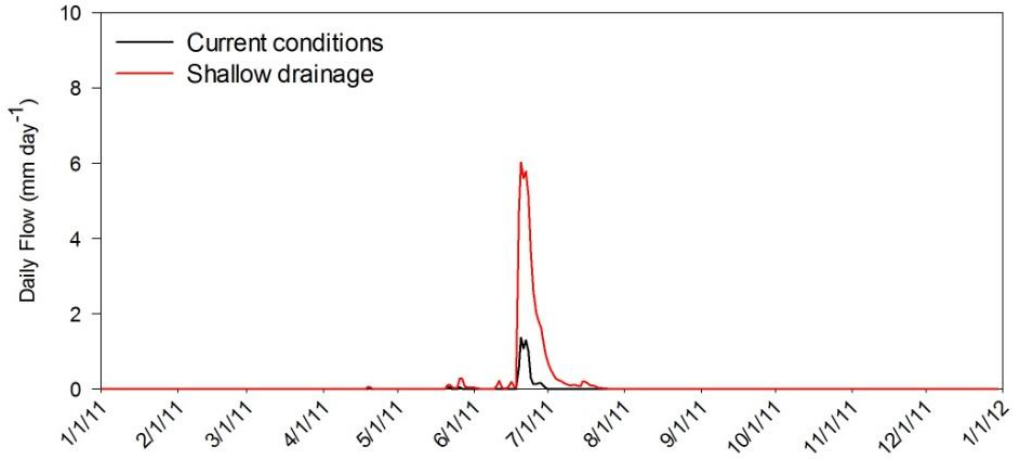

Figure 151 Surface flow for shallow drainage conditions in PAL5, 2011

Subsurface flow

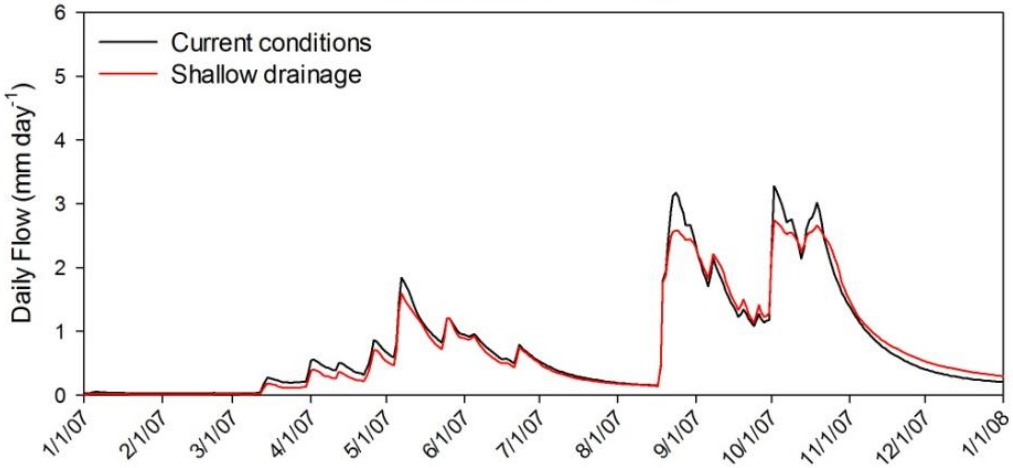

Figure 152 Subsurface flow for shallow drainage conditions in PAL3, 2007

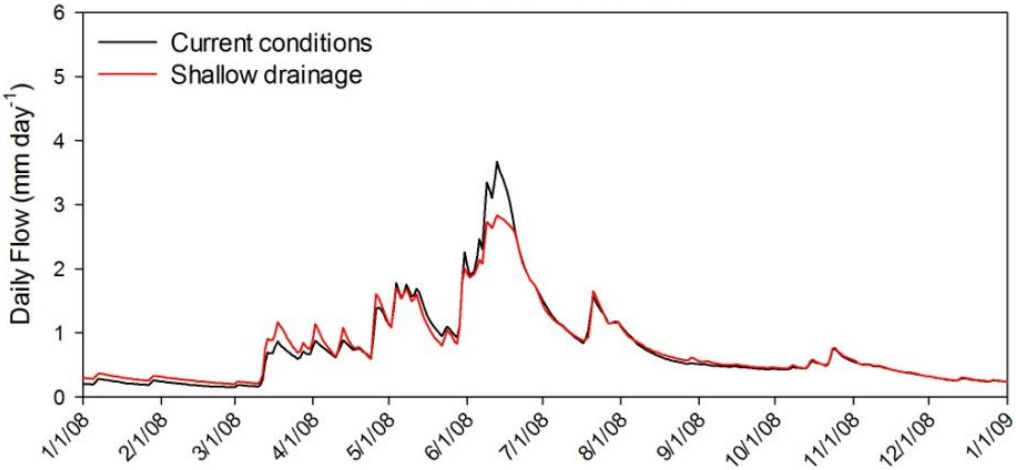

Figure 153 Subsurface flow for shallow drainage conditions in PAL3, 2008

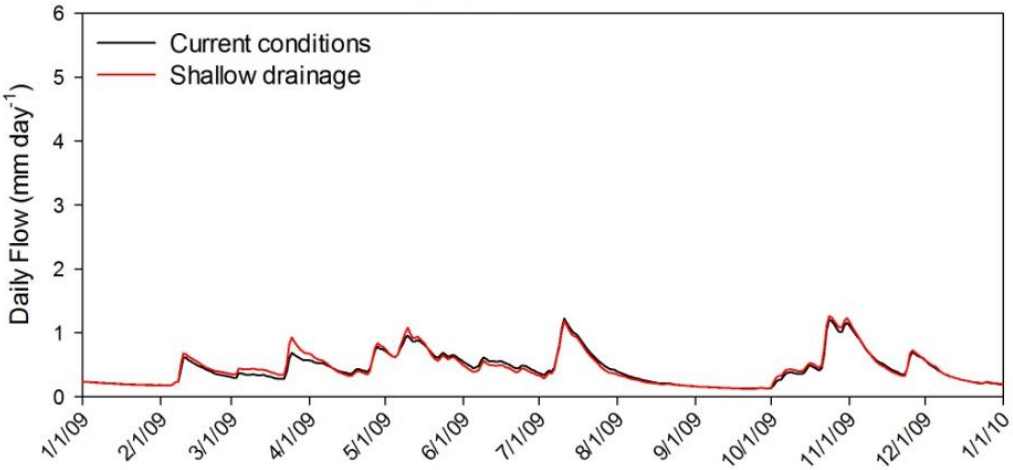

Figure 154 Subsurface flow for shallow drainage conditions in PAL3, 2009

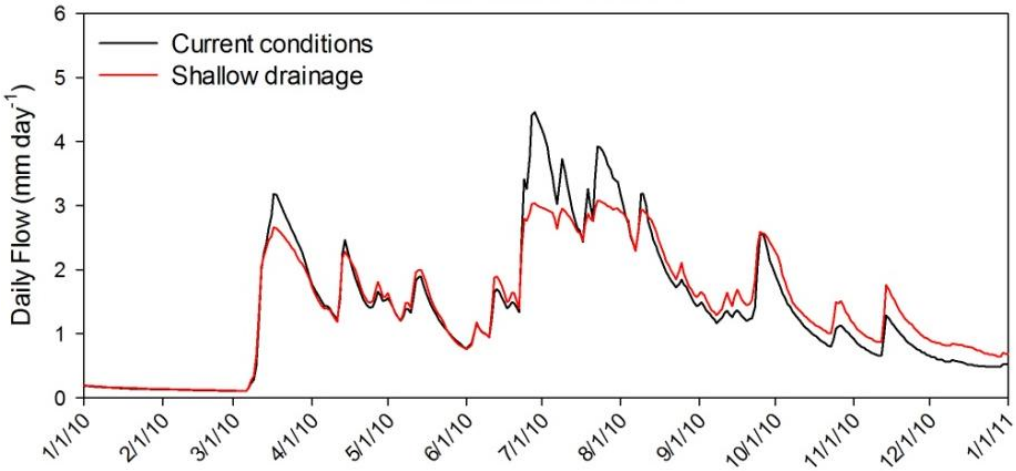

Figure 155 Subsurface flow for shallow drainage conditions in PAL3, 2010

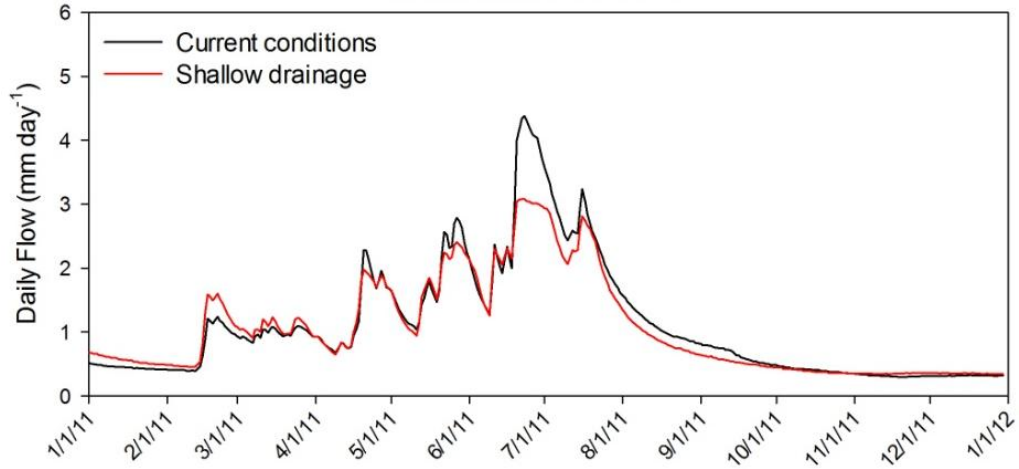

Figure 156 Subsurface flow for shallow drainage conditions in PAL3, 2011

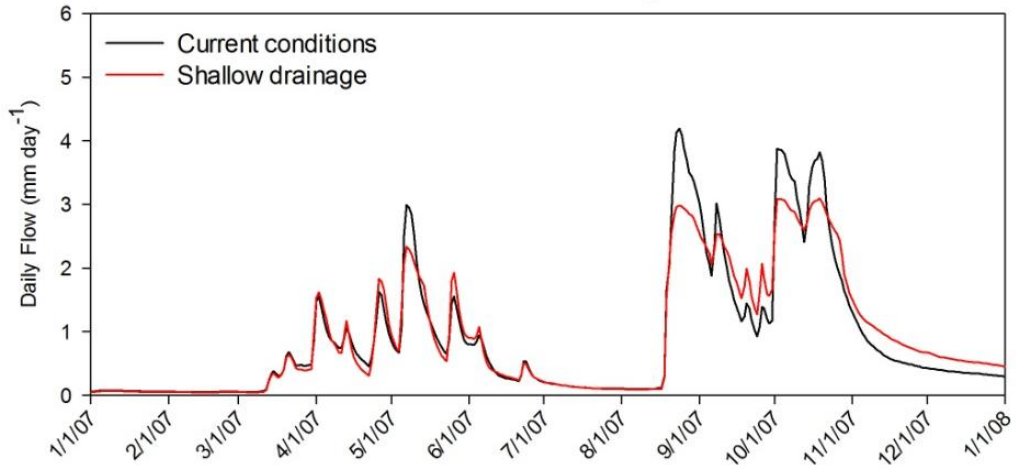

Figure 157 Subsurface flow for shallow drainage conditions in PAL5, 2007

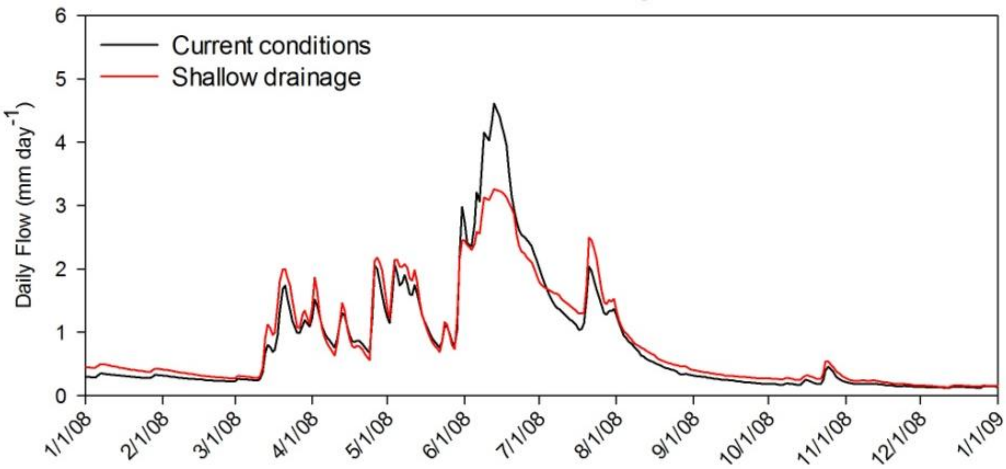

Figure 158 Subsurface flow for shallow drainage conditions in PAL5, 2008

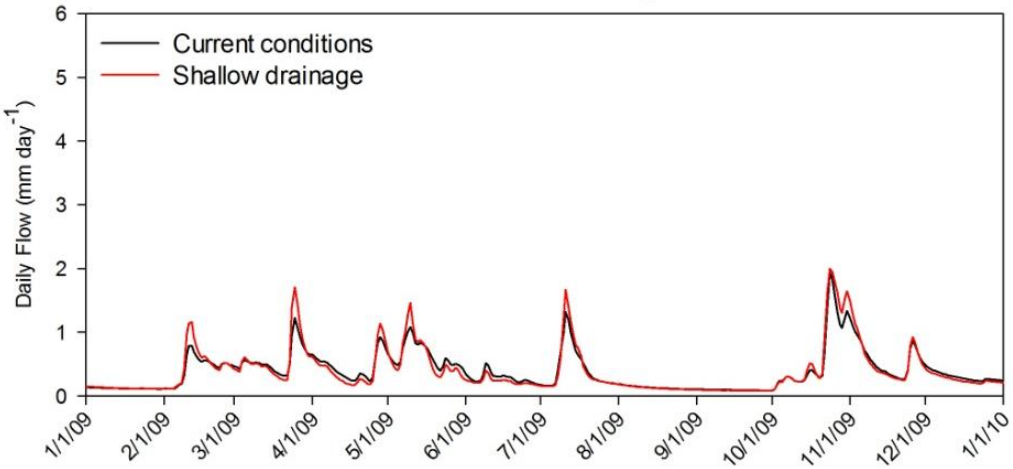

Figure 159 Subsurface flow for shallow drainage conditions in PAL5, 2009

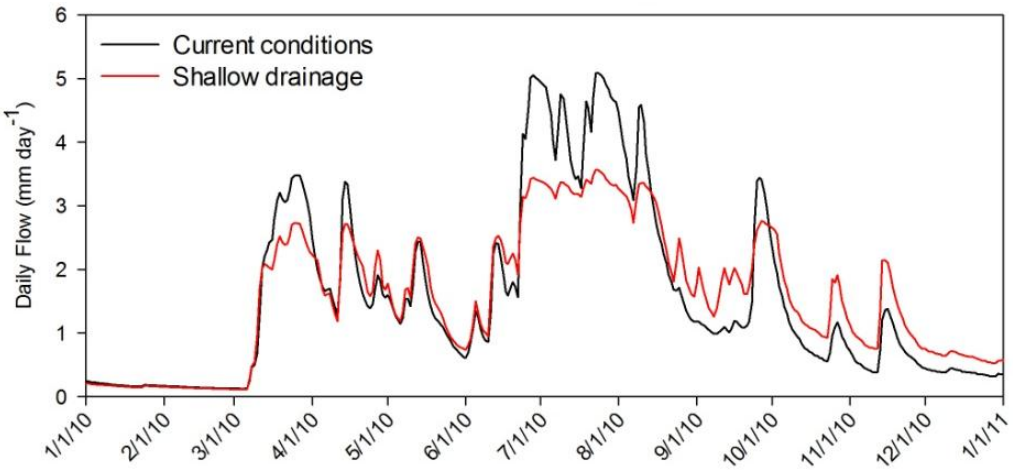

Figure 160 Subsurface flow for shallow drainage conditions in PAL5, 2010

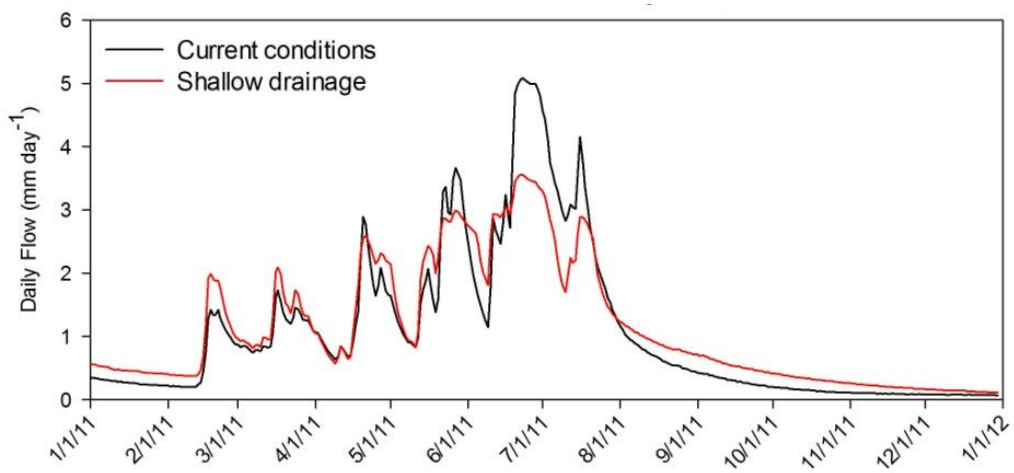

Figure 161 Subsurface flow for shallow drainage conditions in PAL5, 2011

A. 3. 4. Row crop agriculture without drainage infrastructure conditions

Surface flow

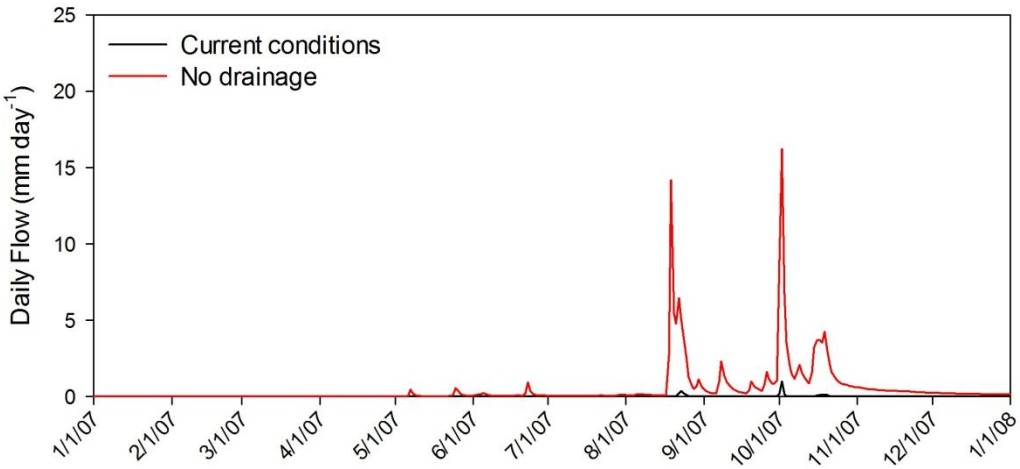

Figure 162 Surface flow for row crop agriculture without drainage infrastructure conditions in PAL3, 2007

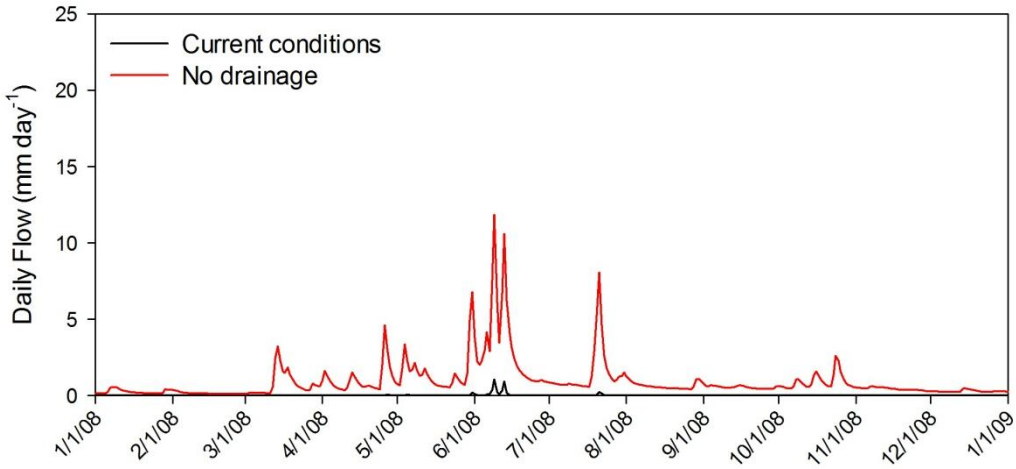

Figure 163 Surface flow for row crop agriculture without drainage infrastructure conditions in PAL3, 2008

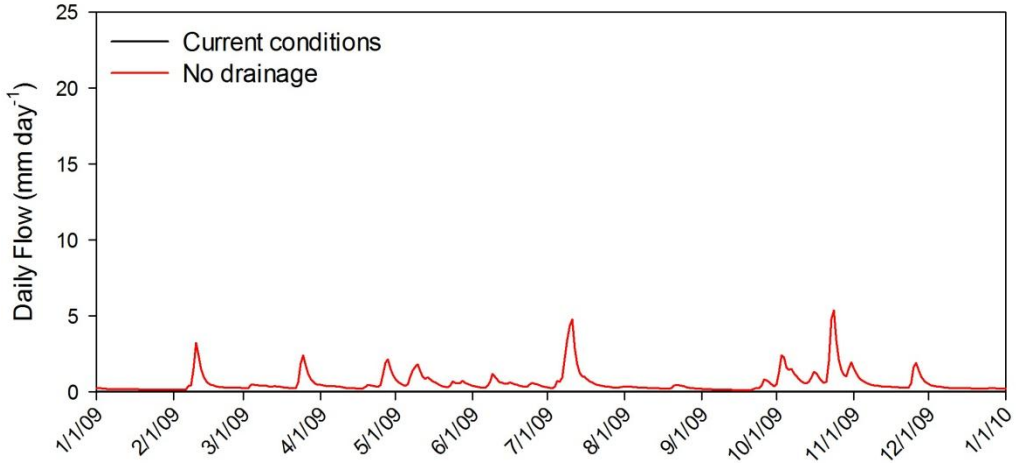

Figure 164 Surface flow for row crop agriculture without drainage infrastructure conditions in PAL3, 2009

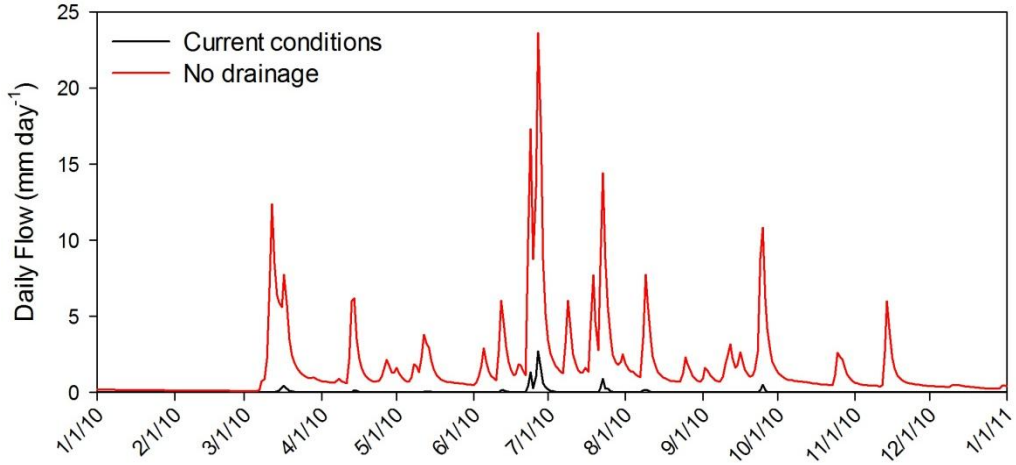

Figure 165 Surface flow for row crop agriculture without drainage infrastructure conditions in PAL3, 2010

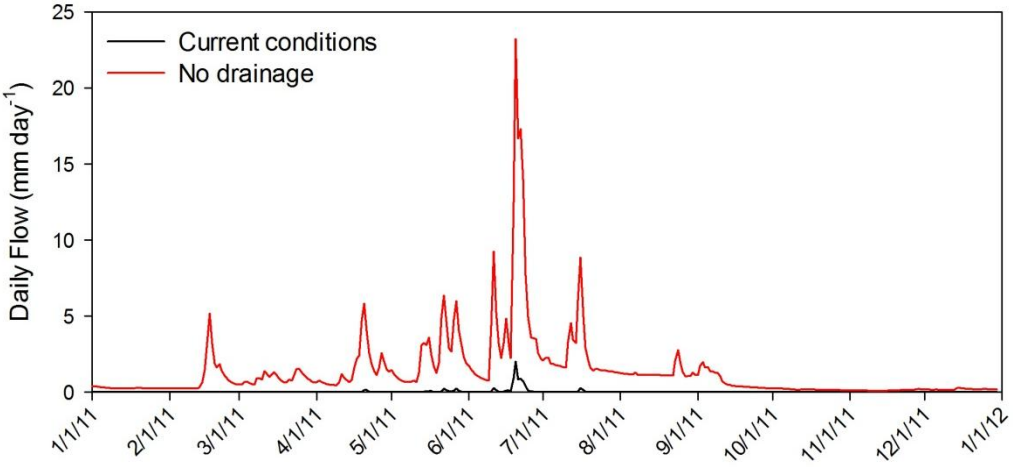

Figure 166 Surface flow for row crop agriculture without drainage infrastructure conditions in PAL3, 2011

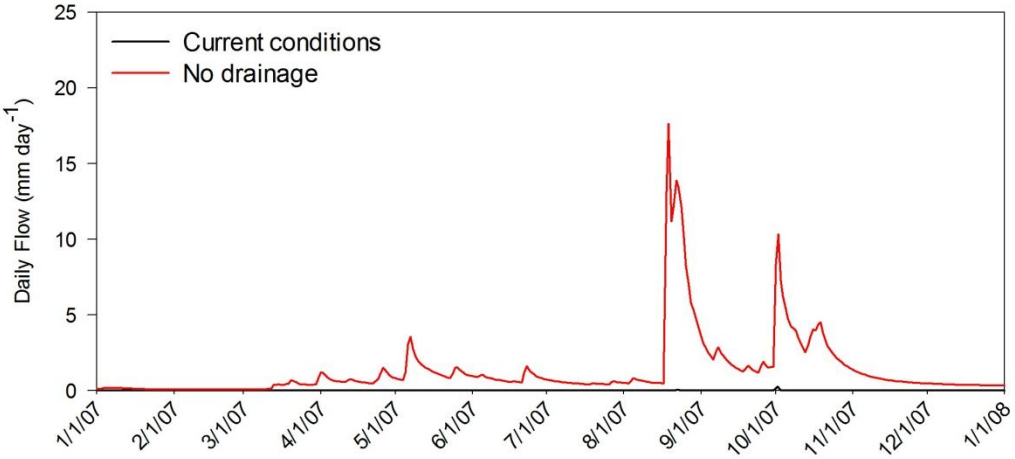

Figure 167 Surface flow for row crop agriculture without drainage infrastructure conditions in PAL5, 2007

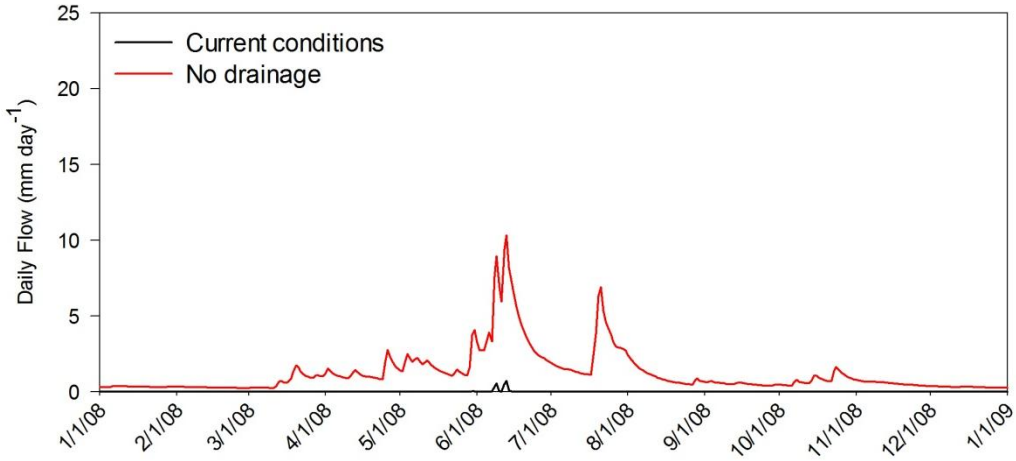

Figure 168 Surface flow for row crop agriculture without drainage infrastructure conditions in PAL5, 2008

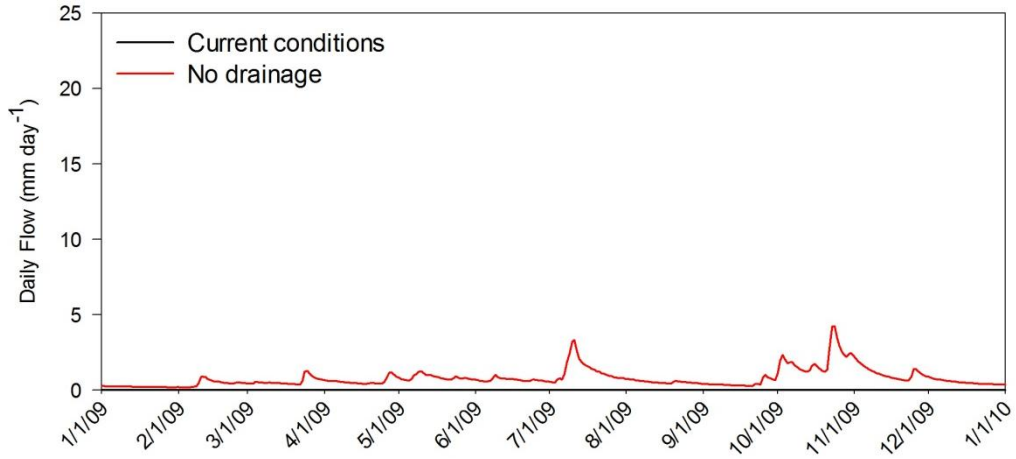

Figure 169 Surface flow for row crop agriculture without drainage infrastructure conditions in PAL5, 2009

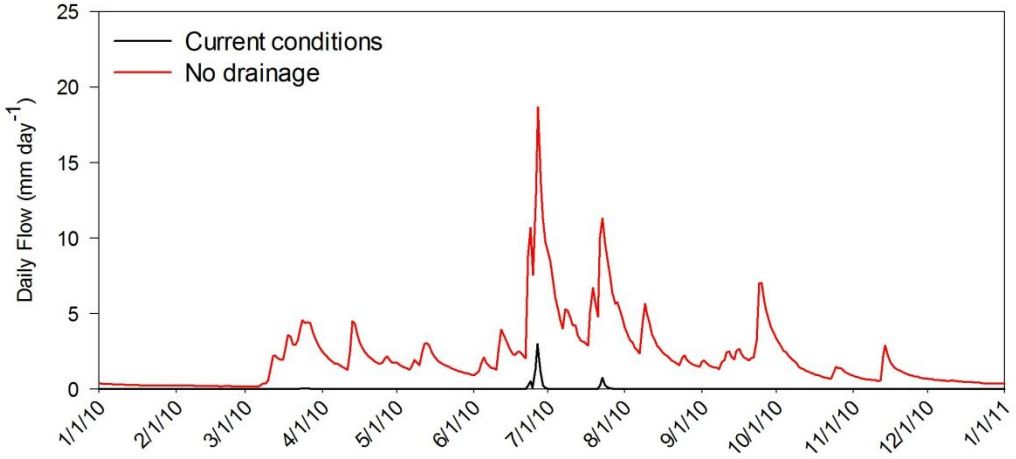

Figure 170 Surface flow for row crop agriculture without drainage infrastructure conditions in PAL5, 2010

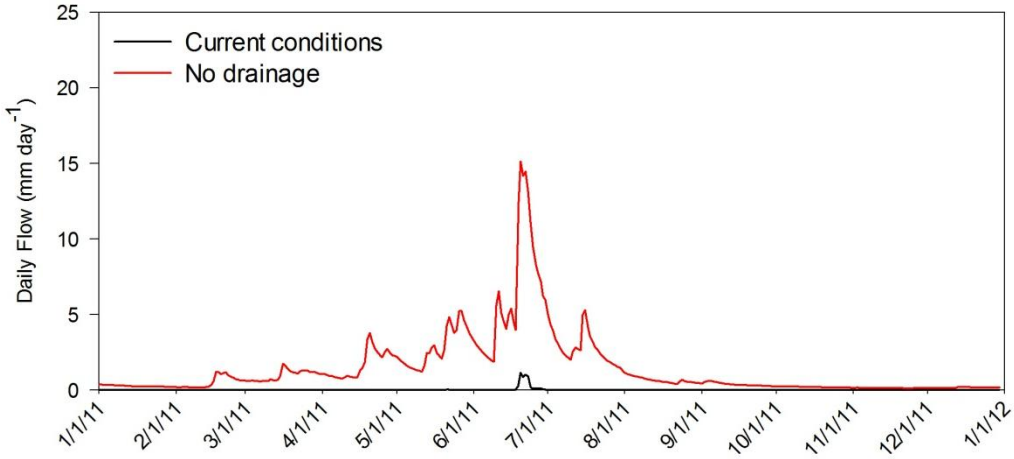

Figure 171 Surface flow for row crop agriculture without drainage infrastructure conditions in PAL5, 2011